



**Technical University of Crete**  
**School of Environmental Engineering**  
Laboratory of Toxic and Hazardous Waste Management

**DEVELOPMENT OF RECYCLING TECHNIQUES  
IN 1ST AND 2ND GENERATION WASTE  
PHOTOVOLTAIC PANELS**

PhD Thesis

Presented to  
The Technical University of Crete  
School of Environmental Engineering  
on July 2, 2019

by

**Vasiliki SAVVILOTIDOU**

Environmental Engineer, M.Sc.

July  
2019





**Πολυτεχνείο Κρήτης**  
**Σχολή Μηχανικών Περιβάλλοντος**  
Εργαστήριο Διαχείρισης Τοξικών και Επικίνδυνων Αποβλήτων

**ΑΝΑΠΤΥΞΗ ΤΕΧΝΙΚΩΝ ΑΝΑΚΥΚΛΩΣΗΣ**  
**ΣΕ ΑΠΟΒΛΗΤΑ ΦΩΤΟΒΟΛΤΑΪΚΑ ΠΛΑΙΣΙΑ**  
**1ΗΣ ΚΑΙ 2ΗΣ ΓΕΝΙΑΣ**

Διδακτορική Διατριβή

Παρουσιάστηκε στο  
Πολυτεχνείο Κρήτης  
Σχολή Μηχανικών Περιβάλλοντος  
στις 2 Ιουλίου 2019

Από τη

**Βασιλική ΣΑΒΒΙΑΩΤΙΔΟΥ**

Μηχανικό Περιβάλλοντος, M.Sc.

Ιούλιος  
2019



## **Examination Committee**

**Evangelos GIDARAKOS** – Supervisor

Professor

School of Environmental Engineering

Technical University of Crete

**Ioannis GENTEKAKIS** – Advisory committee

Professor

School of Environmental Engineering

Technical University of Crete

**Dimitrios KOMILIS** – Advisory committee

Professor

Department of Environmental Engineering

Democritus University of Thrace

**Konstantinos KOMNITSAS**

Professor

School of Mineral Resources Engineering

Technical University of Crete

**Evangelos DIAMADOPOULOS**

Professor, Rector of the Technical University of Crete

School of Environmental Engineering

Technical University of Crete

**George KARATZAS**

Professor

School of Environmental Engineering

Technical University of Crete

**Apostolos GIANNIS**

Assistant Professor

School of Environmental Engineering

Technical University of Crete



Στους γονείς μου και την αδερφή μου

«Το πiónι»

Πολλάκις, βλέποντας να παίζουν σκάκι,  
ακολουθεί το μάτι μου ένα Πiónι  
όπου σιγά-σιγά τον δρόμο βρίσκει  
και στην υστερινή γραμμή προφθαίνει.  
Με τέτοια προθυμία πάει στην άκρη  
όπου θαρρείς πως βέβαια εδώ θ' αρχίσουν  
οι απολαύσεις του κ' οι αμοιβές του.  
Πολλές στον δρόμο κακουχίες βρίσκει.  
Λόγγες λοζά το ρίχνουν πεζόδρομοι·  
τα κάστρα το χτυπούν με τες πλατείες των  
γραμμές· μέσα στα δυο τετράγωνα των  
γρήγοροι καβαλλάρηδες γυρεύουν  
με δόλο να το κάμουν να σκαλώσει·  
κ' εδώ κ' εκεί με γωνιακή φοβέρα  
μπαίνει στον δρόμο του κανένα πiónι  
απ' το στρατόπεδο του εχθρού σταλμένο.

Αλλά γλιτώνει απ' τους κινδύνους όλους  
και στην υστερινή γραμμή προφθαίνει.  
Τι θριαμβευτικά που εδώ προφθαίνει,  
στην φοβερή γραμμή την τελευταία·  
τι πρόθυμα στον θάνατό του αγγίζει!

Γιατί εδώ το Πiónι θα πεθάνει  
κ' ήσαν οι κόποι του προς τούτο μόνο.  
Για την βασίλισσα που θα μας σώσει,  
για να την αναστήσει από τον τάφο  
ήλθε να πέσει στου σκακιού τον άδη.

Κ.Π. Καβάφης (1894)



## Acknowledgements

It is often said that “the journey matters more than the destination itself” or “the doing is more important than the outcome”. In my case this is partly true as reaching my destination and completing my PhD, it is a great reward and relief at the same time. It was a long journey indeed, but like Odysseus’ journey to reach Ithaca, it was not easy and it had many ups and downs, many challenges both at a professional and personal level. I enjoyed the journey and I appreciate the lessons and experiences I lived, the skills I acquired and the person I became.

My research was conducted over the last four years at the Technical University of Crete in the Laboratory of Toxic and Hazardous Waste Management. During these years, I have received support and encouragement from several individuals, to whom I would like to express my sincere and deepest thanks.

First, I would like to express my sincere gratitude to my supervisor Prof. Dr. Evangelos Gidaracos for giving me the opportunity to join his research group and trust in me, as well as for giving me continuous support and advices, for his patience, motivation, and immense knowledge. I have been amazingly fortunate to have an advisor who gave me the freedom to explore on my own, and at the same time the guidance to recover when my steps faltered. I sincerely thank him for the time and effort not only to teach me to do research and encourage me during the difficult times of the research, but also to instruct me over other aspects of life according to his personal experiences and lifetime. I feel that I improved myself in many ways.

I would also like to express my profound gratitude to the thesis committee, namely Prof. Dr. Ioannis Gentekakis, Prof. Dr. Dimitrios Komilis, Prof. Dr. Konstantinos Komnitsas, Prof. Dr. Evangelos Diamadopoulos, Prof. Dr. George Karatzas and Assis. Prof. Dr. Apostolos Giannis, for their expert discussion, the extensive review of the manuscript and their suggestions for improving its quality.

I must acknowledge the General Secretariat for Research and Technology (GSRT) and the Hellenic Foundation for Research and Innovation (HFRI) for the

financial support provided to me, through the scholarship for my doctoral studies at the School of Environmental Engineering of the Technical University of Crete. This scholarship was an important contribution to my studies, as well as a great honor for me personally.

I would like to acknowledge COST Action ES1407 (European network for innovative recovery strategies of rare earth and other critical metals from electric and electronic waste, ReCrew) for networking support and development of research activities, as well as for funding COST meetings, visits and tours in European recycling plants for WEEE. Also, I would like to thank all the ReCrew members for sharing expertise and exchanging knowledge.

I would also like to acknowledge the staff at the Technical University for the support and assistance, and especially:

- Mrs. Maria-Liliana Saru for performing ICP-MS analyses at the School of Environmental Engineering in the Laboratory Hydrogeochemical Engineering and Soil Remediation.
- Mrs. Paola Rotondo for performing XRF analyses at the School of Mineral Resources Engineering in the Laboratory of Petrology and Economic Geology.
- Dr. Eftychia Repouskou for performing and interpreting SEM-EDS analyses at the School of Mineral Resources Engineering in the Laboratory of Petrology and Economic Geology.
- Mr. Stelios Mavrigiannakis for performing uniaxial compressive strength analyses at the School of Mineral Resources Engineering in the Laboratory of Rock Mechanics.
- Dr. Antonios Stratakis for performing and interpreting XRD analyses at the School of Mineral Resources Engineering in the Laboratory of Applied Mineralogy, as well as for offering valuable insights mainly on chapter 6.
- Mrs. Olga Pantelaki and Dr. Anna Kritikaki working at the School of Mineral Resources Engineering in the Laboratory of Ore Processing and Laboratory of

Ceramics and Glass Technology, respectively, for their continuous availability and assistance in some areas covered by this thesis (especially chapter 6).

My sincere thanks go to all the undergraduate and graduate students I worked with at the Laboratory of Toxic and Hazardous Waste Management, and especially to Argiro Lakiotaki, Alexandra Antoniou, Ioanna Papastamati, Nikolaos Sisakis, Maria Tsoka, Ioannis Liarokapis, Nikolia Stoikou, Chrysanthie Makri and Aikaterini Karagianni.

Furthermore, I would like to sincerely thank the current and former colleagues of the Laboratory of Toxic and Hazardous Waste Management, Dr. Maria Aivalioti, Mrs. Eleni Kastanaki, Dr. Ioannis Hahladakis, Dr. Fotini Simantiraki, Mrs. Athanasia Kousaiti, Dr. Frantseska-Maria Pelleri, Mrs. Aikaterini Valouma and Mr. Ioannis Moukazis for the friendly and collaborative environment, the funny and difficult times we spent all these years.

I would also like to thank the technicians of the Technical University of Crete for the technical and practical support, as well as the Secretariats of the School of Environmental Engineering, namely Mrs. Dimitra Pateraki and Mrs. Georgia Poniridou for all the administrative coordination and kind attitude.

Special thanks to Menelaos Xirouchakis for the precious encouragement and everything he has shared with me in this journey. My heartfelt thanks to my friends inside and outside TUC (Elena, Evgenia, Katerina, Marina, Eleni, Evridiki, Pantelis, Sofia, Antonis, Antonis, Electra) for their precious friendship, sharing moments and enriching my life in many ways.

I would also like to thank my friends and relatives for their support and care despite distances. My final thanks go to my family. A special feeling of gratitude to my parents (Kosmas and Chrysanthi) and sister (Maria) for their extraordinary love, for always standing by me and believing in me.

Thank you all!



The research work was supported by the Hellenic Foundation for Research and Innovation (HFRI) and the General Secretariat for Research and Technology (GSRT), under the HFRI PhD Fellowship grant (GA. no. 34413-34414).



Η ερευνητική εργασία υποστηρίχτηκε από το Ελληνικό Ίδρυμα Έρευνας και Καινοτομίας (ΕΛΙΔΕΚ) και από τη Γενική Γραμματεία Έρευνας και Τεχνολογίας (ΓΓΕΤ), στο πλαίσιο της Δράσης «Υποτροφίες ΕΛΙΔΕΚ Υποψηφίων Διδασκτόρων» (αρ. Σύμβασης 34413-34414).

## Summary

Waste electrical and electronic equipment (WEEE) or e-waste is globally considered as one of the fastest growing and complex waste streams. The European Directive on WEEE (2012/19/EU) aims at sustainable production and consumption and sets targets for collection, reuse, recycling and recovery. From 15<sup>th</sup> August 2018 and onwards, WEEE is classified within the six new categories, as stipulated in Annex III of the recast Directive instead of the existing ten categories. End-of-Life (EoL) photovoltaic (P/V) panels consist one of the newest WEEE under category 4 and, thus, a current and future challenge, since their management is yet to be compiled. Because of the P/V market growth and its continuous expansion, the International Renewable Energy Agency (IRENA) has predicted that waste P/V panels will amount to 1.7-8.0 million tonnes by 2030 and to 60-78 million tonnes by 2050. P/Vs are considered as “clean” energy technologies with positive impacts on energy security and climate change, however, the proper management of EoL P/Vs is an indispensable issue that should be particularly addressed and evaluated from a life-cycle viewpoint.

The purpose of this thesis is to develop recycling techniques for P/V panels in order to recover valuable components, taking into consideration that they represent one of the newest and most promising sources of secondary raw materials. P/V panels based on different technology, namely polycrystalline silicon (p-Si) and monocrystalline silicon (m-Si) panels classified in the 1st generation of photovoltaics, as well as copper indium selenide (CIS) and amorphous silicon classified in the 2nd generation of photovoltaics, were studied. Aiming at sustainable management of waste panels, various investigations were carried out including four different approaches, (a) the delamination of P/V panels, (b) the recovery of valuable metals (semiconductors), rather than simple recovery of bulk materials, (c) the reuse of glass or plastic in cement mortar production, and (d) the valorization of glass in the production of glass-ceramics for applications in the construction sector.

One of the main problems in the management of P/V panels is their complex and multilayer structure which differs depending on the cell technology. Initially, investigations were conducted on the delamination of P/V panels by comparing thermal, mechanical and chemical treatment techniques. The comparison and optimal approach were determined based not only on the efficiency of delamination, but also on the mass flow of precious (silver) and critical (indium) metals during these processes. These high-tech metals have been included in the European (EU) list of critical raw materials (CRMs) and their recycling is a priority in order to contribute to a circular economy and reduce the risks pertinent to expensive and scarce resources. The content of silver and indium in the treated mass was determined. Also, their pre-concentration yield and losses in each treatment technique were calculated. Finally, selective recovery of these metals was achieved using a hydrometallurgical process, including leaching and precipitation. Apart from high-value recyclable materials, bulk materials including glass and plastic from P/Vs were recycled and reused as partial replacement of fine aggregates or cement in cement mortar production. Various parameters, among which, the type of waste (glass or plastic), the amount (%) and particle size of waste, as well as the resource replaced (fine aggregates or cement) were studied. Physical, mechanical and thermal properties of cement mortars were determined and compared to reference mortars. Also, the resistance of mortars to corrosive environments, as well as their potential toxicity were examined. The last part of this study was the valorization of specific wastes generated from the energy sector, i.e. P/V glass and lignite fly ash, and the production of glass-ceramics. Various parameters, such as mixing ratio, melting and sintering temperatures, and others were investigated to determine the optimal conditions. The physical and mechanical properties of the produced glass-ceramics were examined. Also, the chemical composition, mineralogy and microstructure, as well as the chemical stability were determined.

Delamination and separation of the major components contained in P/V panels were achieved through a combination of processes, namely a thermal process and a gravimetric separation, leading to intact and reusable components. Under this

combination of processes, 91-94% of silver was pre-concentrated from the p-Si and m-Si panels and around 96% of indium was pre-concentrated from the CIS panel as well. Through selective recovery, i.e. leaching and precipitation,  $\text{In}_2\text{O}_3$  and  $\text{AgCl}$  were recovered achieving 74.8 and 98.7-99.2% recovery. In addition, cement mortars containing up to 20% glass as replacement of sand or cement exhibited high strength and resistance to corrosion comparable with those of reference mortars, whereas plastic addition resulted in enhanced thermal properties by reducing the thermal conductivity of cement mortars (from 0.77 to 0.45 W/m·k). Finally, melting of glass and lignite fly ash mixture at 1200 °C and sintering of the produced glass at 700-800 °C resulted in dense and homogeneous glass-ceramics. Specifically, the results showed that the produced glass-ceramics can be used in the construction sector as brick pavers, since their compressive strength and water absorption were 113-148 MPa and 0.02-0.07% respectively, thus complying with the standard specification, ASTM C 1272.

In conclusion, metal, glass and plastic parts consisting more than 90% of P/V panels can be reused, recovered or recycled towards an integrated sustainable management of waste P/V panels, indicating potential future applications.



## Περίληψη

Τα απόβλητα ηλεκτρικού και ηλεκτρονικού εξοπλισμού (ΑΗΗΕ) αποτελούν μία από τις ταχύτερα αναπτυσσόμενες και πιο πολύπλοκες κατηγορίες αποβλήτων παγκοσμίως. Με στόχο τη βιώσιμη παραγωγή και κατανάλωση ηλεκτρικού και ηλεκτρονικού εξοπλισμού (ΗΕΕ), η Ευρωπαϊκή Οδηγία για τα ΑΗΗΕ (2012/19/ΕΕ) θέτει στόχους για τη συλλογή, επαναχρησιμοποίηση, ανακύκλωση και ανάκτησή τους. Από τις 15 Αυγούστου 2018 και στο εξής το πεδίο εφαρμογής της Οδηγίας περιλαμβάνει έξι κατηγορίες ΑΗΗΕ, όπως ορίζονται στο παράρτημα ΙΙΙ της Οδηγίας, καθώς ολοκληρώνεται η μεταβατική περίοδος η οποία αφορούσε 10 κατηγορίες ΑΗΗΕ. Τα φωτοβολταϊκά (Φ/Β) πλαίσια στο τέλος του κύκλου ζωής τους αποτελούν ένα από τα πλέον πρόσφατα ΑΗΗΕ (κατηγορία 4) και συνάμα μια τρέχουσα και μελλοντική πρόκληση αναφορικά με τη διαχείρισή τους.

Με βάση την συνεχή ανάπτυξη στην αγορά Φ/Β συστημάτων και την επερχόμενη αύξησή τους, εκτιμάται ότι τα απόβλητα Φ/Β πλαίσια θα ανέρχονται συνολικά σε 1.7-8.0 εκατομμύρια τόνους μέχρι το 2030 και 60-78 εκατομμύρια τόνους έως το 2050. Αναμφισβήτητα, τα φωτοβολταϊκά είναι μία από τις πλέον περιβαλλοντικά "καθαρές" τεχνολογίες παραγωγής ενέργειας με θετικό αντίκτυπο στην ενεργειακή ασφάλεια και την κλιματική αλλαγή. Ωστόσο, η ορθή διαχείριση των φωτοβολταϊκών πλαισίων είναι ένα κρίσιμο και καθόλα επίκαιρο περιβαλλοντικό ζήτημα που πρέπει να τεθεί υπό μελέτη.

Ο σκοπός της παρούσας διδακτορικής διατριβής επικεντρώνεται στην ανακύκλωση, ανάκτηση και αξιοποίηση των πολύτιμων υλικών που περιέχονται σε απόβλητα φωτοβολταϊκά πλαίσια, λαμβάνοντας υπόψη ότι μπορεί να αποτελέσουν μία σημαντική πηγή δευτερογενών πρώτων υλών. Καθώς τα φωτοβολταϊκά πλαίσια διαφέρουν ως προς τη σύσταση και τη δομή τους, μελετήθηκαν τέσσερις διαφορετικές τεχνολογίες πλαισίων - οι πιο συχνά απαντώμενες - δηλαδή πολυκρυσταλλικού πυριτίου (p-Si) και μονοκρυσταλλικού πυριτίου (m-Si) πλαίσια τα οποία κατατάσσονται στην πρώτη γενιά φωτοβολταϊκών, καθώς και χαλκού ινδίου σεληνίου (CIS) και άμορφου πυριτίου πλαίσια τα οποία κατατάσσονται στη δεύτερη γενιά φωτοβολταϊκών,

αντίστοιχα. Προς την κατεύθυνση της ολοκληρωμένης και βιώσιμης διαχείρισης των Φ/Β πλαισίων, αναπτύχθηκαν διάφορες τεχνικές, οι οποίες αποτελούνται από πολλαπλά στάδια επεξεργασίας και αποσκοπούν: (α) στην αποστρωματοποίηση της δομής των πλαισίων, (β) στην ανάκτηση πολύτιμων μετάλλων (ημιαγωγών), καθώς και «συμβατικών» υλικών, γ) στην αξιοποίηση γυαλιού ή πλαστικού για την παραγωγή τσιμεντοκονιαμάτων, και δ) στην αξιοποίηση του γυαλιού για την παραγωγή υαλοκεραμικών με χρήσεις στον κατασκευαστικό τομέα.

Ένα από τα κύρια προβλήματα στη διαχείριση των πλαισίων είναι η σύνθετη και πολυστρωματική δομή τους, η οποία διαφέρει ανάλογα με την τεχνολογία των κυττάρων. Στο πρώτο μέρος της διατριβής, διερευνήθηκε η αποστρωματοποίηση της δομής με διάφορες τεχνικές επεξεργασίας, όπως θερμικές, μηχανικές και χημικές μεθόδους. Έπειτα, πραγματοποιήθηκε συνδυασμός των μεθόδων επεξεργασίας προκειμένου να επιτευχθεί αποτελεσματικός διαχωρισμός των κύριων υλικών (γυαλί, κελιά, μεταλλικά ηλεκτρόδια, οργανικά μέρη). Η επιλογή του βέλτιστου συνδυασμού μεθόδων επεξεργασίας προσδιορίστηκε με βάση την απόδοση αποστρωματοποίησης, καθώς επίσης και βάσει των ισοζυγίων μάζας των πολύτιμων (άργυρος) και κρίσιμων (ίνδιο) μετάλλων, που απαρτίζουν τα Φ/Β κύτταρα, προκειμένου να ελαχιστοποιηθούν οι απώλειές τους. Πρέπει να σημειωθεί ότι τα μέταλλα αυτά συμπεριλαμβάνονται στον Ευρωπαϊκό κατάλογο κρίσιμων πρώτων υλών και η ανακύκλωσή τους αποτελεί προτεραιότητα στα πλαίσια της κυκλικής οικονομίας δεδομένου ότι εμφανίζουν υψηλό κίνδυνο διαθεσιμότητας σε παγκόσμιο επίπεδο. Ως εκ τούτου, το δεύτερο μέρος της διατριβής αφορούσε τον προσδιορισμό (α) της περιεκτικότητας του αργύρου και ινδίου στο επεξεργασμένο υλικό, και (β) της απόδοσης προ-συγκέντρωσης και των απωλειών για κάθε συνδυασμό μεθόδων επεξεργασίας λαμβάνοντας υπόψη την περιεκτικότητα στην επεξεργασμένη μάζα ως προς την αρχική περιεκτικότητα στη μη επεξεργασμένη μάζα φωτοβολταϊκού. Επίσης, επιλεκτική ανάκτηση αυτών των μετάλλων επιτεύχθηκε χρησιμοποιώντας υδρομεταλλουργικές διεργασίες, όπως έκπλυση και κατακρήμνιση. Εκτός από την ανάκτηση υψηλής αξίας υλικών, συμβατικά υλικά, όπως γυαλί και πλαστικό που περιέχονται στα πλαίσια, ανακυκλώθηκαν και επαναχρησιμοποιήθηκαν ως

μερική αντικατάσταση λεπτόκοκκων αδρανών ή τσιμέντου για την παραγωγή τσιμεντοκονιαμάτων. Μελετήθηκαν διάφορες παράμετροι, όπως ο τύπος αποβλήτου (γυαλί ή πλαστικό), η ποσότητα (%) και το μέγεθος των σωματιδίων του αποβλήτου, καθώς και το υλικό που αντικαθίσταται (λεπτόκοκκα αδρανή ή τσιμέντο). Οι φυσικές, μηχανικές και θερμικές ιδιότητες των τσιμεντοκονιαμάτων προσδιορίστηκαν και συγκρίθηκαν με τα κονιάματα αναφοράς. Επίσης, εξετάστηκε η αντοχή και ανθεκτικότητα των τσιμεντοκονιαμάτων σε διάφορα περιβάλλοντα διάβρωσης. Το τελευταίο μέρος της διατριβής αφορά στην παραγωγή υαλοκεραμικών από απόβλητα του ενεργειακού τομέα, δηλαδή Φ/Β γυαλί και ιπτάμενη τέφρα λιγνίτη. Διάφορες παράμετροι, όπως η αναλογία ανάμιξης, οι θερμοκρασίες τήξης και πυροσυσσώματωσης-κρυστάλλωσης, κ.α. διερευνήθηκαν για να προταθούν οι βέλτιστες συνθήκες. Αναλύθηκαν οι φυσικές και μηχανικές ιδιότητες των παραγόμενων υαλοκεραμικών. Επίσης, προσδιορίστηκε η χημική και ορυκτολογική σύσταση, η μικροδομή τους, η εν δυνάμει τοξικότητα υπό συνθήκες, καθώς και η χημική σταθερότητα στη διάβρωση.

Τα αποτελέσματα έδειξαν ότι η πιο αποτελεσματική μέθοδος ανάκτησης υλικών ήταν η θερμική επεξεργασία, ακολουθούμενη από βαρυμετρικό διαχωρισμό. Συγκεκριμένα, μετά τη θερμική επεξεργασία το στερεό υπόλειμμα αποτελούταν από γυαλί και Φ/Β κύτταρα καθώς τα οργανικά μέρη αποσυντέθηκαν. Το υπόλειμμα διαχωρίστηκε αποτελεσματικά με βάση τις διαφορετικές πυκνότητες γυαλιού και κυττάρων χρησιμοποιώντας υγρό ενδιάμεσης πυκνότητας. Ο άργυρος προσυγκεντρώθηκε με ποσοστό 91-94% από τα πλαίσια κρυσταλλικού τύπου, p-Si και m-Si, και το ίνδιο προσυγκεντρώθηκε με ποσοστό 96% από το πλαίσιο λεπτού υμενίου, CIS. Με τη χρήση μεθόδων επιλεκτικής ανάκτησης, όπως έκπλυση και κατακρήμνιση, ανακτήθηκαν  $\text{In}_2\text{O}_3$  και  $\text{AgCl}$  επιτυχάνοντας 74.8 και 98.7-99.2% ανάκτηση, αντίστοιχα. Τα τσιμεντοκονιάματα που περιείχαν γυαλί σε ποσοστό 20% ως αντικατάσταση της άμμου ή του τσιμέντου παρουσίασαν υψηλή αντοχή και ανθεκτικότητα στη διάβρωση, συγκριτικά με τα τσιμεντοκονιάματα αναφοράς, ενώ η προσθήκη πλαστικών είχε ως αποτέλεσμα την ενίσχυση των θερμικών ιδιοτήτων των

τσιμεντοκονιαμάτων επιτυγχάνοντας μείωση της θερμικής αγωγιμότητας (από 0.77 σε 0.45 W/m·k). Τέλος, η τήξη του Φ/Β γυαλιού και της ιπτάμενης τέφρας λιγνίτη στους 1200 °C και η πυροσυσσωμάτωση-κρυστάλλωση του παραγόμενου γυαλιού στους 700 ή 800 °C οδήγησαν στην παραγωγή υλικών που χαρακτηρίζονται ως υαλοκεραμικά με βάση τη διεξοδική μελέτη των ιδιοτήτων τους (χημική και ορυκτολογική σύσταση, μικροδομή, αντοχή σε θλίψη, πυκνότητα, κ.α.). Συγκεκριμένα, τα αποτελέσματα έδειξαν ότι τα παραγόμενα υαλοκεραμικά μπορούν να χρησιμοποιηθούν στον τομέα των κατασκευών ως επιστρώσεις για οδικές χρήσεις, καθώς παρουσίασαν αντοχή σε θλίψη με εύρος 113-148 MPa και υδατοαπορροφητικότητα με εύρος 0.002-0.07% πληρώντας τις προδιαγραφές ASTM C 1272 .

Συνολικά, η διατριβή καταδεικνύει ότι τα μέταλλα, το γυαλί και τα πλαστικά μέρη συνιστούν περισσότερο από το 90% κ.β των Φ/Β πλαισίων και μπορούν να επαναχρησιμοποιηθούν, να ανακτηθούν ή να ανακυκλωθούν στα πλαίσια μιας ολοκληρωμένης και βιώσιμης διαχείρισης των Φ/Β πλαισίων.

## Table of contents

Acknowledgements.....	i
Summary.....	v
Περίληψη.....	ix
Table of contents .....	xiii
List of figures.....	xvii
List of tables .....	xxi
Nomenclature.....	xxv
1 Introduction .....	1
1.1 Research topic.....	3
1.2 Objectives .....	4
1.3 Methodology .....	5
1.4 Structure of PhD thesis .....	8
1.5 Original contribution and novelty of PhD thesis .....	10
1.6 List of publications .....	11
1.7 References.....	15
2 Literature review .....	17
2.1 Context and motivation.....	19
2.1.1 Global projections for waste panels .....	20
2.2 European legislation for end-of-life P/Vs .....	22
2.3 Limitations on the management of end-of-life P/Vs.....	23
2.4 Recent advances on P/V panels recycling.....	30
2.4.1 Delamination of P/V panels .....	30
2.4.2 Recovery of high-value materials from P/V panels .....	31
2.4.3 Reuse and recycling options for glass and plastic from P/V panels.....	32
2.5 References.....	34
3 Delamination of P/V panels .....	43

3.1 Overview.....	45
3.1.1 State-of-the-art recycling processes for P/V panels .....	45
3.2 Materials and methods .....	50
3.2.1 Sample collection .....	50
3.2.2 Sample pre-treatment .....	50
3.2.3 Eliminating EVA from the laminated structure .....	52
3.3 Results and discussion .....	55
3.3.1 Evaluation of metal content in P/V panels by ICP-MS.....	55
3.3.2 Delamination through thermal, mechanical and chemical processing.....	58
3.3.3 Comparison of delamination processes.....	66
3.4 Conclusions.....	67
3.5 References.....	68
4 Silver and indium recovery from P/V panels .....	73
4.1 Overview.....	75
4.2 Materials and Methods.....	77
4.2.1 Thermal treatment and gravimetric separation.....	80
4.2.2 Mechanical crushing, sieving and thermal treatment.....	81
4.2.3 Chemical and thermal treatment.....	82
4.2.4 Microwave-assisted digestion and ICP-MS analysis .....	83
4.2.5 Leaching tests.....	83
4.2.6 Precipitation tests .....	84
4.3 Results and discussion .....	85
4.3.1 Thermal and density-based separation process .....	85
4.3.2 Mechanical crushing, sieving and thermal process .....	89
4.3.3 Chemical and thermal process.....	92
4.3.4 Efficiency of treatment routes at the pre-processing stage.....	94
4.3.5 Selective recovery of Ag and In through leaching and precipitation.....	97
4.4 Conclusions.....	99

---

4.5	References.....	100
5	Reuse of glass and plastic in cement mortars.....	107
5.1	Overview.....	109
5.1.1	Why addressing the reuse of glass and plastic from P/Vs or LCDs?.....	110
5.2	Materials and methods.....	111
5.2.1	Glass and plastic waste as raw materials.....	111
5.2.2	Synthesis of cement mortars.....	112
5.2.3	Physical, mechanical and thermal properties of cement mortars.....	113
5.2.4	Resistance of cement mortars to corrosion.....	113
5.3	Results and discussion.....	115
5.3.1	Chemical composition of raw materials.....	115
5.3.2	Physical properties of cement mortars.....	117
5.3.3	Mechanical properties of cement mortars.....	119
5.3.4	Thermal properties of cement mortars.....	124
5.3.5	Resistance of cement mortars to corrosion.....	126
5.4	Conclusions.....	129
5.5	References.....	130
6	Valorization of glass and lignite fly ash in glass-ceramics.....	137
6.1	Overview.....	139
6.1.1	Overview of waste vitrification and sintering.....	140
6.1.2	Perspectives on the production of glass-ceramics from P/V glass and fly ash .....	141
6.2	Materials and methods.....	143
6.2.1	Raw materials.....	143
6.2.2	Production of glasses.....	145
6.2.3	Production of glass-ceramics.....	146
6.3	Results and discussion.....	148
6.3.1	Mineralogical and chemical analyses of raw materials.....	148

6.3.2 Glass production conditions .....	150
6.3.3 Glass characteristics .....	151
6.3.4 Properties of glass-ceramics.....	153
6.3.5 Comparison with other studies .....	163
6.3.6 Chemical stability – Toxicity of glass-ceramics .....	167
6.4 Conclusions.....	169
6.5 References.....	170
7 Conclusions, discussion and future work.....	179
7.1 Main conclusions .....	181
7.2 Discussion .....	182
7.3 Future work.....	184
7.3.1 Recycling design for CdTe.....	184
7.3.2 Recycling design in realistic waste volume cases .....	184
7.3.3 Economic and environmental analyses .....	185
7.4 References.....	185
ANNEXES.....	187
Annex A.....	189
Annex B .....	191
Annex C .....	195
Annex D.....	197
Annex E.....	199

## List of figures

Fig. 1.1: Overview of work and thesis organization.....	8
Fig. 2.1: Solar panel defects (broken glass, hot spots-burnt cells, melted junction box) .	20
Fig. 2.2: Failure rates according to customer complaints (adapted from Weckend et al., 2016).....	21
Fig. 2.3: Overview of global waste panel projections, 2016-2050 (adapted from Weckend et al., 2016) .....	22
Fig. 2.4: Structure of (a) a crystalline silicon, (b) an amorphous/microcrystalline silicon, and (c) a CIS photovoltaic panel (ECOPROGETTI, last access 12.3.2019; Schneider, 2012; Tsai and Tsai, 2014) .....	27
Fig. 2.5: End-of-life recovery potential under regular-loss scenario to 2030 (tonnes) (adapted from Weckend et al., 2016).....	29
Fig. 3.1: Photos after (a) dismantling, i.e. removal of Al frame, junction box and cables, and (b) cutting process (including panel area, junction-box and cables) .....	51
Fig. 3.2: P/V materials after heat treatment and sieving (glass, cells, metal ribbons).....	59
Fig. 3.3: XRD of glass from c-Si panels after thermal treatment .....	60
Fig. 3.4: Double-glass structures of thermally treated thin-film panels .....	60
Fig. 3.5: Photos of mechanical crushing with a cutting mill – not efficient separation ...	61
Fig. 3.6: Photos of EVA residue after mechanical crushing with a blade rotor for (a) p-Si and m-Si panels, as well as for (b) CIS and a-Si panels within 35 and 40 sec, respectively .....	62
Fig. 3.7: Effect of toluene or/and ethyl lactate on the delamination of panel structure....	63
Fig. 4.1: Sketch of the experimental set up .....	79

Fig. 4.2: Components produced after chemical treatment and manual sorting ..... 83

Fig. 4.3: Efficiency comparison of treatment routes in terms of Ag or In pre-concentration (minimum, mean, maximum values) among (a) p-Si panel, (b) m-Si panel, and (c) CIS panel (route 1: thermal treatment at 550 or 500 °C and gravimetric separation (light product for c-Si, heavy product for CIS), route 2: mechanical crushing, sieving (particle size >8.00 mm) and thermal treatment, route 3: chemical (toluene at 25 °C for c-Si panels, ethyl lactate at 25 °C for CIS panel) and thermal treatment) ..... 96

Fig. 4.4: Leaching capacity of Ag or In from (a) p-Si cells and (b) m-Si cells at 20 or 40 °C using HNO<sub>3</sub> or H<sub>2</sub>SO<sub>4</sub>, or from (c) CIS ITO glass using H<sub>2</sub>SO<sub>4</sub> at different solid:liquid ratios. .... 98

Fig. 5.1: Schematic diagram of the experimental methodology ..... 108

Fig. 5.2: Sieve analysis of fine aggregates ..... 112

Fig. 5.3: Compressive strength of cement mortars with glass fragments or plastic pieces ..... 123

Fig. 5.4: Compressive strength of cement mortars with glass powder or plastic grindings ..... 124

Fig. 5.5: Measured positions for penetration of (a) carbon dioxide and (b) chlorides in cement mortars..... 126

Fig. 6.1: Schematic diagram of the experimental methodology ..... 138

Fig. 6.2: (a) Panel chips after shredding, (b) panel chips after thermal treatment at 550 °C, (c) waste P/V glass after sorting ..... 144

Fig. 6.3: DTA of 70G30A glass..... 147

Fig. 6.4: XRD patterns of waste P/V glass and lignite fly ash ..... 148

Fig. 6.5: Photos of (a) waste P/V glass and (b) lignite fly ash, taken with a heating microscope ..... 151

---

Fig. 6.6: XRD patterns of glasses 70G30A and 80G20A produced at 1200 °C.....	152
Fig. 6.7: XRD patterns of glass-ceramics produced at 600, 700 and 800 °C (a) 70G30A, (b) 80G20A.....	155
Fig. 6.8: SEM micrographs of 70G30A (a, c, e) and 80G20A (b, d, f) glass-ceramics produced at 600, 700 and 800 °C.....	158
Fig. 6.9: SEM micrographs and chemical composition of glass matrix and crystals for 70G30A (a, b) and 80G20A (c, d) glass-ceramics produced at 700 and 800 °C.....	159
Fig. D.1: Photos of 60% waste P/V glass and 40% lignite fly ash, taken with a heating microscope.....	197
Fig. E.1: SEM micrographs and chemical composition of glass matrix and crystals for 70G30A and 80G20A glass-ceramics produced at 600, 700 and 800 °C.....	204



---

## List of tables

Table 2.1: Average material composition of P/V panels per technology (%) (Paiano et al., 2015).....	26
Table 3.1: Literature recycling processes specified by type of treatment, panel treated, and targeted and recovered materials .....	46
Table 3.2: Experimental conditions of chemical treatment for a-Si and CIS panels.....	55
Table 3.3: Metal content in photovoltaic panels and junction boxes (mg/kg dry weight).....	56
Table 3.4: Conditions for efficient delamination of p-Si and m-Si panels through chemical processing.....	63
Table 3.5: Conditions for efficient delamination of a-Si and CIS panels through chemical processing .....	63
Table 3.6: Optimal delamination for a-Si and CIS panels using acid solutions.....	65
Table 3.7. Advantages and disadvantages of delamination technologies.....	66
Table 4.1: Content of Ag (mg/kg, dry matter) in the main components of p-Si and m-Si panels after thermal treatment .....	86
Table 4.2: Content of Ag (mg/kg, dry matter) after gravimetric separation of the thermally treated p-Si and m-Si panels.....	87
Table 4.3: Content of In (mg/kg, dry matter) in the main components of CIS panel after thermal treatment .....	87
Table 4.4: Content of In (mg/kg, dry matter) after gravimetric separation of the thermally treated CIS panel.....	88
Table 4.5: Content of Ag (mg/kg, dry matter) after mechanical crushing of p-Si and m-Si panels for 30 sec in a blade rotor and sieving.....	91

Table 4.6: Content of In (mg/kg, dry matter) after mechanical crushing of CIS panel for 45 sec in a blade rotor and sieving .....	91
Table 4.7: Delamination of p-Si and m-Si panels after chemical treatment.....	92
Table 4.8: Delamination of CIS panel after chemical treatment .....	93
Table 4.9: Content of Ag and In (mg/kg, dry matter) after chemical and thermal treatment of panels.....	94
Table 4.10: Leaching capacity and precipitation efficiency of Ag and In.....	99
Table 5.1: Mix proportions .....	113
Table 5.2: XRF analysis of raw materials (% wt) .....	116
Table 5.3: Physical properties of cement mortars. ....	118
Table 5.4: Mechanical properties of cement mortars .....	120
Table 5.5: Thermal conductivity of cement mortars .....	125
Table 5.6: Carbonation depth and chloride ion penetration depth.....	127
Table 5.7: Compressive strength and expansion in length of cement mortars after exposure to sulfate attack .....	129
Table 6.1: XRF analysis of raw materials (% wt) .....	149
Table 6.2: Comparison of TFT-LCD glass and P/V glass composition (% wt).....	150
Table 6.3 XRF analysis of glasses (% wt).....	153
Table 6.4: XRF analysis of glass-ceramics (% wt).....	154
Table 6.5: Properties of glass-ceramics .....	162
Table 6.6: Comparison of properties of glass-ceramics produced from different wastes .....	164

---

Table 6.7: TCLP results for raw materials and glass-ceramics ( $\text{mg L}^{-1}$ ).....	169
Table 7.1: The amount of material saved by recycling P/V panels by 2050 .....	183
Table A.1: Comparison of experimental results to TCLP limits ( $\text{mg/L}$ ).....	189
Table B.1: Chemical composition of the produced fractions after thermal treatment and sieving (p-Si panel).....	191
Table B.2: Chemical composition of the produced fractions after thermal treatment and sieving (m-Si panel).....	192
Table C.1: Content of Ag, In and Sn ( $\text{mg/kg}$ , dry matter) in the main components of a-Si panel.....	195
Table C.2: Content of Ag, In and Sn ( $\text{mg/kg}$ , dry matter) after mechanical crushing of a-Si panel for 45 sec in a blade rotor and sieving.....	195
Table D.1: XRF analysis of raw materials (% wt).....	197



## Nomenclature

a-Si	Amorphous silicon
ABS	Acrylonitrile-butadiene-styrene
CdTe	Cadmium telluride
CIS/CIGS	Copper indium selenide/Copper indium gallium selenide
CRT	Cathode-ray tube
EPR	Extended producer responsibility
EVA	Ethylene vinyl acetate
ITO	Indium tin oxide
LCA	Life cycle analysis
LCD	Liquid crystal display
m-Si	Monocrystalline silicon
PVC	Polyvinyl chloride
P/V panel	Photovoltaic panel
p-Si	Polycrystalline silicon
RES	Renewable energy sources
TCLP	Toxicity characteristic leaching procedure
TCO	Transparent conductive oxide
TFT-LCD	Transistor-liquid crystal display
WEEE	Waste of electrical and electronic equipment



# **1** Introduction



## 1.1 Research topic

Global energy crisis has led to a transition from fossil fuel dependence to renewable energy sources, e.g. solar. Specifically, in 1970s and early 1980s the solar energy gained the international attention in the global energy security context, with heightened production and installation of P/V systems thereafter. Despite the benefits of such a promising technology, the technical lifetime of P/V panels is approximately 25 years, demanding sound waste management solutions (Ashfaq et al., 2017).

The EU has established a regulatory framework, Directive 2012/19/EU, classifying P/V waste as large equipment with a long life cycle. The Directive involves extended producer responsibility (EPR), as well as specific targets for recovery and recycling that should be reached from 15<sup>th</sup> August 2018 (minimum of 85% and 80% of panels' average weight, Annex V). At present, non-profit associations, such as PV cycle, produce an industry-wide take back and recycling system for panel waste (PV CYCLE, 2013). On behalf of industries, Deutsche Solar designed a recycling process for crystalline silicon (c-Si) panels; First Solar developed a recycling process for cadmium telluride (CdTe) panels, while the recycling of the other P/V technologies remains in a pilot scale (Berger et al., 2010).

In this view, recycling strategies for P/V panels have been studied to a considerable extent over the past years. However, these studies neither have been entirely commercialized nor did they anticipate high recovery rate of materials. This is attributed to the technical limitations and cost, as well as to the temporary-limited waste. P/V waste still originates from defects during production, damages during transportation /installation, failures after start-up operations, technical or physical failures caused by severe environmental conditions, and unexpected external factors (e.g. natural disasters) (Tao and Yu, 2015).

It is then expected that research and development of recycling processes for P/V waste is needed to improve the level of technology performance, producing higher value materials from recycling.

## 1.2 Objectives

The main goal of this thesis is to study the recycling potential of photovoltaic panels and especially the recovery of valuable components (i.e. precious or critical metals), as well as bulk materials (i.e. glass or plastic) contained in them. Various treatment technologies, among which recovery, reuse and valorization options of waste panels were developed and evaluated towards a “closed cycle” economy in order to contribute to the reduction of their future disposal and to urge the production of secondary resources. To achieve this goal, four of the most commonly used photovoltaic panel technologies were studied, namely (i) polycrystalline silicon, (ii) monocrystalline silicon, (iii) copper indium selenide, and (iv) amorphous silicon panels.

The following objectives were defined:

- (1) Delamination of P/V panels using different treatment technologies and separation of the major structural components.
- (2) Recovery of silver or indium from c-Si and thin-film panels, respectively, by evaluating the effect of different treatment routes, such as thermal, mechanical, physical and chemical processes and combinations of them, on the mass flow of these high-value metals. Determination of the pre-concentration yield and respective losses at the pre-processing stage, as well as determination of the most suitable conditions for the achievement of maximum leaching capacity and precipitation efficiency at the end-processing stage (purification of metals).
- (3) Reuse of glass or plastic after mechanical treatment for the production of cement mortars, and specifically study on the effect of the type of waste (glass or plastic), the amount of waste (%) as replacement of fine aggregates or cement, and the particle size of waste on the physical, mechanical and thermal properties of the produced cement mortars. Investigation of their resistance to

various corrosive environments and assessment of potential toxicity aiming at their use as construction materials for specific applications.

- (4) Co-valorization of wastes produced from the renewable energy sector, i.e. P/V glass, and the conventional energy sector, i.e. lignite fly ash for the production of glass-ceramics for uses in the construction sector. Investigation of the effect of the mixing ratio, the melting and sintering temperatures on the characteristics of the produced glass-ceramics, i.e. chemical composition, mineralogy, microstructure, physical and mechanical properties, chemical stability and potential toxicity, and evaluation of their use as heavy vehicular paving bricks in the construction sector.

### **1.3 Methodology**

Extensive experimental work was carried out, while theoretical data were obtained from photovoltaic manufacturing or previous research on the management of P/V waste.

#### Literature review

Based on a comprehensive literature review, the structure and composition (%) of P/V panels were derived. A corresponding experimental campaign was designed and the laboratory conditions were established.

#### Experimental investigations (Objectives 1-4)

- The panels were subjected to different treatment processes in order to decompose, cut, swell, or dissolve the organic layer(s), eliminating the laminated panel structure. Delamination was conditioned under different treatment approaches, namely (a) thermal treatment in an electrical furnace, (b) mechanical crushing in a blade rotor and (c) chemical treatment using organic solvents or acid solutions.
- The monitoring of the content of indium and silver during the treatment steps of panels was carried out using inductively coupled mass spectrometry (ICP-MS). The

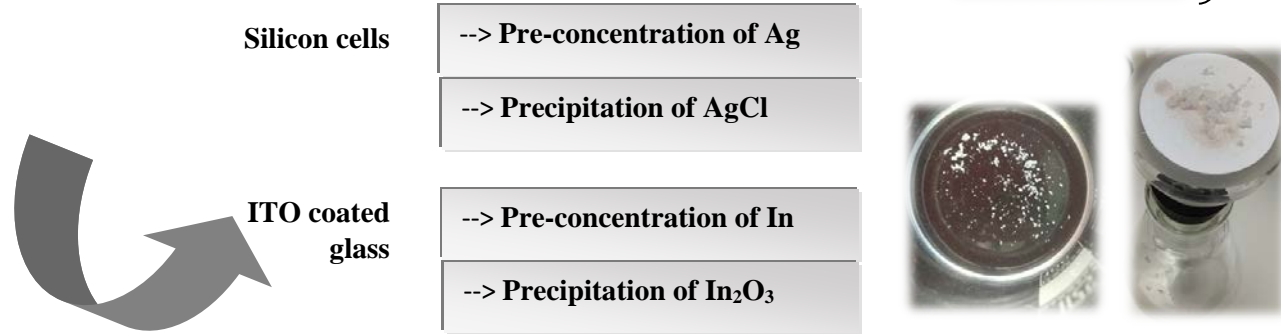
pre-concentration yield and losses were based on the metal content (mg/kg) in the treated mass (%) as compared to the initial content and mass (untreated) used. Prior to ICP-MS analyses, a microwave-assisted digestion was performed. The leaching tests were conducted using inorganic acids and the precipitates were obtained using HCl or NH<sub>4</sub>OH.

- Production of cement mortars from glass or plastic was investigated in terms of waste characteristics (type, amount, particle size, resource replaced) under specific curing conditions. Chemical composition of the raw materials was determined using energy dispersive X-ray fluorescence (ED-XRF); bulk density was measured based on Archimedes' principle and compressive strength using a universal testing machine (MTS model). The resistance of mortars to corrosion was based on existing methods used in the scientific literature. Due to the low rate of material changes caused by the aging mechanisms in service, accelerated conditioning was conducted in order to determine the long-term effects and resistance of the produced cement mortars to corrosive environments.
- Glass-ceramics were prepared under various conditions. Chemical composition, mineralogy and microstructure were identified using ED-XRF, X-ray diffraction (XRD) and scanning electron microscopy (SEM). Also, open porosity, bulk density, water absorption, compressive strength, microhardness, chemical stability and potential toxicity (TCLP) were determined. The produced glass-ceramics were compared to the limits prescribed in ASTM C 1272, standard specifications for heavy vehicular paving brick. A schematic diagram of the experimental methodology is given below.

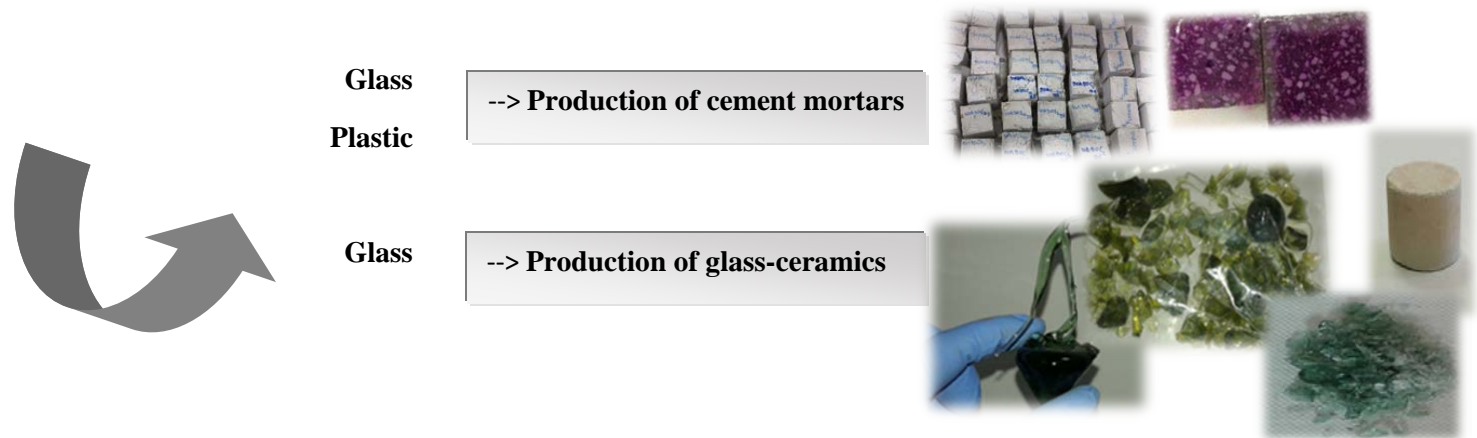
**Delamination**



**Recovery of metals**



**Reuse/valorization**



## 1.4 Structure of PhD thesis

The thesis comprises seven chapters; the content of the main Chapters 3-6 is summarized in **Fig. 1.1**.

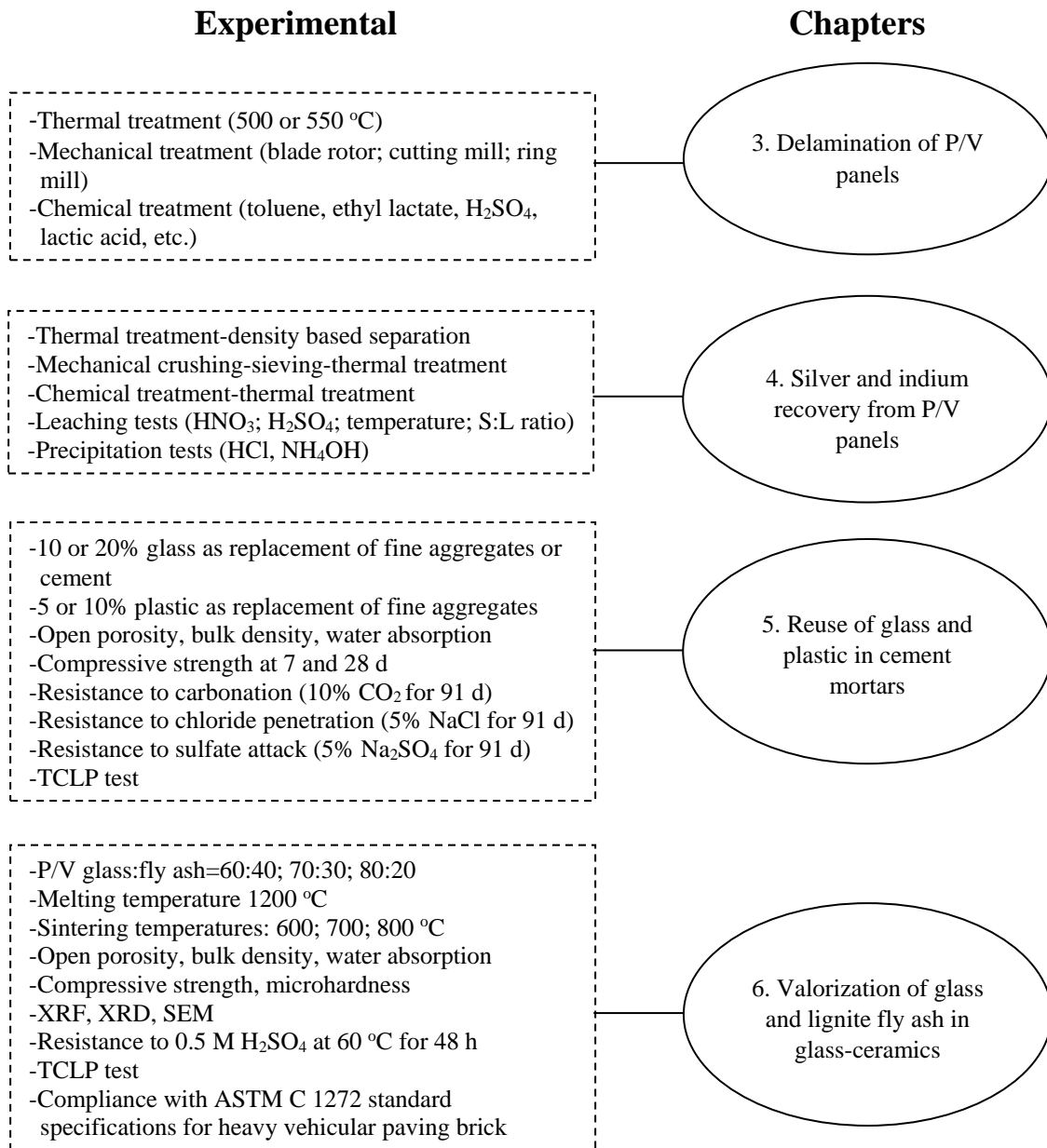


Fig. 1.1: Overview of work and thesis organization

Chapter 2 introduces the specific problems related to the management of waste P/V panels and the possibilities for reuse, recovery and recycling of various P/V components based on a comprehensive literature review.

In chapter 3, delamination of panel structure was investigated in the laboratory through thermal, mechanical and chemical treatment processes resulting in changes in the adhesive thermoplastic, ethylene vinyl acetate (EVA), among which decomposition, swelling or cutting. **Annex A** and **B** complement the discussions of this chapter.

In chapter 4, three treatment routes including various steps were investigated in order to evaluate the mass flow of silver or indium, their pre-concentration yield and losses through the various stages. Selective recovery of these metals was studied in order to achieve high efficiency through leaching and precipitation tests. **Annex C** complements the discussions of this chapter.

In chapter 5, the experiments involve the production of cement mortars using glass or plastic. Two sets of cement mortars were prepared containing 10 and 20% glass as replacement of fine aggregates or cement. Glass from waste computer monitors was also investigated for comparison reasons. In addition, cement mortars with 5 and 10% of plastic as replacement of fine aggregates were produced. The properties of cement mortars were thoroughly evaluated and discussed to determine if they are comparable or superior to those of reference mortars.

Chapter 6 provides extensive examinations on the production of glass-ceramics from P/V glass and lignite fly ash. Three different mixing ratios were investigated, namely 60% glass:40% fly ash, 70% glass:30% fly ash and 80% glass:20% fly ash at a melting temperature of 1200 °C and sintering temperatures of 600, 700 and 800 °C. The objective was to produce construction materials that present characteristics of glass-ceramics and can be used as brick pavers in the construction sector. **Annex D** and **E** complement the discussions of this chapter.

Chapter 7 summarizes the research findings obtained in the previous chapters (2-6) and outlines significant considerations and recommendations for future work.

## 1.5 Original contribution and novelty of PhD thesis

Many studies have focused on life cycle assessment (LCA) and techno-economic analysis of photovoltaic systems in order to evaluate the economic sustainability and environmental impact, however, very few researchers have developed recycling technologies, most of whom focused on one or two approaches, without critically comparing different recycling processes. This thesis makes a significant contribution to this matter, providing thorough investigation of P/Vs treatment both at pre-processing stage and end-processing stage. The innovative aspects of this thesis are briefly summarized here and more complemented in chapters 3-7:

- (a) Referring to delamination and separation of major components contained in P/V panels, this study provides a combination of processes, namely a thermal process, and a subsequent gravimetric separation of glass either from cells or from glass with semiconductors instead of sieving, manual sorting or vibrating table that have been proposed in literature or for industrial use. The application of this combination of processes has not been investigated before, whereas it achieves efficient recovery of intact and reusable components.
- (b) For chemical treatment, among other reagents the use of i) ethyl lactate, or ii) lactic acid was studied for eliminating the laminated structure of panels. These reagents are less toxic and have not so far been used for the treatment of waste panels, as compared to toluene,  $\text{H}_2\text{SO}_4$  or  $\text{HNO}_3$  that are commonly studied in literature.
- (c) The major novelty of this study is the pre-concentration of precious and critical metals (silver, indium) under different treatment routes and their selective recovery through leaching and precipitation. These metals present a supply risk and high economic importance, making their secondary production very promising. Detailed studies focused on the pre-concentration and recovery of silver or indium from waste panels are still lacking. Motivated by this gap, this study investigates the fate of these metals during various treatment stages and suggests the pre-concentration of silver or indium as a critical step to achieve high recovery rates, mitigating the losses.

- (d) This study adds further value by addressing the use of glass or plastic from waste panels for the production of cement mortars. It provides knowledge on the mechanical, physical and thermal properties, as well as the behavior of the produced cement mortars in three different corrosive environments. Such investigations have not so far been considered for P/V waste and may contribute to closing the loop of certain P/V materials.
- (e) For the first time, this study investigates an approach for the valorization of specific wastes generated from the energy sector, and the production of glass-ceramics. Dense and homogeneous glass-ceramics were produced from P/V glass and lignite fly ash. The proposed methodology is considered energy efficient (melting at 1200 °C, sintering at 800 °C) compared to existing approaches. The properties of the produced glass-ceramics allow their use as heavy vehicular paving bricks.

Finally, this thesis highlights the strengths and weaknesses referring to the management of P/V panels and ascertains opportunities and limitations deriving from technological aspects through the pre-processing and end-processing stages. The proposed experimental methodologies might be very useful for further research on this important yet complex topic.

## 1.6 List of publications

### Publications in Scientific Journals

- *Directly related to the PhD Thesis*

**Savvilotidou V.**, Antoniou A., Gidarakos E. (2017). Toxicity assessment and feasible recycling process for amorphous silicon and CIS waste photovoltaic panels. *Waste Management*, 59, 394-402.

**Savvilotidou V.**, Kritikaki A., Stratakis A., Komnitsas K., Gidarakos E. (2019). Energy efficient production of glass-ceramics using photovoltaic (P/V) glass and lignite fly ash. *Waste Management*, 90, 46-58.

**Savvilotidou V.**, Gidakos E. WEEE glass and plastic as raw materials for the production of cement mortars. *Journal of Hazardous Materials*. **Manuscript under review**.

○ *Related to the PhD Thesis area of research*

**Savvilotidou V.**, Hahladakis J.N., Gidakos E. (2014). Determination of toxic metals in discarded Liquid Crystal Displays (LCDs). *Resources, Conservation and Recycling*, 92, 108-115.

**Savvilotidou V.**, Hahladakis J.N., Gidakos E. (2015). Leaching capacity of metals-metalloids and recovery of valuable materials from waste LCDs. *Waste Management*, 45, 314-324.

Batinic B., Vaccari M., **Savvilotidou V.**, Kousaiti A., Gidakos E., Marinkovic T., Fiore, S. (2018). Applied WEEE pre-treatment methods: Opportunities to maximizing the recovery of critical metals. *Global Nest Journal*, 20(4), 706-711. <https://doi.org/10.30955/gnj.002589>.

**Savvilotidou V.**, Kousaiti A., Batinic B., Vaccari M., Kastanaki E., Karagianni K., Gidakos E. (2019). Evaluation and comparison of pre-treatment techniques for recovering indium from discarded liquid crystal displays. *Waste Management*, 87, 51-61.

Sikander A., **Savvilotidou V.**, Jia X., Nicomel N. (2019). The presence of rare earth elements and critical metals in waste electric and electronic equipment: Challenges for Recovery. *Global Nest Journal*, 20(4), 773-777. <https://doi.org/10.30955/gnj.002582>.

Kousaiti A., Hahladakis J.N., **Savvilotidou V.**, Pivnenko K., Tyrovola K., Xekoukoulotakis N., Astrup T.F., Gidakos E. Assessment of tetrabromobisphenol-A (TBBPA) content in post-consumer plastic waste (PCPW) recovered from WEEE. *Journal of Hazardous Materials*. **Manuscript under review**.

**Publications in International Conferences**

**Savvilotidou V.**, Hahladakis J.N., Gidarakos E. (2014). Determination of toxic metals in waste LCDs with emphasis in arsenic. *4th International Conference on Industrial and Hazardous Waste Management, CRETE 2014*, Chania, Crete, Greece, 2 – 5 September.

**Savvilotidou V.**, Gidarakos E. (2015). Recovery strategies of critical Indium from Waste LCDs. *International workshop on Waste Electrical and Electronic Equipment*, University of Salerno, Italy, 12 – 13 November 2015.

**Savvilotidou V.**, Gidarakos E. (2016). Development of valorization options for lignite fly ash. *5th International Conference on Industrial and Hazardous Waste Management, CRETE 2016*, Chania, Crete, Greece, 27 – 30 September.

Antoniou A., **Savvilotidou V.**, Gidarakos E. (2016). Chemical treatment strategies: Dealing with 2nd generation waste photovoltaic panels. *5th International Conference on Industrial and Hazardous Waste Management, CRETE 2016*, Chania, Crete, Greece, 27 – 30 September.

Lakiotaki A., **Savvilotidou V.**, Gidarakos E. (2016). Treatment processes in 1st generation waste photovoltaic panels. *5th International Conference on Industrial and Hazardous Waste Management, CRETE 2016*, Chania, Crete, Greece, 27 – 30 September.

**Savvilotidou V.**, Hahladakis J.N., Gidarakos E. (2016). Indium applications in WEEE: Possible recovery paths. *5th International Conference on Industrial and Hazardous Waste Management, CRETE 2016*, Chania, Crete, Greece, 27 – 30 September.

Batinic B., Vaccari M., **Savvilotidou V.**, Kousaiti A., Gidarakos E., Marinkovic T. (2017). Applied WEEE pre-treatment methods: Opportunities to maximizing the recovery of critical metals. *15th International Conference on Environmental Science and Technology, CEST 2017*, Rhodes, Greece, 31 August – 2 September.

Sikander A., **Savvilotidou V.**, Jia X., Nicomel N. (2017). The Presence of REM and CM in WEEE: Challenges for Recovery. *15th International Conference on Environmental Science and Technology, CEST 2017*, Rhodes, Greece, 31 August – 2 September.

**Savvilotidou V.**, Gidaracos E. (2018). Potentials and challenges of recycled material from photovoltaic panels in cement mortars. *6th International Conference on Industrial and Hazardous Waste Management, CRETE 2018*, Chania, Crete, Greece, 4 – 7 September.

**Savvilotidou V.**, Gidaracos E. (2018). Sustainable Management and valorization of fly ash from lignite-fired power plants in Greece. *6th International Conference on Industrial and Hazardous Waste Management, CRETE 2018*, Chania, Crete, Greece, 4 – 7 September.

**Savvilotidou V.**, Kritikaki A., Stratakis A., Komnitsas K., Gidaracos E. (2018). Production of glass-ceramics from photovoltaic glass and lignite fly ash. *6th International Conference on Industrial and Hazardous Waste Management, CRETE 2018*, Chania, Crete, Greece, 4 – 7 September.

**Savvilotidou V.**, Kousaiti A., Batinic B., Vaccari M., Kastanaki E., Karagianni K., Gidaracos E. (2018). Towards a circular economy of indium in liquid crystal displays: A focus on pre-treatment. *6th International Conference on Industrial and Hazardous Waste Management, CRETE 2018*, Chania, Crete, Greece, 4 – 7 September.

Kousaiti A., **Savvilotidou V.**, Pivnenko K., Tyrovola K., Xekoukoulotakis, Gidaracos E. (2018). Possibilities of brominated flame retardants extraction from polymers of e-waste. *6th International Conference on Industrial and Hazardous Waste Management, CRETE 2018*, Chania, Crete, Greece, 4 – 7 September.

Kousaiti A., Pivnenko K., **Savvilotidou V.**, Astrup T.F., Gidaracos E. (2018). Hexabromocyclododecane, tetrabromobisphenol-A and inorganic additives in polymers

from electric and electronic equipment. *6th International Conference on Industrial and Hazardous Waste Management, CRETE 2018*, Chania, Crete, Greece, 4 – 7 September.

## 1.7 References

- Ashfaq, H., Hussain, I., Giri, A., 2017. Comparative analysis of old, recycled, and new PV modules. *J. King Saud Univ. Eng. Sci.* Manuscript In Press. doi:10.1016/j.jksues.2014.08.004
- Berger, W., Simon, F. G., Weimann, K., Alsema, E. A., 2010. A novel approach for the recycling of thin film photovoltaic modules. *Resour. Conserv. Recycl.* 54(10), 711-718.
- Directive 2012/19/EU of the European Parliament and of the Council of 4 July 2012 on waste electrical and electronic equipment (WEEE), recast. *Off. J. Eur. Union* L197/38.
- PV CYCLE, European Association for the recovery of photovoltaic modules, Annual Report 2013.
- Tao, J., Yu, S., 2015. Review on feasible recycling pathways and technologies of solar photovoltaic modules. *Sol. Energy Mater. Sol. Cells*, 141, 108-124.



## **2 Literature review**



## 2.1 Context and motivation

Global warming has created a push to renewable and low-carbon energy (D'Adamo et al., 2017). Renewable energy sources, i.e. solar, hydro, wind, biomass etc., are getting increasing interest and will supply more and more energy needs on a global scale in order to address the negative environmental impacts of increased fossil fuels exploration and to contribute fundamentally to sustainability (Lee et al., 2013). Solar photovoltaics represent a renewable energy technology, enabling conversion of solar radiation into current electricity (Bio Intelligence Service, 2011).

The P/V industry started in the mid-1980s and early 1990s. Unlike other industries, P/V technology has a particularly long lifetime (between 20 and 25 years) from its production to its withdrawal (McDonald and Pearce, 2010). During the last decade, both European and international electricity markets have witnessed a formidable growth in the photovoltaic sector (Sika et al., 2018). In 2016, the installed solar P/V capacity totaled around 300 GW compared to 5 GW in 2005, following a rapid growth in producing and installing P/V systems (Savvilotidou et al., 2017).

Although the photovoltaic industry is a very dynamic industry and solar energy is practically inexhaustible, there are long-term issues associated with pollution (e.g. release of cadmium or lead; Fthenakis, 2000), yet uncertain, which may indirectly affect humans and the environment in the case of P/Vs disposal. Apart from pollution, a disposal scenario eliminates benefits from recycling and selling P/V materials, i.e. conventional resources such as glass, Al, plastic, as well as valuable metals (Ag, In, Ga, Te, etc.), whereas the latter have been recently determined to be at near-critical supply risk (Dias et al., 2016a). Instead, sound recycling processes can play a key role in protecting the environment by reducing the risks pertinent to hazardous substances such as toxic metals, poly/brominated flame retardants, etc. In addition, recycling is indispensable to avoid the loss of valuable materials and to reduce the demand for new material production, contributing to closing the loop of product life-cycle.

In order to comply with the recovery and recycling targets established by the EU regulations, several treatment and material recovery processes have been proposed for

the waste panels. However, most published approaches focus on specific target components, manifesting the complexity of recycling and the limitations of a “total-recycling” process that covers all recycling steps by combining methods, from panel delamination to material recovery. The recycling processes are complex and not unique as a result of the continuous variations of the panel composition, even with the same P/V technology. Variations in the cost and availability of the raw materials may also affect the development of P/V panels in future.

### 2.1.1 Global projections for waste panels

The life cycle of a typical P/V panel can be divided into three phases: *manufacturing*, *production*, *end life*. Today, most of waste come from defects during *production* that shorten the lifetime of P/V panels, such as decomposition of the ethylene vinyl acetate (EVA) resin due to sun light, demolition of structural materials by outside effects, e.g. broken glass or laminated defects of the cell, manufacturing failures, etc. (Kang et al., 2012) (**Fig. 2.1**). As shown in **Fig. 2.2** the main causes of P/V panel failure are due to optical defect, power loss and defects of the junction boxes and cables reaching cumulatively a rate of 59%.



Fig. 2.1: Solar panel defects (broken glass, hot spots-burnt cells, melted junction box)

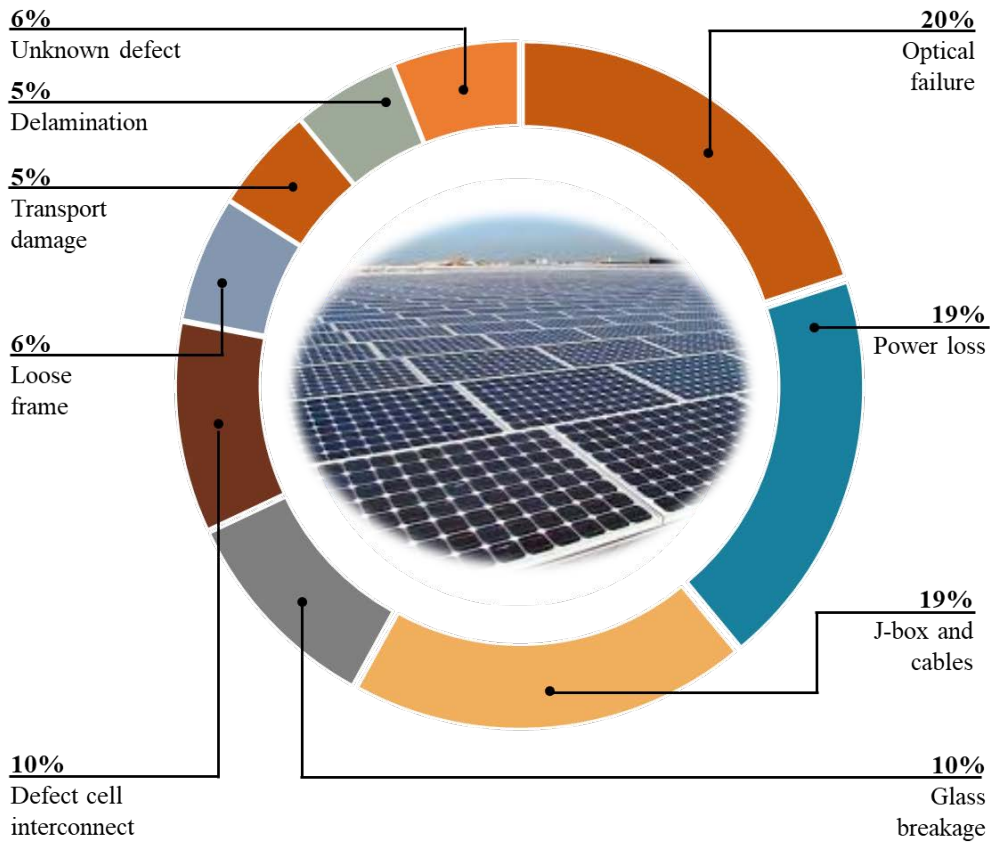


Fig. 2.2: Failure rates according to customer complaints (adapted from Weckend et al., 2016)

With the rapid expansion of P/V industry over the years, it is anticipated that a large amount of discarded P/V panels will be produced, with a forecaste that in 2035 end-of-life panels will account for 1.0 million tonnes (Dias et al., 2016a), whereas they are expected to reach 5.5–6.0 million tonnes by the 2050s (Dias et al., 2018).

Relative estimations published by the International Energy Agency Photovoltaic Power Systems Programme (IEA PVPS) and the International Renewable Energy Agency (IRENA) in 2016 indicate that the waste panels will amount to 1.7–8.0 million tonnes cumulatively by 2030 and to 60-78 million tonnes cumulatively by 2050. The global projections for future P/V waste production until 2050 are shown in **Fig. 2.3** based on two scenarios:

- Regular-loss: Assuming a 30-year lifetime for P/V panels, with no early attrition.

- Early-loss: Taking account of “infant”, “mid-life” and “wear-out” failures before the 30-year lifespan. **Fig. 2.3** indicates a drastic increase of waste panels which is estimated higher for the early-loss scenario.

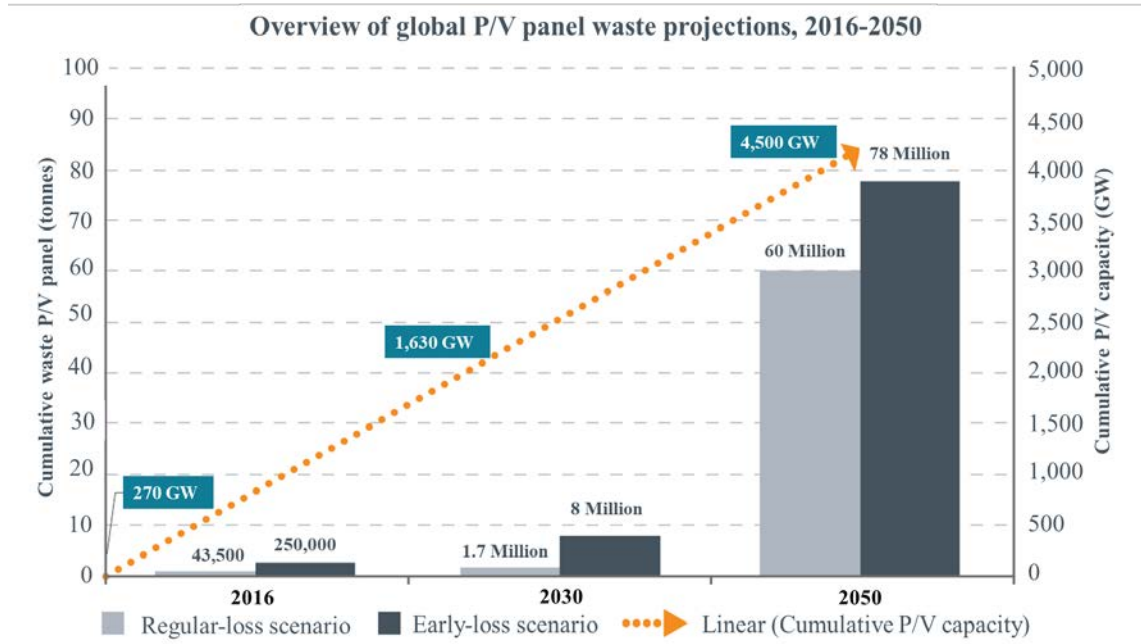


Fig. 2.3: Overview of global waste panel projections, 2016-2050 (adapted from Weckend et al., 2016)

Predictions on volumes of future waste stream, composition analyses and investigations of management technologies for P/V waste are relevant topics in the current literature, supporting the development of a circular economy (D’Adamo et al., 2017). A potential conversion of waste to resource is a strategy that enables multiple benefits, from prevention of improper waste disposal to production of high-value commercial and marketable products, making the economy more resource-efficient and circular. Waste management of P/Vs has therefore been a major concern in recent years, considering that unusable P/V panels can become a valuable source of raw materials for the future.

## 2.2 European legislation for end-of-life P/Vs

In Europe, a drive towards proper management of end-of-life P/V panels has taken form in the Directive **2012/19/EU** on Waste Electrical and Electronic Equipment (WEEE) of

the European Parliament and the Council, according to which decommissioned P/V panels are considered as domestic or professional types of WEEE. The Directive introduces the extended producer responsibility (EPR). Based on this principle, manufacturers and producers are responsible for the management and life cycle impact of their products, by expanding recycling practices and designing easy-to recycle products (eco-design).

The scope of this Directive is to promote the use of secondary raw materials in order to foster more efficient use of natural resources associated with P/V production, by establishing percentages and deadlines for recycling and recovery (up to 80 and 85%, respectively) based on weight per panel from 15<sup>th</sup> August 2018. It is then assumed that since glass recovery already makes up approximately 75-86% of the total P/Vs' weight, this legislation does not guarantee the recovery of precious or critical metals contained in them.

In addition to the regulatory scheme, it is pronounced that analogous recycling technologies must be developed to comply with the increasing requirements of waste panels. Particularly, sufficient attention has to be paid to recycling processes in terms of their technical feasibility, environmental impact and economic profitability in order to satisfy the legislation, regulating the management of P/V panels at reasonable costs.

### **2.3 Limitations on the management of end-of-life P/Vs**

The P/V sector is characterized by a rapid evolution of technologies. The broad categories of P/V technology are classified as 1st, 2nd and 3rd generation based on the type of P/V cell. P/V cell is the fundamental building block of the P/V technology, consisting of semiconductor materials, such as silicon, that exhibit the 'photovoltaic effect' (generating electricity when the light of the sun on falls on its surface).

One of the main limitations to develop universal management of waste panels is the large variety of technologies, i.e. crystalline silicon (c-Si) panels, such as polycrystalline silicon (p-Si) and monocrystalline silicon (m-Si) which represent the 1st generation of photovoltaic technology, as well as copper indium selenide (CIS),

amorphous silicon (a-Si) and cadmium telluride (CdTe) (2nd generation, also known as thin-film panels), and many others considering the three generations of P/V technology (Tao and Yu, 2015). However, regardless of the particular technology, it is important to note that toxic substances to the environment and human health, such as Cd and Pb, are commonly contained in P/V panels.

The crystalline silicon (p-Si and m-Si) panels currently represent the dominant panel technology (85–90% of the P/V market) according to the International Energy Agency. Alternative P/V technologies including a-Si, CdTe and CIS thin-film cells have been developed to mitigate the manufacturing costs. However, the crystalline silicon panels still comprise the technology that guarantees the highest return on investment. Main limitation to the extensive application of thin film technologies is the use of toxic elements (e.g. Cd in CdTe) and/or precious-critical metals (e.g. In, Ga in CIS). Today, ~51% of the P/V market share is covered by p-Si, ~41% by m-Si, ~2% by CIS and 0.7% by a-Si panels (Padoan et al., 2019).

The above mentioned and most commonly used P/V technologies are briefly described, as follows. Novel and/or emerging P/V technologies are not analyzed in this study because they remain in development and demonstration stages.

---

### *Polycrystalline silicon (p-Si) panels*

Polycrystalline, also known as multi-crystalline silicon solar panels, are produced by melted silicon that is poured into a square mould. This silicon is then slowly cooled and sliced into square wafers creating the polycrystalline shape. Silicon is manufactured in such a way that it consists of a number of small crystals, forming grains. The manufacturing process is simpler and cheaper than that of m-Si panels (Leroy, 1986).

### *Monocrystalline silicon (m-Si) panels*

Monocrystalline, also known as single crystalline silicon solar panels, unlike p-Si solar panels, are based on cylindrical silicon ingots, which are cut into wafers. Silicon is manufactured in such a way that it forms a continuous single crystal without grain boundaries. The monocrystalline silicon cells have a typical black or iridescent blue color and long lifespan of 25-year warranty. They provide high efficiency of light conversion attributed to the purity of silicon (typical ~15%; recent developments improved efficiencies up to 22-24%). The manufacturing process of Si crystals is rather complicated. The main disadvantages of the monocrystalline silicon panels are the high manufacturing cost and the mechanical vulnerability (brittle) (Leroy, 1986).

### *Copper indium selenide (CIS) panels*

CIS semiconductor has become a popular new material for solar cells, as it appears the highest efficiency (up to 20%) among the thin-film P/V technologies. The CIS cells are manufactured by thin-film deposition on a substrate, and they are flexible (unlike the silicon cells). Generally, thin-film technology uses solar cells based on very thin layers of P/V materials deposited over an inexpensive material (glass, stainless steel, plastic). Also, the energy payback time for CIS panels is significantly shorter than that of c-Si panels (de Wild-Scholten, 2013).

### *Amorphous silicon (a-Si) panels*

Recent developments have decreased the thickness of silicon used in crystalline cells in order to reduce cost. Thin-film photovoltaic panels, and especially amorphous silicon panels are produced by depositing silicon film onto a substrate material, usually glass. The manufacturing process is based on the formation of non-crystalline silicon using silicon vapour which is quickly cooled. Despite the lower cost thanks to less silicon, they

exhibit lower efficiency, namely ~6%. One of the main advantages of this technology is that amorphous silicon may be deposited on various substrates, which are flexible and come in different shapes, enabling their use in many applications (Chopra et al., 2004).

Recycling technologies for c-Si panels (p-Si and m-Si) and thin-film panels (CdTe and CIS) differ due to differences in the panel structures and the metals contained in them. One important difference is that delamination of thin-film panels aims to recover separately the cover glass and the substrate glass with semiconductor layer (e.g. indium), whereas for c-Si modules the aim is to separate glass from Si cells.

**Table 2.1** and **Fig. 2.4** present the chemical composition and structure of P/V panels, respectively, for the most commonly used technologies. It is seen that despite differences among panel technologies, a typical P/V panel is a great source of glass and other less relevant-mass components, such as metals or plastic present in junction box and connecting cables (Paiano, 2015; Tammaro et al., 2015).

**Table 2.1: Average material composition of P/V panels per technology (%) (Paiano et al., 2015)**

Proportion in %	c-Si	CIGS	a-Si
Glass	74.16	84	86
Aluminum	10.30	12	0.035
Polymers (e.g. EVA)	6.55	3	
Backing film (Tedlar)	3.60		
Adhesive (e.g. silicone)-potting compound-hot melt glue	1.16		0.02
Polyol/MDI (Methylene diphenyl diisocyanate)			12
Copper	0.57	0.8	0.9
Silver	0.004-0.006*		
Tin	0.12		0.043
Zinc	0.12	0.12	
Silicon	3.35		0.0064
Lead	0.06	0.05	
Cadmium		0.0005	
Tellurium			
Indium		0.02	0.5
Selenium		0.03	
Gallium		0.01	
Germanium			0.5

\* 0.07–0.16% according to Peeters et al. (2017)

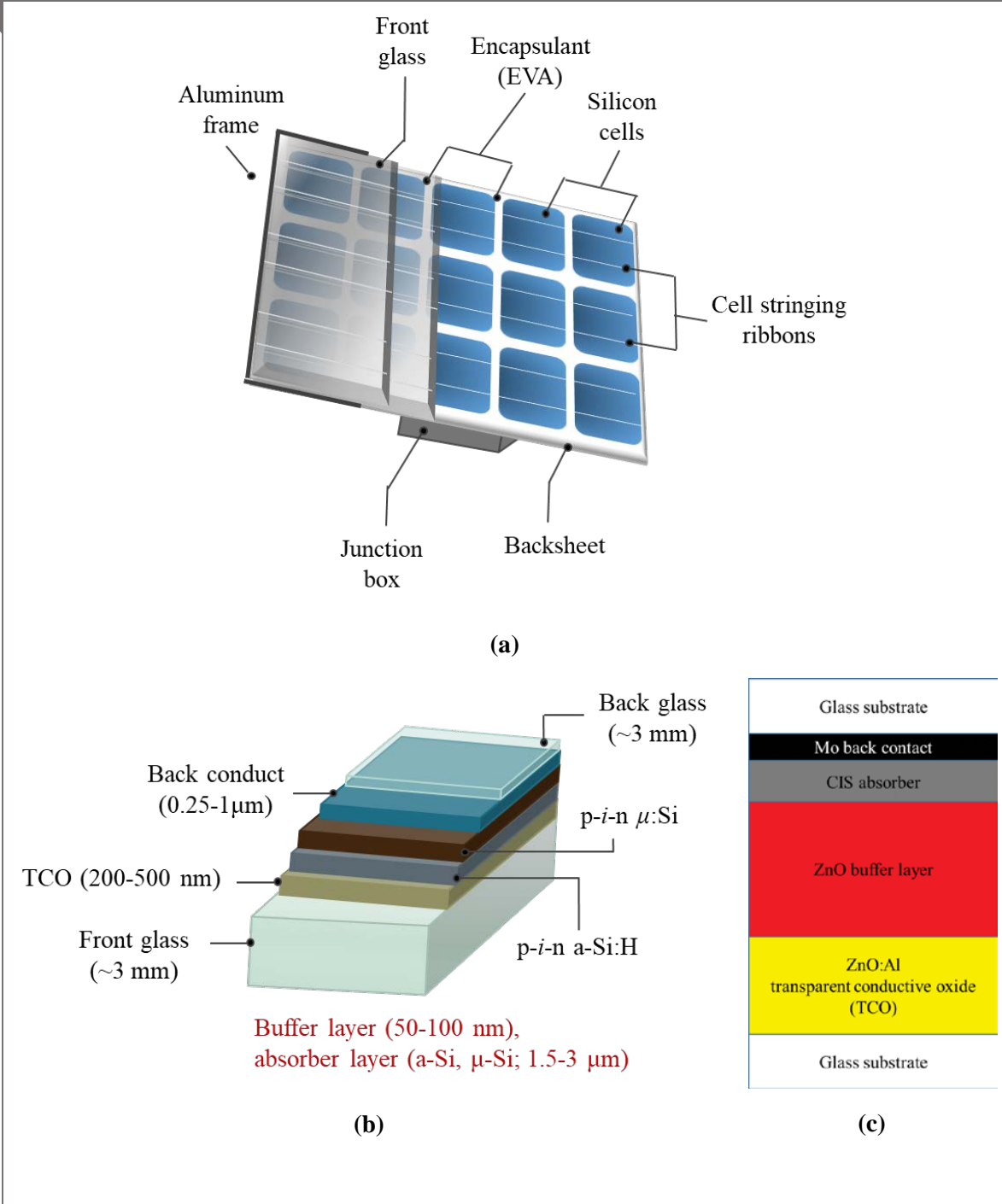


Fig. 2.4: Structure of (a) a crystalline silicon, (b) an amorphous/microcrystalline silicon, and (c) a CIS photovoltaic panel (ECOPROGETTI, last access 12.3.2019; Schneider, 2012; Tsai and Tsai, 2014)

Apart from the diversity based on the panel technology, as well as the intrinsic and/or temporal heterogeneity of the panels, also the feasibility of waste P/V management is indirectly influenced by the cost and availability of the primary resources used in the production of the P/V panels (Padoan et al., 2019). Specifically, the price and scarcity of the raw materials are key drivers for the P/V market.

From a value standpoint, silver is by far the most expensive component per unit of mass of a crystalline panel (m-Si or p-Si), followed by copper, silicon, aluminum, glass and polymer. It is classified as a precious metal and according to literature sources its supply risk for P/V panels may come from limitations on expanding production capacity in the short to medium term, and/or political risk associated with the main supplying countries. In such a context, although silver is not classified in the very risky materials list, its long-term supply is uncertain, considering the demand for emerging P/V technologies, and especially for c-Si panels (Li and Adachi, 2019). Another important resource contained in thin-film panels, and especially in CIS technology, is indium. Although its primary extraction is difficult and costly, its production currently has been increased due to its use in several optoelectronic applications. It is contained in the European critical raw material (CRM) list, as it is mainly produced as a by-product from zinc-sulfide ore mineral sphalerite and is a scarce and rare metal (Grandell and Höök, 2015). China has been the main global supplier of primary indium over the years, representing more than 50% of the world's primary indium production.

Considering the regular loss scenario for waste panel production described in section 2.3 (lifetime of 30 years; cumulative waste volume of 1.7 million tonnes for 2030) and 65-70% efficiency of recycling processes, it is expected that the potential cumulative raw materials recovered (**Fig. 2.5**) will amount to USD 450 million by 2030 (Weckend et al., 2016). This is equivalent to the current raw material value needed to produce 60 million new panels or 18 GW of power-generation capacity. It is also seen that 90 tonnes of silver are estimated to be recovered by 2030, thus we can assume that the limitations of potential recycling that are associated with the scarcity of raw materials may become opportunities to recover valuable materials and reduce their supply risk.

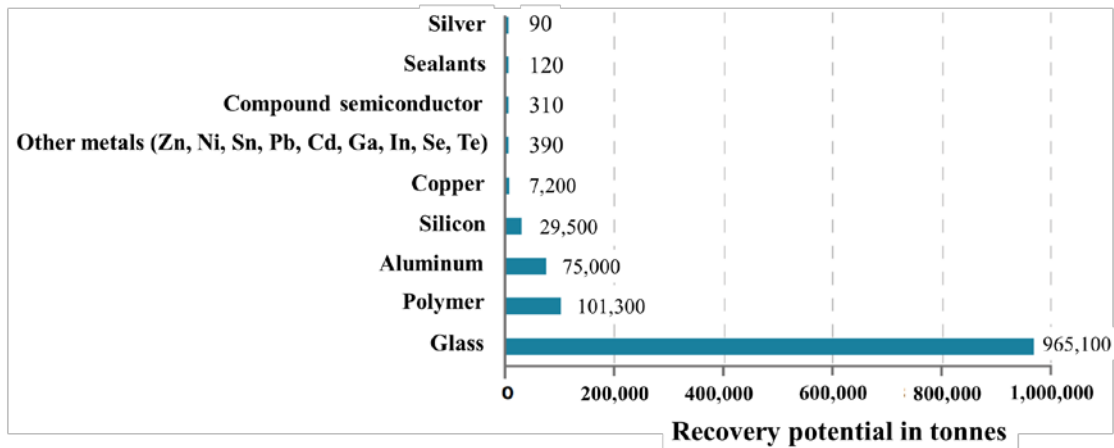


Fig. 2.5: End-of-life recovery potential under regular-loss scenario to 2030 (tonnes) (adapted from Weckend et al., 2016)

The estimated benefits from secondary raw materials motivate the research and development of new recycling techniques, as the industry may significantly benefit by reducing the reliance on primary raw materials and energy.

Since currently only moderate P/V waste quantities exist on the global waste market, there are not sufficient quantities or economic incentives to create dedicated P/V panel recycling plants. On behalf of industries, waste management solutions still are under development, with available operations for specific photovoltaic technologies (i.e. c-Si P/V panels from Deutsche Solar and CdTe from First Solar, as well as take back and recycling system from PV Cycle). Different recycling options have been researched and the produced knowledge may contribute to the development of specialized recycling plants, once the waste streams are sufficiently large for profitable operation. The future recycling processes will need to keep abreast of ongoing P/V cell and panel innovations to obtain the best possible results at acceptable costs. Specifically, such processes will have to include recovery of major components (i.e. glass, aluminum, copper) and other potentially scarce or valuable materials (e.g. silver, indium) at sufficient quality and purity for sale on the world market. Also, they might equally need to handle modest quantities of hazardous and toxic materials (e.g. cadmium).

## 2.4 Recent advances on P/V panels recycling

Based on an extensive literature overview, it can be assumed that the treatment of P/V panels is comprised of two fundamental steps. The first step concerns the delamination of the resistant panel structure, resulting in separation of the major components, i.e. glass, cells, etc., whereas the second step refers to extraction of precious or critical metals from cells, and recycling of pure precious or critical metals.

### 2.4.1 Delamination of P/V panels

The delamination of panel structure is feasible when ethylene vinyl acetate resin (EVA) is removed (i.e. through decomposition, dissolution, comminution, etc.) (Goris et al., 2015). Thermal processes in inert and oxidative conditions (Agroui et al., 2012; De-wen et al., 2004; Frisson et al., 2000; Rimez et al., 2008; Tammaro et al., 2015), as well as chemical processes using organic solvents and ultrasound irradiation (Kim and Lee, 2012; Doi et al., 2001, Savvilotidou et al., 2017) have been used, resulting in EVA's decomposition, and swelling/dissolution, respectively. In addition, physical operations or combinations of treatment technologies, e.g. chemical and thermal processes, have also been investigated (Kang et al., 2012; Granata et al., 2014). Liquid nitrogen treatment to embrittle EVA layer, chemical treatment with the assistance of microorganisms or biodegradation of EVA by inoculating the EVA layers with *Aspergillus niger* (*A. niger*) have been proposed as alternative technologies (Nieland et al., 2012; Sonia and Dasan, 2013).

Although several studies in the scientific literature have focused on the delamination of P/V panels, these remain single investigations, referring to a specific P/V technology or one treatment process, without providing a thorough investigation of conditions and/or detailed comparison of different processes among the panel technologies, while they only consider separation of major components (bulk material recovery) and not the recovery of high-value materials, i.e. metals.

#### ***2.4.2 Recovery of high-value materials from P/V panels***

The recovery of valuable metals from P/V cells has not been extensively studied in literature. Dias et al. (2016a), Dias et al. (2016b) and Berger et al. (2010) explored selective extraction of Ag, Te and In from c-Si, CdTe and CIS panels. These metals present high economic importance and a risk of supply due to political and economic conditions, low recycling rates and increasing demand (European Commission, 2017). For instance, a high demand of Ag occurred over the past ten years, with pressing predictions for a risk of supply in the future (2075) (Dias et al., 2016b; Grandell and Thorenz, 2014; Klugmann-Radzienska and Ostrowski, 2010). The economic benefits for society as a whole by the future recycling of P/V panels still are uncertain (Cucchiella et al., 2015), however, the research community estimates that secondary materials require less processing than that needed for the production of primary raw materials (Doi et al., 2001; Goe and Gaustad, 2014).

Considering that critical and precious metals, found in panels, are worth recycling only after enrichment in separated fractions, it is important to optimize the treatment process (during both pre-processing, i.e. delamination, and end-processing, i.e. purification), especially achieve Ag or In pre-concentration (a fraction enriched in In or Ag) at the pre-processing stage, and also mitigate potential losses, resulting in highly pure In and Ag after selective separation and recovery. Today, most studies either focus on the pre-processing stage aiming only at successful delamination of the panel structure and bulk material recovery, or investigate the end-processing stage (i.e. In/Ag extraction and purification) without evaluating the mass flow of Ag or In during the previous treatment stages. Further investigation is therefore required in order to fill the gaps on both bulk material recycling (glass, Al, etc.) and valuable material recycling, also known as high-value recycling which does not only ensure the recovery of a particular mass percentage of the total P/V panel, but also accounts for minor fractions (In, Ga, Te, Ag, etc.) and determines the life-cycle impact of P/Vs.

### ***2.4.3 Reuse and recycling options for glass and plastic from P/V panels***

Glass and plastic are two of the main components of P/V panels, and both of them can be fully recycled. The glass industry is considered as a large industry; in 2007, the global glass production was 115 million tonnes that increased to 190 million tonnes according to Glass global group report of 2016. The European glass industry contributes to 30-32 million tonnes per year (Wintour, 2015; Glass Alliance Europe, last access 20.11.2018), since glass finds application in several industrial sectors, such as electronics and especially P/Vs (Ma et al., 2016). Its disposal is considered unsustainable, as it is not biodegradable in the environment (Islam et al., 2017). In addition, glass from WEEE is a source of potentially hazardous substances, e.g. cadmium in glass of thin-film P/Vs, arsenic and/or antimony in liquid crystal displays (LCDs) glass, etc., that can affect the environment (Savvilotidou et al., 2014; Savvilotidou et al., 2015; Savvilotidou et al., 2017).

The fast growth of plastic represents another serious impact on the environment (Buekens and Yang, 2014; da Silva et al., 2014; Liguori et al., 2014; Tokiwa et al., 2009). The global annual plastic production totaled more than 300 million tonnes in 2016. Europe is producing around 25.8 million tonnes annually, 8% of which are produced for electrical and electronic equipment (European Commission, last access 20.11.2018). The increasing consumption of plastic (average annual increase of 9%) results in a significant volume of landfilled plastics, most of which are non-biodegradable (da Silva et al., 2014; Liguori et al., 2014; Tokiwa et al., 2009). It must be noted that plastic accounts for 20-30 wt% of the average WEEE composition (Ma et al., 2016; Schlummer et al., 2006) and consist of hazardous substances, namely brominated flame retardants, chlorine, cadmium and antimony in order to exhibit fire resistance (Schlummer et al., 2006).

The pressing need for a systemic transition to a circular economy has pushed for action plans and measures, as held by the European Commission (EC) package (European Commission, 2016a), in priority sectors such as plastics, glass, metals and other waste materials to address sustainability issues (European Commission, 2016b). In

this context, innovative research for reusing or recycling waste materials, namely glass or plastic that are also used in P/Vs, for construction purposes can indicate potential future applications in the recycling and construction sector.

Glass and plastic from waste panels can be considered as materials that enable a circular manner of management; for instance, they can be used as replacement of conventional resources (i.e. fine aggregates or cement). Several benefits are expected by such operations (waste volume reduction, immobilization of hazardous substances, mitigation of natural resources consumption, etc.) (Islam et al., 2017), while technical advantages are also involved. Specifically, glass enhances the cement hydration process by causing a pozzolanic reaction (Islam et al., 2017; Ling and Poon, 2011; Skripkiūnas et al., 2018; Lin et al., 2009), while plastic addition assists thermal insulating properties (Iucolano et al., 2013; Ruiz-Herrero et al., 2016). However, today very few studies have focused on the reuse of P/V materials for construction purposes (Skripkiūnas et al., 2018; Hao et al., 2015; Hao et al., 2013).

Apart from cement mortar production, a promising approach is definitely the production of glass-ceramics from industrial wastes. Lin et al. (2012) explored the P/V glass as raw material for the production of glass-ceramics. The properties of glass-ceramics derived from wastes allow their use as construction and architectural components (Erol et al., 2007; Leroy et al., 2001), exhibiting a wide range of advantageous properties, such as high compressive and bending strength, relatively high hardness, chemical stability, excellent corrosion and abrasion resistance (Aloisi et al., 2006; Baowei et al., 2013; Barbieri et al., 2000; Leroy et al., 2001; Wu et al., 2015; Yoon et al., 2013). Vitrification and sintering of different wastes have been investigated mainly in order to minimize the large waste volumes produced by several industrial sectors (i.e. lignite fly ash, sludge, etc.). Of primary interest is though the co-valorization of wastes and waste glass for the production of glass-ceramics, as described by several earlier studies (Bernardo and Maschio, 2011, Lu et al., 2014, Tian et al., 2011, Vu et al., 2011, Yoon et al., 2013, Zhu et al., 2016, Karamanov et al., 2007, Kourti and Cheesman, 2010, Fan and Li, 2013, Fan and Li, 2014, Kim et al., 2016 and Lin, 2007). This is because

glass enables efficient vitrification at a lower melting point within less time, thus improving the economics of the process (Karamanov et al., 2007; Kourti and Cheesman, 2010). In this context, the glass derived from P/V panels is a new waste source that has not been thoroughly investigated for the production of glass-ceramics.

The above short review is complemented in the following chapters to provide a thorough state-of-the art summary of existing knowledge regarding the recycling techniques that have been developed in waste P/V panels. Based on this review, several techniques were investigated and compared, including four different approaches, namely (a) the delamination of P/V panels, (b) the recovery of silver or indium either from cells or from substrate glass, (c) the reuse of glass or plastic in cement mortars and (d) the valorization of glass for the production of glass-ceramics. The P/V technologies used in the experimental work of this thesis are a polycrystalline silicon panel, a monocrystalline silicon panel, an amorphous silicon panel and a copper indium selenide panel.

## 2.5 References

- Aloisi, M., Karamanov, A., Taglieri, G., Ferrante, F., Pelino, M., 2006. Sintered glass ceramic composites from vitrified municipal solid waste bottom ashes. *J. Hazard. Mater.* 137 (1), 138-143.
- Baowei, L., Leibo, D., Xuefeng, Z., Xiaolin, J., 2013. Structure and performance of glass-ceramics obtained by Bayan Obo tailing and fly ash. *J. Non-Cryst. Solids* 380, 103-108.
- Barbieri, L., Corradi, A., Lancellotti, I., 2000. Bulk and sintered glass-ceramics by recycling municipal incinerator bottom ash. *J. Eur. Ceram. Soc.* 20 (10), 1637-1643.
- Berger, W., Simon, F.G., Weimann, K., Alsema, E. A., 2010. A novel approach for the recycling of thin film photovoltaic modules. *Resour. Conserv. Recycl.* 54(10), 711-718.
- Bernardo, E., Maschio R.D., 2011. Glass-ceramics from vitrified sewage sludge pyrolysis residues and recycled glasses. *Waste Manage.* 31 (11), 2245-2252.

- Bio Intelligence Service, 2011. Study on photovoltaic panels supplementing the impact assessment for a recast of the WEEE directive, Final Report.
- Buekens, A., Yang, J., 2014. Recycling of WEEE plastics: a review. *J. Mater. Cycles Waste Manage.* 16(3), 415-434.
- Chopra, K.L., Paulson, P.D., Dutta, V., 2004. Thin-film solar cells: an overview. *Prog. Photovoltaics* 12(2-3), 69-92.
- Cucchiella, F., Rosa, P., 2015. End-of-Life of used photovoltaic modules: A financial analysis. *Renew. Sust. Energ. Rev.* 47, 552-561.
- D'Adamo, I., Miliacca, M., Rosa, P., 2017. Economic feasibility for recycling of waste crystalline silicon photovoltaic modules. *Int. J. Photoenergy* 2017. Article ID 4184676.
- da Silva, A.M., de Brito, J., Veiga, R., 2014. Incorporation of fine plastic aggregates in rendering mortars. *Constr. Build. Mater.* 71, 226-236.
- De-wen, Z., Born, M., Wambachz, K., 2004. Pyrolysis of EVA and its application in recycling of photovoltaic modules. *J. Environ. Sci.* 16(6), 889-893.
- de Wild-Scholten, M.M., 2013. Energy payback time and carbon footprint of commercial photovoltaic systems. *Sol. Energy Mater. Sol. Cells* 119, 296-305.
- Dias, P.R., Benevit, M.G., Veit, H.M., 2016a. Photovoltaic solar panels of crystalline silicon: characterization and separation. *Waste Manage. Res.* 34(3), 235-245.
- Dias, P., Javimczik, S., Benevit, M., Veit, H., Bernardes, A.M., 2016b. Recycling WEEE: extraction and concentration of silver from waste crystalline silicon photovoltaic modules. *Waste Manage.* 57, 220-225.
- Dias, P., Schmidt, L., Gomes, L.B., Bettanin, A., Veit, H., Bernardes, A.M., 2018. Recycling waste crystalline silicon photovoltaic modules by electrostatic separation. *J. Sustain. Metallurgy* 4(2) 176-186. <https://doi.org/10.1007/s40831-018-0173-5>.
- Doi, T., Tsuda, I., Unagida, H., Murata, A., Sakuta, K., Kurokawa, K., 2001. Experimental study on PV module recycling with organic solvent method. *Sol. Energy Mater. Sol. Cells* 67, 397-403.

- Erol, M., Küçükbayrak, S., Ersoy-Meriçboyu, A., 2007. Production of glass-ceramics obtained from industrial wastes by means of controlled nucleation and crystallization. *Chem. Eng. J.* 132 (1-3), 335-343.
- European Commission. A European strategy for plastics in a circular economy. <http://ec.europa.eu/environment/circular-economy/pdf/plastics-strategy-brochure.pdf> (last access 20.11.2018).
- European Commission, 2017. Communication on the list of Critical Raw Materials for the EU. <<http://eur-lex.europa.eu/legal-content/EN/ALL/?uri=COM:2017:0490:FIN>> (last access 26.09.2018).
- European Commission, 2016a. Circular economy package. Four legislative proposals on waste. <http://www.europarl.europa.eu/EPRS/EPRS-Briefing-573936-Circular-economy-package-FINAL.pdf>.
- European Commission, 2016b. Closing the Loop. New Circular Economy Package. [http://www.europarl.europa.eu/RegData/etudes/BRIE/2016/573899/EPRS\\_BRI\(2016\)573899\\_EN.pdf](http://www.europarl.europa.eu/RegData/etudes/BRIE/2016/573899/EPRS_BRI(2016)573899_EN.pdf).
- Fan, C.S., Li, K. C., 2014. Glass-ceramics produced from thin-film transistor liquid-crystal display waste glass and blast oxygen furnace slag. *Ceram. Int.* 40 (5), 7117-7123.
- Fan, C.S., Li, K.C., 2013. Production of insulating glass ceramics from thin film transistor-liquid crystal display (TFT-LCD) waste glass and calcium fluoride sludge. *J. Clean. Prod.* 57, 335-341.
- Frisson, L., Lieten, K., Bruton, T., Declercq, K., Szlufcik, J., De Moor, H., Goris, M., Benali, A., Aceves, O., 2000. Recent improvements in industrial PV module recycling. 16th European Photovoltaic Solar Energy Conference, 1-5 May, Glasgow, UK.
- Fthenakis, V.M., 2000. End-of-life management and recycling of PV modules. *Energ. Policy* 28(14), 1051-1058.
- Glass Alliance Europe. <https://www.glassallianceeurope.eu/en/industries> (last access 20.11.2018).

- Glass global group. 2016. Glass Market Report and Study. <https://plants.glassglobal.com/admin/downloads/glassglobal%20Glass%20Market%20Study.pdf>.
- Goe, M., Gaustad, G., 2014. Strengthening the case for recycling photovoltaics: An energy payback analysis. *Appl. Energy* 120, 41-48.
- Goris, M.J.A.A., Rosca, V., Geerligs, L.J., de Gier, B., 2015. Production of recyclable crystalline Si PV modules. 31st European photovoltaic solar energy conference and exhibition, 14-18 September.
- Grandell, L., Höök, M., 2015. Assessing rare metal availability challenges for solar energy technologies. *Sustainability* 7(9), 11818-11837.
- Granata, G., Pagnanelli, F., Moscardini, E., Havlik, T., Toro, L., 2014. Recycling of photovoltaic panels by physical operations. *Sol. Energy Mater. Sol. Cells* 123, 239-248.
- Grandell, L., Thorenz, A., 2014. Silver supply risk analysis for the solar sector. *Renew. Energy* 69, 157-165.
- Hao, H., Lin, K.L., Wang, D., Chao, S.J., Shiu, H.S., Cheng, T.W., Hwang, C.L., 2015. Elucidating characteristics of geopolymer with solar panel waste glass. *Environ. Eng. Manage. J.* 14(1), 79-87.
- Hao, H., Lin, K.L., Wang, D., Chao, S.J., Shiu, H.S., Cheng, T.W., Hwang, C.L., 2013. Utilization of solar panel waste glass for metakaolinite-based geopolymer synthesis. *Environ. Prog. Sustain. Energy* 32(3), 797-803.
- Islam, G.S., Rahman, M.H., Kazi, N., 2017. Waste glass powder as partial replacement of cement for sustainable concrete practice. *Int. J. Sustain. Built Environ.* 6(1), 37-44.
- Kang, S., Yoo, S., Lee, J., Boo, B., Ryu, H., 2012. Experimental investigations for recycling of silicon and glass from waste photovoltaic modules. *Renew. Energy* 47, 152-159.
- Karamanov, A., Aloisi, M., Pelino, M., 2007. Vitrification of copper flotation waste. *J. Hazard. Mater.* 140 (1-2), 333-339.

- Kim, Y., Lee, J., 2012. Dissolution of ethylene vinyl acetate in crystalline silicon PV modules using ultrasonic irradiation and organic solvent. *Sol. Energy Mater. Sol. Cells* 98, 317-322.
- Klugmann-Radziemska, E., Ostrowski, P., 2010. Chemical treatment of crystalline silicon solar cells as a method of recovering pure silicon from photovoltaic modules. *Renew. Energy* 35(8), 1751-1759.
- Kourti, I., Cheeseman, C.R., 2010. Properties and microstructure of lightweight aggregate produced from lignite coal fly ash and recycled glass. *Resour. Conserv. Recy.* 54 (11), 769-775.
- Lee, C.H., Hung, C.E., Tsai, S.L., Popuri, S.R., Liao, C.H., 2013. Resource recovery of scrap silicon solar battery cell. *Waste Manage. Res.* 31(5), 518-524.
- Leroy, B., 1986. Silicon wafers for integrated circuit process. *Revue de physique appliquée*, 21(8), 467-488.
- Leroy, C., Ferro, M.C., Monteiro, R.C.C., Fernandes, M.H.V., 2001. Production of glass-ceramics from coal ashes. *J. Eur. Ceram. Soc.* 21 (2), 195-202.
- Li, W., Adachi, T. 2019. Evaluation of long-term silver supply shortage for c-Si PV under different technological scenarios. *Nat. Resour. Model.* 32(1), e12176. <https://doi.org/10.1111/nrm.12176>.
- Lin, K.L., 2007. Use of thin film transistor liquid crystal display (TFT-LCD) waste glass in the production of ceramic tiles. *J. Hazard. Mater.* 148 (1-2), 91-97.
- Lin, K.L., Chu, T.C., Cheng, C.J., Lee, C.H., Chang, T.C., Wang, K.S., 2012. Recycling solar panel waste glass sintered as glass-ceramics. *Environ. Prog. Sustain. Energy* 31(4), 612-618.
- Lin, K.L., Huang, W.J., Shie, J.L., Lee, T.C., Wang, K.S., Lee, C.H., 2009. The utilization of thin film transistor liquid crystal display waste glass as a pozzolanic material. *J. Hazard. Mater.* 163(2-3), 916-921.
- Ling, T.C., Poon, C.S., 2011. Utilization of recycled glass derived from cathode ray tube glass as fine aggregate in cement mortar. *J. Hazard. Mater.* 192(2), 451-456.

- Lu, J., Lu, Z., Peng, C., Li, X., Jiang, H., 2014. Influence of particle size on sinterability, crystallization kinetics and flexural strength of wollastonite glass-ceramics from waste glass and fly ash. *Mater. Chem. Phys.* 148 (1-2), 449-456.
- Iucolano, F., Liguori, B., Caputo, D., Colangelo, F., Cioffi, R., 2013. Recycled plastic aggregate in mortars composition: Effect on physical and mechanical properties. *Mater. Design* 52, 916-922.
- Padoan, F.C.S.M., Altimari, P., Pagnanelli, F., 2019. Recycling of end of life photovoltaic panels: A chemical prospective on process development. *Sol. Energy* 177, 746-761.
- Peeters, J. R., Altamirano, D., Dewulf, W., Duflou, J.R. 2017. Forecasting the composition of emerging waste streams with sensitivity analysis: a case study for photovoltaic (PV) panels in Flanders. *Resour. Conserv. Recycl.* 120, 14-26.
- Rimez, B., Rahier, H., Van Assche, G., Artoos, T., Biesemans, M., Van Mele, B., 2008. The thermal degradation of poly (vinyl acetate) and poly (ethylene-co-vinyl acetate), Part I: Experimental study of the degradation mechanism. *Polym. Degrad. Stab.* 93(4), 800-810.
- Ruiz-Herrero, J.L., Nieto, D.V., López-Gil, A., Arranz, A., Fernández, A., Lorenzana, A., Merino, S., De Saja, J.A., Rodríguez-Pérez, M.Á., 2016. Mechanical and thermal performance of concrete and mortar cellular materials containing plastic waste. *Constr. Build. Mater.* 104, 298-310.
- Savvilotidou, V., Antoniou, A., Gidarakos, E., 2017. Toxicity assessment and feasible recycling process for amorphous silicon and CIS waste photovoltaic panels. *Waste Manage.* 59, 394-402.
- Savvilotidou, V., Hahladakis, J.N., Gidarakos, E., 2015. Leaching capacity of metals–metalloids and recovery of valuable materials from waste LCDs. *Waste Manage.* 45, 314-324.
- Savvilotidou, V., Hahladakis, J.N., Gidarakos, E., 2014. Determination of toxic metals in discarded Liquid Crystal Displays (LCDs). *Resour. Conserv. Recycl.* 92, 108-115.

- Savvilotidou, V., Kousaiti, A., Batinic, B., Vaccari, M., Kastanaki, E., Karagianni, K., Gidarakos, E., 2019. Evaluation and comparison of pre-treatment techniques for recovering indium from discarded liquid crystal displays. *Waste Manage.* 87, 51-61.
- Sica, D., Malandrino, O., Supino, S., Testa, M., Lucchetti, M.C., 2018. Management of end-of-life photovoltaic panels as a step towards a circular economy. *Renew. Sust. Energ. Rev.* 82, 2934-2945.
- Skripiūnas, G., Vasarevičius, S., Danila, V., 2018. Immobilization of copper indium selenide solar module waste in concrete constructions. *Cement Concrete Comp.* 85, 174-182.
- Sonia, A., Dasan, K.P., 2013. Celluloses microfibers (CMF)/poly (ethylene-co-vinyl acetate) (EVA) composites for food packaging applications: A study based on barrier and biodegradation behavior. *J. Food Eng.* 118(1), 78-89.
- Tammaro, M., Rimauro, J., Fiandra, V., Salluzzo, A., 2015. Thermal treatment of waste photovoltaic module for recovery and recycling: Experimental assessment of the presence of metals in the gas emissions and in the ashes. *Renew. Energy* 81, 103-112.
- Tao, J., Yu, S., 2015. Review on feasible recycling pathways and technologies of solar photovoltaic modules. *Sol. Energy Mater. Sol. Cells* 141, 108-124.
- Tian, Y., Zuo, W., Chen, D., 2011. Crystallization evolution, microstructure and properties of sewage sludge-based glass-ceramics prepared by microwave heating. *J. Hazard. Mater.* 196, 370-379.
- Tsai, C.Y., Tsai, C.Y. 2014. Development of amorphous/microcrystalline silicon tandem thin-film solar modules with low output voltage, high energy yield, low light-induced degradation, and high damp-heat reliability. *J. Nanomater.* 2014. Article ID 86174.
- Vu, D.H., Wang, K.S., Nam, B.X., Bac, B.H., Chu, T.C., 2011. Preparation of humidity-controlling porous ceramics from volcanic ash and waste glass. *Ceram. Int.* 37 (7), 2845-2853.

- Weckend, S., Wade, A., Heath, G. 2016. End-of-life management: Solar photovoltaic panels (No. NREL/BK-6A20-66178). National Renewable Energy Lab.(NREL), Golden, CO (United States).
- Wintour, N., 2015. The glass industry: Recent trends and changes in working conditions and employment relations. International Labour Organization. ISBN: 9789221301172; 9789221301189 (web pdf).
- Wu, D., Tian, Y., Wen, X., Zuo, W., Liu, H., Lee, D.J., 2015. Studies on the use of microwave for enhanced properties of glass-ceramics produced from sewage sludge pyrolysis residues (SSPR). *J. Taiwan Inst. Chem. Eng.* 48, 81-86.
- Yoon, S.D., Lee, J.U., Lee, J.H., Yun, Y.H., Yoon, W.J, 2013. Characterization of Wollastonite Glass-ceramics Made from Waste Glass and Coal Fly ash. *J. Mater. Sci. Technol.* 29 (2), 149-153.
- Zhu, M., Ji, R., Li, Z., Wang, H., Liu, L., Zhang, Z., 2016. Preparation of glass ceramic foams for thermal insulation applications from coal fly ash and waste glass. *Constr. Build. Mater.* 112, 398-405.



### **3 Delamination of P/V panels**

Reuse, recycling and recovery technologies must be available in order to address future waste volumes from decommissioned P/V panels. This chapter investigates the first key step of P/V waste processing, and especially the delamination of four different types of P/V waste as a result of the removal of ethylene vinyl acetate (EVA)<sup>1</sup> through decomposition, grinding or swelling. The four P/V panels used are a polycrystalline silicon (p-Si), a monocrystalline silicon (m-Si), a copper indium selenide (CIS) and an amorphous silicon (a-Si), whereas the first two represent the main types of 1st generation P/V panels and the latter two belong to the group of thin-film or otherwise to the 2nd generation P/V panels. Prior to experimental attempts, an analysis of trends in past and current recycling technologies for P/Vs was performed to provide valuable insights on potential developments for panel delamination. Then, in view of the technical characteristics and chemical composition of panels, as well as the mentioned literature overview, various experimental processes were designed and operated, namely thermal, mechanical and chemical treatment. The major differences observed in terms of panel delamination or EVA behavior were associated with the panel technology, demanding a critical selection of operational conditions for each panel. In addition, the selection of an optimal process must be associated with the next steps of recycling and the ultimate goal or else the “targeted” components. For instance, the focus may be a simple separation of the bulk materials and recycling of major components, such as glass (which leaves significant mass of materials mixed or unrecovered) or a high-value recycling including the recovery of precious or critical metals.

---

<sup>1</sup> Ethylene vinyl acetate (EVA) polymer is used as an adhesive and encapsulant in photovoltaic panels.



## 3.1 Overview

### *3.1.1 State-of-the-art recycling processes for P/V panels*

Recycling processes for P/V panels can be divided into those that remove the encapsulant (EVA) from the laminated structure (i.e. delamination and separation of the major structural components) and those that recover the metals from the Si cells or thin-film layers (i.e. metal extraction and purification), after pre-disassembly (removal of the external frames and junction boxes from the panels) (TaO and Yu, 2015).

The primary treatment or else eliminating the encapsulant (usually EVA) from the laminated structure is one of the most difficult and important stages of the recycling process. Several technologies have been under development, showing that utilization of thermal, mechanical, chemical or combination process can cause delamination (Corcelli et al., 2018; Granata et al., 2014; Klugmann-Radziemska, 2013). The combination processes involve thermal and mechanical treatment, thermal and chemical treatment, etc. (TaO and Yu, 2015). Then, metals can be recovered from the obtained separated materials by additional processes, usually chemical treatment such as etching, precipitation, electrowinning and other. **Table 3.1** presents various recycling processes carried out in earlier studies in order to cause delamination and to recover valuable materials from P/V panels of 1st and 2nd generation.

**Table 3.1: Literature recycling processes specified by type of treatment, panel treated, and targeted and recovered materials**

<b>Treatment</b>	<b>Panel type</b>	<b>Targeted and recovered materials</b>	<b>Reference</b>
Cutting, chemical treatment using organic solvents	c-Si	Cells; glass	Doi et al., 2001
Chemical treatment using organic solvents, ultrasonic irradiation	c-Si	EVA dissolution; cells	Kim and Lee, 2012
Recovery of glass using organic solvents, thermal decomposition, etching	c-Si	Glass; Si	Kang et al., 2012
Mechanical crushing and milling, wet mechanical attrition; Combined thermal and mechanical methods; Flotation (pre-concentration) and purification of semiconductors	CIS; CdTe	Glass; semiconductors	Berger et al., 2010
Crushing using blade rotor, thermal treatment; Crushing using blade rotor and hammer crushing; Sieving	c-Si; a-Si; CdTe	Glass	Granata et al., 2014
Pyrolysis in a conveyer belt furnace; Pyrolysis in a fluidized bed reactor; Metal etching	c-Si	Glass; Si	Frisson et al., 2000
Electrothermal process	c-Si (p-Si, m-Si)	Backsheet layer; glass; cell	Doni and Dughiero, 2012
Two-step heating process for PV module thermal delamination; Acid etching to remove tin-lead coating from copper and metal impurities from the silicon wafer	c-Si	Glass; Si; Cu	Wang et al., 2012
Removal of the aluminum coating by etching; Etching for removing Ag coatings, AR coatings and n-p junctions	c-Si	Si	Klugmann-Radziemska and Ostrowski, 2010
Crushing, leaching and self-heating trough ultrasound,	c-Si	Ag; Al; Si	Yi et al., 2014

---

smelting			
Mechanical crushing and sieving, leaching, precipitation; Mechanical crushing and sieving, pyrolysis	c-Si	AgCl	Dias et al., 2016
Mechanical milling, electrostatic separation, thermal process, leaching	c-Si	Ag; Cu; Si; glass; polymers	Dias et al., 2018
Leaching, electrolytic refining process	c-Si	Si; Cu; Ag; Al; Pb	Jung et al., 2016
Thermal treatment, chemical treatment	c-Si	Si	Shin et al., 2017
Mechanical crushing and sieving, thermal oxidation	CIGS	Se oxide	Gustafsson et al., 2014
Mechanical crushing and sieving, thermal oxidation, high-temperature chlorination process	CIS	Ga; In	Gustafsson et al., 2015
Thermal process, leaching, electrowinning, etching, waste handling	c-Si	Glass; Ag; Pb; Cu; Sn	Huang et al., 2017
Triple crushing, thermal treatment and chemical treatment	p-Si; m-Si; a-Si; CdTe	Glass	Pagnanelli et al., 2017
Crushing through a physical disaggregation, pyrolysis and vacuum decomposition process	GaAs	Plastic; glass; Ga	Zhang and Xu, 2016

---

The technologies that combined two or more methods make up the majority of the total. Also, it must be noted that many studies focused on specific target components, whereas other addressed the total process without concentrating on specific components or materials. Some description of the mechanisms involved in the main delamination processes is given in the following boxes.

### *Thermal processes*

Thermal or else combustion techniques have been used for the delamination of panel structures. The result of such processes is the recovery of separated materials, i.e. glass and cells or glass and substrate glass with semiconductor layers, and electrode ribbons. The above expected materials can be recovered without breakage, thus achieving high-value recovered materials for recycling purposes (e.g. recycling of cells into intact wafer if no micro-cracks present), which can be one of the major benefits of this approach. On the other hand, a thermal approach requires treatment of large mass in order to cover the cost and improve efficiency of the entire process. Also, it is important to mitigate the energy consumption by recycling the heat generated from the combustion of organics to the furnace. Finally, countermeasures must be planned for the fluorine gas produced when the back cover, i.e. fluoride-based backsheet, is burned (Komoto et al., 2018).

### *Mechanical processes*

Cutting of EVA (encapsulation layer), scribing of non-glass layers (e.g. backsheet to get removed from the laminated structure), scribing of glass, and crushing/grinding technologies have been examined as a mechanical processing step. The first two technologies can recover glass without breakage, while the other technologies can recover broken glass and cells or glass and substrate glass with semiconductor that present micro-cracks. To get recovered materials of a higher quality, as well as to achieve higher recovery rates, mechanical technologies must be basically combined with some post-treatment steps, such as a chemical process, to separate organics, cells and other metals from the remaining mixture. A mechanical process may consume less energy as compared to a thermal process; however, combinations that involve thermal processing consume even more energy, and combinations with chemical processes may require long processing time, as well as further treatment of the produced waste chemicals (Komoto et al., 2018).

### *Chemical processes*

The chemical processes, such as the use of solvents to delaminate the P/V structures, are technologically feasible, enabling the recovery of glass and cells or glass and substrate glass with semiconductor. However, as previously mentioned, such processes require long treatment times and liquid waste treatment steps as well. Although they may not be suitable for the treatment of large waste volumes, supposing that environmental issues are resolved, they may be suitable for a small-scale on-site treatment, akin to combinations of thermal and mechanical processes for the recovery of cells and metals. In any case, countermeasures for potential gas emissions caused by the chemical reactions, as well as for the disposal of waste acid after the process are significant issues (Komoto et al., 2018).

---

The already proven technologies may offer valuable insights on the waste management decision – makers, however, it seems difficult to get generalized recycling processes due to the constant changes in the manufacturing of P/Vs, the variety of panel technologies (1st and 2nd generation of P/V panels) and the complex panel structure that consists of various components, i.e. aluminum (Al) frame, junction box, glass, EVA resin, cells, electrodes, metals, etc. For instance, a significant structural difference between c-Si and thin-film panels is that the thin-film semiconductor layer is deposited on a substrate glass, while c-Si cells are separate from the cover glass and backsheets/back glass (if exist), thus, in the first case glass cannot be recovered from a thin-film panel by a single recycling method because semiconductor materials remain on the glass surface after delamination, needing additional treatment steps (combination method).

Preparing for future mass treatments, new treatment technologies are necessary to simulate the real treatment conditions in large scale. Several technologies are under development to achieve low cost processes, increase recovery/recycling rates, and improve the quality of the recovered materials. The purpose of this study was to evaluate

the potential of eliminating EVA resin from the laminated P/V structure through thermal, mechanical or chemical process. Various parameters were tested and compared in order to optimize the delamination process and increase its efficiency in four of the most commonly used panel technologies (i.e. p-Si, m-Si, CIS, a-Si). Analogous studies that thoroughly explore delamination based on the use of different crush equipment or different solvents have been very limited. The present study involves innovative aspects as it provides a direct comparison of three delamination processing approaches, addressing the type of treatment, the type of panel and the type of equipment or conditions used. In addition, the use of lactic acid or ethyl lactate as adopted in the present study has not so far been studied in terms of chemical processing.

## **3.2 Materials and methods**

### ***3.2.1 Sample collection***

Panels collection was made from local P/V panel trading/installation companies, located in Chania or Heraklion, Greece. The operational lifetime of the selected panels was completed due to external damage caused by extreme weather conditions or operational failure (i.e. reduced performance in electricity production). Different panel technologies were used, namely a polycrystalline silicon (p-Si) panel obtained from Risen Energy Co., Ltd, a monocrystalline silicon (m-Si) from ExelGroup Ltd, a copper-indium-selenide (CIS) panel from Solar Frontier's KK company and a tandem amorphous hydrogenated/microcrystalline hydrogenated silicon (a-Si:H/ $\mu$ c-Si:H) panel from Sharp company. Note that the p-Si panel was semi-dismantled when received, as its junction box, typically attached to the back of the panel, was missing.

### ***3.2.2 Sample pre-treatment***

In order to recycle P/V panels, they must undergo a series of processes, i.e. dismantling, separation, and recovery. The components produced from such dismantling/separation/recovery processes are mainly classified into frames, encapsulants (mostly EVA), solar cells, copper (Cu) ribbons, glass and backsheets. These components

are essential parts used for the panel manufacturing process. Therefore, it is useful to consider P/V recycling in terms of the degree of interest in certain components, since an “ideal recycling process” may be considered as the reversal of manufacturing.

The separation of the major components such as laminated structures, Al frames and junction boxes (cable and polymers) was the first step. Panels were dismantled by manual operations to remove the surrounded Al frames, junction-boxes and connecting cables (**Fig. 3.1a**). The manual dismantling was chosen in order to avoid further damage to the panels during dismantling, and therefore achieve high recovery rates, as well as high quality materials even if they present in low quantities (Savvilotidou et al., 2019).



(a)



(b)

Fig. 3.1: Photos after (a) dismantling, i.e. removal of Al frame, junction box and cables, and (b) cutting process (including panel area, junction-box and cables)

It is noteworthy that apart from the panels (laminated structures), the other released parts (frames, cables, etc.) also need further specific treatment according to available technologies. For instance, Al from frames or Cu from cables can become part of well-established metal recycling loops, having therefore potential for easy recycling; however, such processes are beyond the scope of this study. Then, the most important and technically difficult process involved the separation of the laminated panel structures consisting of glass, cells or glass substrate with semiconductor, ribbons and polymer layers.

Prior to delamination attempts, the separated parts of P/Vs (panels, junction-boxes and cables) were manually cut and pulverized in a universal cutting mill (FRITSCH, Pulverisette 19) to obtain particle size smaller than 250  $\mu\text{m}$  (**Fig. 3.1b**). The pulverized materials, as produced from the cutting mill, were used in order to determine the chemical composition. Total acid digestion was carried out in a microwave oven (Mars 6) and the digestion conditions were 100 mg of sample diluted into 10 mL solution of  $\text{HNO}_3$  at 180  $^\circ\text{C}$  for 20 min. The digests were diluted and analysed using inductively coupled mass spectrometry (ICP-MS).

### ***3.2.3 Eliminating EVA from the laminated structure***

Delamination was explored through (a) thermal, (b) mechanical and (c) chemical treatment.

#### *(a) Delamination through thermal processing*

The decomposition of EVA starts at 350  $^\circ\text{C}$  and is completed between 470 and 520  $^\circ\text{C}$  (Kang et al., 2012; Berger et al., 2010). During thermal processing, the decomposition of EVA occurs in two stages; the first stage involves deacetylation and release of acetic acid, while the second random/chain scissions giving mainly propane, propene, ethane, butane, hexane-1 and butane-1 (Granata et al., 2014).

The conditions of thermal treatment varied depending on the panel technology. For crystalline silicon (c-Si) panels, the pieces were thermally treated at 550  $^\circ\text{C}$  for 1 h in an electrical furnace (Nabertherm) in order to decompose the organics. At this

temperature the organic layers (EVA, organic dyes, organic polymers, etc) were decomposed resulting in solid residues consisting of glass, cells and Cu ribbons. On the other hand, delamination for CIS and a-Si panels occurred at 500 °C for 1 h, leading to two residue solid components, namely clear glass and glass substrate with semiconductor or else indium-tin oxide (ITO) coated glass. The latter glass serves as a substrate upon which transparent conductive oxides (TCO) are deposited. It must be noted that for thin-film panels, oxidation of the ITO/TCO layer was observed at higher temperatures than 500 °C (e.g. 550 °C).

*(b) Delamination through mechanical processing*

To proceed a mechanical recycling process it is very important to know which technologies and devices are suitable to the creation of crushed material.

P/V pieces with a surface of 2 cm × 2 cm were subjected to mechanical crushing in a blade rotor with a stainless steel bowl in order to break the lamination bond through crushing/scribing glass. In this view, it was expected that glass would be separated from the cells, as the latter would remain encapsulated with EVA (externally EVA coating) for c-Si panels. On the other hand, for thin-film panels the starting estimation was that mechanical processing would result in separation between the two structural glasses (clear glass and ITO coated glass) and the intermediate EVA layer.

The optimal duration of milling was 30 and 45 sec for the first and second type of panels, respectively. The mentioned durations were adequate, as in the first case (i.e. p-Si and m-Si) the glass was nearly crushed in comparison with cells (located between the two EVA layers) that were not grinded due to encapsulation with resin, whereas in the second case (i.e. CIS, a-Si) both glasses were crushed, but EVA pieces remained in the starting dimensions (2 cm × 2 cm). The time was different based on the comminution process that depended on the panel structures.

It should be noted that the selection of this type of mill, blade rotor, for the mechanical crushing was made after preliminary tests using different equipment, namely a ring mill and a cutting mill. However, using a ring mill the elimination of the laminated structure was considered more complicated because some glass portion remained stuck to

the EVA films, imbedding the efficiency of the comminution process and resulting in recovery of components with impurities. Also, the use of a cutting mill led to cutting of EVA and production of two size fractions both consisted of glass mixed with EVA, as it is equipped with a mesh (250  $\mu\text{m}$ ) that controls the size of particles.

*(c) Delamination through chemical processing*

Chemical processing is based on the use of solvent to eliminate the encapsulant from the laminated structures.

Use of organic solvents, namely toluene and ethyl lactate, was carried out in order to cause delamination of p-Si, m-Si, CIS and a-Si pieces, through swelling and/or dissolution of EVA. According to previous studies focused on c-Si panels, toluene presents a high efficiency, causing swelling or dissolution of EVA under certain conditions (i.e. time, temperature, etc.) (Doi et al., 2001; Kang et al., 2012; Kim and Lee, 2012). On the other hand, ethyl lactate is a less toxic solvent, 100% biodegradable and easy to recycle, presenting similar properties to those of toluene; it must be noted that ethyl lactate has not so far been used for the delamination of panel structures. To evaluate the efficiency of the chemical treatment, various conditions were considered, namely the type of solvent (toluene, ethyl lactate, ethyl lactate:ethyl alcohol), the temperature (25-90  $^{\circ}\text{C}$ ), the stirring (0, 500 rpm) and the time of exposure (up to 30 d). The chemical process was performed on panel pieces with a surface of 10 mm X 10 mm or smaller in order to be suitable for small-scale treatment, enabling adequate repetitions of the tests with limited cost. It must be noted that small pieces enable exposure of a larger solid surface to the solution (solid-liquid interface), thereby resulting in quicker EVA swelling and separation of the major components. Small size samples were also used in earlier studies (Kang et al., 2012; Kim and Lee, 2012) in order to allow a direct penetration of the diluent in the panel.

In the case of CIS and a-Si, further experiments were made using dense or diluted organic and inorganic acids (lactic acid,  $\text{HNO}_3$ ,  $\text{H}_2\text{SO}_4$ ,  $\text{HCl}$ ) and a thermostatic water bath for controlling temperature. The diluted acids were prepared by addition of (i) deionized water or, (ii)  $\text{H}_2\text{O}_2$ , in a mixture ratio of 1:1. The efficiency of the solvents was

determined based on the experimental conditions used, such as temperature (25, 50, 70 °C) and agitation (0 or 100 rpm), with a constant S:L ratio of 2:3. Details on the experimental conditions are shown in **Table 3.2**. The solvents used were HNO<sub>3</sub>, HCl, H<sub>2</sub>SO<sub>4</sub>, lactic acid, as well as mixtures of HNO<sub>3</sub>:H<sub>2</sub>O<sub>2</sub>=1:1, HCl:H<sub>2</sub>O<sub>2</sub>=1:1, H<sub>2</sub>SO<sub>4</sub>:H<sub>2</sub>O<sub>2</sub>=1:1, H<sub>2</sub>SO<sub>4</sub>:H<sub>2</sub>O=1:1, lactic acid:H<sub>2</sub>O<sub>2</sub>=1:1 and lactic acid:H<sub>2</sub>O.

**Table 3.2: Experimental conditions of chemical treatment for a-Si and CIS panels**

Parameters	
Solvent (acids or acid mixtures)	HNO <sub>3</sub> , HCl, H <sub>2</sub> SO <sub>4</sub> , lactic acid, HNO <sub>3</sub> :H <sub>2</sub> O <sub>2</sub> , HCl:H <sub>2</sub> O <sub>2</sub> , H <sub>2</sub> SO <sub>4</sub> :H <sub>2</sub> O <sub>2</sub> , H <sub>2</sub> SO <sub>4</sub> :H <sub>2</sub> O, lactic acid, lactic acid:H <sub>2</sub> O <sub>2</sub> , lactic acid:H <sub>2</sub> O
Acid mixture ratio	1:1
Temperature	25, 50, 70 °C
Stirring	0, 100 rpm
S:L ratio	2:3
Sample surface	1 cm <sup>2</sup>

The selected operating parameters were mainly directed to an energy efficient chemical process using gentle temperatures and small volumes of solvents to eliminate liquid emissions and subsequent treatment of wastewater as well.

### 3.3 Results and discussion

#### 3.3.1 Evaluation of metal content in P/V panels by ICP-MS

Prior to delamination, the chemical composition of the tested panels was determined. **Table 3.3** presents the metal content (in mg/kg) in c-Si and thin-film panels, indicating that the composition is significantly associated with panel technology. Specifically, among the four tested panels (p-Si, m-Si, CIS and a-Si) the main differences are related to the metals involved in the semiconductor material, since In, Se and Ga are predominant metals in the CIS layer, while Si, Ag and Al are mainly contained in the

crystalline silicon cells. Also, for amorphous silicon panel, the semiconductor material seems to be rich in Si and In as well.

**Table 3.3: Metal content in photovoltaic panels and junction boxes (mg/kg dry weight)**

Element	Crystalline panels (1st generation)			Thin-film panels (2nd generation)			
	p-Si	m-Si	Junction box	a-Si	Junction box	CIS	Junction box
Al	3201±69	3468±64	10959±184	810±31	51811±328	2218±32	6991±6
Si <sup>2</sup>	2365±7	1205±16	159±0	1191±36	1083±93	440±35	<DL
Cr	180±3	188±2	11582±47	461±3	656±6	340±6	764±14
Cu	273±9	322±3	153678±814	376±4	146889±507	269±12	706929±5415
Zn	207±26	277±15	2537±12	209±2	1381±6	1264±151	14911±327
Ga	<DL	9±0	<DL	3±0	18±0	180±5	<DL
Ge	<DL	<DL	<DL	<DL	<DL	<DL	<DL
As	<DL	<DL	14±2	<DL	<DL	<DL	<DL
Cd	<DL	<DL	19690±159	<DL	<DL	<DL	<DL
In	<DL	<DL	<DL	<DL	4±0	77±1	<DL
Sn	385±15	690±10	28435±216	14200±58	15079±151	712±19	19876±1341
Pb	294±3	360±3	7737±114	<DL	<DL	<DL	<DL
Ti	<DL	<DL	<DL	8±1	538±5	4±0	<DL
Fe	823±26	1089±33	<DL	2892±58	5769±104	1702±21	<DL
Ni	325±20	419±10	987±39	239±2	463±3	152±4	1246±40
Mo	<DL	<DL	<DL	2±0	2±0	12±0	<DL
Hg	<DL	<DL		<DL	6±0	12±0	264±19
Se	<DL	<DL	<DL	<DL	<DL	248±3	<DL

Starting from the crystalline silicon panels, it can be seen that the metal content in p-Si panel is close to that in m-Si panel as a result of their similar structure and manufacturing process. Al is one of the major metals contained in c-Si panels due to the thin Al layer on the rear surface and some Al electrodes (Kang et al., 2012). The content of Si is also high, since it is a principal component of glass and cells, whereas it is also

<sup>2</sup> Si concentration may decline from the present values due to some insoluble amount, since HNO<sub>3</sub> was used as digester, whereas hydrofluoric acid (HF) and HNO<sub>3</sub> solution is more appropriate for the total dilution of Si (Bettinelli et al., 1989; Henssge et al., 2006).

contained in the anti-reflection layer (AR), which covers the P/V cells, in the form of oxides SiO, SiO<sub>2</sub>, etc. (Klugman-Radziemska and Ostrowski, 2010). Other metals contained in lower quantities are Sn, Pb, Zn, Cu and Cr. Actually, Cu and Sn are used for the metal electrodes (i.e. ribbons) of the front surface of the P/V cell (Kang et al., 2012). The ribbons also consist of an alloy composed of Pb or Ag (Tammaro et al., 2015).

The amount of Pb may also be attributed to the Ag paste, facilitating the sintering of Ag paste during manufacturing (Jiang et al., 2016). Finally, metals such as As or Cd were not found, manifesting that crystalline silicon panels may be more environmentally friendly compared to the thin-film technologies (e.g. CdTe, etc.). Apart from the panel area, the composition of the junction box, which is attached to the back cover of the panel and is about 1 – 2.5% of the total panel weight (Tammaro et al., 2015), was determined. The junction box mainly contains Cu in comparison with the other tested metals. High concentrations of Sn and Cd were also observed, which are usually used for plating, metal welding and coating.

For thin-film panels (CIS and a-Si), the high content of Sn and Zn was expected as these metals are highly utilized in the transparent conducting oxide (TCO) layer, i.e. tin oxide (SnO<sub>2</sub>), indium tin oxide (ITO), or zinc oxide (ZnO) (Müller et al., 2004; Tsai and Tsai, 2014). The amount of Al originates from the metal ribbon wiring, as previously mentioned for c-Si panels. Also, it seems that Cd is not contained in CIS panel, although it is typically used as CdS window layer of cells. This may be due to its replacement with a less toxic window layer, Zn(O, S, OH)<sub>x</sub>, during the manufacturing process in order to align with the Restriction of Hazardous Substances (RoHS) Directive (Kushiya, 2014; Schneider, 2012). Another metal found in CIS is Mo; Mo is deposited as a contacting material because of its relatively inert nature during the highly-corrosive deposition conditions in the substrate configuration (Chopra et al., 2004).

The junction boxes, at a first sight present a high content of toxic metals, i.e. Hg, Pb and Ni, raising some concerns; however, Cd and As were not detected. More specifically, Pb only presents in the junction box of a-Si panel, and is probably originating from the lead compounds contained in the PVC (polyvinyl chloride) cable as

thermal stabilizer. The highest Hg concentration (264.53 mg/kg) occurs in the junction-box of CIS panel. At present, the composition and/or potential toxicity of junction boxes used in P/V panels have not been studied yet, despite that open circuit failures may occur (e.g. overheating). However, it must be noted that its contribution to the total panel may not be considerable, since a junction-box typically constitutes around 1% of the total panel weight (Olson et al., 2013). In addition, there is a recent trend for substituting the very toxic amounts of Hg and Pb with increase of less toxic metals Cu, Ag and Ti according to Silicon Valley Toxic Coalition, (2009) and towards an eco-friendly/eco-design manufacturing industry for photovoltaics. **Annex A** presents results on the toxicity potential of panels and junction boxes according to the toxicity characteristic leaching procedure (TCLP).

#### *Comparison with literature data for photovoltaics composition*

A great discrepancy between the metal content reported by the cited works (Chopra et al., 2004; Hahne and Hirn, 2010; Paiano, 2015) and the one of the present study was found. This may be justified by the fact that each study considers one or another fraction of the panel, e.g. Al frames, metal contacts and/or junction boxes. These fractions may or may not be included in the characterized material.

In addition, it is known that P/V market is extremely heterogeneous; also, the evolution of P/V technologies moves towards decreasing the panel metal content in order to reduce the manufacturing cost. For example, referring to silver content the historical data have showed an exponential drop (IRENA and IEA, 2016; Peeters et al., 2017). Accordingly, the quantified metal content is expected to be higher for older panels, which makes the year of manufacture a relevant data to be considered; this data is however missing in most of the published articles (Padoan et al., 2019).

### ***3.3.2 Delamination through thermal, mechanical and chemical processing***

#### *Thermal processing*

After thermal treatment of p-Si and m-Si panels, the polymers were burned, whereas the remaining materials (glass, cells, metal ribbons) were recovered, allowing their

separation either through sieving using four sieve meshes (5.00, 2.00, 0.500 and 0.180 mm, **Fig. 3.2**) or by optical observation and manual sorting.

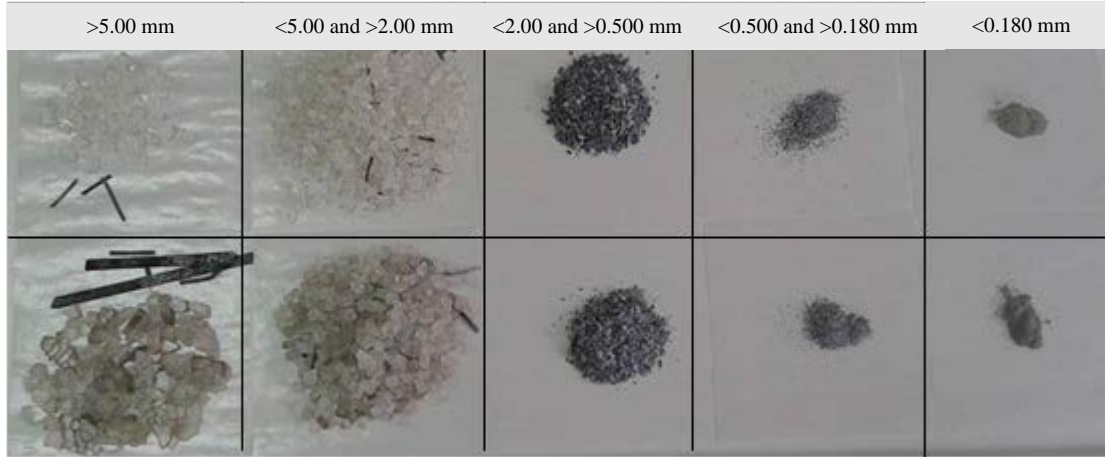


Fig. 3.2: P/V materials after heat treatment and sieving (glass, cells, metal ribbons)

In the first case, it was expected that glass and metal ribbons would be concentrated on the large size fractions, thus achieving a rough separation from cells. The evaluation of size fractions content was carried out using ICP-MS analysis, considering an element that may exist only in cell or glass. Pb, which is used in the manufacturing of cells, was used as the “index metal”. The ICP-MS analysis (see **Annex B; Table B.1** and **2**) indicated that except for the largest fractions which were consisted of glass, the other fractions (<2.00 and >0.500 mm, <0.500 and >0.180 mm, <0.180 mm) contained both cells and glass parts. In any case this rough separation technology, i.e. sieving, can only be considered if waste panels present damages (broken glass and cells).

On the other hand, by optical observation and manual sorting, some quantitative and qualitative information on the quality of glass were obtained. More specifically, the weight loss (%) due to organic combustion was calculated to be 14.5 and 10.7% for p-Si and m-Si panels, respectively, and the separated glass amounted to average rates of 92.0 and 87.1%. XRD patterns for the glass of p-Si and m-Si panels showed two broad humps representing the amorphous phase of glass and no crystalline phases, indicating that the recovered glass is not contaminated with metals from the cells or electrodes (**Fig. 3.3**).

It must be noted that the recovery rates of glass (92.0 and 87.1%) comply with the recycling and recovery targets established by the Directive 2012/19/EC from 15<sup>th</sup> August 2018, i.e. 80 and 85%, respectively.

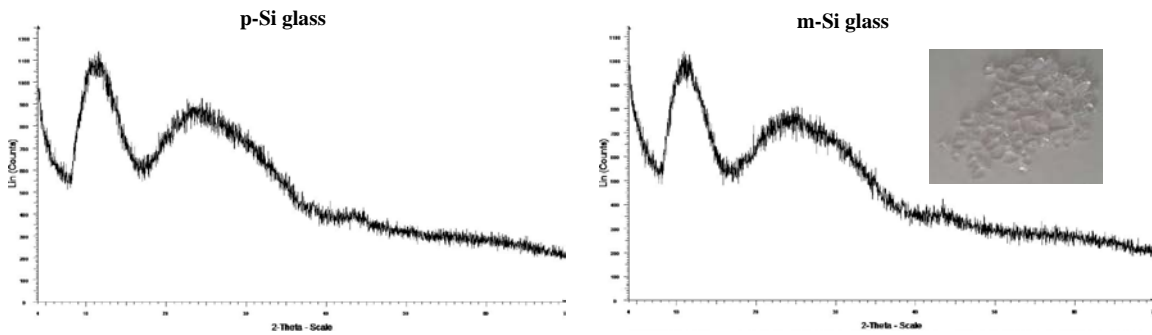


Fig. 3.3: XRD of glass from c-Si panels after thermal treatment



Fig. 3.4: Double-glass structures of thermally treated thin-film panels

For thin-film panels, after separation of the laminated structure through thermal processing, two types of glass were produced, i.e. the cover glass (clear glass), as well as the glass with the semiconductor layer (**Fig. 3.4**). The weight loss was 8.13% and 1.72% for CIS and a-Si panels, respectively, as a result of the burning of polymer components. Then, optical observation and manual sorting enabled the separation of the two glasses. However, due to a structural difference between crystalline and thin-film panels, glass cannot be recovered from a thin-film panel by a single separation method because semiconductor materials remain on the surface of glass after separation, needing subsequent chemical processes, i.e. etching, toward high-value recycling. Therefore,

additional steps are needed to remove the semiconductor materials, after enabling the separation of double-glass structures (i.e. cover glass and semiconductor glass) without any contamination.

#### *Mechanical processing*

The mechanical process was carried out using different mill types namely, a ring mill, a cutting mill or a blade rotor, for the separation and recovery of components such as glass, EVA and cells. Despite the delamination of the panel structure using the first two technologies (ring mill, cutting mill), at a first sight, the produced crushed material was a more complicated mixture as compared to the residue obtained after thermal processing, because the subsequent separation of components was not feasible even by optical observation and manual sorting (**Fig. 3.5**).

More specifically, the cutting mill, which is equipped with a sieve mesh (250  $\mu\text{m}$ ), resulted in two size fractions, the one involving a residual mixture of glass, cells and EVA (or glass, polymers and semiconductor glass depending on the type of panel) with size  $>250 \mu\text{m}$  and the other also consisting of crushed glass, cells and EVA (or glass, polymers and semiconductor glass) with size  $<250 \mu\text{m}$ . Also, the ring mill resulted in some crushed material (powder), as well as in large pieces of EVA with some residual amount of cells, glass or semiconductor glass. In both cases, the recovered glass was a low-grade product due to contaminations with EVA layer, cell or glass with semiconductor material for crystalline silicon or thin-film panels, respectively.

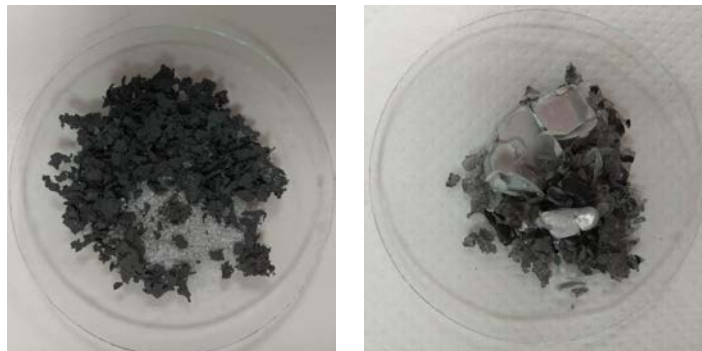


Fig. 3.5: Photos of mechanical crushing with a cutting mill – not efficient separation

On the other hand, efficient crushing was achieved using a blade rotor. Specifically, for crystalline panels, glass was crushed and separated from the other layers, i.e. back surface (tedlar), EVA and encapsulated cells (**Fig. 3.6a**). This is attributed to the different strength behavior of glass and polymers (Savvilotidou et al., 2019).



Fig. 3.6: Photos of EVA residue after mechanical crushing with a blade rotor for (a) p-Si and m-Si panels, as well as for (b) CIS and a-Si panels within 35 and 40 sec, respectively

For thin-film panels, the use of blade rotor led to a crushed material consisting of the two structural glasses, as well as to EVA pieces that contain some portion of the semiconductor layer, as shown in **Fig. 3.6b**.

#### *Chemical processing*

The results showed that toluene is an appropriate solvent with drastic effects on the delamination of crystalline and thin-film panels even at room temperature, as the main components (glass, ribbons, tedlar, cells encapsulated with the swelled EVA or substrate glass with semiconductor depending on panel technology) were separated. However, it is not suitable for the treatment of a-Si panel due to reactions associated with the dissolution of intermediate organic films that influence the quality of the recovered glass, i.e. transparency (**Fig. 3.7**).

Also, ethyl lactate resulted in the delamination of p-Si, m-Si and CIS panels at 90 °C. The delamination of CIS panel was technically feasible even at 25 °C, however, the time required for the reaction was too long.

**Tables 3.4** and **3.5** show the suitable conditions at which the delamination of panels was achieved through chemical processing using toluene or ethyl lactate. Also, **Fig. 3.7** illustrates some selected results after the delamination of panel structures.

**Table 3.4: Conditions for efficient delamination of p-Si and m-Si panels through chemical processing**

Solvent	Temperature (°C)	Stirring (rpm)	Time of exposure (h)	Delamination
Ethyl lactate	90	500	1.5	Complete
Toluene	25	0, 500	2	Complete
	90	0, 500	1.5, 1	Complete

**Table 3.5: Conditions for efficient delamination of a-Si and CIS panels through chemical processing**

Solvent	Temperature (°C)	Stirring (rpm)	Time of exposure	Delamination
<i>a-Si panel</i>				
Toluene:ethyl lactate	90	-	5 h	Complete
<i>CIS panel</i>				
Ethyl lactate	25	0	30 d	Complete
	90	500	1 d	Complete
Toluene	25	0, 500	2 d, 5 h	Complete
	90	0, 500	1.5 h, 1 h	Complete

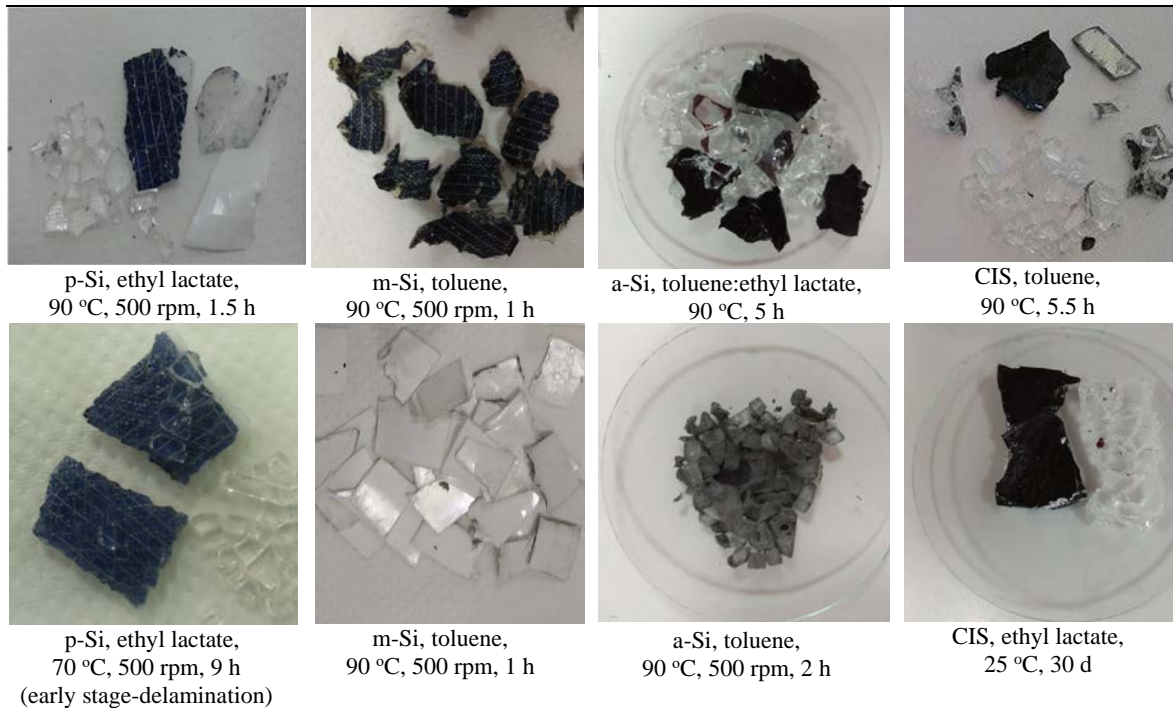


Fig. 3.7: Effect of toluene or/and ethyl lactate on the delamination of panel structure

Apart from organic solvents, also organic and inorganic acids were alternatively used in order to proceed the delamination of thin-film panel structure at temperatures of 25-70 °C.

*Utilization of dense acids at 25, 50, 70 °C for a-Si panel delamination*

Among the inorganic acids, the most drastic behavior was performed by H<sub>2</sub>SO<sub>4</sub> contributing to full dissolution of EVA at 25 °C within 100 min. Agitation highly affected the process leading to a faster separation of the major components. Increase of temperature at 50 °C improved the speed of reactions, resulting in full dissolution of EVA within 40 min. Further increase of temperature (i.e. 70 °C) was considered non-useful, since no significant changes in terms of reaction speed were observed.

Delamination using HCl was considerably slower and insufficient as compared to H<sub>2</sub>SO<sub>4</sub>, requiring long time even at high temperature. HNO<sub>3</sub> exhibited the lowest performance, as the delamination was not achieved; this is in agreement with the findings of earlier studies (Kang et al., 2012). Finally, using lactic acid, full delamination of panel structure was not achieved, since about 50% of the laminated structure was converted into separated components at 25 °C within 4 days.

*Utilization of diluted acids at 25, 50, 70 °C for a-Si panel delamination*

HNO<sub>3</sub> and HCl, diluted or not, were not suitable solvents for the treatment of a-Si panel, whereas lactic acid:H<sub>2</sub>O<sub>2</sub> solution caused defects upon the a-Si panel. On the other hand, the performance of H<sub>2</sub>SO<sub>4</sub> diluted either in deionized water or in H<sub>2</sub>O<sub>2</sub> was as high as in the dense solution requiring less operation time, i.e. 60 and 40 min at 50 and 70 °C, respectively. The less time required indicated that temperature influenced the dissolution of EVA, which was also observed by Kim and Lee (2012).

It must be noted that due to an exothermic reaction (release of heat) when H<sub>2</sub>SO<sub>4</sub> is diluted in H<sub>2</sub>O, an alternative technique was tested, i.e. “serial elution” with H<sub>2</sub>SO<sub>4</sub>, in order to maintain the reaction temperature and mitigate energy demand. Elutions beard the desired effects on delamination within 40 min instead of 100 min using dense H<sub>2</sub>SO<sub>4</sub> at 25 °C. However, the potential applicability of this process in industrial scale is technically troublesome.

*Utilization of dense acids at 25, 50, 70 °C for CIS panel delamination*

The resistance of CIS panel to delamination was higher than that of a-Si panel. HCl and HNO<sub>3</sub> demonstrated very low efficiency at any temperature, with or without agitation. In comparison with a-Si, dense H<sub>2</sub>SO<sub>4</sub> caused damages (rust), and delamination was achieved at 25 °C after 6 d. Rust is a non-desired reaction that can lower the value of the separated components, thus limiting recycling purposes. On the other hand, dense lactic acid led to the separation between glass with EVA, and glass with semiconductor and intermediate polymer layers as well.

*Utilization of diluted acids at 25, 50, 70 °C for CIS panel delamination*

The delamination of CIS panel was accompanied with rust phenomena when H<sub>2</sub>SO<sub>4</sub> diluted in H<sub>2</sub>O<sub>2</sub> was used. However, dilution of lactic acid in deionized water resulted in a stable delamination rate and separation of the main components at 25 °C within 4 days.

The results indicated that the type of solvent has a strong effect on the degradation of EVA. For a-Si panel, optimal delamination was obtained using a solution of H<sub>2</sub>SO<sub>4</sub>:H<sub>2</sub>O=1:1, with S:L=2:3 and 100 rpm at 50 °C for 1 h. For CIS panel, optimal delamination occurred using a solution of lactic acid:H<sub>2</sub>O=1:1 with S:L=2:3 and 100 rpm at 25 °C for 4 d. From an environmental and economical viewpoint, the use of mixture diluents is more sustainable than utilization of dense acids since the required acid volume decreases. Also, “gentle” temperatures, i.e. 25 or 50 °C, mitigate the energy demands of the process. **Table 3.6** includes the suggested conditions for the treatment of thin-film panels.

**Table 3.6: Optimal delamination for a-Si and CIS panels using acid solutions**

P/V type	Solvent (acid mixtures)	Acid mixture ratio	Temperature (°C)	Stirring (rpm)	S:L ratio	Panel surface (cm <sup>2</sup> )	Time
a-Si	H <sub>2</sub> SO <sub>4</sub> :H <sub>2</sub> O	1:1	50	100	2:3	1	60 min
	H <sub>2</sub> SO <sub>4</sub> :H <sub>2</sub> O (“serial” elution)	1:1	Reaction temperature	0	2:3	1	40 min
CIS	Lactic acid:H <sub>2</sub> O	1:1	25	100	2:3	1	4 d

### 3.3.3 Comparison of delamination processes

In order to compare the efficiency of the processes, the advantages and disadvantages of each process are presented in **Table 3.7**. Overall, mechanical treatment is inexpensive, requires less operation time and thus remains competitive in large scale treatment facilities. However, considering the obtained results, it cannot assist recovery of high-value materials, requiring more elaborate treatment. Thermal processes are widely characterized by high energy consumption; the investigation though showed that it separates more efficiently the components leading to intact and reusable components and thus it may be an essential strategic step for the subsequent recycling stages, i.e. the recovery of semiconductor metals (Ag, In, etc.). Finally, chemical treatment requires long time for solvent action and involves high cost of the solvents.

**Table 3.7. Advantages and disadvantages of delamination technologies**

Treatment of panels	Operation conditions/ Equipment	Advantages	Disadvantages
Mechanical process	Appropriate mills; suitable meshes	Simple process; low energy demand; technology widely available	High impurities; ineffective process in terms of major components separation
Chemical process	Appropriate solvents and heating machines	Efficient delamination	Long time; cost of solvents; wastewater treatment; subsequent steps required (e.g. thermal process to remove the swelled EVA)
Thermal process	Electrical furnace (500-550 °C)	No reagents required; full removal of organics; fast processing; applicable in large-scale; enables separation of major components through optical observation and manual sorting	High energy demand; emissions of gases; more steps required for further separation (instead of manual sorting)

Based on the comparative analysis, it is evident that thermal or chemical treatment are more efficient approaches than mechanical crushing in terms of 1st and 2nd

generation panel delamination. In any case, in order to ensure competitiveness for treatment technologies, economic and environmental aspects should also be addressed, considering the industrial capacities and equipment, as well as the multi-stage recycling. Finally, one of the most important criteria to decide suitable delamination is if the aim is a high-value recycling rather than just a bulk separation (which leaves significant mass of materials mixed or unrecovered).

### **3.4 Conclusions**

First, this study provides valuable information on the composition of the most commonly used types of panels, as a fundamental step required prior to any recycling attempt. Attention must be paid to junction boxes, as they can potentially cause adverse effects to the environment and human health due to the high content of toxic metals, necessitating eco-design approaches.

The main part of this study was the investigation of the predominant delamination technologies for P/V panels, and a comparison of their efficiency as well. The results revealed that thermal, mechanical and chemical processes are technically feasible approaches leading to elimination of EVA from the laminated structures either for crystalline silicon panels or for thin-film panels, thus enabling separation of the structural components through further treatment. Among the processes, dry mechanical crushing was considered as the soundest and simplest delamination path, since it does not include either significant air pollution (as in the case of thermal treatment) or any other types of secondary pollution (e.g. direct chemical process associated with produced wastewater); however, it anticipates ineffective component separation due to heightened impurities. Thermal treatment is more advantageous considering the full removal of organics, the fast processing and no need for reagents as compared to the chemical treatment.

The innovative aspects in the present study involve (i) the use of ethyl lactate or lactic acid as compared to toluene, sulfuric or nitric acid that have been proposed for the delamination of panels in earlier studies, and (ii) the investigation of suitable

conditions/equipment in terms of mechanical processing since sufficient attention still has not been paid to.

### 3.5 References

- Ashfaq, H., Hussain, I., Giri, A., 2017. Comparative analysis of old, recycled and new PV modules. *J. King Saud Univ. Eng. Sci.* 29(1), 22-28. doi:10.1016/j.jksues.2014.08.004
- Berger, W., Simon, F.G., Weimann, K., Alsema, E.A., 2010. A novel approach for the recycling of thin film photovoltaic modules. *Resour. Conserv. Recycl.* 54(10), 711-718.
- Chopra, K.L., Paulson, P.D., Dutta, V., 2004. Thin-Film Solar Cells: An Overview. *Prog. Photovolt.: Res. Appl.* 12, 69-92. doi: 10.1002/pip.541.
- Corcelli, F., Ripa, M., Leccisi, E., Cigolotti, V., Fiandra, V., Graditi, G., Sannino, L., Tammaro, M., Ulgiati, S., 2018. Sustainable urban electricity supply chain – Indicators of material recovery and energy savings from crystalline silicon photovoltaic panels end-of-life. *Ecol. Indic.* 94, 37-51. <http://dx.doi.org/10.1016/j.ecolind.2016.03.028>.
- Dias, P., Schmidt, L., Gomes, L.B., Bettanin, A., Veit, H., Bernardes, A.M., 2018. Recycling Waste Crystalline Silicon Photovoltaic Modules by Electrostatic Separation. *J. Sustain. Metallurgy* 4(2), 176-186.
- Dias, P., Javimczik, S., Benevit, M., Veit, H., Bernardes, A.M., 2016. Recycling WEEE: Extraction and concentration of silver from waste crystalline silicon photovoltaic modules. *Waste Manage.* 57, 220-225.
- Directive 2002/95/EC of the European Parliament and of the Council of 27 January 2003 on the restriction of the use of certain hazardous substances in electrical and electronic equipment, *Off. J. Eur. Union* L37/19.
- Directive 2012/19/EU of the European Parliament and of the Council of 4 July 2012 on waste electrical and electronic equipment (WEEE), recast. *Off. J. Eur. Union* L197/38.

- Doi, T., Tsuda, I., Unagida, H., Murata, A., Sakuta, K., Kurokawa, K., 2001. Experimental study on PV module recycling with organic solvent method. *Sol. Energy Mater. Sol. Cells* 67(1-4), 397-403.
- Doni, A., Dughiero, F., 2012. Electrothermal heating process applied to c-Si PV recycling. 38th IEEE Photovoltaic Specialists Conference (pp. 000757-000762). IEEE.
- Frisson, L., Lieten, K., Bruton, T., Declercq, K., Szlufcik, J., De Moor, H., Goris, M., Benali, A., Aceves, O., 2000. Recent improvements in industrial PV module recycling. 16th European Photovoltaic Solar Energy Conference (Vol. 5).
- Granata, G., Pagnanelli, F., Moscardini, E., Havlik, T., Toro, L., 2014. Recycling of photovoltaic panels by physical operations. *Sol. Energy Mater. Sol. Cells* 123, 239-248.
- Gustafsson, A.M., Steenari, B.M., Ekberg, C., 2015. Recycling of CIGS Solar Cell Waste Materials: Separation of Copper, Indium, and Gallium by High-Temperature Chlorination Reaction with Ammonium Chloride. *Sep. Sci. Technol.* 50(15), 2415-2425.
- Gustafsson, A.M., Foreman, M.R.S., Ekberg, C., 2014. Recycling of high purity selenium from CIGS solar cell waste materials. *Waste Manage.* 34(10), 1775-1782.
- Hahne, A., Hirn, G., 2010. Recycling photovoltaic modules. Bine Information Service, Berlin, Germany. <http://www.bine.info/en/publications/publikation/recycling-von-photovoltaik-modulen/> (last access 31.05.2016).
- Huang, W.H., Shin, W.J., Wang, L., Sun, W.C., Tao, M., 2017. Strategy and technology to recycle wafer-silicon solar modules. *Sol. Energy* 144, 22-31.
- IRENA/IEA PVPS Task12, End-of-Life Management: Solar Photovoltaic Panels, 2016.
- Jiang, J., He, Y., Zhang, Z., Wei, J., Li, L., 2016. Pb-free front-contact silver pastes with SnOP2O5 glass frit for crystalline silicon solar cells. *J. Alloy Compd.* 689, 662-668.

- Jung, B., Park, J., Seo, D., Park, N., 2016. Sustainable system for raw-metal recovery from crystalline silicon solar panels: from noble-metal extraction to lead removal. *ACS Sustain. Chem. Eng.* 4(8), 4079-4083.
- Kang, S., Yoo, S., Lee, J., Boo, B., Ryu, H., 2012. Experimental investigations for recycling of silicon and glass from waste photovoltaic modules. *Renew. Energy* 47, 152-159.
- Kim, Y., Lee, J., 2012. Dissolution of ethylene vinyl acetate in crystalline silicon PV modules using ultrasonic irradiation and organic solvent. *Sol. Energy Mater. Sol. Cells* 98, 317-322.
- Klugmann-Radziemska, E., 2013. Current trends in recycling of photovoltaic solar cells and module waste. *Chem. Didact. Ecol. Metrol.* 17 (1-2), 89-95. DOI: 10.2478/cdem-2013-0008.
- Klugmann-Radziemska, E., Ostrowski, P., Drabczyk, K., Panek, P., Marek, S., 2010. Experimental validation of crystalline silicon solar cells recycling by thermal and chemical methods. *Sol. Energ. Mat. Sol. Cells* 94 (12), 2275-2282.
- Komoto, K., Lee, J.S., Zhang, J., Ravikumar, D., Sinha, P., Wade, A., Heath, G., 2018. End-of-Life Management of Photovoltaic Panels: Trends in PV Module Recycling Technologies. IEA PVPS Task 12, International Energy Agency Power Systems Programme, Report IEA-PVPS T12, 10.
- Kushiya, K., 2014. CIS-based thin-film PV technology in solar frontier K.K. *Sol. Energ. Mat. Sol. Cells* 122, 309-313.
- Müller, J., Rech, B., Springer, J., Vanecek, M., 2004. TCO and light trapping in silicon thin film solar cells. *Sol. Energy* 77 (6), 917-930. doi:10.1016/j.solener.2004.03.015.
- Olson, C., Geerligs, B., Goris, M., Bennett, I., Clyncke, J., 2013. Current and future priorities for mass and material in silicon PV modules recycling. 28th European PV Solar Energy Conference and Exhibition (EU PVSEC), Paris; ISBN 3-936338-33-7:4629-33.

- Padoan, F.C., Altimari, P., Pagnanelli, F., 2019. Recycling of end of life photovoltaic panels: A chemical prospective on process development. *Sol. Energy* 177, 746-761.
- Pagnanelli, F., Moscardini, E., Granata, G., Atia, T.A., Altimari, P., Havlik, T., Toro, L., 2017. Physical and chemical treatment of end of life panels: An integrated automatic approach viable for different photovoltaic technologies. *Waste Manage.* 59, 422-431.
- Paiano, A., 2015. Photovoltaic waste assessment in Italy. *Renew. Sustainable Energy Rev.* 41, 99-112.
- Peeters, J.R., Altamirano, D., Dewulf, W., Duflou, J.R., 2017. Forecasting the composition of emerging waste streams with sensitivity analysis: a case study for photovoltaic (PV) panels in Flanders. *Resour. Conserv. Recycl.* 120, 14-26.
- PV CYCLE, European Association for the recovery of photovoltaic modules, Annual Report 2013.
- Schneider, H., 2012. Introduction of Solar Frontier  
. [http://www.nobility.cz/files/Solar\\_Frontier\\_En\\_Nobility\\_Solar\\_Projects.pdf](http://www.nobility.cz/files/Solar_Frontier_En_Nobility_Solar_Projects.pdf) (last access 31.05.2016).
- Shin, J., Park, J., Park, N., 2017. A method to recycle silicon wafer from end-of-life photovoltaic module and solar panels by using recycled silicon wafers. *Sol. Energy Mater. Sol. Cells* 162, 1-6.
- Silicon Valley Toxics Coalition White paper, 2009. Toward a just and sustainable solar energy industry.  
[http://svtc.org/wp-content/uploads/Silicon\\_Valley\\_Toxics\\_Coalition -  
\\_Toward\\_a\\_Just\\_and\\_Sust.pdf](http://svtc.org/wp-content/uploads/Silicon_Valley_Toxics_Coalition_-_Toward_a_Just_and_Sust.pdf) (last access 31.05.2016).
- Tao, J., Yu, S., 2015. Review on feasible recycling pathways and technologies of solar photovoltaic modules. *Sol. Energy Mater. Sol. Cells* 141, 108-124.
- Tsai, C., Tsai, C., 2014. Development of Amorphous/Microcrystalline silicon Tandem Thin-Film Solar Modules with Low Output Voltage, High Energy Yield, Low

- Light-Induced Degradation, and High Damp-Heat Reliability. *J. Nanomater.* doi:10.1155/2014/861741.
- Wang, T.Y., Hsiao, J.C., Du, C.H., 2012. Recycling of materials from silicon base solar cell module. 38th IEEE Photovoltaic Specialists Conference (pp. 2355-2358). IEEE. DOI: 10.1109/PVSC.2012.6318071.
- Yi, Y.K., Kim, H.S., Tran, T., Hong, S.K., Kim, M.J., 2014. Recovering valuable metals from recycled photovoltaic modules. *J. Air Waste Manage. Assoc.* 64(7), 797-807.
- Zhang, L., Xu, Z., 2016. Separating and recycling plastic, glass, and gallium from waste solar cell modules by nitrogen pyrolysis and vacuum decomposition. *Env. Sci. Technol.* 50(17), 9242-9250.

## 4 Silver and indium recovery from P/V panels

Critical raw materials (CRMs), found in waste, have been crucial to the global economy, indicating an urgent need for secondary production through recycling activities. As the photovoltaic (P/V) industry is emerging, damaged P/V cells depending on their technology can be considered as a secondary source of precious or critical metals. However, a circular economy of these high-tech metals may be feasible only if pre-concentration is employed. To this scope, this study first investigates three different treatment routes for waste polycrystalline silicon (p-Si) and monocrystalline silicon (m-Si), as well as copper indium selenide (CIS) photovoltaic panels in order to produce valuable pre-concentrates of Ag and In. The treatment routes, used in various combinations, are (a) thermal treatment and gravimetric separation, (a) mechanical crushing, sieving and thermal treatment, as well as (c) chemical and thermal treatment of the panels. Their evaluation was based on the content of Ag or In (mg/kg) in the treated mass share (%) as compared to the initial content and P/V mass used. Then, the study explores selective recovery of Ag or In from the produced treated fractions, which are enriched in Ag or In. The tests involved acid leaching and precipitation to determine the optimal conditions for obtaining the maximum leaching capacity and precipitation efficiency. The intact target-components produced after thermal treatment and gravimetric separation resulted in the optimal pre-concentration yield of Ag and In, namely 91.42 and 94.25% for p-Si and m-Si panels, and 96.10% for CIS panel. The maximum leaching capacity of Ag and In was obtained using  $\text{HNO}_3$  and  $\text{H}_2\text{SO}_4$  solution, respectively. Pure silver chloride ( $\text{AgCl}$ ) was recovered using  $\text{HCl}$  as precipitating agent and pure indium oxide ( $\text{In}_2\text{O}_3$ ) using  $\text{NH}_4\text{OH}$ . The results reveal that pre-concentration and selective recovery of Ag and In are technically feasible.



## 4.1 Overview

Renewable energy resources, i.e. solar, wind, etc., are becoming more prevalent and necessary; long-term projections indicate that they are expected to provide half of the total energy demands by 2050 (Lee et al., 2013; Islam et al., 2014). Solar energy is practically inexhaustible; however, future disposal of P/V panels creates concerns associated with potential environmental impacts that may affect human health and the environment. Apart from environmental impacts, a disposal scenario eliminates the benefits of recycling and/or selling P/V materials (Dias et al., 2016a). Waste management of P/Vs has therefore been a major concern in current years (Savvilitidou et al., 2017).

The interest upon the recycling of some P/V technologies has been recently raised, as Deutsche Solar and First Solar developed innovative treatments for the recycling of crystalline silicon panels, and cadmium-telluride (CdTe) panels, respectively (Latunussa et al., 2016). However, the recycling of other commonly used P/V technologies has not been entirely commercialized. In laboratory scale, the research community has investigated reuse or recycling practices in waste panels for construction purposes (i.e. production of concrete, geopolymers, glass-ceramics, etc.) (Skripkiūnas et al., 2018; Hao et al., 2015; Hao et al., 2013; Lin et al., 2012). Some research interest is also concentrated on the treatment of waste panels, comprised of two steps, i.e. the simple delamination of the resistant panel structure to separate the major components, such as glass, cells, etc. (pre-processing step)<sup>3</sup>, and the high-value recycling including extraction and recovery of pure precious or critical metals from the cells (end-processing step).

The end-processing step, i.e. purification of metals, has still gained limited interest on behalf of industries and researchers due to the rather low share of the targeted

---

<sup>3</sup> The pre-processing step (delamination of the panel structure) was thoroughly investigated in Chapter 3, involving a review of previous attempts in the field, as well as experiments for the decomposition, cutting, swelling or dissolution of the ethylene vinyl acetate resin (EVA) in various panel technologies.

metals in the total panel mass, as well as the related economic issues (Savvilotidou et al., 2019). Dias et al. (2016a) and Dias et al. (2016b) explored selective separation and extraction of Ag from c-Si cells. Berger et al. (2010) developed a mechanical process, as well as a combination of processes, i.e. mechanical and thermal process, in CdTe and CIS and they obtained pure Te and In, suitable for the production of new panels within the EU-LIFE program (RESOLVED). Based on the literature review, it seems that most studies focus on specific target components or materials, either bulk (glass, aluminum, plastic, etc.) or valuable (Ag, In, etc.), through different processes and combinations of processes. However, research and development of the total recycling process could be very sophisticated considering that critical or precious metals are worth recovering only after pre-concentration (Amato et al., 2017), thus delamination/separation step can significantly influence the recovery of metals.

According to European Commission (2017), Ag and In present high economic importance and a risk of supply due to political and economic conditions, low recycling rates and increasing demand. Klugmann-Radziemska and Ostrowski (2010) refer to a necessity for recovering valuable materials such as Ag from spent P/V panels due to the high demand over the past ten years (20–30% higher compared to the annual mine supply) and the risk of supply in the future (2075) (Dias et al., 2016b; Grandell and Thorenz, 2014). Latunussa et al. (2016) reported that the potentials of In secondary production from P/V waste will enhance the balance between In demand and supply. Relative economic benefits by future recycling of critical metals from P/V panels still are uncertain (Cucchiella et al., 2015). Doi et al. (2001) and Goe and Gaustad (2014) estimated that the production of secondary materials requires less processing than that needed for the production of primary raw materials.

The fate of Ag and In during the treatment of waste panels has not been extensively studied in literature, thus involving various gaps on the optimal pre-processing and end-processing steps. Motivated by these gaps, this study first addresses the pre-concentration of Ag and In as a critical step for integrated high-value recycling of waste panels, and then investigates the suitable conditions for the selective recovery of

the targeted metals. More specifically, in the first part of this study three treatment routes consisted of multiple steps were investigated in order to maximize the recovery of valuable materials (Ag, In), by determination of their content, losses and pre-concentration yield in each treated fraction. In the second part of this study leaching and precipitation of the targeted metals were tested under various solid/liquid ratios and temperatures into HNO<sub>3</sub> and H<sub>2</sub>SO<sub>4</sub> with constant stirring using HCl or NH<sub>4</sub>OH as precipitated agents, and optimized. The present study is a novel contribution towards a sustainable management of spent panels, as it presents, for the first time, a direct comparison of three different treatment routes in terms of Ag and In pre-concentration in a single work, and adds further value by achieving selective recovery of pure Ag and In through leaching extraction and precipitation. Additionally, this study provides worthwhile knowledge on the recovery of the bulk materials contained in the panels (i.e. glass), suggesting at the same time both integrated and individual management practices in the field.

## 4.2 Materials and Methods

The present study focuses on the management of 1st and 2nd generation panels, and especially spent p-Si, m-Si and CIS panels. It should be noted that CIS panels have been considered as the leading thin-film technology, with a respective sharply increase of waste about 45,000 tonnes in 2035 (Rocchetti and Beolchini, 2015), while crystalline silicon panels represent 85 to 90% of the global annual market (Dias et al., 2016a; Klugman-Radziemska and Ostrowski, 2010), thus increasing the motivations to this study.

A p-Si panel obtained from Risen Energy Co., Ltd, a m-Si panel from ExelGroup Ltd and a CIS panel obtained from Solar Frontier's KK Company were used for experiments. The technical characteristics, the composition and potential toxicity of panels are provided in Chapter 3 and **Annex A**. P/V panels typically consist of glass, aluminum frames, EVA layers, solar cells, a junction box, a back film and tapping screws (Kang et al., 2012). Based on the panel structure, the primarily step was the dismantling

of external Al frames and junction box attached to the back surface in order to isolate the panel area. Manual dismantling of such multilayer waste has revealed better results in terms of cost and quality of the recovered components, compared to other methods (e.g. water jet cutting, laser cutting, use of a circular saw) (Silveira et al., 2015). After dismantling, the panels were cut into pieces of  $2\text{ cm} \times 2\text{ cm}$ .

**Fig. 4.1** shows a schematic flow chart of the three treatment routes studied in this work, including various steps at the pre-processing and end-processing stage focusing on Ag and In recovery.

## SILVER AND INDIUM CONTENT AT THE PRE-PROCESSING AND END-PROCESSING STAGE

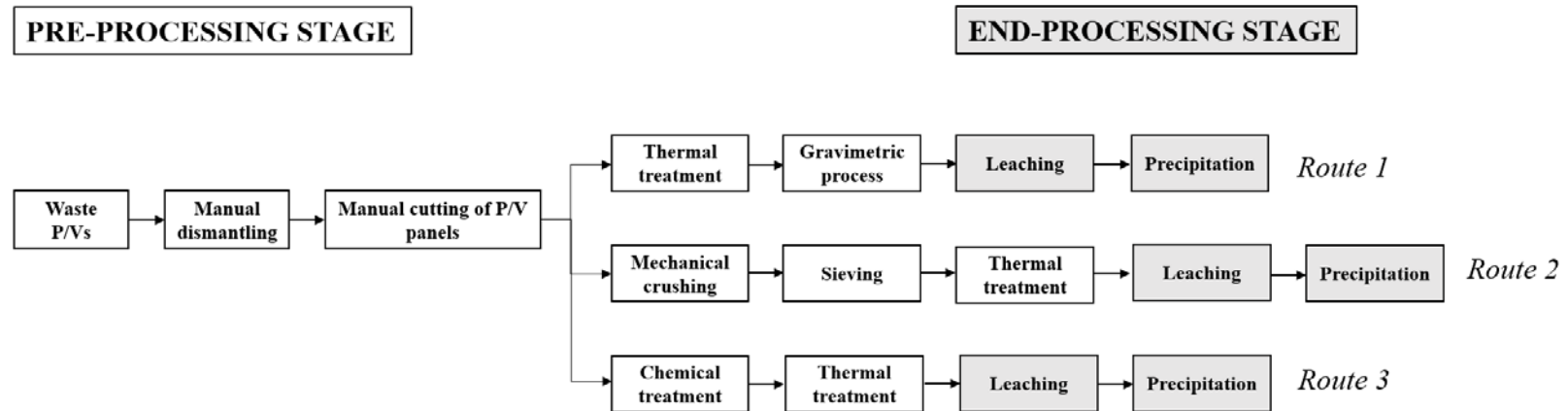


Fig. 4.1: Sketch of the experimental set up

### ***4.2.1 Thermal treatment and gravimetric separation***

After manual cutting, the two crystalline silicon panels were subjected to thermal treatment at 550 °C for 1 h in an electric furnace in order to decompose the intermediate layers of EVA and the back covers (**Fig. 4.1**, Route 1). At this temperature the organic layers (EVA, organic dyes, organic polymers, etc.) were decomposed resulting in a solid residue mainly composed of glass and cells. The decomposition of EVA occurred in two stages; the first stage was deacetylation leading to acetic acid. The second stage was random/chain scissions, releasing mainly propane, propene, ethane, butane, hexane-1 and butane-1 (Granata et al., 2014). After the thermal treatment, a separation between glass and cells containing Ag was achieved based on their densities. Actually, the mixture of glass and cells was placed to a liquid with an intermediate density; after agitation the denser glass was accumulated on the bottom of the separator funnel as heavy product, while the less dense cells were floated on top of the liquid (light product). High density liquid, namely, 1,1,2,2, tetrabromoethene ( $2.97 \text{ g/cm}^3$ ), purchased by Sigma Aldrich, was used by adjusting its density to  $2.40 \text{ g/cm}^3$  with addition of acetone ( $0.8 \text{ g/cm}^3$ ).

Accordingly, the CIS panel was thermally treated at 500 °C for 1 h. The delamination of the panel structure was successfully occurred, resulting in the two structural glasses, namely clear glass and indium-tin oxide (ITO) coated glass. The latter glass serves as a substrate for the deposition of transparent conductive oxides (TCO). The separation between the clear glass and ITO coated glass that is rich in In, was carried out through a density-based process, as previously mentioned for c-Si panels. The density of 1,1,2,2, tetrabromoethene was adjusted to  $2.54 \text{ g/cm}^3$ . The denser (ITO coated) glass was sunk to the bottom of the separator funnel (heavy product), while the less dense (clear) glass was floated on top of the liquid as light product. The content of Ag or In in the heavy and light product was determined by microwave-assisted acid digestion and inductively coupled plasma mass spectrometry (ICP-MS) analysis on the produced separated fractions.

#### ***4.2.2 Mechanical crushing, sieving and thermal treatment***

Another route explored at the pre-processing stage is mechanical crushing and sieving followed by thermal treatment (**Fig. 4.1**, Route 2).

EVA appears flexibility, resilience, crack resistance and ductility as compared to glass which is considered as a brittle material (Alsaed and Jalham, 2012). Taking into account the mentioned characteristics, the panels were subjected to mechanical crushing in a blade rotor with a stainless steel bowl and the produced material was sieved in order to determine the mass distribution and evaluate if the target metals are concentrated in some of the size fractions. Based on the panel technology, it was estimated that glass would be crushed and separated from the cells due to their encapsulation with EVA in the case of crystalline silicon panels. On the other hand, separation between the two structural glasses (clear glass and ITO coated glass) and the intermediate EVA layer was expected in the case of CIS panel crushing. The optimal duration of milling lasted 30 and 45 sec for c-Si and CIS panels, respectively. The mentioned durations were adequate for panel delamination. The time was different based on the comminution process that depended on each panel technology and structure.

The produced material was sieved using five different meshes of 8.00, 1.40, 1.00, 0.500 and 0.250 mm in order to determine which size fraction would present the highest Ag or In content, as well as estimate the potential mass losses using ICP-MS analysis. Specifically, for crystalline silicon panels, it was anticipated that Ag would be found in between the EVA layers in the size fraction >8.00 mm. The largest size fraction was therefore subjected to thermal treatment at 550 °C in order to remove the EVA layers and proceed ICP-MS analysis. For CIS panel, EVA pieces also remained at the mesh of 8.00 mm and were subjected to thermal treatment at 500 °C in order to determine if they were contaminated with some portion of In.

It should be noted that the selection of this type of mill, blade rotor, for the mechanical crushing was based on prior exhaustive tests using different equipment, namely ring mill and cutting mill. However, using ring mill the disintegration of panel pieces was more complicated because of some glass adherence with EVA pieces,

imbedding the efficiency of comminution process. Also, cutting mill led to cutting of EVA producing two size fractions both consisted of glass and EVA, as it is equipped with a sieve mesh (250  $\mu\text{m}$ ). It was therefore estimated that in both processes the resulting crushed-glass fraction was contaminated with the encapsulation layer, allowing recovery of low purity materials or requiring a further processing step.

### ***4.2.3 Chemical and thermal treatment***

Chemical and thermal treatment was another route tested (**Fig. 4.1**, Route 3).

The chemical treatment of panels was explored using toluene or ethyl lactate, anticipating swelling or dissolution of EVA. Earlier studies have shown that toluene exhibits high efficiency in terms of panel delamination resulting in swelling or dissolution of EVA under certain conditions (i.e. time, temperature, etc.) (Doi et al., 2001; Kang et al., 2012; Kim and Lee, 2012). As far as ethyl lactate is concerned, it is a biodegradable solvent with properties similar to those of toluene, whereas it is less toxic than toluene. Ethyl lactate has not so far been used for the removal of EVA. Apart from the type of solvent, various conditions were investigated, such as the temperature (25-90  $^{\circ}\text{C}$ ), the stirring (0, 500 rpm) and the time of exposure (up to 30 d).

In the case of crystalline silicon panels, the chemical treatment resulted in swelling of EVA and subsequent separation of glass from the other components (cells encapsulated with EVA). It must be noted that the separation of the components was feasible only by optical observation and manual sorting. The swelled material, including cells that contain Ag, was thermally treated at 550  $^{\circ}\text{C}$  to remove EVA and thus obtain cells without any contamination. On the other hand for CIS panel, the chemical treatment using ethyl lactate resulted in separation of the two glasses both contaminated with organics, i.e. EVA or other polymeric layers, requiring decomposition through a thermal process, while the chemical treatment using toluene led to delamination and separation of both glasses from EVA and other organic layers, thus requiring a density-separated process to recover the ITO coated glass and clear glass separately. **Fig. 4.2** illustrates the chemically treated and separated through manual sorting components.

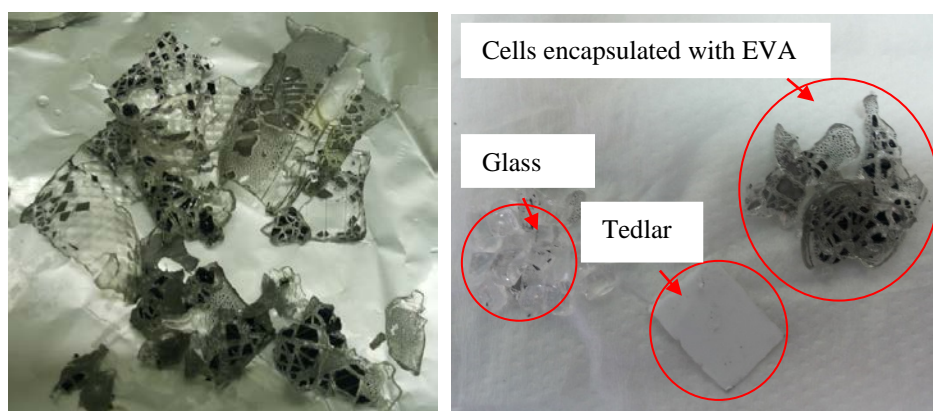


Fig. 4.2: Components produced after chemical treatment and manual sorting

#### ***4.2.4 Microwave-assisted digestion and ICP-MS analysis***

The efficiency of each treatment route was evaluated based on the content of Ag or In in the produced treated fractions. All samples were digested in a microwave Mars 6 CEM reactor. 100 mg of solid sample was diluted into a solution of 10 mL HNO<sub>3</sub> at 180 °C. The content of Ag and In was measured using ICP-MS. The detection and quantification limits were, 3.11 and 10.4 µg/L for Ag and 0.384 and 1.28 µg/L for In, respectively. All measurements were made at least in triplicate. The results were expressed as mg of Ag or In per kg of P/V panel (mg/kg). Also, the treated panel mass was determined (in wt%) as compared to the initial mass used (before treatment) in order to calculate the potential losses of Ag or In during each treatment route. It must be noted that the treated panel mass is decreased during processing, however, this does not mean that the other fractions are definitely lost; for instance, the non-containing Ag or In fraction may be suitable for different reuse purposes (e.g. for glass or aluminum recycling industry).

#### ***4.2.5 Leaching tests***

At the end-processing stage, Ag and In were recovered through leaching and precipitation. It should be noted that during the last years integrated hydrometallurgical processing for recovering critical and precious contained in e-scrap has widely attained much more attention than pyrometallurgical processing (Cui and Zhang, 2008). In this study, batch leaching experiments were performed to investigate the leaching capacity of Ag

contained in p-Si and m-Si cells into acid solutions of H<sub>2</sub>SO<sub>4</sub> (30%) or HNO<sub>3</sub> (30%) at temperatures of 20 or 40 °C with a solid:liquid ratio of 0.02 under mild agitation (150 rpm). The solutions were sampled at 15 min intervals for 60 min, whereas the cells used were ground to pass from a 250 µm sieve. Accordingly for In, the CIS powder was immersed into 1 M H<sub>2</sub>SO<sub>4</sub>, at 90 °C (Silveira et al., 2015) using various S:L ratios, namely 0.01 (1 g:100 mL), 0.02 (2 g:100 mL) and 0.05 (5 g:100 mL), at a stirring rate of 500 rpm for 1 h. Previous studies have concluded that acid concentrations higher than 1 M H<sub>2</sub>SO<sub>4</sub> were not required for In, as its leaching efficiency was not improved from 1 to 6 M (Yang et al., 2013). All experiments were made on a heater plate with a magnetic stirrer and carried out at least in triplicate. A thermometer was installed to obtain constant temperature through experiments. After leaching, the solutions were filtered and stored for analysis using ICP-MS. The leaching capacity (R, mg-element/kg-LCD) was calculated using the initial mass sample (M), the volume of the acid solution used (V) and the concentration of Ag or In into the leachate (C) according to the formula provided in a previous work (Savvilotidou et al., 2015). Also, leaching efficiency was calculated by dividing the weight of Ag or In leached by the weight of Ag or In contained initially in the starting sample (Lee et al., 2013). The leaching efficiency was confirmed by subsequent total digestion of the solid residue (after leaching) in order to compare the concentration of the dissolved Ag or In in the leachate and the non-leached content of the P/V powder, thus obtaining full confirmation of the results.

#### ***4.2.6 Precipitation tests***

The obtained optimal leaching solutions were subjected to precipitation tests. Specifically, for c-Si panels selective recovery of Ag was performed using HCl as precipitating agent; 3 mL of HCl was gradually added into Ag-leachates of 15 mL. For recovering In from CIS panel, precipitation was performed when NH<sub>4</sub>OH was slowly added into the filtered leachates (Silveira et al., 2015) and pH was adjusted between 7.0 and 7.2. After stabilization of pH, the solutions were left for 24 h in order to obtain a precipitate of In<sub>2</sub>O<sub>3</sub>.

Ag and In amount were analyzed using ICP-MS before and after the precipitation tests in order to determine the precipitated amount. The precipitates were collected in filters and their weight was measured. Then, the precipitates on the top of filters were dissolved in high grade dense acid solution for full confirmation of the results. The precipitation efficiency was determined based on the weight of Ag or In in the leachate solution before and after precipitation (Lee et al., 2013).

## 4.3 Results and discussion

### 4.3.1 Thermal and density-based separation process

Pre-concentration of Ag or In in the treated fractions is very important in order to apply an economically viable recovery of these metals, considering that their content in P/Vs is very low, namely 0.004-0.006% Ag and 0.02% In in c-Si and CIS panels, respectively (Paiano et al., 2015). Referring to Ag amount in c-Si panels, other literature sources have mentioned considerably larger quantities, such as 0.053% (Latunussa et al., 2016).

After the decomposition of organics through thermal treatment of c-Si panels, a mixture of glass and cells remained. The content of Ag in the produced thermally treated residue, the manually separated cells and glass (in mg/kg) is shown in **Table 4.1**. Ag content in the mixed residue (glass and cells) was estimated to be 1181 mg/kg treated p-Si panel mass and 1069 mg/kg treated m-Si panel mass. It must be noted that these Ag values refer to 81.16% panel mass based on the typical composition of c-Si panels provided in literature, i.e. 77.16 and 4% average mass of glass and cells for c-Si panels (Tammaro et al., 2015; Paiano et al., 2015). Apart from the mixed residue, **Table 4.1** shows the content of Ag in the glass or cells as separated after optical observation and manual sorting<sup>4</sup>. It is shown that cell is a great source of silver, as p-Si and m-Si cells contain 2.40 and 2.17% Ag respectively, whereas glass is not composed of Ag.

---

<sup>4</sup> The purpose of manual sorting was to determine the accurate Ag content in the targeted materials, glass and cells. The values therefore represent the initial content of Ag in these materials, enabling determination of Ag pre-concentration/losses during the proposed treatment routes. As a result, if lower values occur after treatment steps, it is due to impurities, i.e. cell contaminated with EVA or glass, or losses during operation, reducing the quality of the recovered material.

**Table 4.1: Content of Ag (mg/kg, dry matter) in the main components of p-Si and m-Si panels after thermal treatment**

	Cell	Glass	Mixed residue
p-Si panel			
Treated p-Si panel mass (%)	4*	77.16*	81.16
mg Ag/kg treated p-Si panel	23960±369	<DL	1181±43**
m-Si panel			
Treated m-Si panel mass (%)	4*	77.16*	81.16
mg Ag/kg treated m-Si panel	21691±168	<DL	1069±79**

\*Literature value, \*\*Estimated value

Based on the obtained results, and the fact that crystalline silicon panels are also composed of Al (10.30%), polymers (6.55%), backing film (3.60%) and other components described by Paiano et al. (2015), it was assumed that p-Si panel contains 958 mg Ag/kg and m-Si panel presents 868 mg Ag/kg, respectively. These Ag values are close to those provided in literature (635 mg Ag/kg; Dias et al., 2016b or 8.2-8.8 g/m<sup>2</sup>; García-Olivares, 2015 and Domínguez and Geyer, 2018). Also, it is noteworthy that the amount of Ag in c-Si panels corresponds to that of high grade mineral reserves (1100-800 mg/kg) (Sverdrup et al., 2014), making its secondary production from waste panels very challenging.

Since manual sorting is not considered as a viable process in large scale, the mixed residues were alternatively treated based on a density-separation method using a liquid of 2.40 g/cm<sup>3</sup>, resulting in efficient separation between glass and cells, as shown in **Table 4.2**. It was observed that Ag was concentrated in the light product (cells), as expected, while its amount in the heavy product (glass) was considerably low, namely 4 and 10 mg/kg. Through the gravimetric process, more than 99% of the treated mass was separated. The mass losses may be attributed to agglomeration phenomena among the particles with small size, as they tend to adhere together and form larger agglomerated particles after collision (Savvilotidou et al., 2019; Zhuang et al., 2012). These mass losses, namely 0.3 and 0.8%, correspond to 8.58 and 5.74% Ag losses for p-Si and m-Si panels respectively; accordingly, the pre-concentration yields were 91.42 and 94.25%,

and they were determined based on the content of Ag after the gravimetric process in the treated panel mass divided by the initial Ag content in the panel.

**Table 4.2: Content of Ag (mg/kg, dry matter) after gravimetric separation of the thermally treated p-Si and m-Si panels**

	Heavy Product (Glass)	Light Product (Cell)
p-Si panel		
Treated p-Si panel mass (%)	77.10	3.741
mg Ag/kg treated p-Si panel	4±1	23422±228
m-Si panel		
Treated m-Si panel mass (%)	76.70	3.790
mg Ag/kg treated m-Si panel	10±1	21577±109

The results for CIS panel were different although the same treatment route was applied. This is attributed to the different panel structure. The content of In in a typical CIS panel is 0.02% compared to the major components, i.e. glass 84%, Al 12% and polymers 3% (Paiano, 2015). The external Al frames and polymers were removed through dismantling and thermal treatment, resulting in a treated fraction composed of glass and indium (84.02% of the original CIS panels mass).

At a first sight, after delamination through thermal treatment, the two glass substrates could be separated by optical observation and manual sorting. **Table 4.3** shows the content of In in the two separate glasses (ITO coated glass and clear glass) and their mixture after thermal treatment. The content of In in the mixture was estimated to be 248 mg/kg treated panel mass.

**Table 4.3: Content of In (mg/kg, dry matter) in the main components of CIS panel after thermal treatment**

	ITO coated glass	Clear glass	Glass mixture
Treated CIS panel mass (%)	35.82	48.20	84.02*
mg In/kg treated CIS panel	582±8	<DL	248±20**

\*Literature value, \*\* Estimated value

**Table 4.4: Content of In (mg/kg, dry matter) after gravimetric separation of the thermally treated CIS panel**

	<b>Heavy Product (ITO coated glass)</b>	<b>Light Product (Clear glass)</b>
Treated CIS panel mass (%)	35.71	48.17
mg In/kg treated CIS panel	561±2	<DL

The ITO coated glass (with embedded semiconductor layer) was rich in In (582 mg/kg) containing 0.0582% In in 35.82% treated panel mass, whereas the clear glass substrate did not contain In. It may be assumed that CIS panel contains around 0.0208% In, which is completely in accordance with literature sources (Paiano et al., 2015). Finally, it is noteworthy to mention that In amount is larger in CIS panel (208 mg/kg) than its amount contained in mineral reserves (10–20 mg/kg) (Savvilotidou et al., 2019), reinforcing its secondary production from waste panels.

After thermal treatment, the two glasses were efficiently separated from each other based on their densities, through a physical densimetric approach. The results are shown in **Table 4.4**.

It is revealed that when the thermally treated CIS (glasses) was immersed into 1,1,2,2 tetrabromoethene with a fixed density of 2.40 g/cm<sup>3</sup>, the ITO coated glass was concentrated in the bottom of the liquid (heavy product) and the clear glass was remained in the surface, because of their densities. The selection of liquid density was based on preliminary tests; for instance, when density was controlled to 2.65 g/cm<sup>3</sup>, glass and cells were both floated in the surface. The present density-based separation method for the separation of glass and cells is rather simple and quick, while the solution can be reutilized compared to manual sorting, adopted by Deutsche Solar. The separation of the two glasses was considered quite efficient, as 99.86% of the treated mass was separated. The losses of CIS mass were 0.14% due to some agglomerated material that tended to remain between the top and bottom phases, consisting In losses of 3.90%. The pre-concentration yield of In was therefore 96.10%. It was determined based on the content of In after the gravimetric process in the treated CIS panel mass divided by the initial In content in the untreated CIS panel.

### ***4.3.2 Mechanical crushing, sieving and thermal process***

**Table 4.5** shows the results after mechanical crushing and sieving for the p-Si and m-Si panels. During this process, the components involved were glass, resin and target cells consisting 87.9% of the panels mass. Apart from the content of Ag, the percentage of mass in which Ag was found is presented in order to observe the mass flow of the target metal among the size fractions.

It is seen that a large amount of Ag is concentrated in the finest fraction (<0.250 mm), which represents up to 24% of the initial panels mass. On the other hand, the intermediate fractions do not contain high amount of Ag and in some of them the amount is negligible (below the detection limit). It is then assumed that this fraction probably corresponds to glass and is not suitable for subsequent leaching and precipitation of Ag. Also, it is observed that as the particle size decreases, the amount of Ag increases. Dias et al. (2016a) also found that Ag from crushed panels is accumulated in the smallest particle size (<0.500 mm) compared to those between 1.00 and 0.500 mm or bigger than 1.00 mm. In all the fractions with size lower than 8.00 mm, the total Ag content is only 1.87 and 2.34% for p-Si and m-Si, respectively. As a result, the largest fraction (>8.00 mm) was expected to present the major Ag portion encapsulated with EVA layers. In this case the amount of Ag was determined after thermal treatment to liberate the cells, and thus Ag. The Ag amount at this fraction was considerably high, i.e. 3841 and 3635 mg/kg for p-Si and m-Si panels, respectively. It was deduced that Ag can be recovered by thermal treatment of the largest fraction that contains cells and EVA, while the losses of treated panel mass during mechanical crushing, sieving and thermal treatment are equal to 0.39 and 0.75% for the p-Si and m-Si panels; also, the pre-concentration yields are 89.01 and 89.11%, respectively.

**Table 4.5** shows the results after mechanical crushing and sieving for the CIS panel. The initial mass used at this stage was 87.02% including glass 84%, polymers 3% and indium 0.02% (Paiano, 2015). Apart from the content of indium also the treated CIS mass (%) is provided in order to determine In losses and pre-concentration. The CIS mass losses were 0.63% coming from some material that was not easy to be collected

after crushing and was removed through blade rotor cleaning; the mass losses were mitigated due to the closed milling system. **Table 4.6** also reveals that the majority of In is found in the finest particles (<0.250 mm) in agreement with literature sources (Ferella et al., 2017); however, its amount is very low because it refers to 16.06% of the mass share. Some smaller amount is also distributed in the intermediate layers.

At a first sight, mechanical crushing and sieving reduces the possibilities of efficient and high recovery of In, even if organic layers are separated. This is because In is not anymore located in the ITO coated glass, but it is distributed into the produced crushed material consisting of both glasses. The results also showed that there was an amount of CIS mass (18.19%) which was consisted by a polymeric layer and some retained films. This material, as retained in meshes with size pores of 8.00 mm, was subjected to thermal process (500 °C for 1 hour) in order to recover the remaining glass and/or films and evaluate In content. Almost 75.95% of In content was anticipated to present in the films attached to EVA in the largest fraction (>8.00 mm). This was confirmed by the thermal treatment. The content of In was 779 mg/kg, which is almost four-fold higher than the initial content in the CIS panel. Pre-concentration yield was 68.1% with In losses around 7.85%.

**Table 4.5: Content of Ag (mg/kg, dry matter) after mechanical crushing of p-Si and m-Si panels for 30 sec in a blade rotor and sieving**

	<b>Product &gt;8.00 mm *</b>	<b>Product &lt;8.00 and &gt;1.40 mm</b>	<b>Product &lt;1.40 and &gt;1.00 mm</b>	<b>Product &lt;1.00 and &gt;0.500 mm</b>	<b>Product &lt;0.500 and &gt;0.250 mm</b>	<b>Product &lt;0.250 mm</b>
p-Si panels						
Treated p-Si panel mass (%)	22.21	3.675	2.422	15.24	18.94	24.22
mg Ag/kg treated p-Si panel	3841±15	<DL	48±1	13±0	13±0	51±0
m-Si panels						
Treated m-Si panel mass (%)	21.27	4.210	3.480	14.38	20.85	21.76
mg Ag/kg treated m-Si panel	3635±95	<DL	<DL	<DL	37±9	58±4

\* After thermal treatment

**Table 4.6: Content of In (mg/kg, dry matter) after mechanical crushing of CIS panel for 45 sec in a blade rotor and sieving**

	<b>Product &gt;8.00 mm *</b>	<b>Product &lt;8.00 and &gt;1.40 mm</b>	<b>Product &lt;1.40 and &gt;1.00 mm</b>	<b>Product &lt;1.00 and &gt;0.500 mm</b>	<b>Product &lt;0.500 and &gt;0.250 mm</b>	<b>Product &lt;0.250 mm</b>
Treated CIS panel mass (%)	18.19	3.220	2.872	19.58	22.45	16.06
mg In/kg treated CIS panel	779±4	<DL	28±0	22±1	97±1	190±3

\* After thermal treatment

### 4.3.3 Chemical and thermal process

The results after chemical treatment for c-Si panels are shown in **Table 4.7**. It was observed that toluene caused swelling of EVA contributing on the separation of glass from the P/V structure, even at room temperature. Similar behavior was observed by Kang et al. (2012) within 7-14 days. In the present study, less time of exposure can be attributed to the use of small panel pieces, enhancing the interface between solvent and EVA, as well as due to stirring (Savvilotidou et al., 2017). On the other hand, delamination using ethyl lactate occurred under stirring and heating at 90 °C, while at lower temperatures defects on the panel pieces were observed, possibly due to the extensive time of exposure (1 d). In spite of swelling, dissolution of EVA was not possible at the studied conditions for both solvents, thus requiring thermal treatment of swelled EVA that contained the cells rich in Ag. Prior to thermal treatment, manual sorting was required due to the characteristics of the treated panels (inefficient separation through sieving due to the non-homogenized produced sample, see **Fig. 4.2**), revealing that chemical treatment involves some technical limitations even in small scale experiments.

**Table 4.7: Delamination of p-Si and m-Si panels after chemical treatment**

Solvent	Temperature (°C)	Stirring (rpm)	Time of exposure	Delamination
Ethyl lactate	25	0, 500	30 d	-
	55	0, 500	24 h	-
	75	0, 500	24 h	-
	90	0, 500	12 h, 1.5 h	Non complete, Complete
Toluene	25	0, 500	2 h	Complete
	90	0, 500	1.5 h, 1 h	Complete

The results after the chemical treatment of CIS panel are shown in **Table 4.8**. Toluene was more efficient in EVA swelling compared to ethyl lactate in terms of time and temperature. It should be noted that in the case of toluene the swelling was observed

by the first 15 min, while in the case of ethyl lactate progressive improvement in swelling was considerably slower and not so profound.

**Table 4.8: Delamination of CIS panel after chemical treatment**

Solvent	Temperature (°C)	Stirring (rpm)	Time of exposure	Delamination
Ethyl lactate	25	0	30 d	Complete
	90	500	1 d	Complete
Ethyl lactate 1 M	25, 55, 75, 90	0, 500	1 d	-
Ethyl lactate 3 M	25, 55, 75, 90	0, 500	1 d	-
Toluene	25	0, 500	2 d, 5 h	Complete
	90	0, 500	1.5 h, 1 h	Complete

While toluene resulted in separation of both glasses (clear glass and ITO coated glass) from organics, ethyl lactate resulted in two separated layers, namely the one consisting of the clear glass with EVA and the other one consisting of the ITO coated glass and some intermediate organic layer. In first case, after removal of the two glasses, their mixture may be separated through a gravimetric process, as previously described for route 1. In second case, the produced materials can be separately subjected to thermal treatment in order to decompose organics and obtain ITO coated glass, as well as clear glass, with a perspective of selling the clear reusable glass and recovering In from the ITO coated glass through leaching and precipitation. Although, the effect of toluene was more drastic and quicker, and delamination was carried out within 1 h at 90 °C, ethyl lactate is considered as a more preferable solvent by an environmental point of view. Further experiments were made using ethyl lactate or toluene with the assistance of ultrasonic irradiation. The results (data not shown) were though very poor and no difference was observed, although Kim and Lee (2012) showed that EVA was dissolved in 3 M toluene at 70 °C because of cavitation phenomena.

**Table 4.9** shows the content of Ag and In after chemical and thermal treatment of p-Si, m-Si and CIS panels. First of all, it can be observed that the losses of Ag and In were very low, namely, 5.36, 2.98 and 1.49% for p-Si, m-Si and CIS panels, achieving pre-concentration yield of 94.64, 97.02 and 98.51%, respectively. However, the potential

mass losses of Ag or In during this treatment route in large scale would be considerably higher, inhibiting the targets for efficient recycling of Ag or In. Note that the obtained results refer to small panel pieces, i.e. 2 cm × 2 cm, that allowed an efficient manual sorting of the cells encapsulated with EVA or the ITO coated glass prior to thermal treatment. Thus, an automate sorting of the target components using appropriate equipment would be required for potential industrial applications.

**Table 4.9: Content of Ag and In (mg/kg, dry matter) after chemical and thermal treatment of panels**

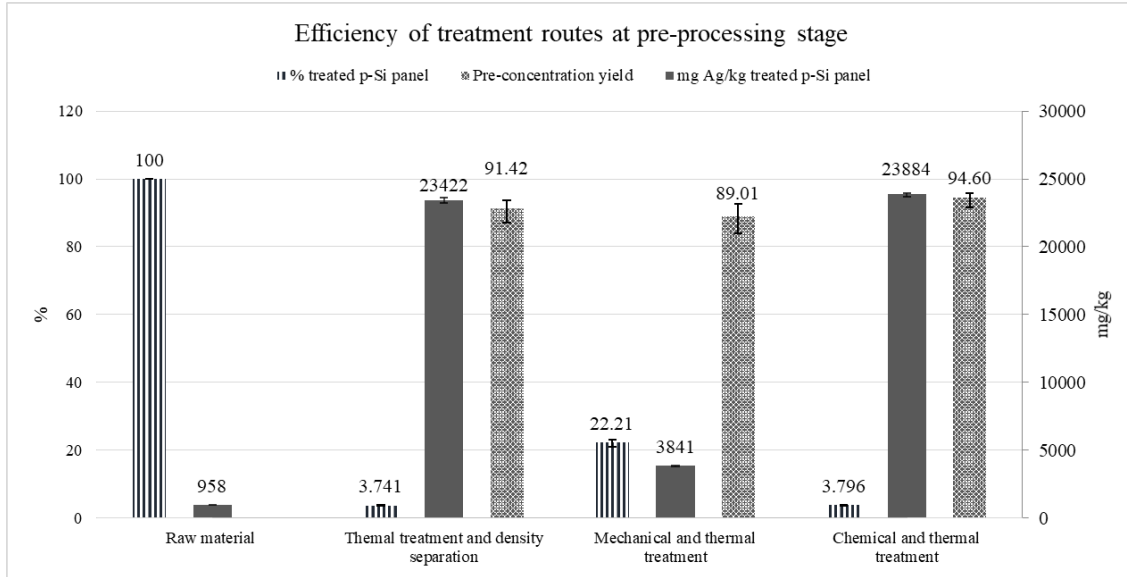
	Chemically and thermally treated residue
p-Si panel	
Treated p-Si panel mass (%)	3.796
mg Ag/kg treated p-Si panel	23884±25
m-Si panel	
Treated m-Si panel mass (%)	3.892
mg Ag/kg treated m-Si panel	21653±31
CIS panel	
Treated CIS panel mass (%)	35.82
mg In/kg treated CIS panel	572±3

#### ***4.3.4 Efficiency of treatment routes at the pre-processing stage***

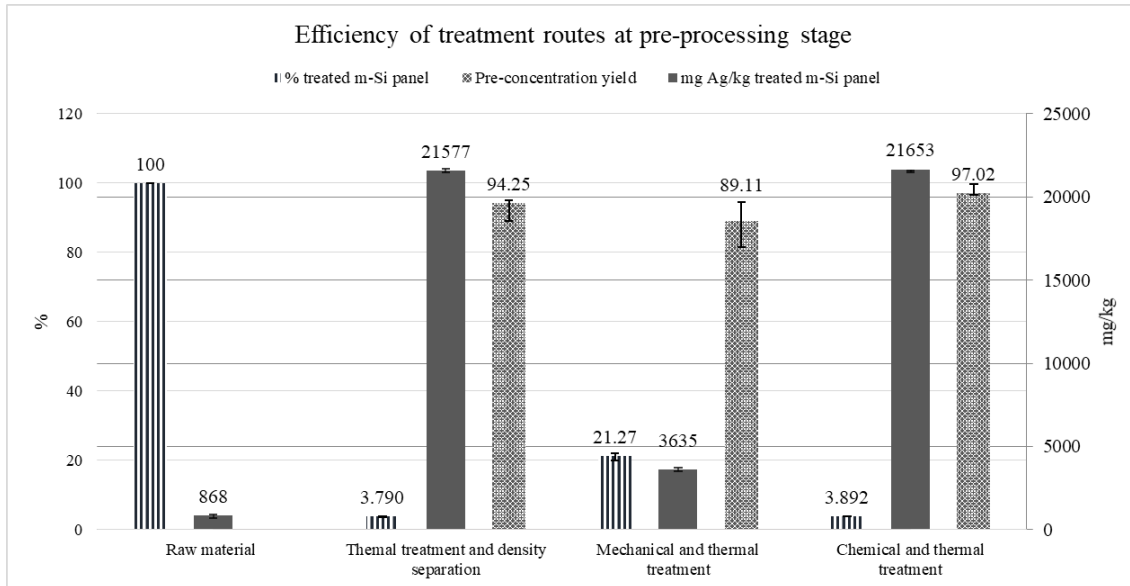
**Fig. 4.3** illustrates a direct comparison on the efficiency of the three treatment routes tested for the waste panels. The efficiency is based on the pre-concentration yield of Ag or In. The average Ag or In content (mg/kg) and its variability are also illustrated per treatment route as determined in the treated panel mass (wt%). It must be noted that for Route 2 (mechanical crushing, sieving, thermal process), only the size fraction >8.00 mm is shown.

The findings demonstrate that thermal treatment followed by a density-based separation process (Route 1) is the most efficient treatment route leading to 91.42 and 94.25% Ag pre-concentration for p-Si and m-Si panels, as well as to 96.31% In pre-concentration for CIS panel. On the other hand, Route 2 that involves mechanical

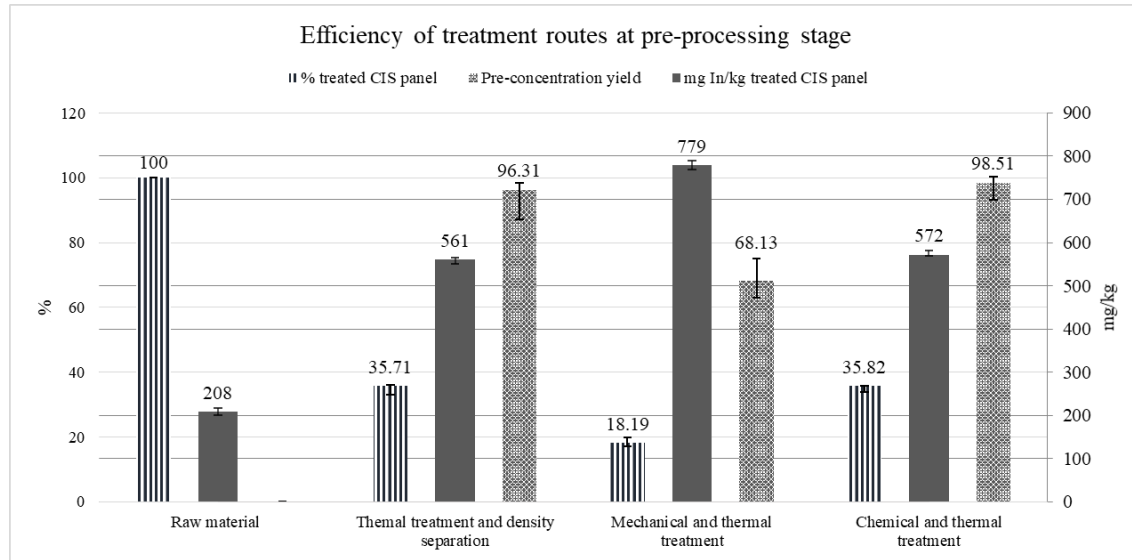
crushing, sieving and thermal process resulted in pre-concentration yield up to 89.11%. This yield is though mainly attributed to the high panel mass in which the metal was distributed and not to the high amount of Ag, i.e. enrichment.



(a)



(b)



(c)

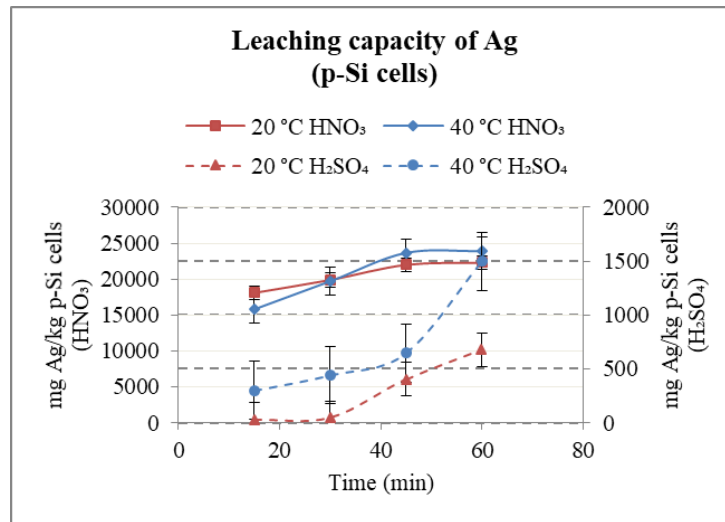
Fig. 4.3: Efficiency comparison of treatment routes in terms of Ag or In pre-concentration (minimum, mean, maximum values) among (a) p-Si panel, (b) m-Si panel, and (c) CIS panel (route 1: thermal treatment at 550 or 500 °C and gravimetric separation (light product for c-Si, heavy product for CIS), route 2: mechanical crushing, sieving (particle size >8.00 mm) and thermal treatment, route 3: chemical (toluene at 25 °C for c-Si panels, ethyl lactate at 25 °C for CIS panel) and thermal treatment)

Specifically, considering that mechanical crushing, sieving and thermal process (Route 2) do not result in intact and directly reusable products, but in materials heavily contaminated, as well as that chemical and thermal process (Route 3) appears technical difficulties (treatment speed, etc.), is high energy intensive and anticipates considerable wastewater volumes, the treatment route that involves a thermal process, followed by gravimetric separation is technically the most efficient route among those tested in the present study.

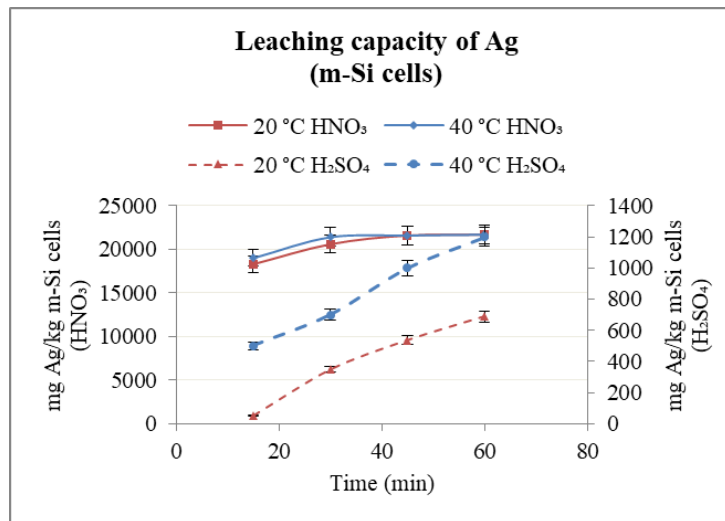
The above results are drawn based on the specific laboratory equipment used, making it difficult to estimate the efficiency of the treatment routes in larger scale. Also, to ensure competitiveness for the treatment technologies, economic and environmental aspects must be addressed. Overall, it is believed that a mitigation of metal losses during the pre-processing stage of waste panels is substantially required in order to achieve economically viable secondary production of silver or indium.

#### 4.3.5 Selective recovery of Ag and In through leaching and precipitation

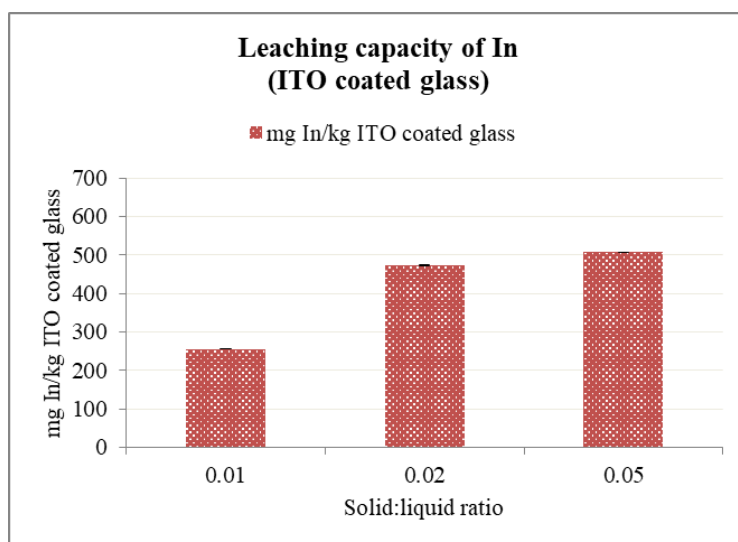
Fig. 4.4a,b illustrates the profile of leaching capacity for Ag using 30% HNO<sub>3</sub> or H<sub>2</sub>SO<sub>4</sub> at temperatures 20 or 40 °C and leaching time of 1 h. Maximum leaching capacity of Ag was observed using HNO<sub>3</sub> as leaching agent compared to H<sub>2</sub>SO<sub>4</sub> within 1 h both for p-Si and m-Si cells. According to earlier studies, sulfuric acid and hydrochloric acid do not assist Ag dissolution because they form insoluble salts of silver sulfate or chloride, while HNO<sub>3</sub> dissolves almost all the silver amount within 1 h (Yi et al., 2014).



(a)



(b)



(c)

Fig. 4.4: Leaching capacity of Ag or In from (a) p-Si cells and (b) m-Si cells at 20 or 40 °C using HNO<sub>3</sub> or H<sub>2</sub>SO<sub>4</sub>, or from (c) CIS ITO glass using H<sub>2</sub>SO<sub>4</sub> at different solid:liquid ratios.

Increase of temperature from 20 to 40 °C did not significantly enhanced the leaching capacity rate. Thus, the most effective leaching conditions were 30% HNO<sub>3</sub>, at controlled temperature of 20 °C and constant agitation of 150 rpm. This temperature was considered sufficient to leach more than 93% of the initial Ag content in the case of p-Si cells and around 100% of Ag in the case of m-Si cells (leaching efficiency, **Table 4.10**), whereas in further experiments made in higher temperatures, e.g. 60 and 80 °C (data not shown), a quite similar leaching capacity was achieved. The efficiency of HNO<sub>3</sub> to leach Ag is in agreement with findings of previous studies (Lee et al., 2013).

The dissolved Ag was then recovered through precipitation tests with HCl. Around 0.80 and 1.30% of Ag remained in the solution after precipitation in the case of p-Si and m-Si cells respectively, resulting in precipitation efficiency of approximately 99% for both tested materials after a period of 4 h.

**Table 4.10: Leaching capacity and precipitation efficiency of Ag and In**

	Leaching capacity	Precipitation efficiency (%)
p-Si panel	mg Ag/kg cells 22331±250	99.2
m-Si panel	mg Ag/kg cells 21691±442	98.7
CIS panel	mg In/kg ITO coated glass	
S:L=0.01	256±1	100
S:L=0.02	474±1	75.3
S:L=0.05	508±0	74.8

Referring to In, **Fig. 4.4c** and **Table 4.10** show the results of the leaching process using 1.0 M H<sub>2</sub>SO<sub>4</sub> with varying solid:liquid ratios at a constant temperature of 90 °C within 1 h. The maximum leaching capacity, 508 mg/kg, was achieved using a solid to liquid ratio of 0.05, corresponding to 87.3% leaching efficiency (by dividing this value with the initial In amount in the powder of ITO coated glass). Rather lower leaching capacity, namely 81.4%, was also reached when solid:liquid ratio was 0.02. Specifically, the results showed that as the solid:liquid ratio increases, the leaching capacity also increases. This tendency was also observed in a previous study focused on In leaching capacity (Savvilotidou et al., 2015). The precipitation efficiency was 75.3 and 74.8% having 0.05 and 0.02 solid:liquid ratio, respectively, as in both cases there was some In amount that was not precipitated. Summarizing the results, it was shown that maximum leaching efficiency (87.3%) and precipitation (74.8%) occurs using H<sub>2</sub>SO<sub>4</sub>, with a solid to liquid ratio of 0.05 at 90 °C for 1 hour by adding NH<sub>4</sub>OH as precipitation agent.

#### 4.4 Conclusions

Secondary production of precious or critical metals, such as Ag or In, receives increasing attention due to their criticality (risk of supply and economic importance). Over the past decade, installation of P/V panels has unprecedentedly grown, surpassing all forecasts. On this basis, the large volume of waste panels makes the recovery of target metals a

major challenge to be addressed, following a circular zero-waste economy. So far, recycling technologies, oriented to precious or critical metals, have not been (well) established; therefore, relative research can play a central role in developing future strategic decisions.

In this study, feasible treatment approaches containing various steps were investigated in order to pre-concentrate and recover Ag and In from waste panels and especially p-Si, m-Si and CIS panels. The multi layered panel structure was successfully delaminated by thermal, physical, mechanical or chemical processes, and combinations of them, resulting in limited losses, high pre-concentration yields and then efficient selective recovery of Ag or In at the end-processing stage. Specifically, the results indicated that a thermal process of waste panels, followed by a gravimetric separation process represent the most efficient route for the pre-concentration of Ag or In as compared to other routes tested that involve mechanical or chemical treatment. Ag and In were highly leached (93-100% and 87.3%) using  $\text{HNO}_3$  and  $\text{H}_2\text{SO}_4$ , respectively. Precipitation of  $\text{AgCl}$  and  $\text{In}_2\text{O}_3$  was identified after leaching in  $\text{HNO}_3$  and  $\text{H}_2\text{SO}_4$  with addition of  $\text{HCl}$  and  $\text{NH}_4\text{OH}$  respectively, resulting in 99.2, 98.7 and 74.8% precipitation for the tested p-Si, m-Si and CIS panels.

For the first time a comprehensive comparison between different treatment routes for waste panels was developed providing valuable insights on the recovery of semiconductor material. The present findings can be very useful for the integration of a circular waste management that will consider the secondary production of precious and critical metals, and especially silver and indium, closing the loop.

## 4.5 References

- Alsaed, O., Jalham, I.S., 2012. Polyvinyl Butyral (PVB) and Ethyl Vinyl Acetate (EVA) as a Binding Material for Laminated Glass. *Jordan J. Mech. Ind. Eng.* 6(2), 127-133.
- Ashfaq, H., Hussain, I., Giri, A., 2017. Comparative analysis of old, recycled and new PV modules. *J. King Saud Univ., Eng. Sci.* 29(1), 22-28.

- Berger, W., Simon, F.G., Weimann, K., Alsema, E.A., 2010. A novel approach for the recycling of thin film photovoltaic modules. *Resour. Conserv. Recycl.* 54(10), 711-718.
- Bilimoria, S., Defrenne, N., 2013. The evolution of photovoltaic waste in Europe. *Renewable Energy World*, 5.
- Bio Intelligence Service, 2011. Study on photovoltaic panels supplementing the impact assessment for a recast of the WEEE directive, Final Report.
- Cucchiella, F., Rosa, P., 2015. End-of-Life of used photovoltaic modules: A financial analysis. *Renew. Sust. Energ. Rev.* 47, 552-561.
- Cui, J., Zhang, L., 2008. Metallurgical recovery of metals from electronic waste: a review. *J. Haz. Mater.* 158(2-3), 228-256.
- De-wen, Z., Born, M., Wambachz, K., 2004. Pyrolysis of EVA and its application in recycling of photovoltaic modules. *J. Environ. Sci.* 16(6), 889-893.
- de Wild-Scholten, M.M., 2013. Energy payback time and carbon footprint of commercial photovoltaic systems. *Sol. Energy Mater. Sol. Cells* 119, 296-305.
- Dias, P.R., Benevit, M.G., Veit, H.M., 2016a. Photovoltaic solar panels of crystalline silicon: characterization and separation. *Waste Manage. Res.* 34(3), 235-245.
- Dias, P., Javimczik, S., Benevit, M., Veit, H., Bernardes, A.M., 2016b. Recycling WEEE: extraction and concentration of silver from waste crystalline silicon photovoltaic modules. *Waste Manage.* 57, 220-225.
- Doi, T., Tsuda, I., Unagida, H., Murata, A., Sakuta, K., Kurokawa, K., 2001. Experimental study on PV module recycling with organic solvent method. *Sol. Energy Mater. Sol. Cells* 67, 397-403.
- Domínguez, A., Geyer, R., 2018. Photovoltaic waste assessment of major photovoltaic installations in the United States of America. *Renew. Energy* 133, 1188-1200.
- European Commission, 2017. Communication on the list of Critical Raw Materials for the EU.  
<http://eur-lex.europa.eu/legal-content/EN/ALL/?uri=COM:2017:0490:FIN>  
(last access 26.09.2018).

- Ferella, F., Belardi, G., Marsilii, A., De Michelis, I., Vegliò, F. 2017. Separation and recovery of glass, plastic and indium from spent LCD panels. *Waste Manage.* 60, 569-581.
- Frisson, L., Lieten, K., Bruton, T., Declercq, K., Szlufcik, J., De Moor, H., Goris, M., Benali, A., Aceves, O., 2000. Recent improvements in industrial PV module recycling. 16th European Photovoltaic Solar Energy Conference, 1-5 May, Glasgow, UK.
- Fthenakis, V.M., 2000. End-of-life management and recycling of PV modules. *Energ. Policy* 28(14), 1051-1058.
- García-Olivares, A. 2015. Substituting silver in solar photovoltaics is feasible and allows for decentralization in smart regional grids. *Environ. Innov. Soc. Tr.* 17, 15-21.
- Goe, M., Gaustad, G., 2014. Strengthening the case for recycling photovoltaics: An energy payback analysis. *Appl. Energy* 120, 41-48.
- Goris, M.J.A.A., Rosca, V., Geerligs, L.J., de Gier, B., 2015. Production of recyclable crystalline Si PV modules. 31st European photovoltaic solar energy conference and exhibition, 14-18 September.
- Granata, G., Pagnanelli, F., Moscardini, E., Havlik, T., Toro, L., 2014. Recycling of photovoltaic panels by physical operations. *Sol. Energy Mater. Sol. Cells* 123, 239-248.
- Grandell, L., Thorenz, A., 2014. Silver supply risk analysis for the solar sector. *Renew. Energy* 69, 157-165.
- Hao, H., Lin, K.L., Wang, D., Chao, S.J., Shiu, H.S., Cheng, T.W., Hwang, C.L., 2015. Elucidating characteristics of geopolymer with solar panel waste glass. *Environ. Eng. Manage. J.* 14(1), 79-87.
- Hao, H., Lin, K.L., Wang, D., Chao, S.J., Shiu, H.S., Cheng, T.W., Hwang, C.L., 2013. Utilization of solar panel waste glass for metakaolinite-based geopolymer synthesis. *Environ. Prog. Sustain. Energy* 32(3), 797-803.

- Işıldar, A., Rene, E.R., van Hullebusch, E.D., Lens, P.N.L., 2018. Electronic waste as a secondary source of critical metals: Management and recovery technologies. *Resour. Conserv. Recycl.* 135, 296-312.
- Islam, M.A., Hasanuzzaman, M., Rahim, N.A., Nahar, A., Hosenuzzaman, M., 2014. Global renewable energy-based electricity generation and smart grid system for energy security. *The Scientific World Journal*, Article ID 197136. <http://dx.doi.org/10.1155/2014/197136>.
- Kang, S., Yoo, S., Lee, J., Boo, B., Ryu, H., 2012. Experimental investigations for recycling of silicon and glass from waste photovoltaic modules. *Renew. Energy* 47, 152-159.
- Kim, Y., Lee, J., 2012. Dissolution of ethylene vinyl acetate in crystalline silicon PV modules using ultrasonic irradiation and organic solvent. *Sol. Energy Mater. Sol. Cells* 98, 317-322.
- Klugmann-Radziemska, E., Ostrowski, P., 2010. Chemical treatment of crystalline silicon solar cells as a method of recovering pure silicon from photovoltaic modules. *Renew. Energy* 35(8), 1751-1759.
- Kuczyńska-Łażewska, A., Klugmann-Radziemska, E., Sobczak, Z., Klimczuk, T., 2018. Recovery of silver metallization from damaged silicon cells. *Sol. Energy Mater. Sol. Cells* 176, 190-195.
- Latunussa, C., Mancini, L., Blengini, G., Ardente, F., Pennington, D., 2016. Analysis of material recovery from photovoltaic panels. EUR 27797. Luxembourg (Luxembourg): Publications Office of the European Union. doi:10.2788/786252.
- Lee, C.H., Hung, C.E., Tsai, S.L., Popuri, S.R., Liao, C.H., 2013. Resource recovery of scrap silicon solar battery cell. *Waste Manage. Res.* 31(5), 518-524.
- Lin, K.L., Chu, T.C., Cheng, C.J., Lee, C.H., Chang, T.C., Wang, K.S., 2012. Recycling solar panel waste glass sintered as glass-ceramics. *Environ. Prog. Sustain. Energy* 31(4), 612-618.
- Paiano, A., 2015. Photovoltaic waste assessment in Italy. *Renew. Sust. Energy Rev.* 41, 99-112.

- Powalla, M., Paetel, S., Hariskos, D., Wuerz, R., Kessler, F., Lechner, P., Wischmann, W., Friedlmeier, T. M., 2017. Advances in cost-efficient thin-film photovoltaics based on Cu(In,Ga)Se<sub>2</sub>. *Engineering* 3(4), 445-451.
- Powalla, M., Bonnet, D., 2007. Thin-film solar cells based on the polycrystalline compound semiconductors CIS and CdTe. *Adv. OptoElectron.* 2007, Article ID 97545. doi:10.1155/2007/97545.
- Rimez, B., Rahier, H., Van Assche, G., Artoos, T., Biesemans, M., Van Mele, B., 2008. The thermal degradation of poly (vinyl acetate) and poly (ethylene-co-vinyl acetate), Part I: Experimental study of the degradation mechanism. *Polym. Degrad. Stab.* 93(4), 800-810.
- Rocchetti, L., Amato, A., Fonti, V., Ubaldini, S., De Michelis, I., Kopacek, B., Vegliò, F., Beolchini, F., 2015. Cross-current leaching of indium from end-of-life LCD panels. *Waste Manage.* 42, 180-187.
- Rocchetti, L., Beolchini, F., 2015. Recovery of valuable materials from end-of-life thin-film photovoltaic panels: environmental impact assessment of different management options. *J. Clean. Prod.* 89, 59-64.
- Savvilotidou, V., Antoniou, A., Gidaracos, E., 2017. Toxicity assessment and feasible recycling process for amorphous silicon and CIS waste photovoltaic panels. *Waste Manage.* 59, 394-402.
- Savvilotidou, V., Hahladakis, J.N., Gidaracos, E., 2015. Leaching capacity of metals–metalloids and recovery of valuable materials from waste LCDs. *Waste Manage.* 45, 314-324.
- Savvilotidou, V., Kousaiti, A., Batinic, B., Vaccari, M., Kastanaki, E., Karagianni, K., Gidaracos, E., 2019. Evaluation and comparison of pre-treatment techniques for recovering indium from discarded liquid crystal displays. *Waste Manage.* 87, 51-61.
- Silveira, A.V.M., Fuchs, M.S., Pinheiro, D.K., Tanabe, E.H., Bertuol, D.A., 2015. Recovery of indium from LCD screens of discarded cell phones. *Waste Manage.* 45, 334-342.

- Skripkiūnas, G., Vasarevičius, S., Danila, V., 2018. Immobilization of copper indium selenide solar module waste in concrete constructions. *Cement Concrete Comp.* 85, 174-182.
- Sonia, A., Dasan, K.P., 2013. Celluloses microfibers (CMF)/poly (ethylene-co-vinyl acetate) (EVA) composites for food packaging applications: A study based on barrier and biodegradation behavior. *J. Food Eng.* 118(1), 78-89.
- Sverdrup, H., Koca, D., Ragnarsdottir, K.V., 2014. Investigating the sustainability of the global silver supply, reserves, stocks in society and market price using different approaches. *Resour. Conserv. Recycl.* 83, 121-140.
- Tamaro, M., Rimauro, J., Fiandra, V., Salluzzo, A., 2015. Thermal treatment of waste photovoltaic module for recovery and recycling: Experimental assessment of the presence of metals in the gas emissions and in the ashes. *Renew. Energy* 81, 103-112.
- Tao, J., Yu, S., 2015. Review on feasible recycling pathways and technologies of solar photovoltaic modules. *Sol. Energy Mater. Sol. Cells* 141, 108-124.
- Wade, A., Sinha, P., Drozdiak, K., Brusch, E., 2017. Beyond waste – The fate of end-of-life photovoltaic panels from large scale PV installations in the EU the socio-economic benefits of high value recycling compared to re-use. 33rd European Photovoltaic Solar Energy Conference and Exhibition (EU PVSEC), Amsterdam, The Netherlands.
- Yang, J., Retegan, T., Ekberg, C., 2013. Indium recovery from discarded LCD panel glass by solvent extraction. *Hydrometallurgy* 137, 68-77.
- Yi, Y.K., Kim, H.S., Tran, T., Hong, S.K., Kim, M.J., 2014. Recovering valuable metals from recycled photovoltaic modules. *J. Air Waste Manage. Assoc.* 64(7), 797-807.
- Zhuang, X., He, W., Li, G., Huang, J., Ye, Y., 2012. Materials Separation from Waste Liquid Crystal Displays Using Combined Physical Methods. *Pol. J. Environ. Stud.* 21(6), 1921-1927.



## **5 Reuse of glass and plastic in cement mortars**

This study investigates the use of materials from waste electrical and electronic equipment (WEEE) in the construction sector. The materials examined were glass, obtained from photovoltaic (P/V) panels or liquid crystal displays (LCDs<sup>5</sup>), and plastic obtained from the junction box or the connecting cables attached to the back surface of P/V panels. Each material was mixed with cement, fine aggregates and water to produce cement mortars. Two sets of cement mortars were prepared to replace part of fine aggregates or cement with 10 and 20% glass content. Also, 5 and 10% of fine aggregates were replaced by plastic. Physical, mechanical and thermal properties of cement mortars were determined. Resistance of cement mortars to carbonation, chloride ion penetration and sulfate attack was studied after three months of exposure to corrosive environment. Cement mortars containing glass exhibited high strength (up to 47.5 MPa at 28 days) and resistance to corrosion, attributed to the inherent glass properties. Cement mortars produced by substituting fine aggregates with plastic exhibited low thermal conductivity (0.45-0.68 W/m·K), encouraging their use as insulators in the construction industry.

---

<sup>5</sup> The investigation of LCD was considered for comparison reasons, as well as due to its increasing utilization in cement mortars according to recent literature. It must be noted that the treatment of waste LCDs and P/V panels is based on similar technologies, since they present a similar multilayer structure consisting of glass, polymers, critical metals, etc.

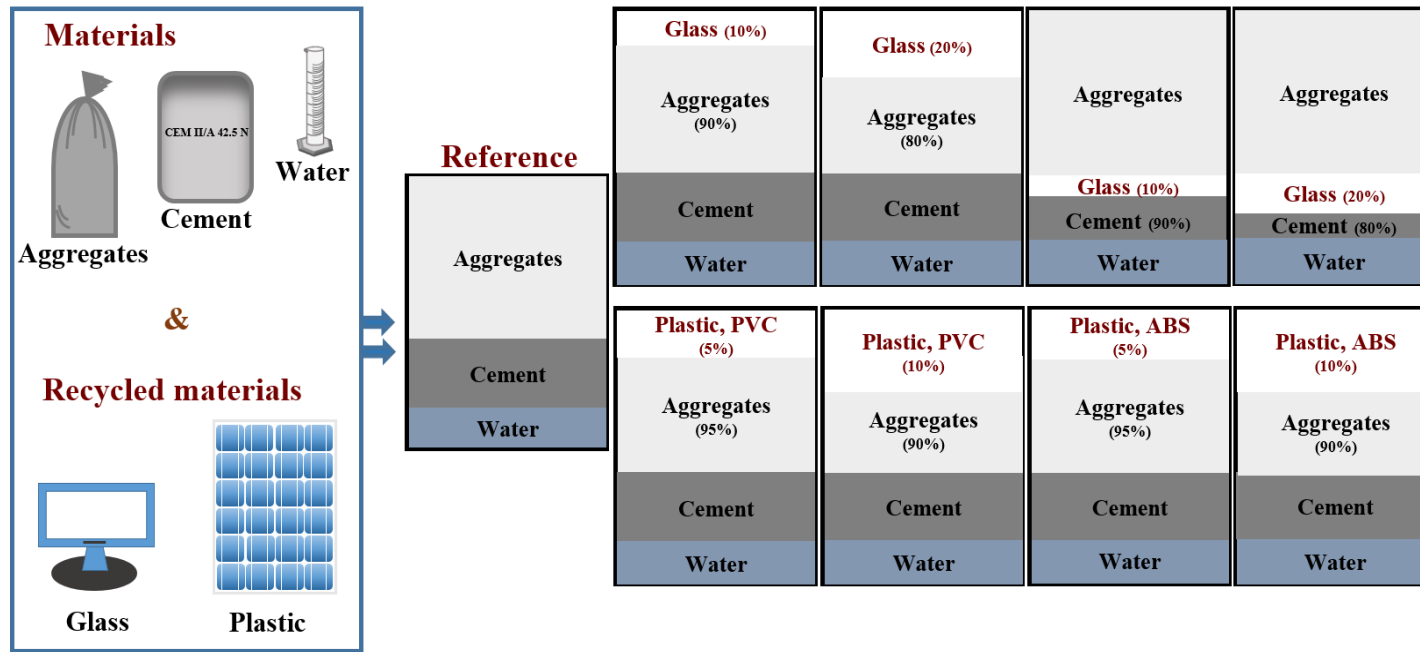


Fig. 5.1: Schematic diagram of the experimental methodology

## 5.1 Overview

Glass is a non-crystalline, amorphous material that finds application in several industrial sectors. Its global production was 115 million tonnes in 2007 (Wintour, 2015) and increased to 190 million tonnes according to Glass global group report of 2016. The disposal of glass is considered unsustainable, as it is not biodegradable in the environment (Islam et al., 2017). Also, some types of glass and especially glass from WEEE, accounting for 5% of the average WEEE composition (Ma et al., 2016), contain an amount of potentially hazardous substances, such as arsenic in LCD glass, cadmium in glass of thin-film P/Vs, etc., that may adversely affect the environment if released (Savvilotidou et al., 2014, 2015, 2017; Ling et al., 2012).

The fast growth of plastic waste is another eternal risk for the environment (Buekens and Yang, 2014). The global annual plastic production totaled more than 300 million tonnes in 2016. The increasing consumption of plastic (average annual increase of 9%) results in a significant volume of landfilled plastics, most of which are non-biodegradable (da Silva et al., 2014; Liguori et al., 2014; Tokiwa et al., 2009). WEEE plastics represent 8% of the total plastic waste (European Commission, last access 20.11.2018). Apart from their huge quantity and non-biodegradability, the majority of WEEE plastics contain hazardous substances, namely brominated flame retardants, chlorine, cadmium and antimony. Also, treatment (i.e. incineration or even recycling) may lead to formation of toxic polybrominated or polychlorinated dioxins causing environmental pollution (Dimitrakakis et al., 2009).

On the other hand, WEEE glass and plastic can be considered as materials that enable a circular manner of management, e.g. in place of conventional resources, such as fine aggregates or cement. Apart from waste volume reduction, immobilization of hazardous substances, mitigation of natural resources consumption (i.e. fine aggregates or others used in cement production) and reduction of greenhouse gas emissions by the manufacturing industry of cement (Islam et al., 2017), technical advantages also are expected by the use of glass or plastic in construction materials. Due to its properties, i.e. composition-mainly silica, smooth surface, low water absorption and pozzolanic nature

(Islam et al., 2017; Ling and Poon, 2012; Skripkiūnas et al., 2018), glass enhances the cement hydration process by causing a pozzolanic reaction, while plastic addition assists thermal insulating properties (Iucolano et al., 2013; Ruiz-Herrero et al., 2016).

### ***5.1.1 Why addressing the reuse of glass and plastic from P/Vs or LCDs?***

In 2016, the installed solar P/V capacity totaled around 300 GW compared to 5 GW in 2005, following a rapid growth in producing and installing P/V systems (Savvilotidou et al., 2017). Typically, P/V panel is a great source of glass (up to 75%) and other less relevant-mass components, such as plastic present in junction box and connecting cables (up to 2.5%) (Tammaro et al., 2015). Another major source of glass derives from discarded LCDs (86.52% mass share) (Savvilotidou et al., 2017). In numbers, more than 2 million of waste units were generated in 2015 corresponding to a global annual weight of 460 million tonnes (Kim et al., 2017). The potential of utilizing glass or plastic waste from P/Vs or LCDs for producing cement mortars is beneficial for both construction and recycling sector, considering that the new materials are economically competitive and environmentally superior to conventional cement mortars.

This study explores the reuse of WEEE glass and plastic for construction purposes. Cube cement mortar specimens were produced and their physical, mechanical and thermal properties were evaluated. Determination of their resistance in various corrosive environments after exposure for 91 days was carried out. Once acceptable performance of cement mortars with substitutes was achieved, further increase of waste amount was also examined. To the author's best knowledge, this study provides valuable knowledge and insights on the reuse of WEEE glass and plastic for construction purposes, by evaluating and comparing for the first time various properties under different conditions (type of waste, particle size of waste, amount of waste, etc.) in a single study.

## 5.2 Materials and methods

### 5.2.1 Glass and plastic waste as raw materials

Crystalline silicon P/V panels, capturing approximately 90% of world P/V market (Gangopadhyay et al., 2013), and LCD monitors from laptop computers, having the largest contribution to WEEE compared to desktop computers or tablets (Statista, last access 21.11.2018), were selected for the tests. The wastes were first treated in order to recover the glass and plastic components.

External frames, junction boxes and connecting cables were dismantled and the isolated P/V panels were cut into pieces. Glass was recovered after thermally treating of pieces at 550 °C for 1 h, manual sorting and sieving with a 4 mm mesh. The produced glass fragments were not spherical, but irregular with sharp edges. An amount of glass fragments was subjected to mechanical crushing using a universal ring mill (FRITSCH) to produce glass powder. Thus, glass fragments of size smaller than 4 mm × 4 mm and glass powder of particles with a median diameter of 55 µm were investigated as replacement of fine aggregates, i.e. sand, or cement.

Laptop computers were dismantled and thermally treated according to a previous study of the author (Savvilotidou et al., 2017). The liquid crystals containing polycyclic aromatic hydrocarbons (Zhang et al., 2017) were then removed using 2% isopropyl alcohol and ultrasonic irradiation for 50 min at 30 °C (Savvilotidou et al., 2019). Two size fractions of LCD glass were used as replacement of fine aggregates or cement, namely (a) fragments of size smaller than 4 mm × 4 mm through manual cutting and (b) powder of particles with median diameter 80 µm obtained by a ring mill.

Plastic from the junction box made of acrylonitrile butadiene styrene copolymer (ABS) and from the connecting cables made of polyvinyl chloride (PVC) was cut separately into size fractions, namely, pieces of size less than 4 mm × 4 mm and grindings smaller than 3 mm × 1 mm. The obtained size fractions were used to replace fine aggregates. Note that ABS is the main thermoplastic used in WEEE plastics accounting for 30%, whereas PVC contains high chlorine content making its recycling rather complex (López et al., 2011; Yang et al., 2013; Zhang and Yu, 2016).

Energy Dispersive X-ray fluorescence (XRF) analysis was carried out in all raw materials (except for plastics) in order to compare the oxide content of waste glasses to that of conventional resources (fine aggregates and cement).

### 5.2.2 Synthesis of cement mortars

Cement mortar specimens of 5 cm × 5 cm × 5 cm were prepared. CEM II/A-P 42.5 Portland-pozzolana cement was used as hydraulic binder. Local limestone sand and potable water were also used for preparing all mixtures. Sand fraction (%) passing through 4 mm mesh was only operated, as illustrated by the grading curve in **Fig. 5.2**.

To evaluate the effect of waste in cement mortars, various conditions were investigated, namely, (a) the type of waste (glass or plastic) and its origin (P/V or LCD for glass and ABS or PVC for plastic), (b) the amount of waste (%), (c) the particle size of waste and (d) the replacement of fine aggregates or cement (in the case of glass). The mix proportions are provided in **Table 5.1**. A constant ratio of cement to aggregates, 1:2.5, was applied according to ASTM C109. The ratio of water to cement was varied between 0.4 and 0.7 to ensure workability of the fresh paste. The fresh mortars were casted in steel molds for 24 h and then removed and placed for curing under water at 23±2 °C for 7 and 28 days.

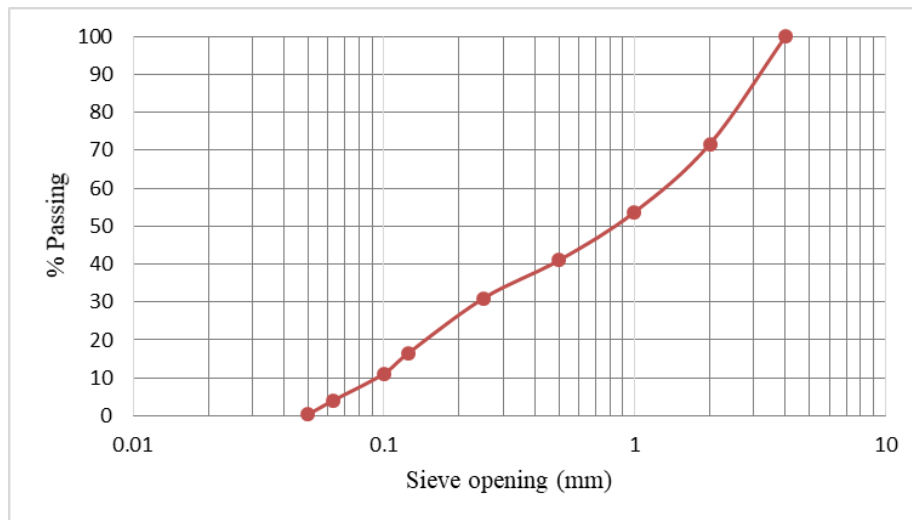


Fig. 5.2: Sieve analysis of fine aggregates

**Table 5.1: Mix proportions**

Type of waste	Size of waste	Replaced sand (wt%)	Replaced cement (wt%)
P/V glass	Fragments	10, 20	-
	Powder	10, 20	10, 20
LCD glass	Fragments	10, 20	-
	Powder	10, 20	10, 20
Plastic from junction box, ABS	Pieces	5, 10	-
	Grindings	5, 10	-
Plastic from connecting cables, PVC	Pieces	5, 10	-
	Grindings	5, 10	-

Codes are provided for all cement mortar specimens explored depending on their mix proportions. For instance, the code 10PVG90S represents the use of 10% P/V glass as replacement of natural aggregates. The first number is the amount of waste (%) and the second number is the percentage of sand (S) or cement (C) used.

### ***5.2.3 Physical, mechanical and thermal properties of cement mortars***

Bulk density was provided by Archimedes’ principle. Open porosity and water absorption were determined according to relative formulas by Skripkiūnas et al. (2018). The uniaxial compressive strength of the hardened cement mortars was determined according to ASTM C109 after 7-day and 28-day aging. The tests were performed at a constant loading rate of 0.5 MPa/s until failure. Sets of three to five specimens were used for each measurement. Thermal conductivity of specimens was measured using the transient plane source (TPS 1500, Sweden) thermal characterization technique.

### ***5.2.4 Resistance of cement mortars to corrosion***

#### ***5.2.4.1 Carbonation test***

Carbonation is a natural aging process in cement-based construction materials, due to reaction between calcium oxide and calcium silicate hydrate that form calcium carbonate in the presence of carbon dioxide and relative humidity. Cement mortars containing P/V

or LCD glass were exposed to constant 10% CO<sub>2</sub> at 25 °C and humidity of 65±5% during 91 days (Morandeu et al., 2014). The test was applied to 28-day aged into water specimens (a) before being subjected to compressive strength test – undamaged and (b) after being subjected to compressive strength test – damaged, so as to evaluate the deterioration in case of cracks. An epoxy resin was first used to cover the five out of six surfaces of the specimens, while one surface was left free of epoxy resin. After spraying a solution of phenolphthalein on the surface of split specimens into the height of 4 cm, parallel to the target-surface, the degree of carbonation was evaluated depending on the color formed on that surface (Lee et al., 2012). The colorless region was carbonated (pH<8), the red-purple or magenta region was noncarbonated (pH>9.5) and the pink region was medium carbonated (8<pH<9.5) (Ruiz-Herrero et al., 2016). Note that the degree of carbonation is associated with the distance from the exterior surface. The color in the middle of split surfaces was primarily considered as measurement focusing on axial penetration of CO<sub>2</sub>. However, six further measurements per side were performed using a caliper to count the potential surrounding colorless area (Morandeu et al., 2014).

#### ***5.2.4.2 Chloride ion penetration***

Chloride ion penetration is mostly critical for constructions close to marine environment, as it can cause damage due to corrosion. The test was performed to cement mortars with P/V or LCD glass and their performance was compared to that of reference mortars. All sides of specimens (28-day aging), except for the target-surface, were primarily coated with an epoxy resin in order to achieve axial penetration. After 91 days of exposure to 5% NaCl solution, the specimens were split into 4 cm height and sprayed across the split surface with 0.1 N silver nitrate (AgNO<sub>3</sub>) solution (Higashiyama et al., 2012). The chloride ion diffusion was then determined by the color observed on the sprayed surface. The white regions indicated the presence of chlorides due to silver chloride (AgCl) precipitation and the brown regions indicated the absence of chlorides, as AgNO<sub>3</sub> reacted with hydroxide ions to form silver oxide (AgO) (Camarini et al., 2013).

#### ***5.2.4.3 Sulfate attack***

Sulfate attack may be caused by contaminated ground water or seawater. In this case, internal cracks and ultimate failure of cement mortars may be observed (Chen et al., 2006). Specimens (28-day aging) with P/V or LCD glass were covered by an epoxy resin on each side except for the sixth one. The specimens were then immersed into 5% Na<sub>2</sub>SO<sub>4</sub> aqueous solution for 91 days. Length expansion and compressive strength were determined and compared to those of reference mortars in order to consider the damages. Also, a comparison between the strength of cement mortars cured into the solution and cured naturally was carried out.

### **5.3 Results and discussion**

#### ***5.3.1 Chemical composition of raw materials***

XRF results for P/V and LCD glass, fine aggregates and cement are shown in **Table 5.2**. The major oxides present in P/V glass are SiO<sub>2</sub> (78.3%), CaO (9.07%) and Na<sub>2</sub>O (7.73%), while LCD glass mainly contains SiO<sub>2</sub> (71.0%), Al<sub>2</sub>O<sub>3</sub> (13.0%) and CaO (7.07%). Due to the high silicon and calcium content, both materials are anticipated to exhibit a cementitious behavior, if they are finely ground (Wang, 2011). It is also indicated that they can be employed as a part of fine aggregates, as they present high amount of CaO.

**Table 5.2: XRF analysis of raw materials (% wt)**

Oxide (%)	CaO	SiO <sub>2</sub>	Al <sub>2</sub> O <sub>3</sub>	Fe <sub>2</sub> O <sub>3</sub>	MgO	K <sub>2</sub> O	P <sub>2</sub> O <sub>5</sub>	MnO	SrO	As <sub>2</sub> O <sub>3</sub>	BaO	Cr <sub>2</sub> O <sub>3</sub>	Na <sub>2</sub> O
P/V glass	9.07	78.3	1.46	0.85	1.63	0.69	<DL	0.03	<DL	<DL	<DL	<DL	7.73
LCD glass	7.07	71.0	13.0	0.43	<DL	0.21	0.11	<DL	6.44	0.47	0.32	0.09	<DL
Natural aggregates	96.3	0.25	<DL	<DL	1.20	0.20	<DL	<DL	<DL	<DL	<DL	<DL	1.00
Cement	58.0	22.8	5.22	4.13	2.32	0.68	0.07	<DL	0.05	<DL	<DL	0.03	0.42

DL: Detection limit

### ***5.3.2 Physical properties of cement mortars***

**Table 5.3** demonstrates the results for open porosity, bulk density and water absorption. The use of P/V glass fragments reduced water absorption compared to the reference mortars due to the presence of glass, which is impermeable and hydrophobic (Wang and Huang, 2010) leading to superior workability of fresh mortar. Also, a decrease of open porosity was observed with increase of glass fragment proportion from 0 to 10% replacement of sand or cement. Bulk density did not fluctuate significantly compared to that of reference mortars; cement mortars containing 10% P/V glass fragments as replacement of sand presented higher density value ( $2.26 \text{ g/cm}^3$ ), in agreement with results obtained by other studies (Skripkiūnas et al., 2018; Bhandari and Tajne, 2013). In contrast to fragments, addition of P/V glass powder resulted in higher open porosity and water absorption, and lower density (Ling and Poon, 2013). This was attributed to the low workability, as the fine glass particles necessitated larger demand of water during the synthesis of mortar. The larger amount of water caused low compactness and high porosity of the produced cement mortars (Jang et al., 2015). A similar behavior was observed by Rashad (2015), who found that glass particles in the size range 5-2.36 mm increased the workability of fresh mortar, though, finer particles (1.18-0.6 mm) relatively decreased workability. On the other hand, it should be noted that fine glass powder may exhibit beneficial pozzolanic properties if glass content, particle size of aggregates and type of cement are properly controlled (Bhandari and Tajne, 2013).

**Table 5.3: Physical properties of cement mortars.**

<b>Size of waste</b>	<b>Sample</b>	<b>Open porosity (%)</b>	<b>Bulk density (g/cm<sup>3</sup>)</b>	<b>Water absorption (%)</b>
	Reference (0% waste)	10.9	2.22	4.83
P/V glass fragments	10PVG90S	7.24	2.26	3.19
	20PVG80S	8.08	2.22	3.63
P/V glass powder	10PVG90S	7.88	2.18	3.60
	20PVG80S	10.4	2.13	4.87
	10PVG90C	9.12	2.16	4.20
	20PVG80C	11.6	2.14	5.37
LCD glass fragments	10LCDG90S	8.70	2.20	3.93
	20LCDG80S	11.1	2.13	5.76
LCD glass powder	10LCDG90S	9.40	2.15	4.36
	20LCDG80S	10.5	2.12	4.95
	10LCDG90C	12.1	2.10	5.73
	20LCDG80C	13.2	2.05	6.40
PVC pieces	5PVC95S	9.80	2.08	5.69
	10PVC90S	13.7	2.06	6.25
PVC grindings	5PVC95S	10.2	2.07	5.82
	10PVC90S	12.4	2.01	6.11
ABS pieces	5ABS95S	11.9	1.97	5.38
	10ABS90S	12.1	1.96	6.06
ABS grindings	5ABS95S	12.4	1.94	5.74
	10ABS90S	13.5	1.83	6.92

Cement mortars with LCD glass exhibited lower bulk densities (2.05-2.20 g/cm<sup>3</sup>) than those obtained for cement mortars with P/V glass (2.13-2.26 g/cm<sup>3</sup>). This is mainly due to the different density between LCD glass, i.e. 2.3 g/cm<sup>3</sup> (Zhuang et al., 2012), and P/V glass, i.e. 2.5 g/cm<sup>3</sup> (Green Rhino Energy, last access 17.8.2018), or other properties associated with the type of glass (composition, shape of fragments, particle size etc.). For

instance, the use of P/V glass is more advantageous compared to LCD glass due to its alkali content which activates the dissolution and hydration of cement (calcium silicates and calcium aluminate phases) (Harbec et al., 2016). Accordingly, the values of open porosity and water absorption were higher than those of cement mortars without waste or those of cement mortars with P/V glass (except for cement mortars with 10% LCD glass as replacement of fine aggregates). These observations are more profound in cement mortars with LCD glass powder and can be attributed to the larger surfaces of fine glass aggregates, which entrap more air in the mortar matrix (Harbec et al., 2016).

The use of plastic in cement mortars demonstrates a decrease in the bulk density by increasing the percentage of plastic in the mixture. More specifically, the values decreased from 2.22 (reference mortar) to 1.83 g/cm<sup>3</sup> (mortar composed of 10% ABS aggregates). This reduction may be attributed to the low specific weight of plastic (Senhadji et al., 2015) and is compatible with previous findings (Ruiz-Herrero et al., 2016). In case of higher replacement ratios, this could result in production of lightweight mortar which appears resistant to water penetration (Manjunath, 2016). As far as the type of plastic is concerned, this highly affects the physical properties of mortar, with a more pronounced effect on density. Apart from the type of plastic, its size is another influence factor (da Silva et al., 2014). Plastic grindings resulted in lower density compared to the obtained density using pieces, because they interrupted the bonding and the complete hydration of the cement paste (Sharma and Bansal, 2016). Also, the use of plastic resulted in higher porosity and water absorbency with increasing plastic amount due to inhomogeneity, formation of voids, and thus poor chemical compatibility between plastic and inorganic fraction (Iucolano et al., 2013).

### ***5.3.3 Mechanical properties of cement mortars***

Mechanical behavior of cement mortars cured for 7 and 28 days is shown in **Table 5.4**. For all tested cement mortars, compressive strength increased, as expected, with the curing age. The rate of this increase depended on the type of waste, its amount or particle size, and the resource replaced.

**Table 5.4: Mechanical properties of cement mortars**

Sample	Code of sample	Compressive strength (MPa)	
		7 days	28 days
	Reference (0% waste)	39.1	42.6
P/V glass fragments	10PVG90S	30.5	42.8
	20PVG80S	35.3	39.8
P/V glass powder	10PVG90S	27.8	39.1
	20PVG80S	29.2	36.2
	10PVG90C	29.5	36.0
	20PVG80C	23.8	31.3
LCD glass fragments	10LCDG90S	39.4	47.5
	20LCDG80S	31.0	37.3
LCD glass powder	10LCDG90S	23.8	33.4
	20LCDG80S	17.1	28.1
	10LCDG90C	18.1	27.9
	20LCDG80C	14.6	23.9
PVC pieces	5PVC95S	26.5	32.4
	10PVC90S	18.9	22.9
PVC grindings	5PVC95S	23.7	31.1
	10PVC90S	18.2	20.9
ABS pieces	5ABS95S	20.2	24.1
	10ABS90S	17.7	21.5
ABS grindings	5ABS95S	19.1	22.7
	10ABS90S	16.6	20.1

P/V glass fragments affected the strength of samples mostly in the first 7 days of curing, with a decrease varying between 22 and 10% (for 10 and 20% replacement of sand, respectively). Decrease in strength was also observed by Kim et al. (2017) on the first 3 days. However, when the cement mortars were cured for 28 days, strength values approached those of reference mortars. The maximum value (42.8 MPa) was measured in cement mortars with 10% P/V glass fragments as replacement of sand. The results are in

close agreement with observations of other researchers, who found that waste material from P/V panels (10-20% replacement of fine aggregates and 5-10% replacement of cement) improves the compressive strength of mortar (Cheng, 2014). Specifically, an increase of 9% in compressive strength occurred when 10% of cement was replaced with glass, followed by a decrease when the glass content was 15% (Aliabdo et al., 2016).

The replacement of aggregates with glass powder caused lower strength values than those obtained using glass fragments due to not efficient granulometric distribution of the waste glass, worse workability and weak adhesion between glass and cement (Ling and Poon, 2013). Rashad (2015) showed that large particle range of glass considerably increases the strength providing more continuous particle size distribution due to smoother surfaces. However, as previously mentioned, if glass particles are adequately fine, e.g. smaller than 38  $\mu\text{m}$  (Soliman and Tagnit-Hamou, 2016), a pozzolanic behavior of glass occurs that affects the cement hydration reactions improving the mechanical behavior of cement mortars (Bhandari and Tajne, 2013). Due to relatively larger particle size of glass powder used in the present study, it cannot be considered as a pozzolanic material. In any case, its potential of pozzolanic effect could be well-observed by comparing the strength with those of reference mortars after a long aging of at least 90 days.

LCD glass also affected the mortar strength, while its particle size played a substantial role. The use of LCD glass fragments (<4 mm) substantially improved compressive strength when it replaced 10% of the fine aggregates, with values (39.4 and 47.5 MPa for 7 and 28 days of curing, respectively) considerably exceeding those of the reference mortars (39.1 and 42.6 MPa). The enhanced mechanical behavior in hardened mortar may be justified by the characteristics of fresh mortar. Due to the nature of glass, that is impermeable, the preparation of the mixture required limited amount of water to achieve the desired workability (Soliman and Tagnit-Hamou, 2016). Also, the smooth surface of glass allowed good adherence between cement mortar and glass. Thus, an increase (%) of glass in the mix proportion (from 0 to 10%) lead to an increase in mortar flow and then higher strength (Bhandari and Tajne, 2013). However, the amount of waste

is a critical factor; a 20% replacement of fine aggregates with glass fragments (<4 mm) resulted in lower compressive strength (around 13% decrease) than that of reference mortars. Wang and Huang (2010), who tested various mix proportions (20-80%), found that the lowest mix proportion (20% LCD glass of the total aggregates) was the optimal one in terms of strength. It is then deduced that high substitution rates lower the strength in cement mortars.

LCD glass as partial replacement of cement resulted in lower strengths than those exhibited in cement mortars based on fine aggregates substitution or reference mortars. This is in agreement with the low densities showed in **Table 5.3** and is attributed to the high water demand and low workability of fresh mortars (Wang and Wang, 2017), as also mentioned for the P/V glass powder. In terms of particle size effect, the LCD glass powder did not enhance the compressive strength in cement mortars. The lowest strength was observed in cement mortars with 20% glass powder as replacement of cement.

The increasing amount of plastic affects negatively the mechanical properties of cement mortars, resulting in decrease of compressive strength in the tested conditions (days of aging, mix proportions, type of polymers and particle size). Decrease in strength was also observed by previous studies due to the low bond between plastic and cement paste that normally differs from that between natural aggregates and cement paste (Senhadji et al., 2015). Also, the high water to cement ratio required during the preparation of cement mortars is responsible for the loss of strength (Saikia and Brito, 2013). Optimum compressive strength was measured in cement mortars of 5% plastic as replacement of natural aggregates against 10% amount of plastic for both polymers tested (PVC or ABS). During the synthesis of fresh mortars, the mixtures with ABS polymer required more water compared to the mixtures with PVC polymer. This is a possible reason why the cement mortars contained PVC polymer obtained higher strength than those produced by addition of ABS polymer. In particular, addition of 5% PVC pieces present around 27% reduction of compressive strength compared to the reference mortar, while approximately 43% reduction is presented in cement mortars with 5% ABS pieces. Also, taking into account the mechanical properties of these typical polymers and

comparing the data on their compressive strength (65 MPa for ABS and 57-83 MPa for PVC), it was estimated that the type of polymer affects the compressive strength in a higher degree than the particle size of plastics, which causes little difference in strength between the two sets of cement mortars (PVC and ABS). The smaller particles of plastic represent larger area that should be homogenized in the cement paste to increase the workability, resulting in low strength. The reduction of compressive strength in cement mortars, as a function of the increasing amount of plastic and its particle size, is confirmed by similar tests, in which replacement of 5-50% of fine aggregates with plastic of varying particle size (0.01-20 mm) was carried out (Ismail and Al-Hashmi, 2008; Saikia and Brito, 2012; Iucolano et al., 2013).

**Figs. 5.3 and 5.4** show a direct comparison of compressive strength between cement mortars with glass or plastic and reference mortars. Each result represents the mean value, while the minimum and maximum values are also provided.

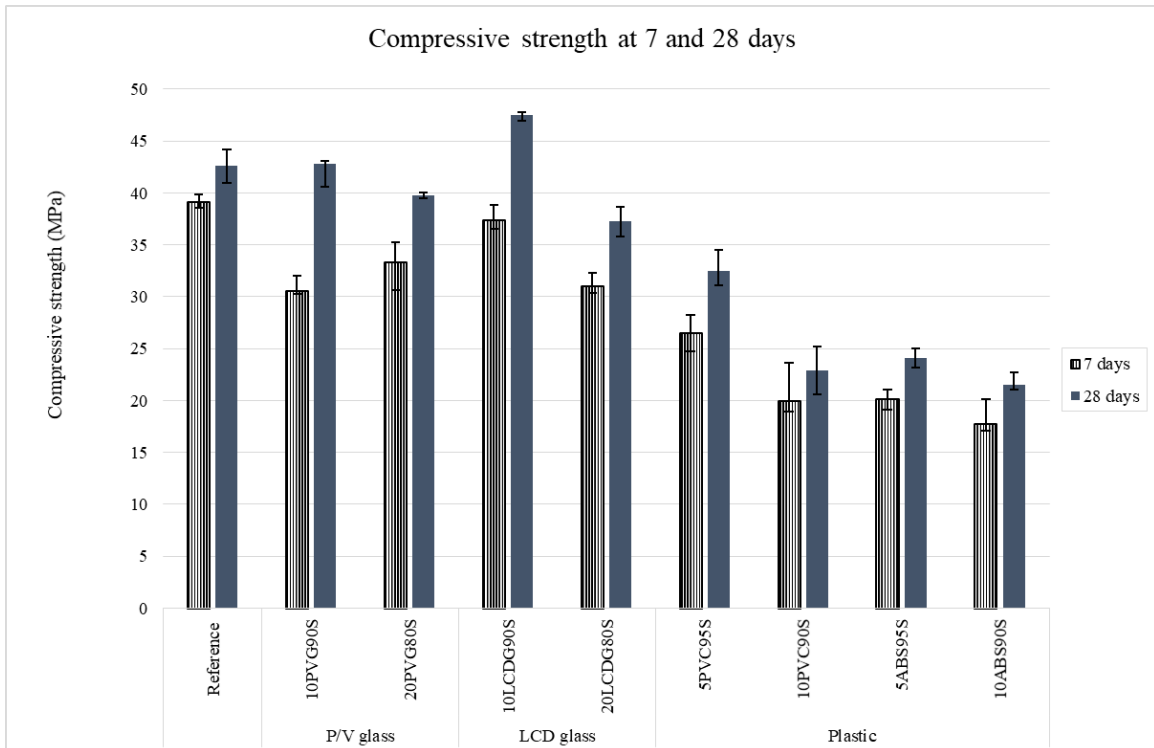


Fig. 5.3: Compressive strength of cement mortars with glass fragments or plastic pieces

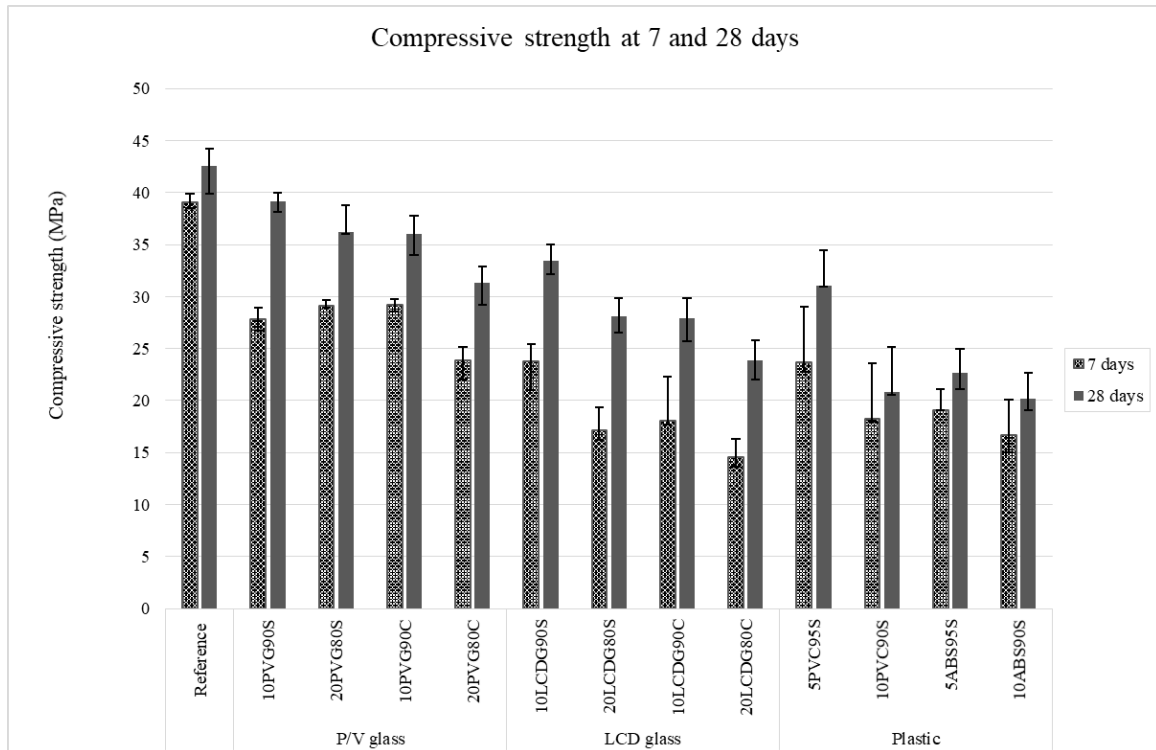


Fig. 5.4: Compressive strength of cement mortars with glass powder or plastic grindings

In case of glass fragments (**Fig. 5.3**), the most efficient mechanical performance is exhibited by 28-day aged cement mortars with 10% as replacement of fine aggregates. In case of plastic pieces, 28-day aged cement mortars with 5% PVC plastic pieces exhibited the highest strength among the tested mortars. The same tendencies are observed for glass powder and plastic grindings (**Fig. 5.4**). Finally, the comparative analysis showed that for all tests, small amount of waste (i.e. 10% for glasses and 5% for plastic) with large particle size (i.e. glass fragments and plastic pieces) resulted in better strengths.

#### 5.3.4 Thermal properties of cement mortars

The results of thermal conductivity are shown in **Table 5.5**.

**Table 5.5: Thermal conductivity of cement mortars**

Code of sample	Thermal conductivity (W/m·K)
Reference (0% waste)	0.77
10PVG90S	0.64
20PVG80S	0.61
10PVG90C	0.63
20PVG80C	0.62
10LCDG90S	0.60
20LCDG80S	0.54
10LCDG90C	0.62
20LCDG80C	0.61
5PVC95S	0.68
10PVC90S	0.62
5ABS95S	0.50
10ABS90S	0.45

Referring to thermal properties of cement mortars, both glass and plastic influence the thermal insulation of cement mortars, as a result of their low thermal conductivity and density (Sikora et al., 2017). In fact, the greatest improvement is observed in cement mortars with plastic (0.45-0.68 W/m·K), followed by those with LCD glass (0.54-0.62 W/m·K) and P/V glass (0.61-0.64 W/m·K). In all cases, as the amount of waste increases, thermal conductivity decreases. For cement mortars with glass, the changes are more profound when partial replacement of aggregates occurs. This is because aggregates and not cement are in a larger proportion in the mixtures. Also, regarding the type of plastic polymers, ABS appears as a better thermal insulator compared to PVC matrix. The results are in agreement with previous researches, among which Liguori et al. (2014) and Lucolano et al. (2013), showing that plastic use in cement mortars is beneficial due to thermal degradation, fire resistance and thermal conductivity improvement.

### 5.3.5 Resistance of cement mortars to corrosion

**Fig. 5.5a** illustrates the noncarbonated region in the middle of the sprayed surface, indicating that CO<sub>2</sub> did not penetrate in the tested height (at 1 cm depth), and also the penetration of CO<sub>2</sub> from the other sides occurs at a low degree despite of the epoxy resin layer (**Table 5.6**).

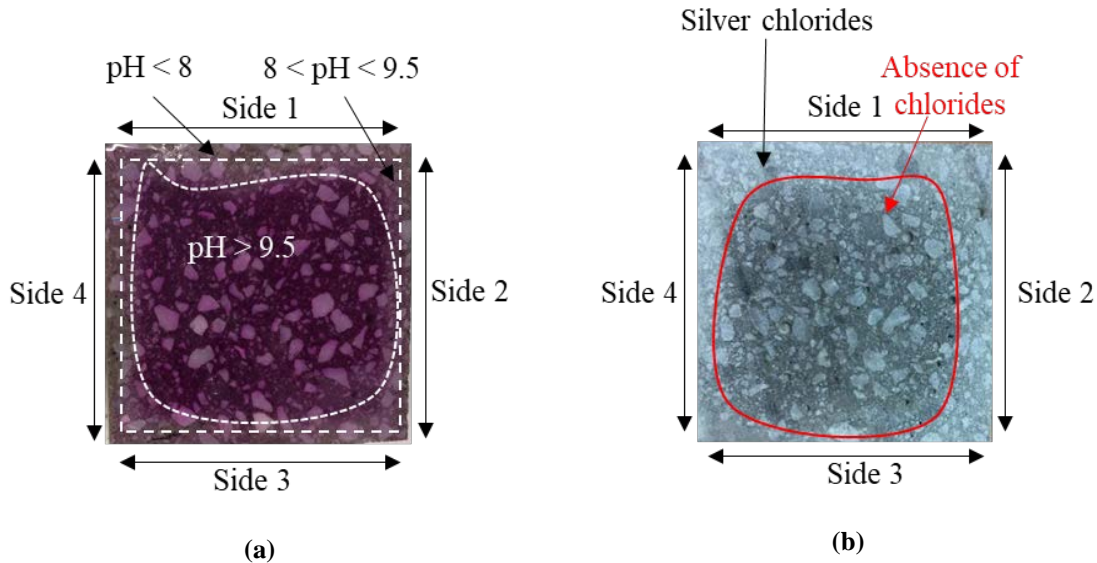


Fig. 5.5: Measured positions for penetration of (a) carbon dioxide and (b) chlorides in cement mortars

Even the cracked cement mortars with P/V or LCD glass were fairly not carbonated, although the diffusion of CO<sub>2</sub> was higher in their case due to the damages and cracks (Jiang et al., 2017). The findings can be explained by the porosity values, since cement mortars were characterized by lower porosity compared to that of reference mortars. The degree of carbonation in cement mortars of 20% replacement of sand or cement with P/V glass was slightly higher, though remaining lower than in reference mortars. This is also observed by Rashad (2015) who mentioned that substitution of natural aggregates with glass is associated with weaker carbonation resistance due to voids and trapped air into the mortar matrix which permit CO<sub>2</sub> penetration. It is therefore deduced that addition of glass up to 20% does not deteriorate the cement mortars, however, it is expected that higher substitution rates may deliver detrimental effects on cement mortars due to carbonation.

**Table 5.6: Carbonation depth and chloride ion penetration depth**

Code of sample	Depth of carbonation in damaged cement mortars (mm)				Chloride ion penetration depth (mm)			
	Side 1	Side 2	Side 3	Side 4	Side 1	Side 2	Side 3	Side 4
Reference (0% waste)	2.40	2.31	1.78	2.07	3.78	3.61	3.87	3.73
10PVG90S	0.00	0.00	0.00	0.00	2.38	1.13	0.00	1.56
20PVG80S	1.12	0.75	0.00	0.00	0.47	0.00	0.00	0.00
10PVG90C	0.00	0.00	0.00	0.00	0.00	0.00	3.32	2.65
20PVG80C	0.84	0.00	0.75	0.00	0.00	1.60	0.00	2.11
10LCDG90S	0.00	0.00	0.00	0.00	0.14	0.00	0.00	1.11
20LCDG80S	0.00	0.00	0.00	0.00	0.00	0.00	0.00	3.29
10LCDG90C	0.00	0.00	0.00	0.00	0.27	0.00	0.00	1.12
20LCDG80C	0.00	0.00	0.00	0.00	0.00	0.00	0.00	0.00

Regarding chloride ion resistance, the results reveal the absence of chlorides in the tested height (at 1 cm depth) (**Fig. 5.5b**). The penetration depth decreases as the amount of glass increases (Rashad, 2015) and is lower than that in reference mortar. This decrease was observed by the penetration through the other sides, although they were covered with epoxy resin (**Table 5.6**). The high resistance in penetration of chloride ions is explained by the low water absorption and porosity values of cement mortars with glass. More specifically, as the number of pores decreases, the penetration of water or aqueous solutions that may contain corrosive or chemical substances is also reduced (Wang and Huang, 2010). Previous studies that examined the durability of construction materials consisting of glass against chloride ion penetration (Chen et al., 2006; Islam et al., 2017) also proved the high resistance to chloride transport. Zuo et al. (2017) compared the effect of 5% NaCl solution on specimens with a glass rate of 5-20% and glass particle size that varied (0.250-0.038 mm) and found that 10% glass and glass particle size of 0.125 mm resulted in the highest resistance to chlorine ion penetration. Not only the particle size may influence the chlorine ion penetration (Wang and Huang, 2010), but also the aging of cement mortars (Wang et al., 2009). Considering the obtained results, cement mortars with glass content could be used in construction sector, such as in bridge decks, pavements etc. which are usually exposed to the respective corrosive effects (Nassar and Soroushian, 2011).

The resistance of cement mortars to sulfate attack was assessed after a 91-day exposure of cement mortars to 5% Na<sub>2</sub>SO<sub>4</sub> solution (Hossack and Thomas, 2015). The length change and the compressive strength were determined in order to consider the damages (**Table 5.7**).

Expansion of cement mortars after sulfate attack was not apparent in all dimensions, but through the target-surface, as the epoxy resin effectively protected the covered surface from sulfate attack allowing a monoaxial ingress. A decrease of the compressive strength and an expansion of maximum 0.05% were measured in all cement mortars due to the contact with the sulfate solution. However, as the amount of glass increases from 10 to 20% glass, the resistance of cement mortars to sulfate increases

(Wang and Huang, 2010). As referred in literature, weight loss of mortar due to sulfate corrosion is mitigated with the increase of glass content, thus, resistance to sulfate attack is efficiently improved (Rashad, 2015).

**Table 5.7: Compressive strength and expansion in length of cement mortars after exposure to sulfate attack**

Code of sample	Mechanical strength (MPa)		Expansion in length (%)
	Sulfate attack (91 days)	Natural hardening (91 days)	
Reference (0% waste)	40.6	51.3	0.03
10PVG90S	46.9	52.8	0.03
20PVG80S	43.8	48.0	0.01
10PVG90C	36.2	45.1	0.05
20PVG80C	35.5	43.3	0.02
10LCDG90S	50.4	56.7	0.05
20LCDG80S	39.6	44.4	0.04
10LCDG90C	40.3	46.2	0.03
20LCDG80C	35.2	39.4	0.01

Overall, the results showed that the use of WEEE glass increases the life-time and resistance of cement mortar to corrosive environments. Also, according to the toxicity characteristic leaching procedure (TCLP), the produced cement mortars are considered non-hazardous, as Cd, As, Ag, Pb, Hg and Se values were below the limits.

### 5.4 Conclusions

The sharp increasing volume of glass and plastic waste has become a major threat for the environment. Towards a circular economy, conversion of waste to construction material is a strategy that enables various benefits, from prevention of inappropriate disposal to production of commercial and marketable products.

This study addresses the issue of using glass and plastic waste from WEEE to replace conventional materials for construction purposes. The tests involved the production of cement mortars with addition of P/V glass, LCD glass or plastic (ABS,

PVC). The results demonstrated that some properties may be enhanced and others may be defected with the inclusion of WEEE glass or plastic in the cement mortars. This should be critically considered based on the specific application for which mortar would be utilised. The main conclusions drawn are that: (a) glass can be used as suitable partial-substitute either for natural aggregates or cement, enabling high strength and resistance to corrosive environments, and (b) plastic can be used for the production of insulating cement mortars, as it reduces thermal conductivity. The proposed approach can contribute to a resource-efficient, circular economy.

## 5.5 References

- Aliabdo, A.A., Abd Elmoaty, A.E.M., Aboshama, A.Y., 2016. Utilization of waste glass powder in the production of cement and concrete. *Constr. Build. Mater.* 124, 866-877.
- Bhandari, P.S., Tajne, K.M., 2013. Use of waste glass in cement mortar. *Int. J. Civ. Struct. Eng.* 3(4), 704.
- Buekens, A., Yang, J., 2014. Recycling of WEEE plastics: a review. *J. Mater. Cycles Waste Manage.* 16(3), 415-434.
- Camarini, G., Bardella, P.S., Barbosa, D.C., 2013. Chloride Penetration Depth in Silica Fume Concrete. *Int. J. Eng. Technol.* 5(6), 717.
- Chen, C.H., Huang, R., Wu, J.K., Yang, C.C., 2006. Waste E-glass particles used in cementitious mixtures. *Cement Concrete Res.* 36(3), 449-456.
- Cheng, A., 2014. Effects of waste material from solar panels on mechanical properties and durability of cement based materials. *Mater. Res. Innov.* 18(sup2), S2-344.
- da Silva, A.M., de Brito, J., Veiga, R., 2014. Incorporation of fine plastic aggregates in rendering mortars. *Constr. Build. Mater.* 71, 226-236.
- Dimitrakakis, E., Janz, A., Bilitewski, B., Gidaracos, E., 2009. Small WEEE: determining recyclables and hazardous substances in plastics, *J. Hazard. Mater.* 161(2-3) 913-919.

- European Commission. A European strategy for plastics in a circular economy. <http://ec.europa.eu/environment/circular-economy/pdf/plastics-strategy-brochure.pdf> (last access 20.11.2018).
- Gangopadhyay, U., Jana, S., Das, S., 2013. State of art of solar photovoltaic technology. Conference Papers in Science. Hindawi. Article ID 764132. <http://dx.doi.org/10.1155/2013/764132>.
- Glass global group. 2016. Glass Market Report and Study. <https://plants.glassglobal.com/admin/downloads/glassglobal%20Glass%20Market%20Study.pdf>.
- Green Rhino Energy. [http://www.greenrhinoenergy.com/solar/technologies/solar\\_glass.php](http://www.greenrhinoenergy.com/solar/technologies/solar_glass.php) (last access 17.8.2018)
- Harbec, D., Tagnit-Hamou, A., Gitzhofer, F., 2016. Waste-glass fume synthesized using plasma spheroidization technology: Reactivity in cement pastes and mortars. *Constr. Build. Mater.* 107, 272-286.
- Higashiyama, H., Sappakittipakorn, M., Sano, M., Yagishita, F., 2012. Chloride ion penetration into mortar containing ceramic waste aggregate. *Constr. Build. Mater.* 33, 48-54.
- Hossack, A.M., Thomas, M.D., 2015. The effect of temperature on the rate of sulfate attack of Portland cement blended mortars in Na<sub>2</sub>SO<sub>4</sub> solution. *Cement Concrete Res.* 73, 136-142.
- Islam, G.S., Rahman, M.H., Kazi, N., 2017. Waste glass powder as partial replacement of cement for sustainable concrete practice. *Int. J. Sustain. Built Environ.* 6(1), 37-44.
- Ismail, Z.Z., Al-Hashmi, E.A., 2008. Use of waste plastic in concrete mixture as aggregate replacement. *Waste Manage.* 28(11), 2041-2047.
- Jiang, C., Huang, Q., Gu, X., Zhang, W., 2017. Experimental investigation on carbonation in fatigue-damaged concrete. *Cement Concrete Res.* 99, 38-52.

- Jang, H., Jeon, S., So, H., So, S., 2015. Properties of different particle size of recycled TFT-LCD waste glass powder as a cement concrete binder. *Int. J. Precis. Eng. Man.* 16(12) 2591-2597.
- Kim, S.K., Kang, S.T., Kim, J.K., Jang, I.Y., 2017. Effects of particle size and cement replacement of LCD glass powder in concrete. *Adv. Mater. Sci. Eng.* Article ID 3928047. <https://doi.org/10.1155/2017/3928047>.
- Lee, H.J., Kim, D.G., Lee, J.H., Cho, M.S., 2012. A study for carbonation degree on concrete using a phenolphthalein indicator and fourier-transform infrared spectroscopy. *Int. J. Civ. Environ. Eng.* 34(62), 184-190.
- Liguori, B., Iucolano F., Capasso, I., Lavorgna, M., Verdolotti, L., 2014. The effect of recycled plastic aggregate on chemico-physical and functional properties of composite mortars. *Mater. Design* 57, 578-584.
- Lin, K.L., Huang, W.J., Shie, J.L., Lee, T.C., Wang, K.S., Lee, C.H., 2009. The utilization of thin film transistor liquid crystal display waste glass as a pozzolanic material, *J. Hazard. Mater.* 163(2-3) 916-921.
- Ling, T.C., Poon, C.S., 2013. Effects of particle size of treated CRT funnel glass on properties of cement mortar. *Mater. Struct.* 46(1-2), 25-34.
- Ling, T.C., Poon, C.S., 2011. Utilization of recycled glass derived from cathode ray tube glass as fine aggregate in cement mortar. *J. Hazard. Mater.* 192(2), 451-456.
- Ling, T.C., Poon, C.S., Lam, W.S., Chan, T.P., Fung, K.K.L., 2012. Utilization of recycled cathode ray tubes glass in cement mortar for X-ray radiation-shielding applications, *J. Hazard. Mater.* 199, 321-327.
- López, A., de Marco, I., Caballero, B.M., Laresgoiti, M.F., Adrados, A., 2011. Dechlorination of fuels in pyrolysis of PVC containing plastic wastes. *Fuel Process. Technol.* 92(2), 253-260.
- Iucolano, F., Liguori, B., Caputo, D., Colangelo, F., Cioffi, R., 2013. Recycled plastic aggregate in mortars composition: Effect on physical and mechanical properties. *Mater. Design* 52, 916-922.

- Ma, C., Yu, J., Wang, B., Song, Z., Xiang, J., Hu, S., Su, S., Sun, L., 2016. Chemical recycling of brominated flame retarded plastics from e-waste for clean fuels production: a review. *Renew. Sust. Energ. Rev.* 61, 433-450.
- Manjunath, B.A., 2016. Partial replacement of e-plastic waste as coarse-aggregate in concrete. *Procedia Environ. Sci.* 35, 731-739.
- Morandea, A., Thiery, M., Dangla, P., 2014. Investigation of the carbonation mechanism of CH and CSH in terms of kinetics, microstructure changes and moisture properties. *Cement Concrete Res.* 56, 153-170.
- Nassar, R.U.D., Soroushian, P., 2011. Field investigation of concrete incorporating milled waste glass. *J. Solid Waste Technol. Manage.* 37(4), 307-319.
- Rashad, A.M., 2015. Recycled cathode ray tube and liquid crystal display glass as fine aggregate replacement in cementitious materials. *Constr. Build. Mater.* 93, 1236-1248.
- Ruiz-Herrero, J.L., Nieto, D.V., López-Gil, A., Arranz, A., Fernández, A., Lorenzana, A., Merino, S., De Saja, J.A., Rodríguez-Pérez, M.Á., 2016. Mechanical and thermal performance of concrete and mortar cellular materials containing plastic waste. *Constr. Build. Mater.* 104, 298-310.
- Saikia, N., Brito, J.D., 2013. Waste polyethylene terephthalate as an aggregate in concrete. *Mater. Res.* 16(2), 341-350.
- Savvilotidou, V., Antoniou, A., Gidarakos, E., 2017. Toxicity assessment and feasible recycling process for amorphous silicon and CIS waste photovoltaic panels. *Waste Manage.* 59, 394-402.
- Savvilotidou, V., Hahladakis, J.N., Gidarakos, E., 2014. Determination of toxic metals in discarded Liquid Crystal Displays (LCDs). *Resour. Conserv. Recycl.* 92, 108-115.
- Savvilotidou, V., Hahladakis, J.N., Gidarakos, E., 2015. Leaching capacity of metals–metalloids and recovery of valuable materials from waste LCDs. *Waste Manage.* 45, 314-324.

- Savvilotidou, V., Kousaiti, A., Batinic, B., Vaccari, M., Kastanaki, E., Karagianni, K., Gidarakos, E. 2019. Evaluation and comparison of pre-treatment techniques for recovering indium from discarded liquid crystal displays. *Waste Manage.* 87, 51-61. <https://doi.org/10.1016/j.wasman.2019.01.029>.
- Senhadji, Y., Escadeillas, G., Benosman, A.S., Mouli, M., Khelafi, H., Ould Kaci, S., 2015. Effect of incorporating PVC waste as aggregate on the physical, mechanical, and chloride ion penetration behavior of concrete. *J. Adhes. Sci. Technol.* 29(7), 625-640.
- Sharma, R., Bansal, P.P., 2016. Use of different forms of waste plastic in concrete—a review. *J. Clean. Prod.* 112, 473-482.
- Sikora, P., Horszczaruk, E., Skoczylas, K., Rucinska, T., 2017. Thermal properties of cement mortars containing waste glass aggregate and nanosilica. *Procedia Eng.* 196, 159-166.
- Skripkiūnas, G., Vasarevičius, S., Danila, V., 2018. Immobilization of copper indium selenide solar module waste in concrete constructions. *Cement Concrete Comp.* 85, 174-182.
- Soliman, N.A., Tagnit-Hamou, A., 2016. Development of ultra-high-performance concrete using glass powder—Towards ecofriendly concrete. *Constr. Build. Mater.* 125, 600-612.
- Statista, Shipment forecast of tablets, laptops and desktop PCs worldwide from 2010 to 2021 (in million units). <https://www.statista.com/statistics/272595/global-shipments-forecast-for-tablets-laptops-and-desktop-pcs/> (last access 21.11.2018).
- Tamaro, M., Rimauro, J., Fiandra, V., Salluzzo, A., 2015. Thermal treatment of waste photovoltaic module for recovery and recycling: Experimental assessment of the presence of metals in the gas emissions and in the ashes. *Renew. Energy* 81, 103-112.
- Tokiwa, Y., Calabria, B.P., Ugwu, C.U., Aiba, S., 2009. Biodegradability of plastics. *Int. J. Mol. Sci.* 10(9), 3722-3742.

- Wang, C.C., Wang, H.Y., 2017. Assessment of the compressive strength of recycled waste LCD glass concrete using the ultrasonic pulse velocity. *Constr. Build. Mater.* 137, 345-353.
- Wang, H.Y., 2011. The effect of the proportion of thin film transistor–liquid crystal display (TFT–LCD) optical waste glass as a partial substitute for cement in cement mortar. *Constr. Build. Mater.* 25(2), 791-797.
- Wang, H.Y., Huang, W.L., 2010. Durability of self-consolidating concrete using waste LCD glass. *Constr. Build. Mater.* 24(6), 1008-1013.
- Wang, Z., Shi, C., Song, J., 2009. Effect of glass powder on chloride ion transport and alkali-aggregate reaction expansion of lightweight aggregate concrete. *J. Wuhan Univ. Technol. Mat. Sci. Ed.* 24(2), 312-317.
- Wintour, N., 2015. The glass industry: Recent trends and changes in working conditions and employment relations. International Labour Organization. ISBN: 9789221301172; 9789221301189 (web pdf).
- Yang, X., Sun, L., Xiang, J., Hu, S., Su, S., 2013. Pyrolysis and dehalogenation of plastics from waste electrical and electronic equipment (WEEE): A review. *Waste Manage.* 33(2), 462-473.
- Zhang, L., Wu, B., Chen, Y., Xu, Z., 2017. Treatment of liquid crystals and recycling indium for stripping product gained by mechanical stripping process from waste liquid crystal display panels. *J. Clean. Prod.* 162, 1472-1481.
- Zhang, S., Yu, Y., 2016. Dechlorination behavior on the recovery of useful resources from WEEE by the steam gasification in the molten carbonates. *Procedia Environ. Sci.*, 31, 903-910.
- Zhuang, X., He, W., Li, G., Huang, J., Ye, Y., 2012. Materials Separation from Waste Liquid Crystal Displays Using Combined Physical Methods. *Pol. J. Environ. Stud.* 21(6).
- Zuo, J., Li, H., Dong, B., Luo, C., Chen, D., 2017. Mechanical properties and resistance to chloride ion permeability of epoxy emulsion cement mortar reinforced by glass flake. *Constr. Build. Mater.* 155, 137-144.



## **6 Valorization of glass and lignite fly ash in glass-ceramics**

This study investigates an innovative approach for the valorization of specific wastes generated from the energy sector and the production of glass-ceramics. The wastes used were photovoltaic (P/V) glass, produced from the renewable energy sector, and lignite fly ash, produced from the conventional energy sector. The process first involved the production of glass after melting specific mixtures of wastes, namely i) 70% P/V glass and 30% lignite fly ash, and ii) 80% P/V glass and 20% lignite fly ash, at 1200 °C for 1 hour as revealed by the use of a heating microscope. The results indicated that the P/V glass, as a sodium-potassium-rich inorganic waste, reduces energy requirements of the melting process. The produced glass was then used for the production of glass-ceramics. Dense and homogeneous glass-ceramics, exhibiting high chemical stability and no toxicity, were produced after controlled thermal treatment of glass at 800 °C. The mechanical (compressive strength, Vickers hardness) and physical (open porosity, bulk density and water absorption) properties of the produced glass-ceramics were evaluated. X-ray diffraction (XRD) and Energy Dispersive X-ray fluorescence (ED-XRF) were used for the characterization of the raw materials and the produced glass-ceramics. Scanning electron microscopy (SEM) provided further insights on the microstructure of the final products. The properties of the produced glass-ceramics, namely water absorption and compressive strength, render them suitable for applications in the construction industry. The waste valorization approach followed in this study is in line with the principles of circular economy.

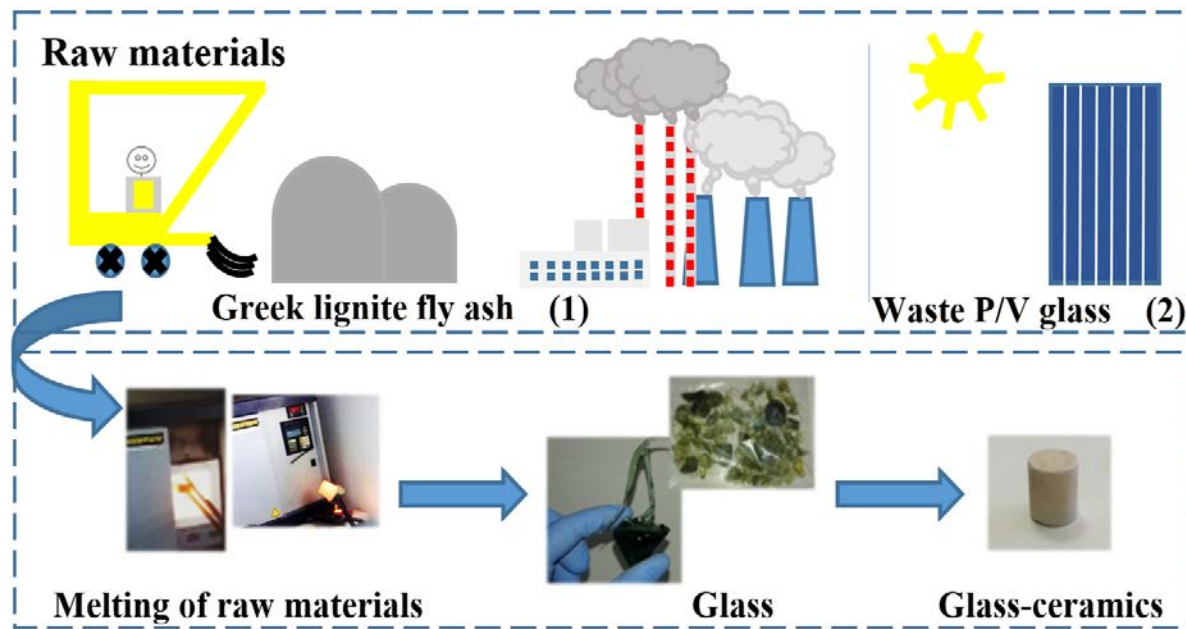


Fig. 6.1: Schematic diagram of the experimental methodology

## 6.1 Overview

As a result of industrialization and population growth, the volume of produced inorganic wastes and by-products, such as fly ashes, slags and sludges, steadily increases (Karamberi et al., 2007). Valorization techniques, including waste conversion into glass and glass-ceramics, are explored in order to control the potential release of contaminants or/and to fabricate products with tailored properties (Wu et al., 2015; Leroy et al., 2001). Sintered glass-ceramic composites are considered for the immobilization of toxic metals, metalloids or radioactive elements present in a wide range of wastes, such as bottom and fly ashes, municipal solid waste (MSW) ashes, industrial residues, nuclear waste (McCloy and Goel, 2017), zeolitized volcanoclastic deposits rich in Cs and Sr (Cappelletti et al., 2011), volcanic ashes (Vu et al., 2011), slags and sludges (Erol et al., 2009).

*“Glass-ceramics are inorganic, non-metallic materials prepared by controlled crystallization of glasses via different processing methods. They contain at least one type of functional crystalline phase and a residual glass. The volume fraction crystallized may vary from ppm to almost 100%”* (Deubener et al., 2018). Depending on the number of nuclei and their dispersion, heterogeneous nucleation (i.e. uncontrolled crystallization or otherwise devitrification) may occur either on the surface or the substrate of glass, reducing its mechanical strength (Deubener et al., 2018; Paul, 1982; Shelby, 2007). In heterogeneous nucleation, nuclei are formed on the surface of a foreign substrate mainly due to contact with container material, impurity particles, exposure to atmosphere, etc. (Deubener et al., 2018). In material science, functional glass-ceramics can be used in i) the building industry (Wu et al., 2015) for architectural and decorative applications (e.g. floors, roofs), ii) the medical sector as biomaterials (e.g dental filling and bone replacement materials), iii) the metallurgical and optical industry, iv) the chemical processing industry, and v) as coating materials for industrial dies (Yoon et al., 2013).

The properties of glass-ceramics derived from wastes allow their use as construction and architectural components (Erol et al., 2007; Leroy et al., 2001). They

usually exhibit advanced properties, comparable with those of traditional products, including high compressive and bending strength, hardness, chemical stability, excellent corrosion and abrasion resistance (Aloisi et al., 2006; Baowei et al., 2013; Wu et al., 2015).

Valorization approaches for fly ash have been developed since 1960 (Yilmaz, 2012). Vitrification or glassification is a well-established alternative which transforms the waste into a stable and homogeneous glass. During the process, ash is mixed with other additives and heated at temperatures up to 1500 °C (Prasad and Shih, 2016). Although the high energy demand still remains an important barrier (Binhussain et al., 2014; Lu et al., 2014), energy savings may be achieved with the addition of glass-forming materials and fluxes (borax, sodium carbonate, waste glass etc.) that increase the glass forming ability and lower the melting temperature and/or the required time (Lazău and Vancea, 2014; Prasad and Shih, 2016). Viscous flow sintering, also known as sinter crystallization, is another important thermal process, through which the glass powder is transformed into a dense material (glass-ceramic) at much lower temperatures, up to 1100 °C, compared to those used for vitrification/melting (Bernardo and Maschio, 2011; Prasad and Shih, 2016).

### ***6.1.1 Overview of waste vitrification and sintering***

In recent years, vitrification and sintering of different wastes have been investigated mainly as a result of the urgent need to minimize the large waste volumes produced by several industrial sectors. Of primary interest is the use of waste glass, mainly from display monitors, as raw material for the production of glass-ceramics in order to improve the economics of the process. Glass-ceramics were produced from waste cathode ray tube funnel glass and coal fly ash (Lv et al., 2018). Also, Andreola et al. (2005) investigated the synthesis of glass-ceramics from panel or funnel glass of waste cathode ray tubes with dolomite and alumina. Fan and Li (2014) and (2013) used mixtures of waste glass from thin film transistor liquid crystal displays (LCDs) with blast oxygen furnace slag or calcium fluoride sludge respectively, for the production of glass-

ceramics. Lin (2007) and Kim et al. (2016) also investigated the production of ceramic tiles using glass from LCDs. Furlani et al. (2010) obtained glass-ceramics from steel slag and glass cullet from energy saving lamps. Wu et al. (2015) and Tian et al. (2011) used sewage sludge pyrolysis residues (SSPR) to synthesize glass-ceramics, while further improvement of end materials' properties was achieved by microwave irradiation for 10 min at 750 °C. Bernardo and Mascio (2011) improved glass-ceramics' durability, produced from a mixture of SSPR and recycled glass, through microwave heating. Lu et al. (2014) investigated the effect of the particle size during sintering of a mixture 70 wt% waste glass and 30 wt% fly ash for the production of wollastonite glass-ceramics. Coal fly ash and waste glass in a ratio of 2:3 were also examined as raw materials for the production of glass-ceramic foams (Zhu et al., 2016). A mixture of hazardous iron-rich waste arising from slag flotation during copper production, waste glass, sand and limestone was also investigated for the production of glass-ceramics by sinter-crystallization (Karamanov et al., 2007). Furthermore, waste glass and coal fly ash were mixed at percentages 65 wt% and 35 wt% respectively for the production of glass-ceramics (Yoon et al., 2013), while Vu et al. (2011) produced superior ceramic materials by vitrifying mixtures of volcanic ash and waste glass (30 wt% to 70 wt%, respectively). Most of the aforementioned efforts for the synthesis of glass-ceramics were based on mixing waste glass and several industrial wastes; however, a new waste source, namely the P/V glass derived from waste panels has been recently classified as waste of electrical and electronic equipment (WEEE) and, to the author's best knowledge, has not been investigated yet for the production of glass-ceramics.

### ***6.1.2 Perspectives on the production of glass-ceramics from P/V glass and fly ash***

Lignite is currently the prime domestic energy source of Greece. Despite the various benefits associated with electricity generation (abundant, easily accessible and low cost fuel that offers energy independence), multiple environmental impacts are associated with lignite combustion. For example, around 10,000 kilotonnes of fly ash are produced annually as a result of lignite combustion in Greek power plants (Kourti and Cheeseman,

2010). In order to valorize these large waste volumes, numerous attempts have been made over the last decades with only limited success. A fraction of fly ash may be utilized for the production of lightweight aggregates and zeolites, or as partial replacement of sand and cement in the concrete industry (Kourti and Cheeseman, 2010; Mouhtaridis et al., 2003). However, one of the inherent characteristics of the Greek lignite fly ash is the presence of a widespread glassy phase, up to 40% of its weight depending on the lignite quality and combustion conditions, which consists of SiO<sub>2</sub> and CaO and may be used for the production of glass-ceramics (Kostakis, 2009).

Apart from the conventional energy sector derived wastes, in recent years the valorization of wastes produced by the renewable energy sector is also explored. Due to the global energy concerns associated with the use of conventional fuels (Cappelletti et al., 2011), the industry is focused on the use of Renewable Energy Sources (RES), as a result of the increasing integration of P/V technology (Savvilotidou et al., 2017). The worldwide growth of the P/V sector shows an exponential curve for more than two decades (Tao and Yu, 2015). In 2016, the installed solar P/V capacity totaled around 300 GW compared to 5 GW in 2005 (Savvilotidou et al., 2017), whereas it has been predicted that waste P/V panels will amount to 1.7-8.0 million tonnes by 2030 and 60-78 million tonnes by 2050 (Komoto et al., 2018). Thus, new challenges emerge for the recovery of the raw materials contained in End of Life (EoL) P/V panels as they have been included in the waste catalogue of the Directive 2012/19/EU, which sets targets for recycling (80 wt%) and recovery (85 wt%) from 15<sup>th</sup> August 2018. It has been noted that in typical crystalline P/V panels, which are the lion's share among the P/V technologies, the core layers consist of glass (up to 75 wt%), cells, Ethylene Vinyl Acetate polymer (EVA), ribbons and Tedlar (Kang et al., 2012; Klugmann-Radziemska and Ostrowski, 2010; Tammaro et al., 2015). In this perspective, if most P/V glass is recovered and recycled, the minimum Directive's requirements will be met.

Predictions on volumes of future waste streams, as well as composition and management of lignite fly ash and waste P/V panels are relevant aspects in the current literature, following the principles of circular economy (D'Adamo et al., 2017).

However, today the degree of valorization of the Greek lignite fly ash is considered rather poor, as only 15% of its volume is utilized for commercial applications (i.e. in cement production), while the remaining volumes are mainly stockpiled and cause various environmental problems (Itskos et al., 2010). Also, insufficient attention has been paid to recycling of waste P/V glass, thus the development of sustainable practices is considered urgent.

This study investigates for the first time a valorization approach involving two industrial wastes generated by the energy sector, namely waste P/V glass and lignite fly ash, for the production of glass-ceramics. Aiming at the development of a novel energy efficient process, mixing ratios of the raw materials, temperature, additives and other parameters were thoroughly explored. Also, various properties of the produced glass-ceramics were evaluated and compared to those of products used in the construction sector.

## 6.2 Materials and methods

### 6.2.1 Raw materials

A 19.5 kg waste poly-crystalline panel, with dimensions 1640 (l) × 992 (w) × 40 (h) mm, consisting of 3.2 mm thick tempered glass, was obtained from RISEN ENERGY Co., Ltd. (China). Sound dismantling of the aluminium frame and junction box (Savvilitidou et al., 2017), shredding of the panel in pieces of approximately 2 cm × 2 cm (**Fig. 6.2a**) and thermal treatment of the pieces were carried out to recover the waste P/V glass from the highly resistant panel structure. Thermal treatment was applied in an electrical furnace (Nabertherm), at 550 °C for 1 hour to degrade the EVA layer, since EVA resin's decomposition starts at 350 °C and is completed between 470 and 520 °C (Berger et al., 2010; Kang et al., 2012). In specific terms, the decomposition of EVA occurs in two stages; the first stage involves deacetylation and release of acetic acid, while the second random/chain scissions giving mainly propane, propene, ethane, butane, hexane-1 and butane-1 (Granata et al., 2014). The separated recyclable materials obtained after thermal treatment are shown in **Fig. 6.2b**. More specifically, they contain P/V glass fragments,



1992). This batch extraction test is widely used for assessing the toxicity of a waste, as it simulates the worst-case scenario, which involves disposal in landfills (Chichester and Landsberger, 1996; Cohen et al., 1999). It has been reported that TCLP leachates obtained from WEEE components exhibited significantly higher concentration of metals compared to the leachates obtained after the use of the European leaching test (EN 12457) (Komilis et al., 2013).

### ***6.2.2 Production of glasses***

The thermal treatment of inorganic wastes for the production of glass is normally carried out between 1200 and 1500 °C (Barbieri et al., 2000; Vu et al., 2011). Temperature depends mainly on the type and chemical composition of the waste, the particle size (Barbieri et al., 1997; Lu et al., 2014) and the additives (i.e. glass modifiers, etc.) (Zhu et al., 2016) used to form eutectic mixtures with lower melting points and decreased viscosity. In this study, a heating microscope was initially used to observe the overall flattening/melting behavior of the raw materials in order to select the most appropriate mixing ratios and temperature required for glass production. Four characteristic temperatures at which the materials exhibit structural changes were determined, namely the initial deformation temperature (IDT), the softening temperature (ST), the hemispherical temperature (HT) and the fluid temperature (FT).

Considering the FT of the raw materials, all tests were carried out in a Nabertherm furnace at 1200 °C for 1 hour. Molten glass was first produced in alumina crucibles and then was rapidly cooled to room temperature after its direct removal from the furnace. Glass was synthesized after thermally treating mixtures of wastes, namely i) 70% P/V glass and 30% lignite fly ash, and ii) 80% P/V glass and 20% lignite fly ash. The code 70G30A refers to the glass produced from a starting mixture consisting of 70% waste P/V glass and 30% fly ash, while the code 80G20A refers to the glass produced from 80% waste P/V glass and 20% fly ash. Sodium carbonate (4.5 wt%) and borax (4.5 wt%), as supplied by Fluka and Sigma Aldrich respectively, were also used as fluxes to decrease viscosity of the molten phase at the studied temperature (Zhu et al., 2016).

### **6.2.3 Production of glass-ceramics**

The produced glasses were pulverized ( $d_{50}=31\mu\text{m}$ ) and then uniaxially pressed at 50 MPa (Zuo et al., 2009) so that cylindrical specimens of 30 mm diameter and 20 mm height were obtained. Five specimens were produced for each mixture of raw materials and each selected temperature. The code 70G30A refers to the products obtained after heating of 70G30A glasses, while the code 80G20A refers to the products obtained after heating of 80G20A glasses.

As previous studies showed, optimum nucleation usually occurs at a temperature between 50 to 100 °C above transition temperature ( $T_g$ ) (Wu et al., 2015). Also, the process is effective if the heating temperature is higher than the dilatometric softening point of the glasses, which represents a threshold temperature for obtaining viscous flow (Bernardo and Maschio, 2011). Based on these remarks, Differential Thermal Analysis (DTA) was used to determine the glass  $T_g$  and crystallization peak temperature ( $T_c$ ). The glass powders were heated from room temperature to 1100 °C with a heating rate of 10 °C/min using a Perkin Elmer Pyris DTA/TG analyser. Referring to the thermal behavior of 70G30A glass (**Fig. 6.3**), an endothermic peak is shown at 587 °C, i.e.  $T_g$  and an exothermic peak at 641 °C, i.e.  $T_c$  in the thermal spectrum. The endothermic peak indicates the glass transition temperature due to the absorption of heat, while the exothermic peak is due to the release of heat of crystallization. Also, 80G20A glasses exhibit very similar behavior with peaks at slightly lower temperatures ( $T_g$  and  $T_c$ ). Since low heating rates assist exothermic peak at relatively low temperatures (Lin et al., 2012), a heating rate of 3 °C/min was finally carried out in specimens in order to achieve efficient production of glass-ceramics. The specimens were heated to 600, 700 and 800 °C in a furnace (Nabertherm) with a heating rate of 3 °C/min in order to convert the glasses into glass-ceramics. The desired temperatures were maintained for 1 hour and afterwards the specimens were cooled to room temperature in the furnace.

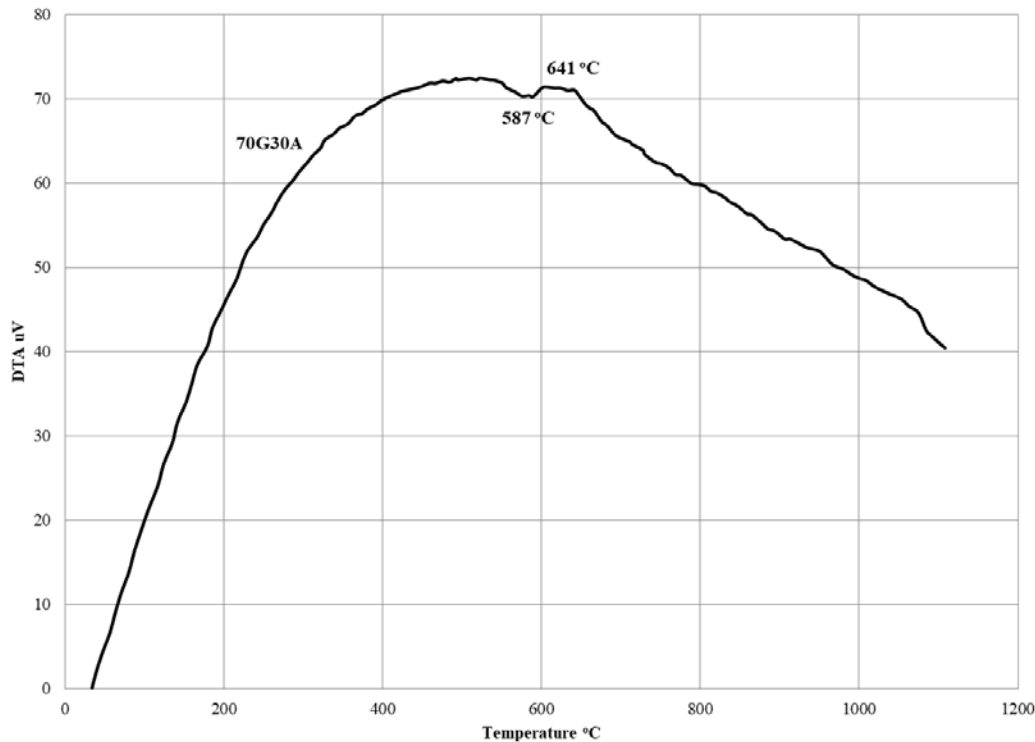


Fig. 6.3: DTA of 70G30A glass

Several physical and mechanical properties of glass-ceramics, namely open porosity, bulk density, water absorption, compressive strength and microhardness, were determined. The mechanical behavior of glass-ceramics was assessed by using cylindrical specimens in a universal testing machine (MTS model) with load and displacement control. Microhardness (Vickers hardness) testing was accomplished by a microhardness tester FM-700 (FUTURE-TECH CORP.) with a load of 500 g and dwell time of 5 sec. The microstructure of glass-ceramics was evaluated through SEM studies using a JEOL 6380LV scanning electron microscope equipped with an energy dispersive spectrometer (EDS) INCA microanalysis system.

The chemical stability of the produced glass-ceramics was determined by immersing specimens into an acidic solution (0.5 M  $H_2SO_4$ ) at 60 °C for 48 hours according to Yoon et al. (2013). The weight loss of specimens was recorded. Finally, the potential toxicity of the produced glass-ceramics was assessed.

## 6.3 Results and discussion

### 6.3.1 Mineralogical and chemical analyses of raw materials

The XRD patterns of P/V glass and lignite fly ash are illustrated in **Fig. 6.4**.

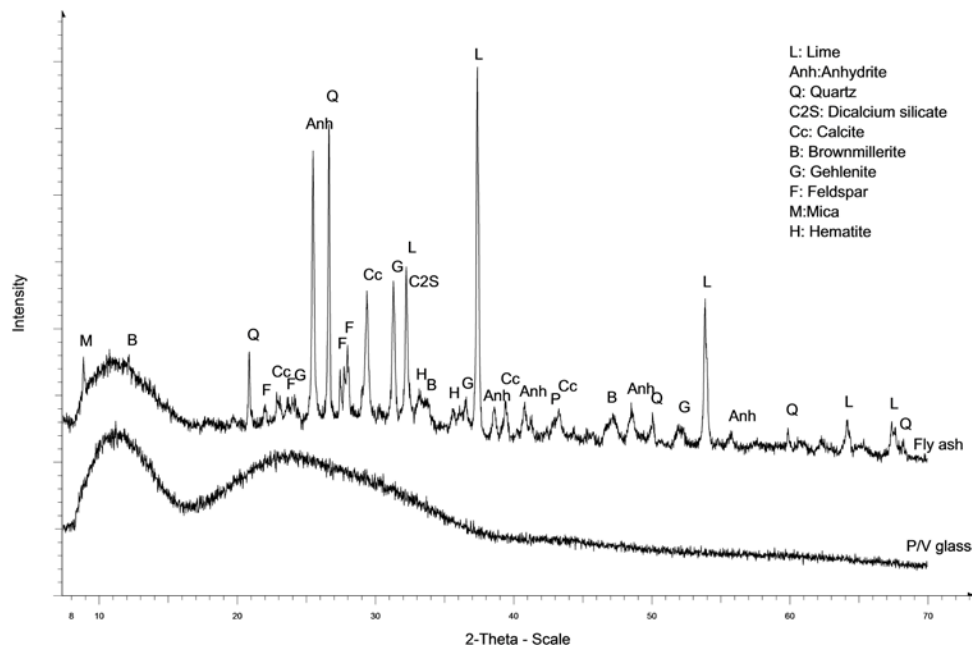


Fig. 6.4: XRD patterns of waste P/V glass and lignite fly ash

Two broad humps are shown representing the amorphous phase of the P/V glass. The mineral phases that were identified in lignite fly ash were amorphous phase, feldspars ( $\text{CaAl}_2\text{Si}_2\text{O}_8$ ,  $(\text{Na,K})(\text{Si}_3\text{Al})\text{O}_8$ ), calcite ( $\text{CaCO}_3$ ), lime ( $\text{CaO}$ ), quartz ( $\text{SiO}_2$ ), anhydrite ( $\text{CaSO}_4$ ), gehlenite ( $\text{Ca}_2\text{Al}_2\text{SiO}_7$ ), brownmillerite ( $\text{Ca}_2(\text{Al,Fe})_2\text{O}_5$ ), mica  $\text{KAl}_2(\text{AlSi}_3\text{O}_{10})(\text{F,OH})_2$ , dicalcium silicate ( $\text{Ca}_2\text{SiO}_4$ ), periclase ( $\text{MgO}$ ) and hematite ( $\text{Fe}_2\text{O}_3$ ).

The XRF analyses of the raw materials, in the form of oxides, are shown in **Table 6.1**. P/V glass mainly contains  $\text{SiO}_2$ ,  $\text{CaO}$ ,  $\text{Na}_2\text{O}$  and also some  $\text{Al}_2\text{O}_3$  and  $\text{K}_2\text{O}$ , while  $\text{SiO}_2$ ,  $\text{CaO}$  and  $\text{Al}_2\text{O}_3$  are the major components present in fly ash. The presence of  $\text{SiO}_2$ ,  $\text{CaO}$ , and  $\text{Al}_2\text{O}_3$  in the starting mixture demonstrates the potential of thermal treatment

for the production of glasses and glass-ceramics (Kritikaki et al., 2016; Yoon et al., 2013; Prasad and Shih, 2016).

**Table 6.1: XRF analysis of raw materials (% wt)**

Oxide	Waste P/V glass	Fly ash
CaO	9.07	29.6
SiO <sub>2</sub>	78.3	33.9
Al <sub>2</sub> O <sub>3</sub>	1.46	14.5
Fe <sub>2</sub> O <sub>3</sub>	0.85	5.07
SO <sub>3</sub>	0.18	5.33
MgO	1.63	3.58
K <sub>2</sub> O	0.69	0.99
TiO <sub>2</sub>	<DL	0.68
P <sub>2</sub> O <sub>5</sub>	<DL	0.06
MnO	0.03	0.05
Na <sub>2</sub> O	7.73	0.22

<DL: below detection limit

Oxides such as SiO<sub>2</sub> and Al<sub>2</sub>O<sub>3</sub> serve as glass formers, also known as glass network formers or glass forming oxides (Karamberi et al., 2007). Alkali oxides (Na<sub>2</sub>O and K<sub>2</sub>O) and alkaline earth oxides (CaO and MgO) act as network modifiers that partially break up the SiO<sub>2</sub> network and lower melting and softening temperatures (Hülsenberg et al., 2008). In the present study the composition of P/V glass (high content of Na<sub>2</sub>O and moderate content of K<sub>2</sub>O) increases the content of non-bridging oxygens and decreases silica network connectivity (Hülsenberg et al., 2008), while Fe<sub>2</sub>O<sub>3</sub>, as glass intermediate, also results in low viscosity and low melting temperature (Erol et al., 2007; Lin et al., 2015; Lin et al., 2012).

As most studies for the production of glass-ceramics from WEEE have focused on valorization of TFT-LCD glass (Savvilotidou et al., 2015; Savvilotidou et al., 2019), a comparison between the P/V glass and TFT-LCD glass composition is provided in **Table 6.2**. For instance, the content of CaO and MgO in P/V glass (9.07 and 1.63%), which typically increases the durability (Almasri et al., 2017), is higher compared to the

respective content in a typical TFT-LCD glass (1.5 and 1.16%) (Fan and Li, 2014, 2013). Additionally, the higher amount of Na<sub>2</sub>O and Fe<sub>2</sub>O<sub>3</sub> in P/V glass (7.73 and 0.85% in our study) in comparison to the low respective content in TFT-LCD glass (up to 0.3 and between 0-0.025%) (Fan and Li, 2013; Fan and Li, 2014; Kim et al., 2016; Lin et al., 2009; Lin, 2007) indicates that P/V glass will exhibit a better behavior during melting.

**Table 6.2: Comparison of TFT-LCD glass and P/V glass composition (% wt)**

Oxide	TFT-LCD glass			P/V glass	
	Fan and Li, 2014; Fan and Li, 2013	Kim et al., 2016	Lin et al., 2009	Lin et al., 2007	Present work
CaO	1.50	3-8 (7.6)	20.06		9.07
SiO <sub>2</sub>	61.20	58-64 (60.1)	72.84	64	78.3
Al <sub>2</sub> O <sub>3</sub>	16.30	15-20 (16.8)			1.46
Fe <sub>2</sub> O <sub>3</sub>		~0.025			0.85
MgO	1.16	0-4 (0.44)			1.63
K <sub>2</sub> O					0.69
MnO					0.03
Na <sub>2</sub> O			0.3	0.3	7.73
B <sub>2</sub> O <sub>3</sub>	10.72	7-11 (10.3)			

### 6.3.2 Glass production conditions

Photos of the raw materials' flattening/melting behavior are presented in **Fig. 6.5** which also includes the original form (at 550 °C). It is seen that for P/V glass, the FT is considerably lower, 1200 °C (**Fig. 6.5a**), compared to the respective temperature for lignite fly ash, 1350 °C (**Fig. 6.5b**).

It is then anticipated that addition of more glass in the starting mixture will decrease the FT and the required heating time. The mixing ratios investigated (i.e. 70% P/V glass to 30% fly ash, 80% P/V glass to 20% fly ash) were selected after carrying out several preliminary tests. For instance, mixtures of 60% P/V glass to 40% fly ash were excluded from further studies because the molten glass produced at 1200 °C exhibited

very high viscosity indicating that higher temperature and/or longer heating times are required. This was first witnessed by the heating microscope, as the FT of the mixture was 1245 °C (see **Annex C**).

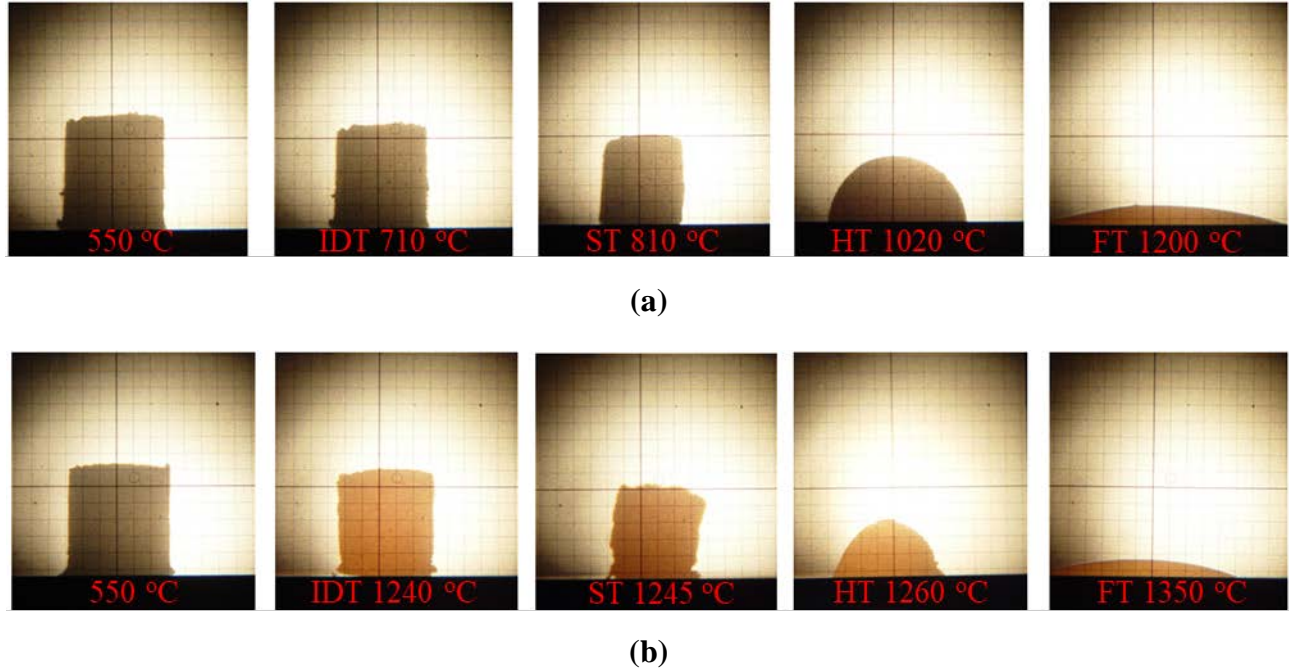


Fig. 6.5: Photos of (a) waste P/V glass and (b) lignite fly ash, taken with a heating microscope

### 6.3.3 Glass characteristics

The XRD patterns of the produced glasses indicate the presence of an amorphous phase which denotes the conversion of the raw materials' mixture to glass (**Fig. 6.6**). The glasses were transparent, homogeneous and bubble-free. Non-formation of bubbles was attributed to the homogeneous starting mixture. Specifically, P/V glass was milled in order to obtain a similar particle size distribution with fly ash, resulting in relatively homogeneous glasses; thus agglomeration of particles, which trap atmospheric gases and are externally surrounded by the melt (Shelby, 2007), did not occur. At this point, it must be noted that the material produced after thermal treatment of a mixture containing 60% P/V glass to 40% fly ash at 1200 °C, had a partly glassy matrix with peaks of various

intensities for anhydrite, feldspar and others, thus it does not exhibit the proper characteristics of glass.

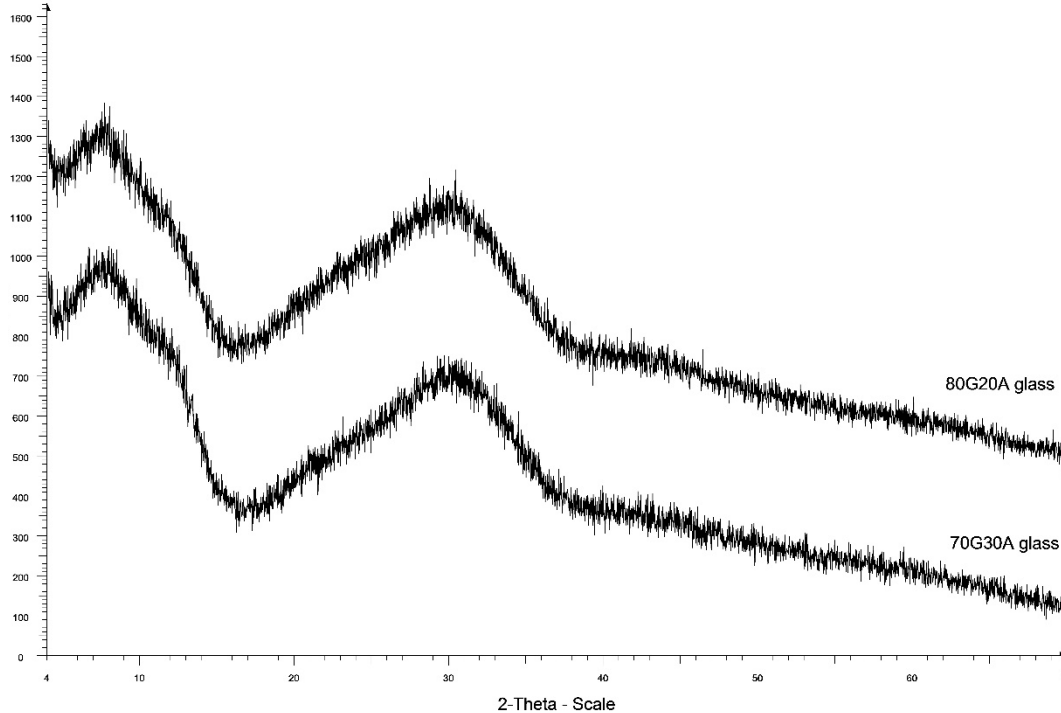


Fig. 6.6: XRD patterns of glasses 70G30A and 80G20A produced at 1200 °C

The XRF analysis of the produced glasses at 1200 °C is shown in **Table 6.3**. Their compositions are similar, presenting a high proportion of Si, Ca and Na oxides; specifically, 80G20A glass contains a higher content of Na<sub>2</sub>O and a lower content of Fe<sub>2</sub>O<sub>3</sub> and Al<sub>2</sub>O<sub>3</sub>, which was attributed to the higher proportion of P/V glass and the relatively lower proportion of fly ash compared to 70G30A glass.

By comparing the composition of glasses to those of the initial raw materials it has been confirmed that there was no reactivity between the melt and the crucible for both compositions (i.e. 70G30A, 80G20A). Also, the results indicate that the composition of glasses is suitable for the production of glass-ceramics and presents qualitative and quantitative similarities with those referred to in previous studies (Almasri et al., 2017; Lin et al., 2012). The high content of Na<sub>2</sub>O (**Table 6.3**) will assist sintering mainly at temperatures varying between 500 and 800 °C (Nel et al., 2015).

Also, the content of Fe<sub>2</sub>O<sub>3</sub> is anticipated to improve the microstructure resulting in dense glass-ceramics (Zuo et al., 2009). It is therefore expected that the produced glasses will exhibit good sintering behavior.

**Table 6.3 XRF analysis of glasses (% wt)**

Oxide	70G30A	80G20A
CaO	18.2	14.1
SiO <sub>2</sub>	64.7	64.8
Al <sub>2</sub> O <sub>3</sub>	3.51	3.15
Fe <sub>2</sub> O <sub>3</sub>	2.38	1.71
SO <sub>3</sub>	1.05	0.76
MgO	1.81	2.88
K <sub>2</sub> O	0.40	0.28
TiO <sub>2</sub>	0.30	0.20
P <sub>2</sub> O <sub>5</sub>	<DL	<DL
MnO	0.03	0.03
Na <sub>2</sub> O	5.43	10.5

<DL: below detection limit

### 6.3.4 Properties of glass-ceramics

#### 6.3.4.1 Chemical composition, mineralogy and microstructure

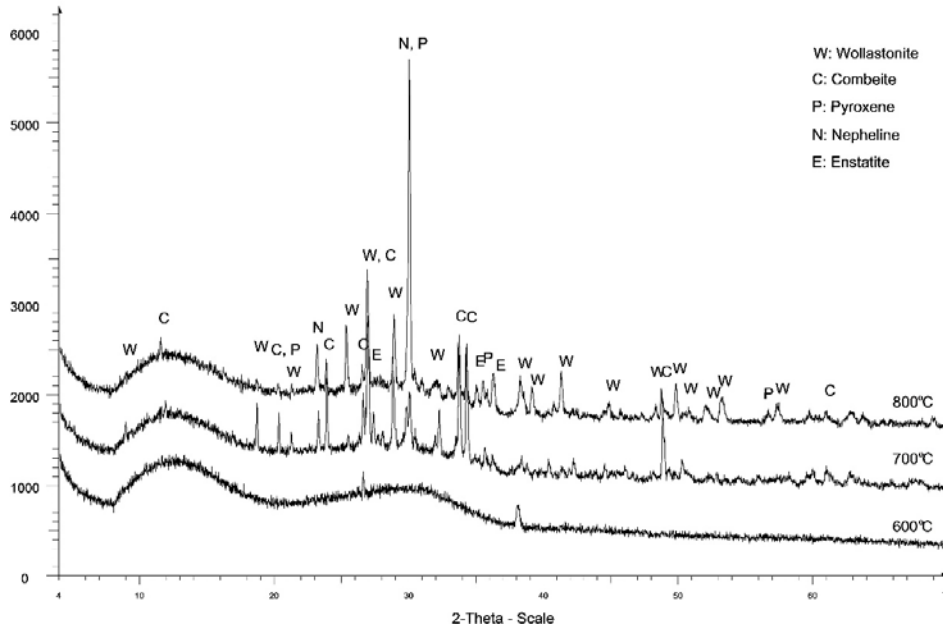
The composition of glass-ceramics, obtained from the respective glasses, is shown in **Table 6.4**. The obtained SiO<sub>2</sub>-CaO-Na<sub>2</sub>O glass-ceramic system with an average composition of more than 85% (w/w) SiO<sub>2</sub>, CaO and Na<sub>2</sub>O may be justified by the chemical composition of the glasses (70G30A and 80G20A, **Table 6.3**), whose major oxides were SiO<sub>2</sub>, CaO and Na<sub>2</sub>O.

**Fig. 6.7** shows the XRD patterns of the glass-ceramics obtained from glasses 70G30A and 80G20A, respectively. The products obtained after heating glasses at 600 °C are mainly amorphous and the only mineral phase identified, exhibiting peaks of low intensity, is wollastonite. More specifically, two low intensity peaks in the case of 70G30A and only one in the case of 80G20A are shown, indicating that crystallization is

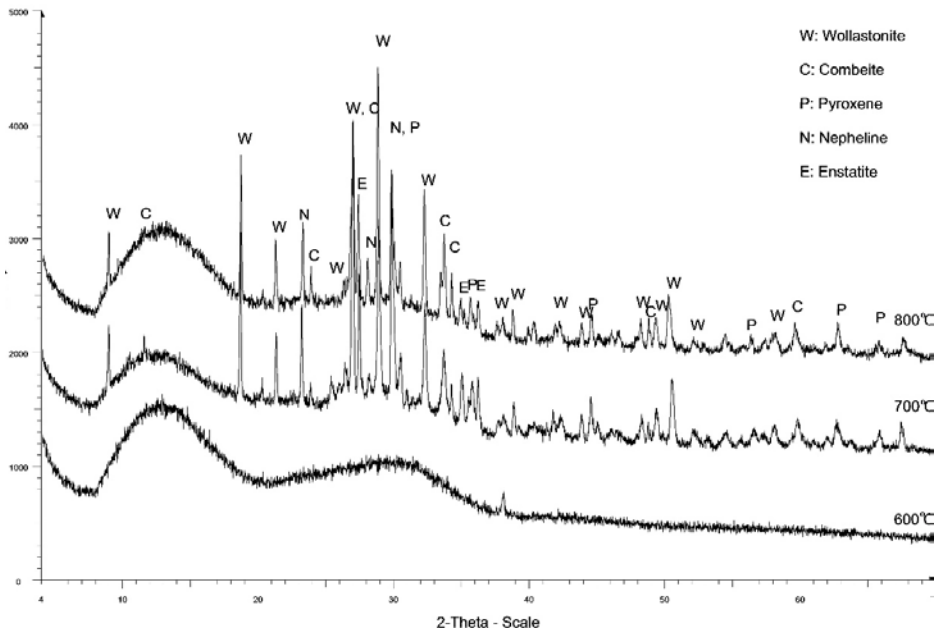
poor, thus the products cannot be characterized as glass-ceramics. The high amorphicity is attributed to the low sintering efficiency at 600 °C, as it is nearly below the crystallization temperature (641 °C). On the other hand, the products obtained after heating glasses at 700 and 800 °C exhibited various crystalline phases, namely wollastonite ( $\text{CaSiO}_3$ ), combeite ( $\text{Na}_2\text{Ca}_2\text{Si}_3\text{O}_9$ ), pyroxene ( $\text{CaMgSi}_2\text{O}_6 - \text{CaFe}^{2+}\text{Si}_2\text{O}_6$ ), nepheline ( $\text{Na}_3\text{KAl}_4\text{Si}_4\text{O}_{16}$ ) and enstatite ( $(\text{Mg,Fe})_2\text{Si}_2\text{O}_6$ ), thus exhibiting the characteristics of glass-ceramics. More specifically, it is seen that the predominant crystalline phases for the 70G30A products are nepheline and pyroxene, while for the 80G20A products the main phase is wollastonite. Another difference observed is that in the first case lower-intensity broad humps are shown indicating higher crystallinity compared to the 80G20A products.

**Table 6.4: XRF analysis of glass-ceramics (% wt)**

Oxide	70G30A 600 °C	80G20A 600 °C	70G30A 700 °C	80G20A 700 °C	70G30A 800 °C	80G20A 800 °C
CaO	19.1	19.3	19.3	16.7	19.1	16.7
SiO <sub>2</sub>	55.6	55.8	55.2	58.5	55.7	58.1
Al <sub>2</sub> O <sub>3</sub>	3.34	2.67	3.37	2.74	3.14	2.89
Fe <sub>2</sub> O <sub>3</sub>	1.80	1.83	1.84	1.53	1.84	1.52
SO <sub>3</sub>	1.55	1.73	1.76	1.28	1.58	1.29
MgO	1.70	1.50	1.40	1.40	1.70	1.70
K <sub>2</sub> O	0.45	0.49	0.54	0.43	0.47	0.42
TiO <sub>2</sub>	0.21	0.23	0.22	0.16	0.20	0.16
Na <sub>2</sub> O	14.9	14.7	15.3	16.0	14.8	16.0



(a)



(b)

Fig. 6.7: XRD patterns of glass-ceramics produced at 600, 700 and 800 °C (a) 70G30A, (b) 80G20A

Earlier studies also show the formation of wollastonite in glass-ceramics produced from coal fly ash mixed with waste glass (Lu et al., 2014; Yoon et al., 2013). The formation of wollastonite can be attributed to the devitrification of P/V glass, which is stimulated by the presence of CaO in fly ash (Ponsot et al., 2015). The formation of combeite is caused by the presence of Na<sub>2</sub>O (Pirayesh and Nychka, 2013; Thomas and Bera, 2016). Pyroxene is formed as a result of the presence of CaO, MgO, Al<sub>2</sub>O<sub>3</sub>, SiO<sub>2</sub> as well as the alkaline oxides (Na<sub>2</sub>O, K<sub>2</sub>O) in glasses (Kamseu et al., 2008; Yoon et al., 2013). Also, the content of Na<sub>2</sub>O and Al<sub>2</sub>O<sub>3</sub> causes the formation of nepheline (Almasri et al., 2017). In the author's opinion, the content of alkaline oxides in the starting waste P/V glass played a key role in this notable crystallization, as the produced glasses, i.e. 70G30A and 80G20A, were prone to form crystalline phases, such as combeite, pyroxene and nepheline.

Overall, the XRD patterns of glasses (70G30A and 80G20A) heated at 700 and 800 °C indicate the efficient production of glass-ceramics with higher crystallization degree in the latter case (800 °C); such tendency has also been observed by Erol et al. (2007). Several studies showed that the sintering temperature of glasses and the heating time play an important role on the mineralogy of the produced glass-ceramics (Lu et al., 2014; Lin et al., 2009; Wu et al., 2015). In the current study, data on the sintering of glasses at temperatures higher than 800 °C is not provided because the products were melted and lost their shape due to extensive viscous flow sintering.

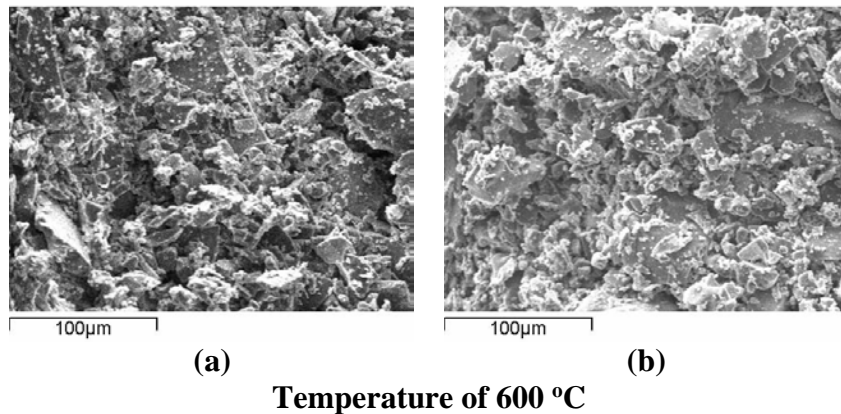
SEM studies (micrographs in **Fig. 6.8**) revealed that the microstructure of the products varied with the heating temperature of glasses and their composition. The products obtained after heating glasses at 600 °C (**Fig. 6.8a** and **b**) are not characterized as glass-ceramics since sintering was poor. They were granulated and exhibited rough texture and weak bonds between particles. The loose compaction among the particles was due to the absence of a liquid phase. When the temperature increased from 600 to 700 °C (**Fig. 6.8c** and **d**), the products exhibited a quite smooth surface and higher homogeneity as a result of better sintering.

The products obtained after heating glasses at 800 °C (**Fig. 6.8e** and **f**) exhibit the

characteristics of glass-ceramics. They are characterized by a dense and homogeneous microstructure as a result of the improved viscous flow sintering, while crystals are homogeneously dispersed into the matrix. The formation of crystals was the result of ion diffusion and rearrangement into the glassy phase. Due to the action of a viscous flow phase key mechanism and the presence of a sufficient liquid fraction, originating from the amorphous phase, open pores were filled by the liquid while the number of isolated (closed) pores, as well as the bulk density increased (Fan and Li, 2013; Lin et al., 2012).

SEM analysis also provided information on the shape, morphology and size of crystals after sintering. At 700 and 800 °C there exist identically distributed crystal grains with size varying (up to 30 µm in length), which according to EDS correspond to wollastonite (**Fig. 6.9**).

**Fig. 6.9** shows that the sizes of the crystals formed at 700 °C are smaller than those formed at 800 °C. Thus, sintering at 700 °C allows the conversion of few glass droplets into crystals, whereas the glassy phase is dominant. **Fig. 6.9a** illustrates the formation of small wollastonite crystals (~10 µm) and also the glassy phase present in 70G30A glass-ceramics. A similar structure is observed for 80G20A glass-ceramics (**Fig. 6.9c**), where many tiny crystals, as well as boundaries between the crystalline grain-area and the glassy-matrix are observed. However, crystals were not identified due to their small size and background counts. It is estimated that the growth of crystals could be enhanced achieving better sintering behavior either at higher temperature than 700 °C or using finer glass particles than those studied.



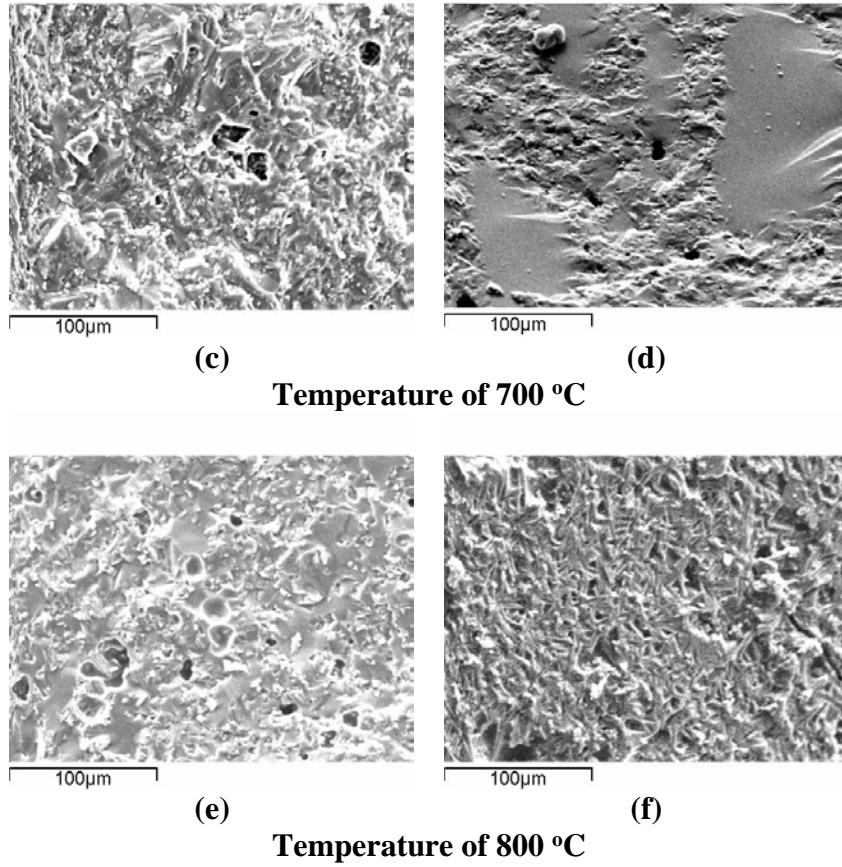
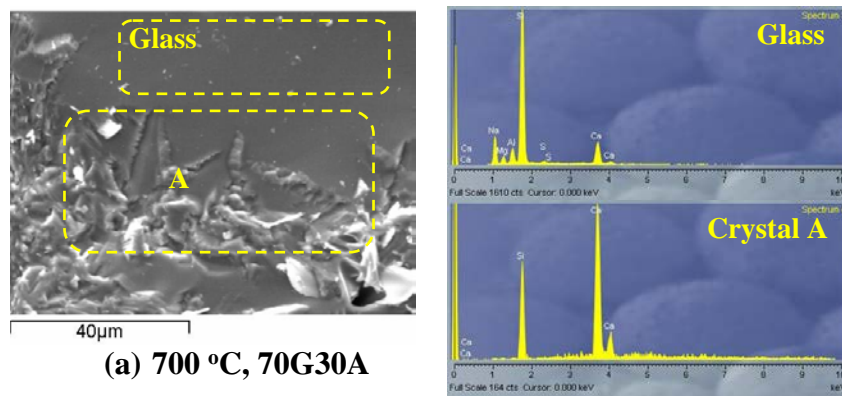


Fig. 6.8: SEM micrographs of 70G30A (a, c, e) and 80G20A (b, d, f) glass-ceramics produced at 600, 700 and 800 °C



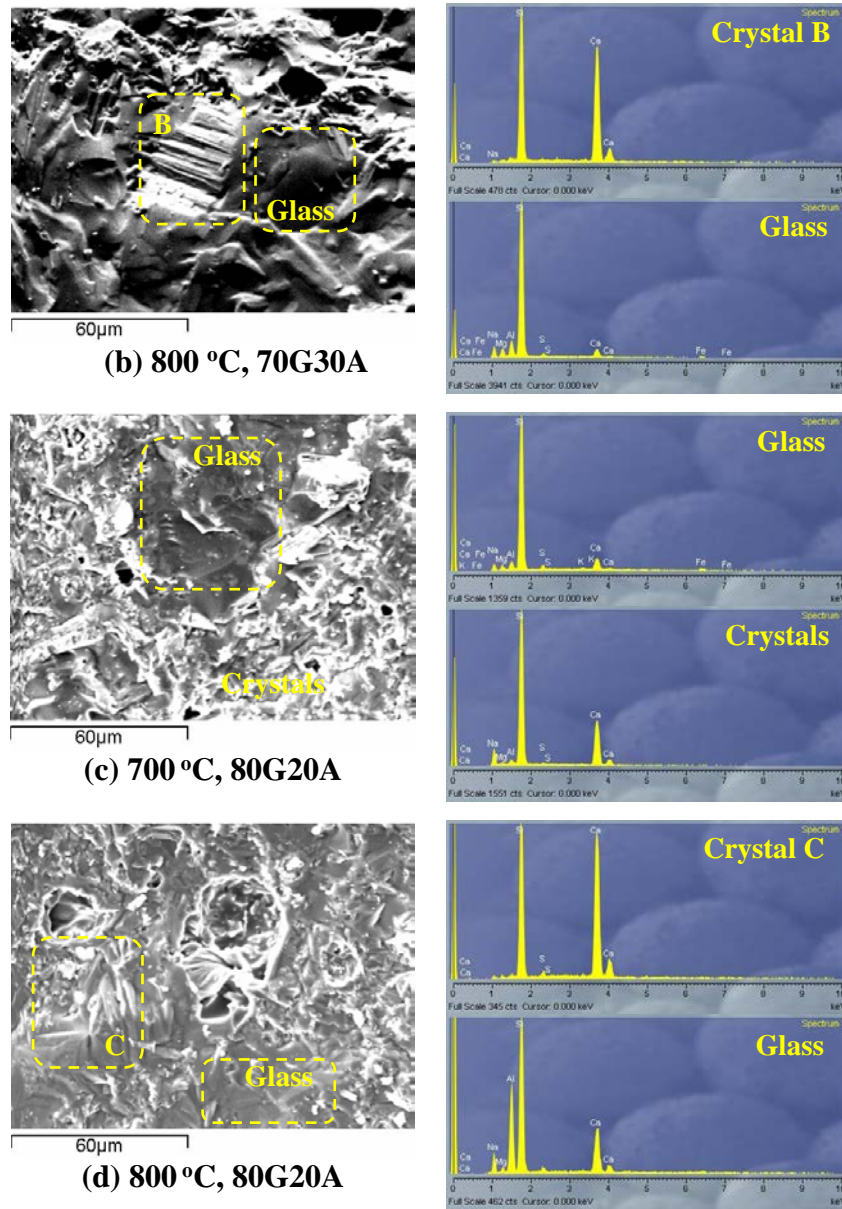


Fig. 6.9: SEM micrographs and chemical composition of glass matrix and crystals for 70G30A (a, b) and 80G20A (c, d) glass-ceramics produced at 700 and 800 °C.

At 800 °C, the microstructure of the products is obviously better, whereas crystals have grown and their interlocking is more visible. The crystal size is almost two times bigger than that of 700 °C, and this indicates that without changing the particle size this temperature was more suitable for the formation of glass-ceramics. During crystallization, there was a re-adjustment of particles, as a result of the sintering viscous flow, and the particles joined via sintering necks (Almasri et al., 2017), which were

developed when glasses softened enough to allow particle adhesion and development of grain boundaries as a function of temperature and time. This is the reason why the pore size of the glass-ceramics at 800 °C is low, whereas a growth of grains and elongated cavities are also observed. **Fig. 6.9b,d** show the formation of tabular crystals (B) of wollastonite, with length of approximately 30 µm for 70G30A and 10-15 µm for 80G20A glass-ceramics, surrounded by amorphous phase (glass matrix with conchoidal fracture) and other crystals. **Annex E** illustrates further SEM micrographs.

The microstructure of glass-ceramics produced at 700 and 800 °C is in agreement with the mineralogical studies obtained by XRD. The degree of crystallization and densification could be further enhanced by increasing the sintering time or/and adding binders, i.e., aqueous polyvinyl alcohol, in the grounded glass before its pressing (Erol et al., 2009). Such parameters though were not investigated in the present study.

#### ***6.3.4.2 Physical and mechanical properties***

**Table 6.5** demonstrates the physical and mechanical properties of the glass-ceramics, as well as their chemical stability. Glasses sintered at 700 and 800 °C were transformed into pore-free glass-ceramics with negligible water absorption and high density, within the range of 2.41-2.83 g/cm<sup>3</sup>. At these sintering temperatures, the products exhibit higher densification (Cao et al., 2016; Erol et al., 2008; Fan and Li, 2013) whereas open pores tend to disappear and closed pores tend to increase Lin et al. (2012). Previous studies (Binhussain et al., 2014) stated that density of glass-ceramics produced from wastes is normally in the range of 1.83-2.63 g/cm<sup>3</sup>, which is in good agreement with the results of the present study.

Regarding the mechanical properties of glass-ceramics, it was demonstrated that compressive strength and microhardness increase in proportion to the sintering temperature. The compressive strength of the produced glass-ceramics varied and depended mainly on the sintering temperature, rather than the initial compositions of the raw materials (i.e. glasses 70G30A, 80G20A) and increased from 6 to 148 MPa when the sintering temperature was 800 °C for 70G30A. The variations associated with the initial composition are less profound, with 70G30A glass-ceramics exhibiting better mechanical

performance than 80G20A glass-ceramics. Finally, as expected, the glass-ceramics that were produced at the highest sintering temperature (800 °C) exhibited the highest degree of crystallization and obtained the maximum microhardness values (Erol et al., 2007; Lin et al., 2009). Also, the glass-ceramics derived from 70G30A glasses exhibit higher microhardness values than 80G20A glass-ceramics.

The obtained values were compared to the limits prescribed in ASTM C 1272. A maximum average value of 6% for water absorption and a minimum average value of 69.0 MPa for compressive strength are required to comply with ASTM C 1272 standard specifications for heavy vehicular paving brick. Other requirements, including freeze thaw resistance and abrasion resistance were not investigated in the present study. Based on the comparative analysis, it is deduced that the values obtained at 700 and 800 °C exceeded the minimum requirements for their use as brick pavers for heavy vehicular traffic uses, as well as those obtained by other studies (Wu et al., 2015; Yoon et al., 2013).

It should be mentioned that 70G30A glass-ceramics produced at 800 °C exhibited the highest strength, thus better mechanical performance as bricks. Considering that the same parameters (i.e. particle size (31 µm) and temperature at 800 °C) were used for the production of 70G30A and 80G20A glass-ceramics, the difference may be attributed to their compositions. The higher proportion of CaO in 70G30A than in 80G20A glass-ceramics (**Table 6.4**) offered higher stability, microhardness and strength (Almasri et al., 2017; Barbieri et al., 1997). Therefore, a careful control of oxide content is required to obtain glass-ceramics with tailored properties depending upon their application.

**Table 6.5: Properties of glass-ceramics**

<b>Sample</b>	<b>Temperature (°C)</b>	<b>Open porosity (%)</b>	<b>Bulk density (g/cm<sup>3</sup>)</b>	<b>Water absorption (%)</b>	<b>Compressive strength (MPa)</b>	<b>Vickers Hardness (GPa)</b>	<b>Weight loss (%)</b>
70G30A	600	22.1±0.2	2.01±0.06	11.2±0.5	6.89±1.10	5.47±0.24	4.42
80G20A	600	23.6±0.4	1.97±0.04	12.0±0.5	5.60±0.80	5.28±0.47	3.81
70G30A	700	0.05±0.00	2.79±0.18	0.02±0.00	117±1	7.05±0.37	0.013
80G20A	700	0.19±0.01	2.41±0.16	0.07±0.00	113±0	6.79±0.25	0.012
70G30A	800	0.21±0.03	2.83±0.11	0.06±0.02	148±1	8.89±0.24	0.008
80G20A	800	0.10±0.00	2.69±0.26	0.07±0.00	129±2	7.78±0.22	0.005

### **6.3.5 Comparison with other studies**

The results obtained in the present study (**Table 6.5**) were compared to those of previous studies (**Table 6.6**) that investigated the production of glass-ceramics from various other wastes.

Referring to the physical properties, density is in the same range with the values found by Bernardo and Maschio (2011), Lin et al. (2015), Lu et al. (2014), Wu et al. (2015), Yoon et al. (2013) and other studies listed in **Table 6.6**. Also, focusing on open porosity and water absorption, similarities are observed between the values of the present study and those of Ji et al. (2016), Kim et al. (2016), Lin (2007), Lin et al. (2015), Fan and Li (2013) and Fan and Li (2014).

Compressive strength (max. 148 MPa, **Table 6.5**) is higher than the values obtained (between 5 and 67 MPa) in other studies (Zhu et al., 2016) and (Zhang et al., 2015a), or lower compared to the values reported (up to 237 MPa) by Lin et al. (2015), Yoon et al. (2013) and Zhang et al. (2015b) (**Table 6.6**). The values of microhardness obtained in the present study are in the same range with the values listed in **Table 6.6**, as well as those obtained in studies investigating the production of glass-ceramics from other wastes, such as mine tailings (Ye et al., 2015), sugar cane bagasse ash (Teixeira et al., 2014 and references therein) or cement kiln dust (Khater, 2010). However, it must be noted that microhardness values obtained in the present study (5.47-8.89 GPa) exceeded those obtained in an earlier study (2.52-5.73 GPa) investigating the production of glass-ceramics from fly ash mixed with red mud or ferronickel slag at 800 °C (Kritikaki et al., 2016). This is mainly attributed to the large differences in the composition of the raw materials and the mixing ratio used (e.g. the lower value mentioned, 2.52 GPa, refers to glass ceramics produced from a starting mixture consisting of 50% fly glass and 50% red mud). Also, microhardness values of glass–ceramics produced at 800 °C in the present study are higher than those (3.01 GPa) obtained for glass-ceramics produced from TFT-LCD waste glass after sintering at the same temperature (800 °C) (Lin et al., 2009).

**Table 6.6: Comparison of properties of glass-ceramics produced from different wastes**

Waste mixtures	Vitrification/melting conditions	Sintering conditions	Mechanical strength (MPa)	Vickers hardness (GPa)	Density (g cm <sup>-3</sup> )	Porosity (%)	Water absorption (%)	Reference
Sewage sludge (52 wt%) with CaO (21 wt%) and waste glass (21 wt%)	1450 °C for 2 h	820 °C for 90 min (nucleation) and 1000 °C for 120 min (crystallization)	Bending strength: 70.2	6.28	-	-	-	Tian et al., 2011
Sewage sludge pyrolysis residues (80 wt%) with CaO (10 wt%) and SiO <sub>2</sub> (10 wt%)	1400 °C for 2 h	800 °C for 60 min (nucleation) and 1000 °C for 120 min (crystallization)	Bending strength: 72.23	5.28	2.47	-	-	Wu et al., 2015
Sewage sludge with recycled soda–lime–silica glass and kaolin clay; Sewage sludge with recycled borosilicate glass and kaolin clay	1300 °C for 1 h	1050 for 30 min; 1000 °C for 30 min	Bending strength: 49.0; 62.1	5.2; 5.8	2.50; 2.47	11; 7	Negligible	Bernardo and Maschio, 2011
Coal fly ash (35 wt%) and waste glass (65 wt%)	1400 °C for 3 h	850-1050 °C for 1 h	Compressive strength: 162.7-238.6, bending strength: 60.8-94.1	Max. 5.3 (1050°C)	2.19-2.49	-	-	Yoon et al., 2013
Volcanic ash (30 wt%) and waste glass (70 wt%)	-	800 °C for 5 min	Bending strength: 6.58	-	1.34	52.08	-	Vu et al., 2011
Waste soda–lime–silica glass (70 wt%) and fly ash (30 wt%)	1450 °C for 2 h	Sintering of 15 wt% lime and 85 wt% of produced	Flexural (bending) strength: 76 (fine powder);	-	2.0-2.2	-	-	Lu et al., 2014

		glass at 1100 °C	60 (coarse powder)					
Coal fly ash (40 wt%) and waste glass (60 wt%) with borax (30 wt%) and calcium carbonate (0.5 wt%)		800 °C for 45 min	Compressive strength ~5	-	0.46	~79	-	Zhu et al., 2016
Oil shale fly ash and municipal solid waste incineration bottom ash	1500 °C for 1 h	1000 °C for 2 h	Compressive strength: 67	-	1.92	-	-	Zhang et al., 2015a
Oil shale fly ash with CaO and Al <sub>2</sub> O <sub>3</sub>	1500 °C for 1 h	850-1050 °C for 2 h	Compressive strength: max. 186 (for CaO/SiO <sub>2</sub> =0.5); Bending strength: 78 (for CaO/SiO <sub>2</sub> =0.5)	-	-	-	-	Zhang et al., 2015b
Fly ash and calcium carbonate	-	Sintering at the range of 1200–1350 °C	Flexural (bending) strength: 34-90	-	-	> 35	-	Wei et al., 2016
Coal fly ash, rich in alumina (60 wt%) with quartz (4 wt%), clay (20 wt%) and feldspar (16 wt%)	-	1200 °C	Rapture modulus: 51.28	-	-	1.1	0.47	Ji et al., 2016
High-aluminum fly ash	-	1600 °C for 2 h	Compressive strength: 169	-	2.78	1.20	-	Lin et al., 2015
Thin film transistor liquid crystal display (TFT-LCD) waste glass	-	900–1200 °C for 6 h	Flexural (bending) strength ranged	2.5-6.5	1.6-2.3	0-40	0-25	Lin, 2007

---

(0–50%) with clay			from 7-17					
Liquid crystal display glass (0-20 wt %)	-	1100 °C or 1150 °C for 1 h	-	-	1.9-2.4	-	0-15	Kim et al., 2016
Thin-film transistor liquid-crystal display waste glass with blast oxygen furnace slag (7:3) and MgO (10, 20 wt%), Al <sub>2</sub> O <sub>3</sub> (10, 20 wt%)	1400 °C for 30 min	780-980 °C	Flexural (bending) strength of 0-200	-	1.8-2.8	0-0.4	0-20	Fan and Li, 2013
Thin film transistor-liquid crystal display (TFT-LCD) waste glass and calcium fluoride sludge with 5 wt% MgO	1450 °C for 30 min	780-980 °C	Flexural (bending) strength max. 160	-	0.5-2.8	0-40	0-22	Fan and Li, 2014

---

Apart from the properties of the final products, it is critical to compare the conditions under their manufacturing. Melting of wastes is commonly carried out in temperatures greater than 1400 °C. Also, sintering processes are mostly feasible at temperatures of 1000 or 1050 °C. The comparison indicates that the present approach is low-energy intensive (1200 and 700-800 °C, respectively) and this mitigates the entire cost.

Finally, a comparison between the obtained findings and those of earlier studies should be critically considered depending on the specific application for which the produced glass-ceramics will be utilized. For instance, the glass-ceramics obtained at 800 °C exhibited similar properties (density, porosity, water absorption and microhardness) with those of glass-ceramics produced by Erol et al. (2007), Erol et al. (2008), Erol et al. (2009) and were considered suitable for tiling and cladding applications. Also, based on the results of water absorption and open porosity obtained by Ji et al. (2016), which are very similar to the results of the present study, the standard requirements (ISO 13006) for ceramic wall tiles (fine earthenware tile, stoneware tile and fine stoneware tile) are met. Additionally, the microhardness values (up to 8.89 MPa) of glass-ceramics, as determined in the present study, allow their use as coating plates for buildings according to Teixeira et al. (2014) who found mean value of 5.44 GPa in glass-ceramics produced from sugar cane bagasse ash and compared their microhardness with that of natural stones.

### ***6.3.6 Chemical stability – Toxicity of glass-ceramics***

High chemical stability is one of the requirements of glass-ceramics that define their use in the construction industry. Immersion of glass-ceramics produced at 700 and 800 °C into 0.5 M H<sub>2</sub>SO<sub>4</sub> (49 g·L<sup>-1</sup>) at 60 °C for 48 hours resulted in negligible weight loss (**Table 6.5**), namely, 0.013 and 0.008% for 70G30A glass-ceramics, and 0.012 and 0.005% for 80G20A glass-ceramics produced at 700 and 800 °C, respectively. On the other hand, the weight loss for 70G30A and 80G20A glass-ceramics obtained at 600 °C was 4.42 and 3.81%, representing a low chemical stability.

Although the test simulates a highly corrosive environment, the calculated weight loss of glass-ceramics produced at 700 and 800 °C was much lower than the values, 0.13 to 0.15% and 0.085%, reported by Yoon et al. (2013) and Wu et al., 2015. It should be noted that in the first case glass-ceramics were produced from 65% waste glass (from bottles, automobile windows etc.) and 35% fly ash by sintering between 850 to 1050 °C, while in the second case powder of glass-ceramics produced from sewage sludge pyrolysis residues was immersed into 10% H<sub>2</sub>SO<sub>4</sub> solution at 100 °C for 2 hours. Even if the glass-ceramics exhibited better structural integrity than those produced in other studies, these comparative results are only indicative since different waste types and synthesis conditions were used in each study. Also, it must be highlighted that the conditions used in this test are extreme and no direct exposure of glass-ceramics in such environments is anticipated.

**Table 6.7** presents the TCLP results for P/V glass, fly ash and produced glass-ceramics. It is clear from this data that the concentrations of toxic elements in the leachates are well below the given thresholds.

In the TCLP leachates for fly ash, no element concentration exceeds the limits. The highest concentration values were 0.995 mg·L<sup>-1</sup> and recorded for Cr and Ba.

For the produced glass-ceramics, the concentration of Ba, Cr, Pb, and Hg in the leachates has been further decreased compared to the respective concentrations in the leachates produced from fly ash. This decrease may be associated with the increased crystallinity, entrapment, incorporation and immobilization of metals into a stable glass-ceramic structure (Vu et al., 2011; Yang et al., 2009). It is therefore indicated that the use of glass-ceramics as construction materials is safe and no health risks are anticipated. Another issue that needs to be considered, in terms of potential toxicity, is the presence of volatile elements in the raw materials and their volatilization during the production of glass or glass-ceramics (Zhang et al., 2015a; Zhu et al., 2011).

However, in our case no such elements were present in the raw materials investigated. If present, air control systems are required to prevent emissions of volatile toxic metals in the off-gases.

**Table 6.7: TCLP results for raw materials and glass-ceramics (mg·L<sup>-1</sup>)**

Element	P/V glass	Fly ash	Concentration (mg·L <sup>-1</sup> )						TCLP limits
			70G30A, 600 °C	80G20A, 600 °C	70G30A, 700 °C	80G20A, 700 °C	70G30A, 800 °C	80G20A, 800 °C	
As	<DL	<DL	<DL	<DL	<DL	<DL	<DL	<DL	5.0
Ba	<DL	0.994	0.049	0.064	0.017	0.016	0.017	0.018	100.0
Cd	<DL	<DL	<DL	<DL	<DL	<DL	<DL	<DL	1.0
Cr	<DL	0.995	0.124	0.151	0.111	0.043	0.089	0.074	5.0
Pb	0.004	0.002	0.001	0.000	0.001	<DL	0.001	0.001	5.0
Hg	<DL	0.056	0.039	0.051	0.042	0.055	0.046	0.048	0.2
Se	<DL	0.216	<DL	<DL	<DL	<DL	<DL	<DL	1.0
Ag	<DL	<DL	<DL	<DL	<DL	<DL	<DL	<DL	5.0

<DL: below detection limit

## 6.4 Conclusions

This innovative study raises a key environmental issue and deals with the sustainable management and valorization of industrial wastes produced from the energy sector. For the first time, P/V glass, a waste derived from the renewable energy sector and lignite fly ash, a by-product of the conventional lignite combustion, were treated for the production of glass-ceramics. Glass was first produced at 1200 °C, while the optimum temperature for the production of glass-ceramics was 800 °C. Both temperatures are substantially lower than those normally used in similar studies and confirm that the valorization approach considered in the present study is energy efficient.

The properties of the produced novel SiO<sub>2</sub>-CaO-Na<sub>2</sub>O glass-ceramics, namely open porosity, bulk density, water absorption, compressive strength and microhardness indicate that they can be used as bricks for heavy vehicular traffic uses (e.g. in streets, commercial driveways, and other places where there is a high volume of heavy vehicular traffic). However, additional research efforts are required to improve the properties of the produced functional glass-ceramics and broaden the range of their applications in other industrial sectors.

## 6.5 References

- Almasri, K.A., Sidek, H.A.A., Matori, K.A., Zaid, M.H.M., 2017. Effect of sintering temperature on physical, structural and optical properties of wollastonite based glass-ceramic derived from waste soda lime silica glasses. *Results Phys.* 7, 2242-2247.
- Aloisi, M., Karamanov, A., Taglieri, G., Ferrante, F., Pelino, M., 2006. Sintered glass ceramic composites from vitrified municipal solid waste bottom ashes. *J. Hazard. Mater.* 137 (1), 138-143.
- Andreola, F., Barbieri, L., Corradi, A., Lancellotti, I., Falcone, R., Hreglich, S. 2005. Glass-ceramics obtained by the recycling of end of life cathode ray tubes glasses. *Waste Manage.* 25(2), 183-189.
- Baowei, L., Leibo, D., Xuefeng, Z., Xiaolin, J., 2013. Structure and performance of glass-ceramics obtained by Bayan Obo tailing and fly ash. *J. Non-Cryst. Solids* 380, 103-108.
- Barbieri, L., Corradi, A., Lancellotti, I., 2000. Bulk and sintered glass-ceramics by recycling municipal incinerator bottom ash. *J. Eur. Ceram. Soc.* 20 (10), 1637-1643.
- Barbieri, L., Manfredini, T., Queralt, I., Rincon, J.M., Romero, M., 1997. Vitrification of fly ash from thermal power stations. *J. Glass Sci. Technol.* 38 (5), 165-170.
- Berger, W., Simon, F.G., Weimann, K., Alsema E.A., 2010. A novel approach for the recycling of thin film photovoltaic modules. *Resour. Conserv. Recy.* 54 (10), 711-718.
- Bernardo, E., Maschio R.D., 2011. Glass-ceramics from vitrified sewage sludge pyrolysis residues and recycled glasses. *Waste Manage.* 31 (11), 2245-2252.
- Binhussain, M.A., Marangoni, M., Bernardo, E., Colombo, P., 2014. Sintered and glazed glass-ceramics from natural and waste raw materials. *Ceram. Int.* 40 (2), 3543-3551.

- Cao, J., Lu, J., Jiang, L., Wang, Z., 2016. Sinterability, microstructure and compressive strength of porous glass-ceramics from metallurgical silicon slag and waste glass. *Ceram. Int.* 42 (8), 10079-10084.
- Cappelletti, P., Rapisardo, G., de Gennaro, B., Colella, A., Langella, A., Graziano, S.F., Bish, D.L., de Gennaro, M. 2011. Immobilization of Cs and Sr in aluminosilicate matrices derived from natural zeolites. *J. Nucl. Mater.* 414(3), 451-457.
- Chichester, D. L., Landsberger, S., 1996. Determination of the leaching dynamics of metals from municipal solid waste incinerator fly ash using a column test. *J. Air Waste Manage. Assoc.* 46(7), 643-649.
- Cohen, B., Lewis, A.E., Petersen, J., Von Blottnitz, H., Drews, S.C., Mahote, S.I., 1999. The TCLP and its applicability for the characterisation of worst case leaching of wastes from mining and metallurgical operations. *Adv. Environ. Res.* 3(2), 152-165.
- Directive 2012/19/EU of the European Parliament and of the Council of 4 July 2012 on waste electrical and electronic equipment (WEEE), recast. *Off. J. Eur. Union* L197/38.
- Deubener, J., Allix, M., Davis, M.J., Duran, A., Höche, T., Honma, T., Komatsu, T., Krüger, S., Mitra, I., Müller, R., Nakane, S. Pascual, M.J., Schmelzer J.W.P., Zanotto, E.D., Zhou, S., 2018. Updated definition of glass-ceramics. *J. Non-Cryst. Solids* 501, 3-10. DOI: 10.1016/j.jnoncrysol.2018.01.033.
- Erol, M., Küçükbayrak, S., Ersoy-Meriçboyu, A., 2008. Comparison of the properties of glass, glass-ceramic and ceramic materials produced from coal fly ash. *J. Hazard. Mater.* 153 (1-2), 418-425.
- Erol, M., Küçükbayrak, S., Ersoy-Meriçboyu, A., 2007. Production of glass-ceramics obtained from industrial wastes by means of controlled nucleation and crystallization. *Chem. Eng. J.* 132 (1-3), 335-343.
- Erol, M., Küçükbayrak, S., Ersoy-Meriçboyu, A., 2009. The influence of the binder on the properties of sintered glass-ceramics produced from industrial wastes. *Ceram. Int.* 35 (7), 2609-2617.

- Fan, C.S., Li, K.C., 2014. Glass-ceramics produced from thin-film transistor liquid-crystal display waste glass and blast oxygen furnace slag. *Ceram. Int.* 40 (5), 7117-7123.
- Fan, C.S., Li, K.C., 2013. Production of insulating glass ceramics from thin film transistor-liquid crystal display (TFT-LCD) waste glass and calcium fluoride sludge. *J. Clean. Prod.* 57, 335-341.
- Furlani, E., Tonello, G., Maschio, S. 2010. Recycling of steel slag and glass cullet from energy saving lamps by fast firing production of ceramics. *Waste Manage.* 30(8-9), 1714-1719.
- Granata, G., Pagnanelli, F., Moscardini, E., Havlik, T., Toro, L., 2014. Recycling of photovoltaic panels by physical operations. *Sol. Energy Mater. Sol. Cells* 123, 239-248.
- Hülseberg, D., Harnisch, A., Bismarck, A., 2008. *Microstructuring of glasses*. ISBN 978-3-540-49888-9.
- ISO 13006: Ceramic Tiles – Definitions, Classification, Characteristics and Marking, 1998. International Organization for Standardization.
- Itskos, G., Itskos, S., Koukouzas, N., 2010. Size fraction characterization of highly-calcareous fly ash. *Fuel Process. Technol.* 91(11), 1558-1563.
- Ji, R., Zhang, Z., Yan, C., Zhu, M., Li, Z., 2016. Preparation of novel ceramic tiles with high Al<sub>2</sub>O<sub>3</sub> content derived from coal fly ash. *Constr. Build. Mater.* 114, 888-895.
- Kamseu, E., Boccaccini, D.N., Sola, A., Rizzuti, A., Leonelli, C., Melo, C.U., Billong, N., 2008. Sintering behaviour, microstructure and mechanical properties of low quartz content vitrified ceramics using volcanic ash. *Adv. Appl. Ceram.* 107(1), 19-26.
- Kang, S., Yoo, S., Lee, J., Boo, B., Ryu, H., 2012. Experimental investigations for recycling of silicon and glass from waste photovoltaic modules. *Renew. Energy* 47, 152-159.

- Karamanov, A., Aloisi, M., Pelino, M., 2007. Vitrification of copper flotation waste. *J. Hazard. Mater.* 140 (1-2), 333-339.
- Karamberi, A., Orkopoulos, K., Moutsatsou, A., 2007. Synthesis of glass-ceramics using glass cullet and vitrified industrial by-products. *J. Eur. Ceram. Soc.* 27 (2-3), 629-636.
- Khater, G.A., 2010. Glass-ceramics in the CaO–MgO–Al<sub>2</sub>O<sub>3</sub>–SiO<sub>2</sub> system based on industrial waste materials. *J. Non-Cryst. Solids* 356(52), 3066-3070.
- Kim, K., Kim, K., Hwang, J., 2016. Characterization of ceramic tiles containing LCD waste glass. *Ceram. Int.* 42 (6), 7626-7631.
- Klugmann-Radziemska, E., Ostrowski P., 2010. Chemical treatment of crystalline silicon solar cells as a method of recovering pure silicon from photovoltaic modules. *Renew. Energy* 35 (8), 1751-1759.
- Komilis, D., Tataki, V., Tsakmakis, T., 2013. Leaching of heavy metals from personal computer components: comparison of TCLP with a European leaching test. *J. Environ. Eng.* 139(11), 1375-1381.
- Komoto, K., Lee, J.S., Zhang, J., Ravikumar, D., Sinha, P., Wade, A., Heath, G., 2018. End-of-Life Management of Photovoltaic Panels: Trends in PV Module Recycling Technologies. IEA PVPS Task 12, International Energy Agency Power Systems Programme, Report IEA-PVPS T12, 10.
- Kostakis, G., 2009. Characterization of the fly ashes from the lignite burning power plants of northern Greece based on their quantitative mineralogical composition. *J. Hazard. Mater.* 166 (2), 972-977.
- Kourti, I., Cheeseman, C.R., 2010. Properties and microstructure of lightweight aggregate produced from lignite coal fly ash and recycled glass. *Resour. Conserv. Recy.* 54 (11), 769-775.
- Kritikaki, A., Zaharaki, D., Komnitsas, K., 2016. Valorization of industrial wastes for the production of glass-ceramics. *Waste Biomass Valor.* 7 (4), 885-898. DOI: 10.1007/s12649-016-9480-x.

- Lazău, I., Vancea, C., 2014. New vitreous matrix for chromium waste immobilization. *Open Chem.* 12(7), 763-768. <https://doi.org/10.2478/s11532-014-0509-3>.
- Leroy, C., Ferro, M.C., Monteiro, R.C.C., Fernandes, M.H.V., 2001. Production of glass-ceramics from coal ashes. *J. Eur. Ceram. Soc.* 21 (2), 195-202.
- Lin, B., Li S., Hou, X., Li, H., 2015. Preparation of high performance mullite ceramics from high-aluminum fly ash by an effective method. *J. Alloys Compd.* 623, 359-361.
- Lin, K.L., Chang, W.K., Chang, T.C., Lee, C.H., Lin, C.H., 2009. Recycling thin film transistor liquid crystal display (TFT-LCD) waste glass produced as glass-ceramics. *J. Clean. Prod.* 17 (16), 1499-1503.
- Lin, K.L., 2007. Use of thin film transistor liquid crystal display (TFT-LCD) waste glass in the production of ceramic tiles. *J. Hazard. Mater.* 148 (1-2), 91-97.
- Lin, K.L., Chu, T.C., Cheng, C.J., Lee, C.H., Chang, T.C., Wang, K.S., 2012. Recycling solar panel waste glass sintered as glass-ceramics. *Environ. Prog. Sustain. Energy* 31(4), 612-618.
- Lu, J., Lu, Z., Peng, C., Li, X., Jiang, H., 2014. Influence of particle size on sinterability, crystallization kinetics and flexural strength of wollastonite glass-ceramics from waste glass and fly ash. *Mater. Chem. Phys.* 148 (1-2), 449-456.
- Lv, J., Yang, H., Jin, Z., Zhao, M., 2018. Lead extraction and glass-ceramics synthesis from waste cathode ray tube funnel glass through cooperative smelting process with coal fly ash. *Waste Manage.* 76, 687-696.
- McCloy, J.S., Goel, A., 2017. Glass-ceramics for nuclear-waste immobilization. *MRS Bull.* 42(3), 233-240. <https://doi.org/10.1557/mrs.2017.8>.
- Mouhtaridis, Th., Charistos, D., Kantiranis, N., Filippidis, A., Kassoli-Fournaraki, A., Tsirambidis, A., 2003. GIS-type zeolite synthesis from Greek lignite sulphocalcic fly ashes promoted by NaOH solutions. *Microporous Mesoporous Mater.* 61 (1-3), 57-67.

- Nel, M.V., Strydom, C.A., Schobert, H.H., Beukes, J.P., Bunt, J.R., 2015. Effect of sodium compounds on the sintering propensity of coal-associated minerals. *J. Anal. Appl. Pyrol.* 111, 94-99.
- Paul, A., 1982. *Chemistry of glasses*. Chapman and Hall, London. ISBN 978-94-009-5918-7.
- Pirayesh, H., Nychka, J.A., 2013. Sol–Gel Synthesis of Bioactive Glass-Ceramic 45S5 and its in vitro Dissolution and Mineralization Behavior. *J. Am. Ceram. Soc.* 96(5), 1643-1650.
- Ponsot, I., Bernardo, E., Bontempi, E., Depero L., Detsch, R., Chinnam, R.K., Boccaccini, A.R., 2015. Recycling of pre-stabilized municipal waste incinerator fly ash and soda-lime glass into sintered glass-ceramics. *J. Clean. Prod.* 89, 224-230.
- Prasad, M.N.V., Shih, K., 2016. *Environmental materials and waste: resource recovery and pollution prevention*. Academic Press. ISBN: 978-0-12-803837-6.
- Savvilotidou, V., Antoniou, A., Gidarakos, E., 2017. Toxicity assessment and feasible recycling process for amorphous silicon and CIS waste photovoltaic panels. *Waste Manage.* 59, 394-402.
- Savvilotidou, V., Hahladakis, J.N., Gidarakos, E., 2014. Determination of toxic metals in discarded Liquid Crystal Displays (LCDs). *Resour. Conserv. Recy.* 92, 108-115.
- Savvilotidou, V., Hahladakis, J.N., Gidarakos, E., 2015. Leaching capacity of metals–metalloids and recovery of valuable materials from waste LCDs. *Waste Manage.* 45, 314-324.
- Savvilotidou, V., Kousaiti, A., Batinic, B., Vaccari, M., Kastanaki, E., Karagianni, K., Gidarakos, E. 2019. Evaluation and comparison of pre-treatment techniques for recovering indium from discarded liquid crystal displays. *Waste Manage.* 87, 51-61. <https://doi.org/10.1016/j.wasman.2019.01.029>.
- Shelby, J.E., 2007. *Introduction to glass science and technology*. Royal Society of Chemistry. ISBN 0-85404-639-9.

- Tammaro, M., Rimauro, J., Fiandra, V., Salluzzo, A., 2015. Thermal treatment of waste photovoltaic module for recovery and recycling: Experimental assessment of the presence of metals in the gas emissions and in the ashes. *Renew. Energy* 81, 103-112.
- Tao, J., Yu, S., 2015. Review on feasible recycling pathways and technologies of solar photovoltaic modules. *Sol. Energ. Mat. Sol. Cells* 141, 108-124.
- Teixeira, S.R., Souza, A.E., Carvalho, C.L., Reynoso, V.C.S., Romero, M., Rincón, J.M., 2014. Characterization of a wollastonite glass-ceramic material prepared using sugar cane bagasse ash (SCBA) as one of the raw materials. *Mater. Charact.* 98, 209-214. DOI:10.1016/j.matchar.2014.11.003.
- Thomas, A., Bera, J., 2016. Crystallization and sintering behavior of Glass-ceramic powder synthesized by Sol-Gel Process. *J. Austr. Ceram. Soc.* 52(2), 1-5.
- Tian, Y., Zuo, W., Chen, D., 2011. Crystallization evolution, microstructure and properties of sewage sludge-based glass-ceramics prepared by microwave heating. *J. Hazard. Mater.* 196, 370-379.
- US EPA, 1992. Method 1311, Toxicity Characteristic Leaching Procedure.
- Vu, D.H., Wang, K.S., Nam, B.X., Bac, B.H., Chu, T.C., 2011. Preparation of humidity-controlling porous ceramics from volcanic ash and waste glass. *Ceram. Int.* 37 (7), 2845-2853.
- Wu, D., Tian, Y., Wen, X., Zuo, W., Liu, H., Lee, D.J., 2015. Studies on the use of microwave for enhanced properties of glass-ceramics produced from sewage sludge pyrolysis residues (SSPR). *J. Taiwan Inst. Chem. Eng.* 48, 81-86.
- Yang, J., Xiao, B., Boccaccini, A.R., 2009. Preparation of low temperature glass-ceramics from municipal waste incineration fly ash. *Fuel* 88 (7), 1275-1280.
- Ye, C., He, F., Shu, H., Qi, H., Zhang, Q., Song, P., Xie, J., 2015. Preparation and properties of sintered glass-ceramics containing Au-Cu tailing waste. *Mater. Design* 86, 782-787.

- Yilmaz, G., 2012. Structural characterization of glass-ceramics made from fly ash containing  $\text{SiO}_2 - \text{Al}_2\text{O}_3 - \text{Fe}_2\text{O}_3 - \text{CaO}$  and analysis by FT-IR – XRD – SEM methods. *J. Mol. Struct.* 1019, 37-42.
- Yoon, S.D., Lee, J.U., Lee, J.H., Yun, Y.H., Yoon, W.J., 2013. Characterization of Wollastonite Glass-ceramics Made from Waste Glass and Coal Fly ash. *J. Mater. Sci. Technol.* 29 (2), 149-153. <https://doi.org/10.1016/j.jmst.2012.12.002>.
- Zhang, Z., Zhang, L., Li, A., 2015a. Development of a sintering process for recycling oil shale fly ash and municipal solid waste incineration bottom ash into glass ceramic composite. *Waste Manage.* 38, 185-193.
- Zhang, Z., Zhang, L., Li, A., 2015b. Remedial processing of oil shale fly ash (OSFA) and its value-added conversion into glass-ceramics. *Waste Manage.* 46, 316-321.
- Zhu, J., Zhao, L., Chen, M., Zhang, F.S., 2011. Removal of heavy metals from hazardous waste incinerator fly ash by vacuum-aided heat treatment. *Environ. Eng. Sci.* 28 (10), 743-748.
- Zhu, M., Ji, R., Li, Z., Wang, H., Liu, L., Zhang, Z., 2016. Preparation of glass ceramic foams for thermal insulation applications from coal fly ash and waste glass. *Constr. Build. Mater.* 112, 398-405.
- Zuo, R., Wang, M., Ma, B., Fu, J., Li, T., 2009. Sintering and electrical properties of  $\text{Na}_0.5\text{K}_0.5\text{NbO}_3$  ceramics modified with lanthanum and iron oxides. *J. Phys. Chem. Solids* 70 (3-4), 750-754.



## **7** Conclusions, discussion and future work

This section presents a summary of the conclusions obtained by this thesis with a particular focus on the implementation of the results in future recycling design for P/V waste.



## 7.1 Main conclusions

Considering the high number of P/V panels that are expected to reach end-of-life and the opportunities for materials recovery therein, technical innovations are necessary in terms of developing recycling technologies that can recover all valuable materials at high rates and low cost as well. In this thesis, the technical feasibilities and limitations related to developing a viable recycling technology for the most commonly used P/V technologies were identified leading to the following conclusions:

### *Delamination of P/V panels*

Delamination of P/V panels was achieved through thermal, mechanical or chemical processing, resulting in the removal of EVA. Thermal processing produced intact separated materials that are directly reusable as compared to mechanical and chemical processing. The most important criteria though to decide appropriate delamination are associated with the aim of recycling, i.e. if it is a high-value recycling including the recovery of precious and critical metals (Ag, In) or a simple separation and recovery of bulk materials, such as glass and Al.

### *Silver and indium recovery from P/V panels*

Due to the small share of silver or indium, their selective recovery from waste panels is worth only after pre-concentration. Silver and indium were first pre-concentrated through a combination of treatment processes, namely thermal treatment and gravimetric processes, and then recovered through a hydrometallurgical process involving leaching and precipitation steps. The recovery of critical raw materials, such as silver or indium, is a priority for the EU economy. The findings of this thesis may contribute towards an integrated circular waste management that will consider the secondary production of these high-tech metals from waste panels.

In addition to material separation and recovery from waste panels, how the recovered materials can be reused or valorized is also significant, as they often lack quality. This

thesis closed this gap, enabling not only methods for the separation and recovery of materials, but also efficient reuse and valorization potentials for the recovered materials.

#### *Reuse of glass and plastic in cement mortars*

Glass or plastic from waste panels were used as raw materials in place of sand or cement for the production of cement mortars. The results showed that the mechanical properties and corrosion resistance of cement mortars containing glass were comparable or superior to those of reference mortars. Specifically, the produced cement mortars were sufficiently resistant to carbonation, chloride ion penetration and sulfate attack, and thus suitable for exterior uses. In addition, plastic improved the thermal properties of cement mortars, enabling their use as insulators in the construction sector.

#### *Valorization of glass and lignite fly ash in glass-ceramics*

P/V glass and lignite fly ash were melted, and the obtained glasses were sintered for the production of glass-ceramics. The proposed approach is considered energy efficient as compared to those used in relevant studies, mitigating the entire cost. The properties of the novel  $\text{SiO}_2\text{-CaO-Na}_2\text{O}$  glass-ceramics, and especially the obtained compressive strength and water absorbance allow their use as heavy vehicular paving bricks in the construction sector according to ASTM C 1272 standard specifications.

## **7.2 Discussion**

#### *Estimation of P/V material saved by 2050 according to the recycling plan of this thesis and available data*

Assuming that 4,843,891 of c-Si and 950,058 tonnes of c-Si and CIS panel waste will be cumulatively produced by 2050 (Paiano, 2015), the amount of material saved according to the proposed recycling planning of this thesis was estimated. For the calculations, the material share in panel (%) according to Dias et al. (2016), Paiano (2015) and Tammaro et al. (2015), the separation/recycling/recovery yield (%) achieved in chapters 3-6, and the estimated total amount of waste per technology (tonnes) by 2050, as reported by Paiano (2015), were used. The calculations were based on the following formula:

*Estimation of saved material by 2050 = Amount of panel technology by 2050 (tonnes) × Material share in P/V panel (%) × Recovered material yield (%)*

**Table 7.1** presents the amount of material that could be saved by recycling waste panels by 2050. EVA, Tedlar and plastic from junction boxes were not considered in the calculations. Based on the findings, the total amount of saved material from 1st and 2nd generation panels until the year 2050 is 4,976,422 tonnes. Specifically, recycling can save up to 4,360,742 tonnes of glass, 612,828 tonnes of aluminum, 2,731 tonnes of silver and 121 tonnes of indium. However, it must be noted that the manufacturing of P/V panels is continuously changing, making it difficult to adopt universal recycling practices for the treatment of past, current and future panels efficiently, as well as to claim accurate predictions of the future saved material.

**Table 7.1: The amount of material saved by recycling P/V panels by 2050**

Material	Glass	Al	EVA	Tedlar	Ag	In
<i>c-Si</i>						
Percentage of material in P/V panel (%)	74.16	10.30	6.55	3.6	0.0635	-
Material yield from P/V panel waste (%)	99.2	100	X	X	88.8*	-
Estimation of saved material by 2050 (tonnes)	3,563,491	498,821	X	X	2,731	-
<i>CIS</i>						
Percentage of material in P/V panel (%)	84	12	3	-	-	0.02
Material yield from P/V panel waste (%)	99.9	100	X	-	-	63.2*
Estimation of saved material by 2050 (tonnes)	797,251	114,007	X	-	-	121

\*The value was considered based on the pre-concentration yield, the leaching capacity and precipitation efficiency of the metal.

As the findings of this thesis underline, the recycling of P/V panels at their end-of-life can unlock an estimated stock of million tonnes of valuable components globally by 2050, thereby reducing the extraction of raw materials. If the recovered materials are then injected back into the economy, they can either serve for the production of new panels or be sold into global commodity markets, securing the supply of raw materials

for the future. Preliminary estimates suggest that by 2050 the raw materials technically recoverable from waste panels could cumulatively yield a value that is higher than USD 15 billion. This is equivalent to the amount of raw materials that is currently needed to produce approximately 2 billion panels, or 630 GW of power-generation capacity (IRENA and IEA, 2016).

At the end, the P/V sector may become one of the biggest contributors to shaping a circular economy, applying the key metaphor of “what is waste” which can broadly be defined as the “waste is resource” metaphor. However, to accomplish the expectations for the years to come, there is a necessity for a collaborative approach among the business community, policy makers, and institutions that ideally have the same vision, mission, and code of conduct towards the circular economy goals.

### **7.3 Future work**

This section outlines research topics that were beyond the scope of this work and should be addressed in the future to complement the present study.

#### ***7.3.1 Recycling design for CdTe***

This work focused on 1st and 2nd generation P/V waste, investigating the recycling potentials of p-Si, m-Si, CIS and a-Si panels. However, it must be noted that CdTe type is an emerging technology and its recycling is very challenging due to the toxicity of cadmium and tellurium criticality. Recycling and recovery investigations for CdTe are suggested for future research, as they will offer further insights on the recycling design for end-of-life thin-film panels.

#### ***7.3.2 Recycling design in realistic waste volume cases***

The recycling processes in this thesis were limited to small scale experiments in order to achieve repetitions and to mitigate the cost (such as large wastewater volumes, etc.). They were also dependent on the capacity of the available laboratory equipment. Though,

due to variations in composition from panel to panel, it is very important to proceed the treatment in larger waste volumes, under realistic conditions using industrial equipment.

### ***7.3.3 Economic and environmental analyses***

Several studies have explored the life cycle impact of P/V panels. However, their end-of-life phase has been either excluded or neglected from such analyses, mainly due to the very low number of panels that reached the disposal yet, and the missing data about their end-of-life. The P/V community is working on this topic to develop cost effective and environmentally friendly recycling systems. However, in recent literature assessments on the chemicals, energy consumption, material recovery rate, by-products of the whole process and of every single step of process are not complete. To this direction, the results obtained in this thesis can be used to investigate the cost and environmental impact of each recycling, recovery or reuse process for P/V panels using life cycle assessment (LCA).

## **7.4 References**

- IRENA/IEA PVPS Task12, End-of-Life Management: Solar Photovoltaic Panels, 2016.
- Dias, P., Javimczik, S., Benevit, M., Veit, H., Bernardes, A.M., 2016. Recycling WEEE: extraction and concentration of silver from waste crystalline silicon photovoltaic modules. *Waste Manage.* 57, 220-225.
- Paiano, A., 2015. Photovoltaic waste assessment in Italy. *Renew. Sustainable Energy Rev.* 41, 99-112.
- Tammaro, M., Rimauro, J., Fiandra, V., Salluzzo, A., 2015. Thermal treatment of waste photovoltaic module for recovery and recycling: Experimental assessment of the presence of metals in the gas emissions and in the ashes. *Renew. Energy* 81, 103-112.



## **ANNEXES**



## Annex A

P/V waste characterization as “hazardous” or “non-hazardous waste” is based on the typical waste characterization leaching test methods in the US (US Environment Protection Agency method 1311, TCLP), Germany (DIN EN German Institute for Standardization standard 12457-4:01-03) or Japan (Ministry of Environment Notice 13/JIS K 0102:2013 method (JLT-13)). TCLP was used for the characterization of panels in this thesis, as it is one of the most important characterization metrics used in P/V waste classification across the world at this time, which simulates the worst-case scenario, involving disposal in landfills. The results revealed that no panel exceeds the TCLP limits (**Table A.1**).

**Table A.1: Comparison of experimental results to TCLP limits (mg·L<sup>-1</sup>)**

Element	Concentration (mg·L <sup>-1</sup> )				TCLP Limit (mg·L <sup>-1</sup> )
	p-Si	m-Si	a-Si	CIS	
As	<DL	<DL	<DL	<DL	5.0
Cd	<DL	<DL	<DL	<DL	1.0
Cr	<DL	0.415	0.059	0.150	5.0
Pb	3.243	0.744	0.133	<DL	5.0
Hg	<DL	<DL	<DL	<DL	0.2
Se	<DL	<DL	<DL	0.040	1.0
Ag	<DL	<DL	<DL	<DL	5.0

<DL: below detection limit



## Annex B

**Table B.1: Chemical composition of the produced fractions after thermal treatment and sieving (p-Si panel)**

Element	p-Si sieved after thermal treatment		Cells	Glass
	<2.00 and >0.500 mm	<0.500 and >0.180 mm		
Li	<DL	<DL	<DL	<DL
B	14±1	9±0	21±1	40±6
Na	<DL	<DL	<DL	2025±36
Mg	113±0	113±0	113±0	249±4
Al	12459±73	7685±30	16461±334	682±56
Si	68±0	386±1	159±0	204±1
K	5684±518	5479±515	6999±803	5672±636
Ca	1885±20	1749±21	2430±62	1295±29
Ti	288±4	1050±2	76±3	19±5
V	3±0	<DL	2±0	<DL
Cr	286±1	148±1	123±1	308±1
Mn	30±9	18±3	24±3	274±146
Fe	734±35	504±11	826±21	1330±405
Co	<DL	<DL	<DL	<DL
Ni	115±2	62±1	43±0	184±2
Cu	198±3	685±1	101±1	131±236
Zn	122±2	111±2	136±4	236±6
As	<DL	<DL	<DL	<DL
Se	<DL	<DL	<DL	<DL
Sr	8±1	8±0	13±0	7 ±2
Y	<DL	<DL	<DL	<DL
Zr	<DL	<DL	6±1	5±1
Cd	<DL	<DL	<DL	<DL
Sn	430±13	2062±11	433±10	312±69
Sb	24±0	25±0	24±0	31±0

Cs	<DL	<DL	<DL	<DL
Ba	27±3	42±1	19±1	86±43
Hg	<DL	<DL	<DL	<DL
Pb	678±6	2949±3	419±2	<DL
Bi	235±3	227±1	241±2	5±0
U	<DL	<DL	<DL	<DL

**Table B.2: Chemical composition of the produced fractions after thermal treatment and sieving (m-Si panel)**

Element	m-Si sieved after thermal treatment		Cells	Glass
	<2.00 and >0.500 mm	<0.500 and >0.180 mm		
Li	1±0	1±0	1±0	0±0
B	4±0	5±0	7±0	2±0
Na	<DL	<DL	990±24	2160±19
Mg	204±1	295±0	113±0	476±1
Al	8003±58	11732±26	12368±72	318±5
Si	68±0	659±1	159±0	432±2
K	5798±570	5022±480	6208±525	5933±574
Ca	1522±33	2385±28	1930±24	1703±5
Ti	100±2	150±3	77±0	3±0
V	3±0	4±0	1±0	<DL
Cr	326±1	277±1	116±0	215±0
Mn	22±6	18±2	15±1	125±0
Fe	642±17	596±9	321±8	596±5
Co	<DL	<DL	<DL	<DL
Ni	130±3	125±2	46±1	115±1
Cu	47±1	283±2	66±2	258±2
Zn	103±2	141±0	154±2	206±4
As	<DL	<DL	<DL	<DL
Se	<DL	<DL	<DL	<DL
Sr	81±1	158±3	140±1	3±0
Y	<DL	<DL	<DL	<DL

---

Zr	4±1	<DL	<DL	45±1
Cd	<DL	<DL	<DL	<DL
Sn	29±6	1150±2	367±12	131±2
Sb	7±0	31±0	6±0	91±1
Cs	<DL	<DL	<DL	<DL
Ba	585±12	1093±6	123±1	15±0
Hg	<DL	<DL	<DL	<DL
Pb	619±7	2009±14	577±2	<DL
Bi	675±5	1219±9	1154±11	20±3
U	<DL	<DL	<DL	<DL

---



## Annex C

For a-Si panel, selective recovery of the target metal was rather complicated. Although literature supports that a typical a-Si panel contains semiconductors based on In or Sn, the present work did not confirm considerable amounts of these metals, as provided in **Table C.1**.

**Table C.1: Content of Ag, In and Sn (mg/kg, dry matter) in the main components of a-Si panel**

	TCO coated glass	Clear glass
mg Ag/kg treated a-Si panel	<DL	<DL
mg In/kg treated a-Si panel	<DL	<DL
mg Sn/kg treated a-Si panel	13±0	9±0

\*Literature value, \*\* Estimated value

Also, the gravimetric experiment for separating the two glasses was not efficient due to no difference in the density of the two glasses of the a-Si panel. The mechanical crushing and sieving followed by thermal processing gave the following results, indicating once again that the semiconductor layer is not rich in Ag, In or Sn (**Table C.2**).

**Table C.2: Content of Ag, In and Sn (mg/kg, dry matter) after mechanical crushing for 45 sec of a-Si panel in a blade rotor and sieving**

Sample	Product >8.00 mm*	Product >1.40 mm	Product <1.40 and >1.00 mm	Product <1.00 and >0.500 mm	Product <0.500 and >0.250 mm	Product <0.250 mm
mg Ag/kg treated a-Si panel	688±6	33±0	4±0	121±3	10±3	32±0
mg In/kg treated a-Si panel	<DL	<DL	<DL	<DL	<DL	<DL
mg Sn/kg treated a-Si panel	27±0	15±0	5±0	135±7	12±0	11±0

\*After thermal treatment



## Annex D

The glass-ceramics were prepared from starting mixtures of 70% P/V glass and 30% fly ash, as well as 80% P/V glass and 20% fly ash. Initially, further mixture ratios were explored, such as 60% P/V glass to 40% fly ash; in the latter case, the molten glass exhibited very high viscosity at 1200 °C indicating that higher temperature and/or longer heating times are required. This was first profound by the heating microscope as shown in **Fig. D.1**.

Also, the XRF studies showed that the major oxides in 60G40A glasses were Si, Ca and Al oxides (**Table D.1**). No further investigation was made for 60G40A glasses due to the poor results that may be related to the low content of Na<sub>2</sub>O.

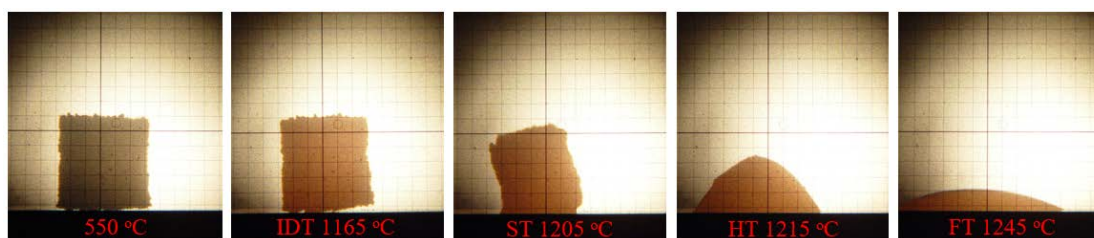


Fig. D.1: Photos of 60% waste P/V glass and 40% lignite fly ash, taken with a heating microscope

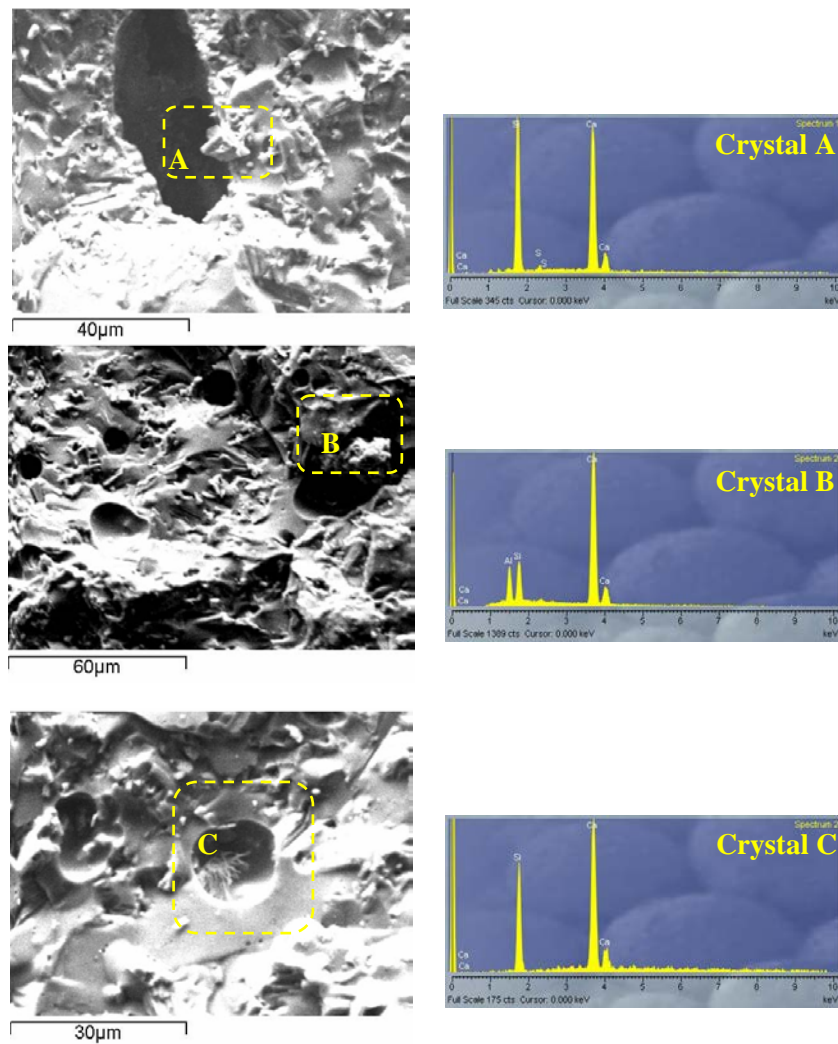
**Table D.1: XRF analysis of raw materials (% wt)**

Oxide	60G40A
CaO	25.8
SiO <sub>2</sub>	51.4
Al <sub>2</sub> O <sub>3</sub>	7.09
Fe <sub>2</sub> O <sub>3</sub>	3.92
SO <sub>3</sub>	2.33
MgO	2.10
K <sub>2</sub> O	0.79
TiO <sub>2</sub>	0.49
Na <sub>2</sub> O	4.90

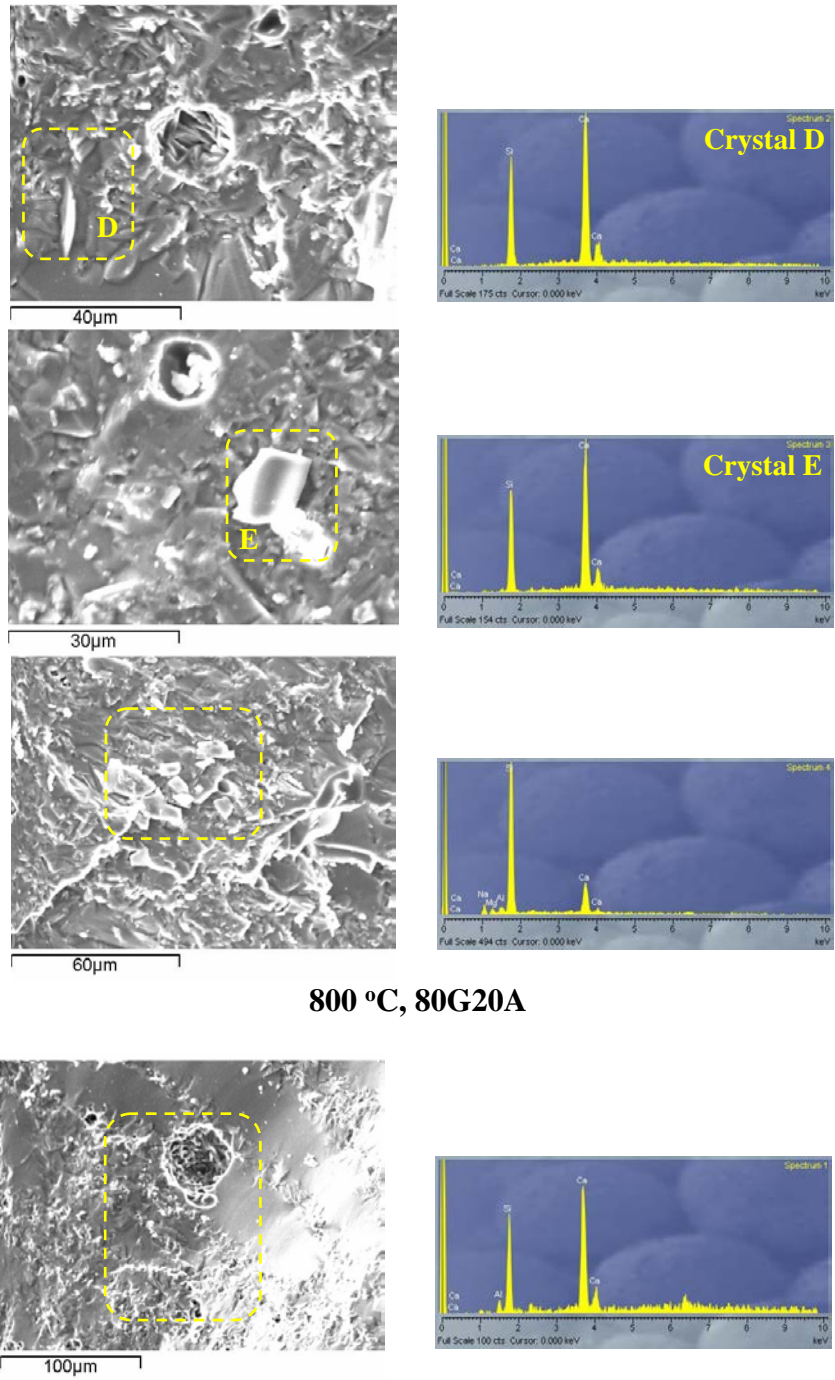


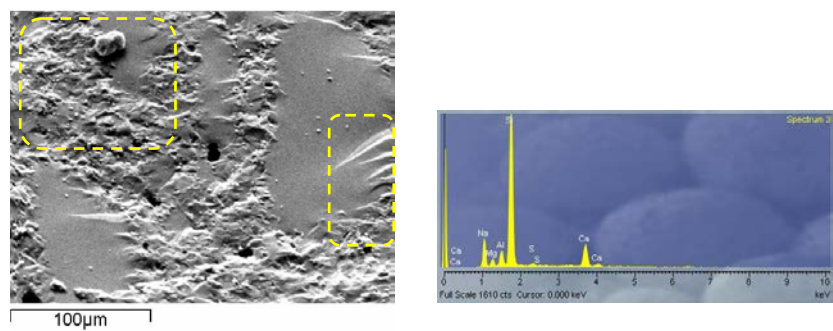
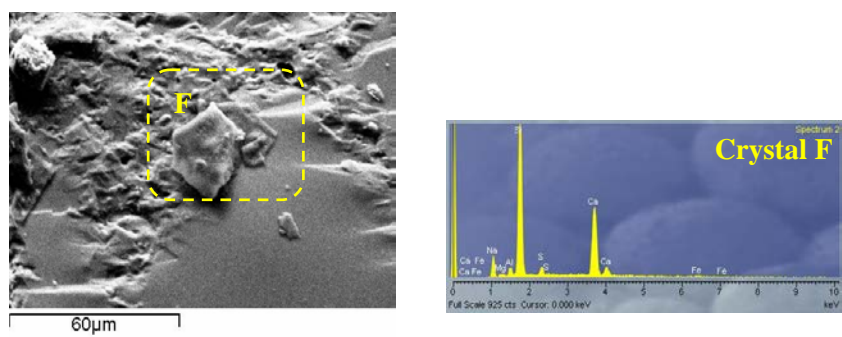
## Annex E

**Fig. E.1** illustrates the microstructure of glass-ceramics, revealing the formation of various crystals with different shapes and sizes, most of which correspond to wollastonite.

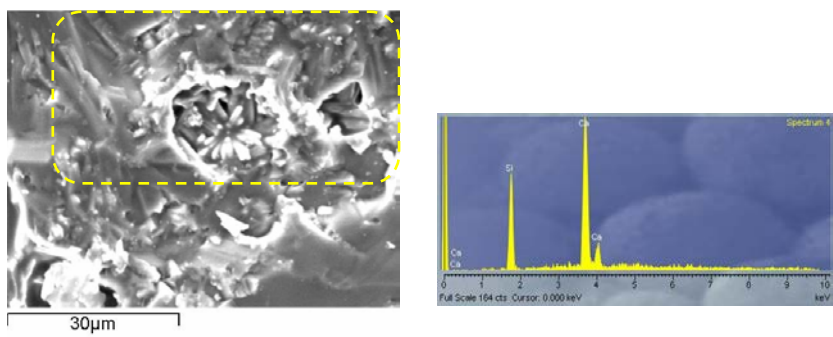
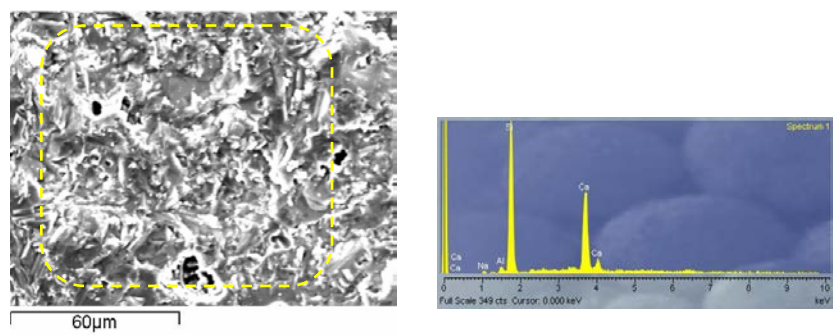


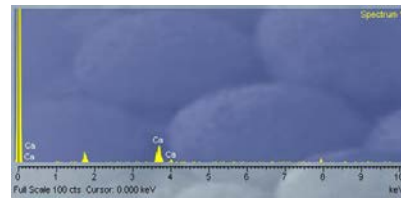
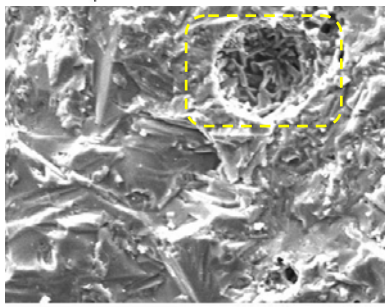
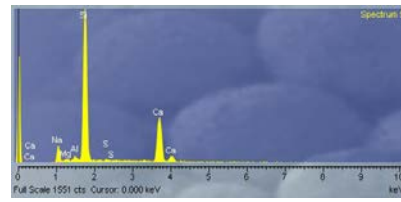
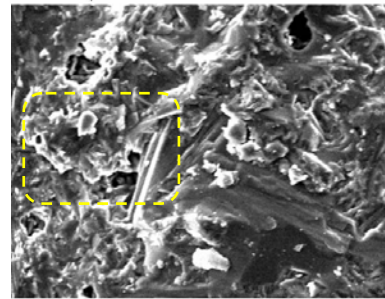
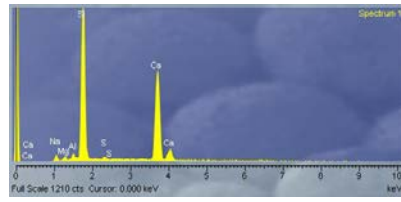
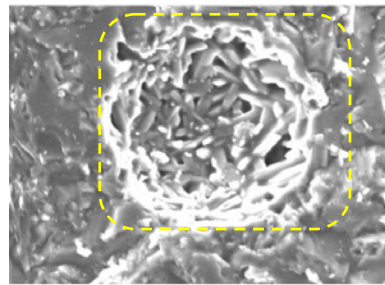
800 °C, 70G30A



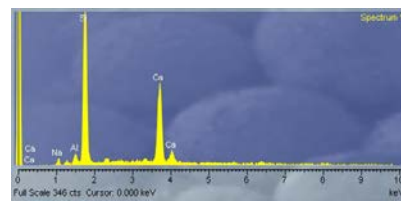
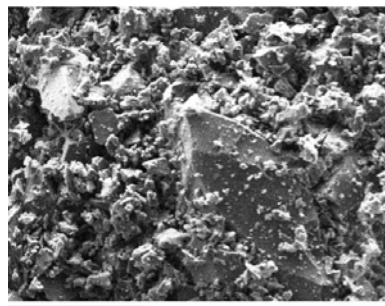


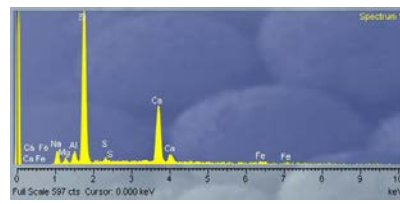
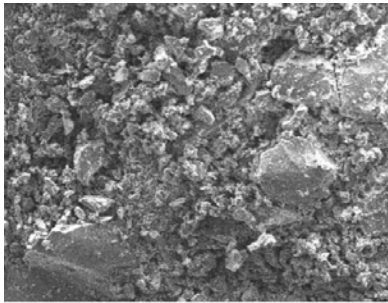
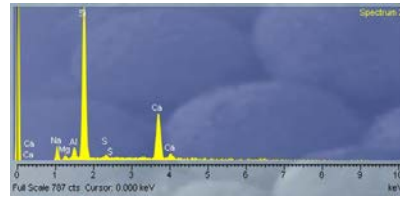
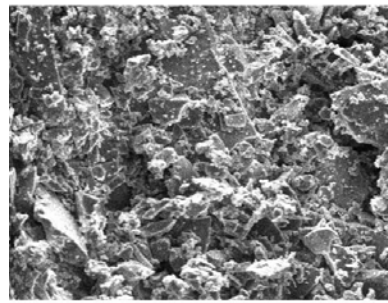
700 °C, 70G30A



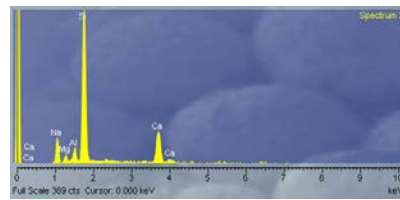
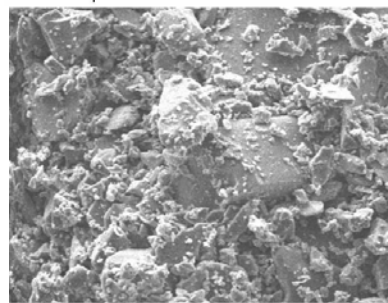
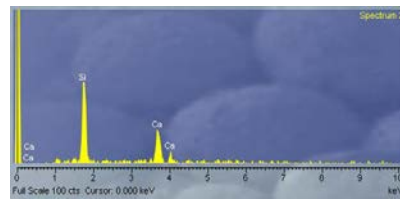
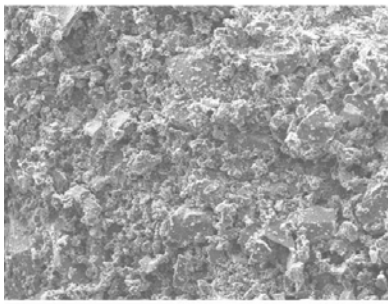


**700 °C, 80G20A**





**600 °C, 70G30A**



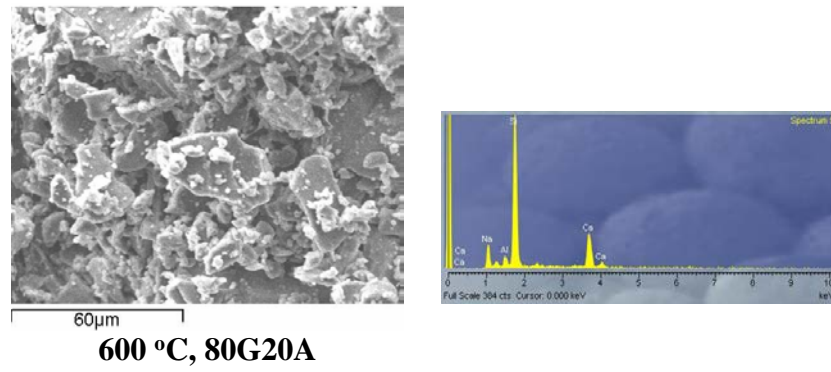


Fig. E.1: SEM micrographs and chemical composition of glass matrix and crystals for 70G30A and 80G20A glass-ceramics produced at 600, 700 and 800 °C.



